Performance optimization modelling of a horizontal roughing filter for the treatment of mixed greywater

by

Mtsweni Sphesihle

Submitted in fulfilment of the requirements for the degree of Doctor of Engineering in the Department of Chemical Engineering in the Faculty of Engineering and the Built Environment at Durban University of Technology, KwaZulu-Natal, South Africa

February 2021

Supervisors: Professor S. Rathilal Professor B.F. Bakare

Dedication

To my family the Mtswenis, MaMatswa, Ns and “N”, for your ever holistic support!

Declaration

I, **Sphesihle Mtsweni**, declare that:

(i) This research reported in this thesis except where otherwise indicated is my own original work.

(ii) This thesis has not been submitted for any degree or examination at any other University or academic institution.

(iii) This thesis does not contain other persons' data, pictures, graphs or other information, unless specifically acknowledged as being sourced from other persons.

(iv) This thesis does not contain other persons' writing, unless specifically acknowledged as being sourced from other researchers. Where other written sources have been quoted, then:

a) Their words have been re-written but the general information attributed to them has been referenced;

b) Where their exact words have been used, their writing has been placed inside quotation marks, and referenced.

(v) Where I have reproduced a publication of which I am an author, co-author or editor, I have indicated in detail which part of the publication was actually written by myself alone and have fully referenced such publications.

(vi) This thesis does not contain text, graphics or tables copied and pasted from the Internet, unless specifically acknowledged, and the source being detailed in the thesis and in the references sections

Signed: _____

As the candidate's Supervisors we have approved this thesis for submission

Professor S. Rathilal

Professor B.F. Bakare

Acknowledgements

I would like thank my supervisors for their support and guidance throughout this research and I will be always grateful to them. I would also like to thank Mangosuthu University of Technology particularly the Teaching and Learning Development Centre, Research Department and Skills Development Unit including Chemical Engineering Department in terms of financial support throughout my entire research. I would also like to thank the Department of Higher Education and Training for the provision of funding support since the inception of my research work and following participation in a six-year comprehensive development and induction programme, the New Generation of Academics Programme (nGAP) for aspiring academics over the past six years. I would also like to thank Dr Phiwayinkosi Gumede and the staff in Chemical Engineering department for the provision of holistic support in all aspects of my research. I would also like to thank Dr Bwaphwa and the rest of my colleagues in various academic disciplines within the institution for being helpful in terms of guidance and sharing of informative research ideas.

My special thanks to MaMatswa for your optimistic character since the inception of this research and for always being a source of encouragement, the rest of my family and close friends for always being ever supportive to me and not least to the population at large in Umhlabeni informal settlements and the entire community representatives within the area for good cooperation while conducting the study.

List of authored publications

MTSWENI, S., RATHILAL, S. AND BAKARE, B.F. (2021). Application of neural network for the prediction of filter duration and turbidity in a horizontal roughing filter using domestic wastewater, (In prep.).

MTSWENI, S., RATHILAL, S. AND BAKARE, B.F. (2021). Prediction of domestic greywater effluent turbidity from a horizontal roughing filter using feedforward neural network, (In prep.).

MTSWENI, S., BAKARE, B.F. AND RATHILAL, S. (2019). Performance of a horizontal roughing filter using principal component regression and multiple linear regression treating informal settlement greywater, *Proceedings of the world congress on engineering and computer science* (WCECS), October 22-24, San Francisco, USA.

BAKARE, B.F., MTSWENI, S. AND RATHILAL, S. (2019). Pilot study of a horizontal roughing filtration system treating greywater generated from peri-urban community in Durban, South Africa, *Journal of Water Reuse and Desalination*, 9(3), 330-337.

BAKARE, B.F., MTSWENI, S. AND RATHILAL, S. (2017). Characteristics of greywater from different sources within households in a community in Durban, South Africa, *Journal of Water Reuse and Desalination*, 7(4), 520-528.

Abstract

The growing demand of development of appropriate and relevant wastewater treatment technology is drastically increasing in rural and urban communities in many parts of the world including South Africa. This is largely exacerbated by the escalation of water demand and decreasing potable water availability. As a result, advanced research related to the development and optimization of water treatment technologies is becoming an urgent necessity including research focusing on wastewater recycling and reclamation. Meanwhile, horizontal roughing filter (HRF) technology is one such physical water pre-treatment system that can effectively and efficiently treat wastewater and thus reduce the reliance on potable water use. Therefore, this study aimed at modelling HRF in order to investigate the option of domestic greywater reuse for delivering desired water quality for non-potable applications.

The overall aim of the study was modelling the HRF in order to improve its performance and several objectives were investigated in this study. The first one was the characterization of biological and physico-chemical strength of greywater originated from kitchen, bath and laundry sources. The second objective investigated the HRF performance/efficiency after treating various domestic greywater pollutants. The third objective investigated the controlling factors affecting the performance and optimization of the HRF during its operation. This was investigated based on design of experiments (DOE) and response surface methodology (RSM). Based on the artificial neural network (ANN), the first objective investigated the filter duration in a HRF using ANN modelling for high level of contaminants in domestic greywater. Secondly, the ANN models applicable to a HRF were investigated and used for the prediction of greywater quality variables from the output stream of the HRF based on experimental data obtained from the operation of the HRF equipment.

The first step in water treatment processes requires quality analysis in order to understand the constituent of water pollutants. Therefore, the experimental analysis of biological and physico-chemical contents in greywater sources was conducted in this study. The next aspect involved treatment of mixed domestic greywater using a three compartment HRF unit which was fixed at a low filtration rate of 0.3 m/h. The effect of operating parameters on the HRF performance was studied factorial design and optimization. The factorial design application in HRF defines

performance based on derivation of right factor settings for the effective operation of HRF. The aspect of ANN was undertaken to investigate the applicability, effectiveness and predictive ability of ANN within a HRF equipment. The use of ANN in HRF can serve as a monitoring tool in terms of performance and also as an indicator of any quality deviation that might be occurring during the filter operation.

The key findings were obtained on qualitative analysis of domestic greywater originating from a peri-urban community for the quantification of biological and physico-chemical contaminants. The significant quality difference was recorded in greywater sources and the kitchen greywater source recorded the highest load of pollutants compared to the laundry and bathing sources at $p<0.05$ significant level. Furthermore, the quality difference was evident in greywater sources in terms of daily households' social conditions, activities and practices. Also, the analysis of microbes in domestic greywater recorded high values of Escherichia coli (E. coli) and total coliform contamination which poses health related risks in domestic greywater reuse. Therefore, further treatment of domestic greywater prior to reuse remained necessary. The effectiveness of HRF was evident in removing biological and physico-chemical pollution load in domestic greywater at 0.3 m/h filtration rate. An average of 90% turbidity removal was obtained with 86% removal of conductivity and 84% of total solids and more than 50-70% removal of chemical oxygen demand (COD) within the HRF system. The E. coli and total coliforms were totally removed in the three compartment HRF. Based on DOE analysis, the significant factors identified were flowrate, gravel media, filter bed height and filter length and most significant contributing factor identified was filtration rate. Furthermore, the optimization of the HRF resulted in a high efficiency of 76% for the removal of turbidity.

Results on ANN modelling for the prediction of turbidity of the effluent stream from the HRF showed good learning abilities of the ANN and the optimal ANN structure obtained was 4-7-1 structure using the trainlm algorithm. The mean square error (MSE) value below 10% was obtained after training and the R correlation coefficient >0.9 was obtained in training, testing, validation and all data sets. For the prediction of COD, the optimal ANN architecture was 3-10-1 which was obtained with trainlm training algorithm. A satisfactory mean absolute percentage error (MAPE), low mean absolute error (MAE) and high R correlation coefficients close to 1 for the training and testing sets were also recoded for this ANN model for the prediction of COD. The other objective

was the investigation of filter duration in HRF using ANN and a 4-8-2 optimal structure was obtained with the trainlm algorithm which outperformed other training algorithms for the prediction of filter duration along with turbidity. Also, a high *R* correlation coefficient and low MSE value was obtained for this optimal ANN model for the predicted filter duration. For this model, satisfactory *R* correlation values for training, testing, validation and all data were close to 1.

Results on feedforward multi-input multi-output (MIMO) ANN showed good accuracy in predicting multioutput parameters of domestic greywater effluent from the HRF. The optimal ANN architecture obtained through a trial-and-error approach for MIMO ANN was 7-15-4. During training, different structures of ANN were investigated through varying training functions, neurons and combination of physico-chemical parameters and learning functions. For the optimal ANN model, the MSE of 0.001 was finally obtained based on the training data set. Furthermore, the *R* correlation values above 0.9 for training, testing, validation and all data sets were obtained. The optimal ANN model also showed good prediction and satisfactory accuracy when a new set of sample data was presented to the network.

Therefore, based on the objectives and findings of this study, the pollution load in domestic greywater characteristics can contain a number of pollutants and can significantly vary with greywater sources. It is also important to note that the HRF significantly showed effectiveness in treating physical pollutants and large amounts of chemical and biological pollutants. From the findings and based on the HRF, it was also noted that the chemical pollutants can be significantly removed using a combination of physical and chemical treatment processes in order to remove more pollutants. This was observed by a high removal of physical pollutants such as turbidity, conductivity and solids while domestic greywater biodegradability ratio was lower than 0.5. Furthermore, for the DOE/RSM techniques, it was also observed that the effective filter performance of the HRF is a function of multi-design parameters such as filtration rate, filter length, gravel media and bed height and multi factor optimization was useful in this research work. Finally, the ANN showed effective characteristics and accuracy in the HRF equipment for the prediction of multi-output variables of the effluent greywater from the HRF following mixed domestic greywater pre-treatment.

Definitions of keywords

Activation functions - is a mathematical equation responsible for the learning of the network by transform/set the relationship between inputs to the corresponding outputs (Wang et al., 2020).

Artificial neural network - is a computational and mathematical technique which was motivated and inspired by the studies of brain / nervous systems in biological organisms (Qiao et al., 2018).

Biological oxygen demand - measures the amount of oxygen used by microorganisms to degrade organic matter present under aerobic settings (Morel and Diener, 2006).

Chemical oxygen demand - is described as the quantity of oxygen required to oxidize the organic content in the greywater (Morel and Diener, 2006).

Electrical conductivity - is the indicator of the dissolved soluble salts often present in the greywater (Rakesh et al., 2020; Morel and Diener, 2006).

Epoch-the number of training data cases processed (Shallue et al., 2019).

Error function - is the function that describes the deviation between the predicted and observed outcomes which is minimized during artificial neural network training (Durstewitz et al., 2019).

Greywater - refers to the wastewater generated from household washing activities such as bathing, laundry and dish washing; the definition excludes toilet water source (Ludwig, 2006; Jefferson et al., 2004).

Learning rate - is the parameter that is responsible for scaling and controlling the magnitude of weight changes (Ojha et al., 2017).

MATLAB Neural Network Toolbox - is a simulation software programme that is used to train and evaluate a suitable neural network.

Neural network architecture - is the number of layers, nodes and connections in a particular network (Wagarachchi and Karunananda, 2017).

Roughing filter (RF) - is a physical water pre-treatment technology that removes pollutants in water based on transportation mechanism, mainly sedimentation (Wegelin, 1996).

Training algorithm - is a mathematical procedure that adjust the weights and bias of the network in searching of the optimal artificial neural network by minimizing the error between the target and network output (Talaee, 2014).

Turbidity - Turbidity is the measure of the transparency of water and microorganisms present in water (De Roos, 2017).

Table of contents

List of figures

List of tables

List of abbreviations

Adj-R^2	Adjusted R-squared
AGS	Aerobic granular sludge
ANFIS	Adaptive neuro-fuzzy inference system
ANM	Artificial neuron model
ANN	Artificial neural network
ANOVA	Analysis of variance
BOD	Biological oxygen demand
BPNN	Back propagation neural network
BWW	Brewery wastewater
CCD	Central composite design
Chl-a	Chlorophyll-a
cm	Centimeter
CNN	Convolutional neural network
CNW	Cellulose nanowhisker
COD	Chemical oxygen demand
DNN	Deep neural network
DO	Dissolved oxygen
DOE	Design of experiments
E	Error
E. coli	Escherichia coli (E. coli)
EC	Electrical conductivity
ELU	Exponential linear unit
EPA	Environmental protection agency
FA	Factor analysis
FC	Faecal coliform

FFANN	Feedforward artificial neural network
GD	Gradient descent
GDP	Gross domestic product
HMs	Hybrid models
hr	Hour
HRF	Horizontal roughing filter
HRT	Hydraulic retention time
l	Litre
m	Miter
MAE	Mean absolute error
MANOVA	Multivariate analysis of variance
MAPE	Mean absolute percentage error
MIMO	Multi-input multi-output
min	Minute
MISO	Multi-input single-output
MLP	Multilayer perceptron
MLP ANN	Multilayer perceptron artificial neural network
MLR	Multiple linear regression
mm	Millimeter
MSE	Mean square error
NN	Neural network
NTU	Nephelometric turbidity units
NWQS	National water quality standards
PCA	Principal component analysis
PCR	Principal component regression
PLS	Partial least squares
Pred-R^2	Predicted R-squared
PRELU	Parametric rectified linear unit

p-value	Probability value
R^2	Coefficient of determination
RBFNN	Redial basis function neural network
R-correlation	Correlation coefficient
RELU	Rectifier linear unit
RMS	Root mean square
RNN	Recurrent neural network
RO	Reverse osmosis
RSM	Response surface methodology
SD	Disk depth
SIMCAT	Simulated catchment model
SISO	Single-input single-output
SLP	Single layer perceptron
SPSS	Statistical package for the social sciences
SS	Suspended solids
SWAT	Soil water assessment tool
TDS	Total dissolved solids
TKN	Total kjeldahl nitrogen
TN	Total nitrogen
TNIA	Tancredo Neves international airport
TOC	Total organic carbon
TP	Total phosphorus
TS	Total solids
TSS	Total suspended solids
UK	United Kingdom
USA	United States of America
USDA	United States department of agriculture

USEPA	United States environmental protection agency
WASP	Water quality analysis simulation program
WQI	Water quality index
WTP	Waste treatment plant
WWTP	Wastewater treatment plant

Chapter 1

Introduction

1.0 Background

Access to potable water remains a necessity to preserve, support and sustain life in many parts of the world today, particularly in developing countries. However, the water challenges such as water availability - a lack and access to fresh water, escalating levels of water drought, potable water demand, lacking recycling and reuse strategies are becoming the biggest challenges facing the world's population (Singh, 2017; Voulvoulis, 2018). Such challenges are now becoming more evident in most parts of the world especially in undeveloped and poorest countries (Misra, 2014). Therefore, there is a growing need for viable and operational wastewater treatment techniques and alternative solutions in order to achieve minimization of water scarcity and better reuse of wastewater.

With insufficient potable water supply and limited water reuse technology of domestic wastewater in South Africa, filtration technology can be useful in the context of social and economic benefits. Filtration remains one of the simplest water treatment technology for removing contaminants in surface water through the reduction of solid mass pollutants in water (Wegelin, 1996; Bakare et al., 2017, Nkwonta et al., 2010). In water treatment, filtration remains one of the oldest, simplest, useful technique for removing contaminants in surface water. In practice, there are various filtration units that are applicable in water treatment. The most common include slow sand filtration and roughing filtration based on the design and operational procedure and the application in water treatment (Ives and Sholji, 1965; Wegelin, 1996).

In South Africa, the escalating water drought levels are being observed in most parts of the country with most provinces recently declared drought disaster areas (Enqvist and Ziervogel, 2019; Oteng-Peprah et al., 2018; Hanjra and Qureshi, 2010; WWF-SA, 2016). To this end, wastewater reuse and treatment technologies including water modelling techniques are advancing and becoming preferred methods in response to water challenges in many countries (Bailey et al., 2020; Sarkhosh et al., 2016). In water treatment, the roughing filters are used for pre-treatment purposes prior to sand filtration (Jayalath and Padmasiri, 1996; Jayalath, 1994). During operation, the

removal efficiency in roughing filters is strongly related on filter design, particulate, and water quality parameters (Boller, 1993; Wegelin, 1986). Therefore, roughing filters are an alternative for wastewater pre-treatment prior to reuse or recycling. The advantage of roughing filtration is its ability to remove high percentage of physical pollutants and microbes in water including the advantage to remove solid mass in a cost effective manner (Wegelin, 1996).

1.1 Research justification

In South Africa, the worst water drought was experienced in 1983 with the national average dam level reaching 34% while the water stress is projected to increase by 2030 to about 32% due to industrial and population growth. At the same time, the focus in wastewater technology and reuse is becoming an urgent matter as water scarcity and water drought levels are being observed and remains a recurrent crisis in most parts of the nine provinces of South Africa since the year 2014 to date (WWF-SA, 2016; Masih et al., 2014; Orimoloye et al., 2019). A lack of freshwater supply including water reuse and recycling scheme challenges is the overall demonstration of the level and depth of water challenges. Domestic greywater has a great potential for reuse due to its availability and various existing technologies can be very useful if water quality measures are well monitored using water treatment quality modelling techniques. At the same time, many researchers, scientists and government organizations have all undertaken the challenge and currently make great efforts to come up with feasible alternatives to minimize potable water challenges and demands. This includes water quality modeling techniques applicable in water treatment systems.

This research intended to explore the possibility to optimize the performance of the HRF using existing modelling techniques. This included modelling the HRF based on empirical and current modelling techniques in order to predict greywater effluent quality from the HRF. Secondly, the possibility to effectively and efficiently use a horizontal roughing filter that utilizes locally available filter media for the prediction of filter efficiency using neural network.

1.1.1 Research contributions

Research on domestic wastewater reuse schemes including treatment options continues to grow in South Africa, thus, it is anticipated that this work will add valuable contribution as the building

block for future work on domestic wastewater management. In this research, the main contributions are the following:

- Gaining the insight and exploration of the quality of domestic greywater originating from a disadvantaged community and its potential for reuse based on its quality following the application of HRF equipment.
- Give insight on considerations of design and optimization techniques for the roughing filtration equipment, particularly the HRF equipment based on empirical and ANN modelling techniques for the estimation/monitoring of filter performance.

1.2 Aims and objectives

This research intends to optimize HRF equipment in order to improve its water treatment performance by using selected and applicable modelling techniques. Research questions were:

- Is it possible to optimize the performance of a horizontal roughing filter using existing modelling techniques?
- Is it possible to effectively and efficiently use a horizontal roughing filter that utilizes locally available filter media and predict filter efficiency using neural networks?

In order to achieve the central aims of this research study, the following objectives were considered:

- To characterize domestic greywater for qualitative assessment of various contaminants such as physical, biological and chemical contaminants which are often present in domestic greywater.
- To investigate and quantify design variables that affect the performance/efficiency of a HRF equipment using RSM.
- To optimize the HRF performance using RSM based on the design variables of a HRF equipment.
- To study and estimate filter duration of a HRF based on domestic greywater with high pollution load and to develop the ANN model for the prediction of filter duration.
- To predict various pollutants of domestic greywater from the HRF equipment using ANN technique following domestic greywater treatment in a HRF.

1.3 Thesis outline

The thesis is structured as follows:

Chapter 1 discusses the background of the study on water challenges and its significance on potable water requirement including the significance of domestic greywater characteristics and implications on qualitative assessment within the HRF equipment. **Chapter 2** discusses existing literature related to greywater quality, roughing filtration and available roughing filter models and studies on design of experiments, principles and algorithms related to water treatment. **Chapter 2** also covers aspects related to neural network algorithms and its potential application in modelling roughing filters. **Chapter 3** focuses on the methodological approaches followed in this study. The chapter presents aspects related to the mathematical approach used to gain an understanding of the operational aspect of the roughing filter and the methodological approach on the development of ANN models for the prediction of various pollutants of domestic greywater effluent from the HRF equipment. **Chapters 4-6** outlines findings of this research, the detailed discussion of all findings related to domestic greywater characteristics and HRF performance including the findings on empirical and ANN modelling of the HRF system. **Chapter 7** presents conclusions and recommendations of the thesis through addressing the study objectives, the implications of findings and significance of this research work. The structure of thesis with its main parts is presented in the next Figure 1-1.

The structure of thesis for the modelling of HRF performance with its main components is presented below having research background, previous and current research studies, research approach techniques, research findings including conclusion and recommendations that are formally organized as shown:

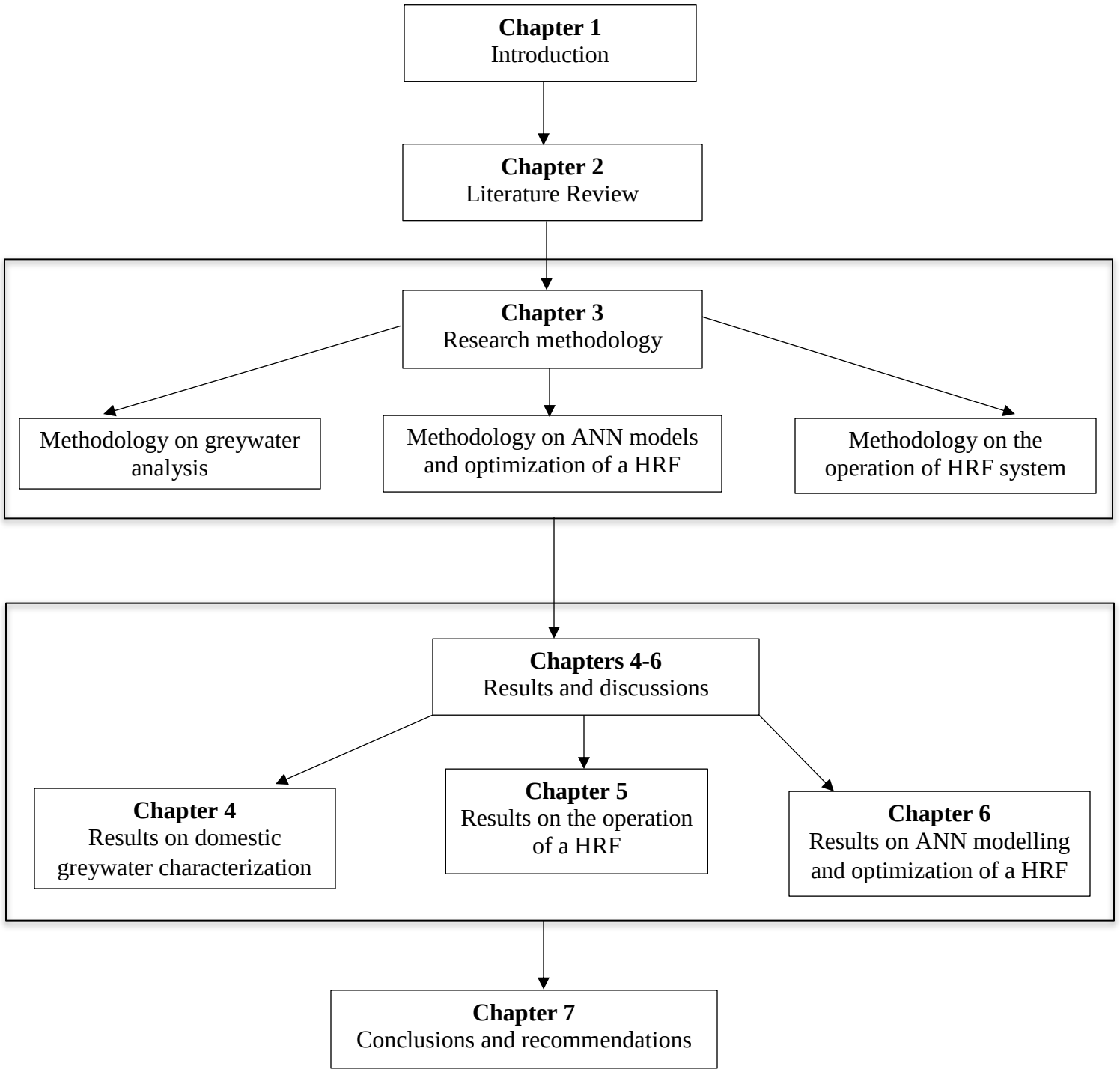

Figure 1-1: The structure of thesis with its main components

Chapter 2

Literature review

2.0 Background

This chapter discusses existing literature related to greywater characteristics and quality and its potential reuse option for non-potable application purposes. The chapter also focuses on roughing filtration and operational aspects of the roughing filtration and available literature on roughing filters including studies on design of experiments, principles and algorithms related to water treatment. Furthermore, it also covers aspects related to various water quality models and neural network algorithms and its potential application in modelling roughing filters while focusing on neural network algorithms and their application for developing roughing filter models. The literature review also deals with the water quality models by giving background about various modelling techniques, to identify knowledge gaps in the field related to the present study conducted for modelling HRF equipment.

2.1 Greywater characteristics

Greywater is becoming one of the dominant factors in wastewater management and resources and it accounts for approximately 60 - 70% of the total domestic wastewater by volume in larger parts of the developed countries (Finley et al., 2009; Friedler, 2004). Non-sewered areas seem to account for almost all water as greywater with the exception of only that used for potable purposes according to Carden et al. (2006). In many countries including South Africa, there is still a minimum or even a lack of formal greywater infrastructures and greywater is simply disposed of onto the ground or as runoffs by inhabitants/households due to a lack of these established and existing infrastructures to handle and recycle greywater for reuse purposes (Oh et al., 2018; Muanda, 2009, Carden et al., 2006; Mashabela, 2015; Allen et al., 2010).

The variation in greywater quality and its chemistry due to pollution and nature of contaminants often requires the development of scientific data monitoring techniques for the assessment of greywater quality (Wurochekke et al., 2016; Boano et al., 2020; Ghawi, 2019). As a result, the biological and physico-chemical pollutants are amongst the major and essential contaminants in greywater that are often used to assess the quality of greywater (Oteng-Peprah et al., 2018;

Edokpayi et al., 2017). In greywater, the composition varies mainly as a function of greywater application, greywater source, detergents and the nutrients level dissolved in greywater (Hernández-Leal et al., 2007; Eriksson et al., 2007). To better understand greywater quality, the application of cluster analysis (CA), factor analysis (FA) and principal component analysis (PCA) are often used for comprehensive and complex data matrix analysis and interpretations (Boyacioglu et al., 2005).

Factor analysis is a statistical tool used to study correlations in multi-variables in raw data and to relate underlying variables known as common factors. In many areas of research, factor analysis has been used for surface water analysis and ground water quality assessment including environmental research (Praus, 2005). A study by Shihab (1993) used principal component analysis to investigate water quality in Saddam dam reservoir and in his findings it was discovered that 90 percent of variation in water quality was attributed to three parameters which were algae, electrical conductivity (EC) and total solids (TS). Boyacioglu et al. (2005) applied factor analysis in assessment of surface water quality in western Turkey; two underlying factors in 19 stations/sites monitored for a total number of 45 water parameters were identified. Factor 1 explained 63% of the total variance and factor 2 explained 21% of the total variance. Factor 1 had strong positive loadings on electrical conductivity, sulfate, sodium and total Kjeldahl nitrogen (TKN). Factor 2 had strong positive loadings on biochemical oxygen demand (COD), biological oxygen demand (BOD) and total coliforms. The two factors indicated inorganic contamination-factor 1 and organic contamination-factor 2.

The wastewater recycling, reclamation or reuse can become a viable option in minimization of water challenges (Chen et al., 2012). The recycled wastewater is mostly and often used for different purposes and activities. These activities largely include irrigation, toilet flushing and industrial cooling purposes including a number of other possible applications (Karpiscak et al., 1990). For example, greywater has a great potential for reuse due to its unlimited abundance and its availability contributes up to 70% of the total domestic wastewater (Li et al., 2009). Except the exclusion of toilet wastewater, greywater is generally less polluted and often contains low levels of pollutants than the combined household wastewater (Almeida et al., 1999). Therefore, greywater can highly support and substitute potable water activities (NSW, 2008).

In terms of quality, greywater may contain a number of contaminants such as oils, grease, fats, hair, soaps, cleansers, and lint and fabric softeners including other chemical pollutants (Mangio et al., 2017). Greywater may also contain high levels of chemicals such as sodium, borax, chlorides and sulfates. As a result, a general care and standard guidelines must be followed in greywater use due to its high pH levels that may have harmful effects to some plants and even washing activities (Ludwig, 2006). Therefore, reclaimed wastewater may be beneficial largely in agriculture. Also, landscape irrigation, toilet flushing, industrial processes and replenishment of groundwater basin (Jhansi and Mishra, 2013).

2.2 Water treatment technologies

Currently, there are various wastewater treatment technologies that have been developed that are very useful for reuse purposes. These technologies can be applied for recycled or reclaimed wastewater in order to ensure sufficient quality to satisfy most of the non-potable demand standards (Tortajada and Nambiar, 2019; Asanoa, 2006). In water treatment, the various forms of water treatment processes mainly include chemical, physical and biological treatment (Oteng-Peprah et al., 2018; Hernández-Leal et al., 2007; Laaffat et al., 2019). For instance, the physical systems include sand filters and membranes and have good efficiency with minimum maintenance costs (Pidou et al., 2007). Whereas, the chemical processes for greywater largely involve photo-catalytic oxidation, ion exchange, coagulation and granular activated carbon (Li et al., 2009). Again, some of the biological water treatment systems include membrane bioreactors, cyclic activated sludge systems, conventional activated sludge processes, and integrated fixed film activated sludge (Al-Jayyousi, 2003).

2.3 Roughing filtration

The roughing filtration is more advantageous due to its ability to remove a wide range of physical and chemical pollutants contained in water and the reduction of the solid mass and turbidity removals ranging from 60 to 90% (Wegelin, 1996; Bakare et al., 2019). For instance, the roughing filters are characterized by gravel media in range larger than 2 mm (Boyacioglu et al., 2005). Also, the normal range of gravel media fractions in three compartment horizontal roughing filters range from 25 mm down to 4 mm from the filter inlet-outlet water flow direction. In addition, these filters include down flow, up-flow and horizontal roughing filters (Wegelin, 1996; Wegelin, 1986; Zeng et al., 2020). A typical form of roughing filter normally consists of a series of graded gravel

beds arranged in compartments. The first bed normally consists of the coarsest gravel fractions and the finest gravel media fractions are in the last compartment with reference to the direction of water flow (Patil et al., 2012). In the early 1800s, Baker (1948) reported the application of coarse gravel filtration for water treatment and thereafter in Scotland for water pre-treatment. Therefore, the roughing filters can significantly reduce high amounts of solids in water prior to the sand filtration (Jayalath and Padmasiri, 1996).

2.4 Design variables in roughing filtration technology

The gravel media fractions, filtration rate, filter bed depth and filter length are the main parameters that affect solid removal efficiency, especially the suspended solids (SS) in roughing filters (Cleary, 2005). The filter removal efficiency is also strongly a function of the amount of particulates, filter design and water quality parameters, the various types and concentration of organics and suspended matter (Boller, 1993; Wegelin, 1986). In terms of design, the normal filtration rate in horizontal roughing filters is in range of 0.3-1m/h (Nkwonta, 2010; Aulenbach, 1993). Furthermore, the HRF mainly has extended bed lengths than up-flow and down-flow filters and has maximum solid capacity for the removal of solids. This results in minimized cleaning frequencies at the expense of bigger space requirement. After all, roughing filtration performs significantly well in removing physical and chemical contaminants in water using different graded gravel media fractions (Clarke et al., 1996).

Lebcir (1992) conducted a study to identify some of the controlling factors on a laboratory scale HRF. Based on this study, filtration rate proved to be significant in filter performance. Other studies in roughing filtration suggest that the Reynolds number should be maintained below a value of 10. This will result in laminar flow conditions which will in turn favor high removals within the roughing filters. Furthermore, the effect of low filtration rate on filtration performance with minimal Reynolds Number were confirmed by Ives and Sholji (1965), that is, low filtration rates significantly improve filter efficiency. Using HRF, Mukhopadhay (2009), investigated neural network and empirical modelling methods in order to estimate the performance of the HRF using local pond water which had a concentration of SS in range from 40 to 150 mg/l. In this study, the neural network model showed better prediction accuracy than empirical modelling techniques.

In water treatment, roughing filters have been widely applied especially in developing counties and remains essential in wastewater treatment (Oteng-Peprah et al., 2018; Tepong-Tsindé et al., 2015; Mtsweni et al., 2019). Firstly, the advantage of roughing filters is essentially related to their ability to improve water quality by removing physical, chemical and biological pollutants in wastewater (Affam and Adlan, 2013; Cleary, 2005). This includes good efficiency to remove pathogens/microorganisms with minimal operational and maintenance costs (Wegelin, 1996). For instance, the HRFs can significantly handle high turbid raw water and achieve good removals due to their good design, extended filter lengths and high silt storage capacity (Maung, 2006). The physical treatment processes in water mainly include coarse gravel, sand and membrane filtration and chemical treatment processes include ion exchange, granular activated carbon, coagulation and photo-catalytic oxidation (Tansel, 2008; Zhang et al., 2015).

The removal ability in roughing filters depends largely upon water characteristics, the type of contaminants (organics and inorganics), suspended matter, viscosity and social and geographic conditions (Clarke et al., 1996). For instance, the composition in greywater strongly correlates with the source and nutrients dissolved in greywater (Wegelin 1986; Eriksson et al., 2007). Many studies on greywater revealed that laundry and kitchen greywater have higher physical and organic pollutants than mixed and bathroom greywater (Li et al., 2009). Compared to general wastewater, the greywater from laundry and bath generally contains high levels of dissolved solids, high turbidity, low nutrients and pathogens (Al-Jayyousi, 2003). Although, the application of roughing filters can effectively remove the suspended matter, fine particles, turbidity and colloidal matter including non-settleables and microorganisms, the reduction of surfactants, nutrients and organics may further require an application of chemical processes (Li et al., 2009). Contrary, physical treatment processes can provide limited removal efficiencies for chemical parameters in greywater but are highly recommended for the removals of physical parameters in greywater (Pidou et al., 2007; Ghrair et al., 2014). Specifically, they can provide significant high removals of turbidity, SS and microorganisms (Ramon et al., 2004). In essence, the physical processes can be applied for bathing and laundry greywater treatment while the kitchen source will require further treatment processes due to the presence of high levels of the surfactants, nutrients and organics (Li et al., 2009).

The influent solids concentration strongly affect the filter efficiency where removal ability will be greater with high influent concentrations. According to 1/3 and 2/3 filter theory, each layer removes one-third of the particles while letting two-thirds to the next layer. In addition, the filtration process continues at each layer and more particles are removed in the first layer due to higher concentration of particles in the first layer (Wegelin, 1996). For instance, the removal of turbidity can range between 60-90% and high removal of coliforms without any chemical addition. Therefore, the higher the turbidity of the initial influent water, the higher the removal that can be achieved (Wegelin, 1996). As a result, the pore sizes of the filtration media will progressively be reduced with the continuation of particle deposition process (Ahsan, 1995). Therefore, the understanding and knowledge of the solids characteristics in suspension is an important step particularly for the prediction of removal efficiency of the particles in roughing filters (Lin et al., 2006).

During water treatment, the monitoring of water quality, especially greywater, remains critical particularly in minimization of public health risk, household water stress and negative impact on the environment (Yerel, 2010; Ayeni et al., 2011). Therefore, water quality assessment is often assessed by measuring the presence of the level of biological, chemical and physical pollution loads in water (Hamzah et al., 2016). For example, water quality index (WQI) is one of the existing water quality techniques dating back to the past decades and according to Zin et al. (2017), many studies often applied WQI in river water, streams, and sites and in various water quality related monitoring systems. The basis of this water quality technique is water parameters such as total suspended solids (TSS), electrical conductivity (EC), biological oxygen demand (BOD), pH, total dissolved solids (TDS), total coliforms and all other existing measurable water parameters (Tavakol et al., 2017).

2.5 Water modelling techniques

2.5.1 Data driven models

Multivariate statistical analysis is one other common approach largely used in water quality data analysis. In water quality modelling, many researchers recommend multivariate statistical techniques because of its ability to analyze the relationship amongst variables using the multivariate approach including its power to summarize the correlation in variables of the large data by using relatively few variables (Mazlum et al., 1999; Yerel, 2010). Additionally, they are

also useful in identification of components or underlying dimensions and the level of variance within the data. In terms of use, the common applications of multivariate statistical techniques for the analysis of water quality include PCA, FA, DA and multivariate analysis of variance (MANOVA) (Gajbhiye et al., 2015; Tavakol et al., 2017; Nathan et al., 2017). For example, a study using cluster CA and PCA was conducted by Couto et al. (2013) in Brazil, Tancredo Neves International Airport (TNIA) using greywater effluent from the airport. In this study, greywater effluent was successfully assessed including its reuse potential.

The multivariate statistical methods on water parameters are also useful in understanding the underlying information including the impact of significant factors in water treatment (Boyacioglu, et al., 2005). These include multiple linear regression (MLR), PCA and partial least squares (PLS) analysis. In the past years, multivariate regression methods including FA techniques have been widely applied in the analysis of water treatment and water quality monitoring, for instance, Mazlum et al. (1999) investigated water quality in Porsuk Tributary-Sakarya river and a number of factors such as nitrification, domestic and industrial waste discharge and seasonal effects were identified as source of water quality variations based on PCA. Also, Ieong et al. (2015) studied the comparison of principal component regression (PCR), hybrid models (HMs) and ANN for the application in the prediction of phytoplankton abundance which was studied in Macau storage reservoir. Based on the findings of this study, the ANN outperformed PCR and HMs. In India, Iyer et al. (2003) worked on a statistical model using PCA in Cochin coast and identified a relationship of physical and chemical variables in coastal water. Wuttichaikitcharoen and Babel (2014) also used PCA in a river basin in Thailand to study the suspended sediment yield content. The predictors of sediment yield that were identified included rainfall distribution, channeling network, basin size and steepness, and land use.

The traditional modelling involving varying one factor at a time/one-variable-at-a-time to achieve optimal conditions has been extensively used over the years (Bowden et al., 2019; Murray et al., 2016). However, this modelling procedure fails to capture and resolve the underlying relationship between multi-variables because of the complexity and influence of these factors to the dependent variables. This modelling approach is further described as laborious, time consuming and expensive because of the requirement of a high number of experimental runs (Dejaegher and Heyden, 2011). To overcome this challenge, DOEs and RSMs are normally used because of their

effectiveness in studying the effect of multi-variables on dependent factors using minimum number of experimental runs (Murray et al., 2016; Tye, 2004). The RSM is, therefore, a good mathematical modelling technique to build regression models while assessing/evaluating the effects of multiple variables which allows optimization conditions for obtaining desirable responses (Ryad et al., 2010).

Recently, Murdani et al. (2018) investigated electrocoagulation performance using RSM with Box-Behnken design in hospital wastewater through the electrocoagulation process. This was used in order to ensure that water meets effluent standards before it was discharged. In this work, the contact time, voltage and electrolytes concentration were used as independent parameters and COD removal efficiency as the response variable. In the findings, a satisfactory quadratic model was reported with 69.51% COD reduction and 18.36% minimum COD reduction with an R^2 value of 0.9945. In Morocco, Karboubi et al. (2014) investigated the influence of water temperature, pH and conductivity as indicators of pollution-COD and TSS using RSM-CCD for wastewater from the treatment plant of the city of Settat. The study investigated the influence of independent variables on the effectiveness of the treatment process. It was found that the performance of the station was efficient and was able to reduce COD and TSS by 80% and 83%, respectively.

Ghanim (2014) applied RSM to optimize pollutants removal from textile wastewater using electrocoagulation. A RSM with CCD was used in this study for the investigation of the effect of operation time and current density on COD, TSS and turbidity as response variables which was carried out under an ambient temperature of 25 °C and pH of 4.52. The optimum time and current density for COD were found to be 56.54 min and 20 mA/cm^2, respectively. For TSS, the operation time and current density were 53.13 min and 20 mA/cm^2, respectively and 54.74 min and 20 mA/cm^2 for turbidity. The RSM thus showed that the operation time and current density had significant effects on the removal of pollutants by electrocoagulation.

Luo et al. (2019) used RSM for zero valent iron powder and pH and reaction time dosage of zero valent iron powder as input variables. The maximum removal efficiency of 99.66% was obtained which occurred from 2772.23 µg/l uranium content with 0.6 g dose of zero valent iron powder and reaction time of 52.5 min with a pH of 5. Subsequently, the removal efficiency of uranium obtained under an optimized condition was 98.79%. Mohamed et al. (2019) applied RSM in a vertical

multilayer ceramic filter system for laundry greywater treatment to investigate or evaluate efficiency of this treatment system and to identify the physical and chemical characteristics of greywater. The treatment system was optimized based on different hydraulic retention times (HRT) and sample volumes. Results showed that both HRT and sample volumes were significant factors for the treatment system. The optimal values for COD, phosphate and sodium reduction were obtained at 2 hours HRT with 2 litre sample volumes. The study also showed the effectiveness of a ceramic filter system in removing pollutants in the laundry greywater.

A study conducted by Manhokwe et al. (2019) investigated the effect of temperature and cultured bacteria on the performance of a biological wastewater treatment system from a yeast producing plant in Zimbabwe. The CCD was used in this study for experimental design and RSM for optimization. The findings of the study showed that biological treatment was an effective process for removing organic load and color effect in wastewater under optimized conditions. The dependent variables were COD removal and color reduction and 13 experiments were conducted using temperature and bacteria concentration as independent variables. In terms of findings, a COD removal efficiency of 26% was obtained and 44% decolourization efficiency was recorded for wastewater treatment under optimized conditions. The maximum COD reduction was obtained at 25°C and 16.37 g/L of bacterial culture with a desirability value of 0.634.

Mhaske et al. (2014) conducted a study on phytorid sewage treatment plant in India for the removal of turbidity in sewage water. The Box-Behnken design was used for experimental design and RSM to determine optimum conditions. The study used three 2 level factors which were dilution, hydraulic loading and spatial length. The optimization of turbidity using RSM was evident in this study for the efficient removal of turbidity in sewage water. Ibrahim et al. (2017) also used Box-Behnken design and RSM for the optimization of a sequencing batch reactor for the aerobic granular sludge (AGS) using domestic wastewater. The two-level factor setting of independent factors were temperature and time (days) and response variables were COD and phosphorus removal. In this research study, the simulation results showed that the RSM can be useful to predict aerobic granular sludge parameters well under optimum conditions.

Taheriyoun et al. (2020) studied industrial wastewater treatment of Mobarekeh steel complex in Iran using RSM. The study was intended to optimize coagulation - flocculation processes for COD

removal of galvanized wastewater treatment plant. The input variables were pH, input turbidity and concentrations of coagulant aid which were studied in five levels. The RSM was found effective in modelling and optimizing of the coagulation-flocculation processes for the COD removal. Based on the findings of the RSM, the optimum coagulant-ferric chloride obtained was 350 mg/l, 0.14 mg/l for the coagulant aid - polyelectrolyte, pH of 11 and 79 Nephelometric Turbidity Units (NTU) for input turbidity.

ANN overview

Artificial neural network is a computational mathematical modelling technique that consists of a number of processing elements that receive and map input information and deliver outputs based on their defined algorithms and activation functions (Sildir et al., 2020). The structure of ANNs simulate neural networks in animals and human beings which contains nearly 100 billion neurons that are interconnected by thousands synapses to each other (Martins et al., 2019). Using learning algorithms, the interconnected nodes can have the ability to solve problems just like a human brain, recognize the hidden patterns and correlations in the given raw data and can even cluster and classify it over some time through the learning process (Maren et al., 1990). The ANN is also a powerful tool suitable to model complex problems in real-life applications to the extent of modelling complex and non-linear problems that cannot be easily modelled using simple defined empirical modelling (Rath et al., 2017; Pasini, 2015). In modelling, the ANNs can also make good generalization and reveal hidden relationships in the input data including being able to make pattern recognition and powerful predictions (Hinton, 1992; Puskarczyk, 2019).

In 1943, the artificial neuron model (ANM) was firstly introduced by Warren McCulloch and Walter Pits prior to the existence of commercial computers (Husbands and Holland, 2012). McCulloch and Pitts began exploring how the small networks of artificial neurons could possibly mimic brain-like processes and this was through modelling a simple neural network using electrical circuits. In 1949, Donald Hebb further reinforced the idea of neurons through his work - the Organisation of Behaviour which pointed out the concept that neural pathways are strengthened each time they are used (Markram et al., 2011; Langille and Brown, 2018; Unar, 1999). Further explorations led by Nathanial Rochester from IBM research laboratories resulted to the first effort to simulate neural networks in the 1950s and this brought significant advancement in the computers and neural research (Yin, 2018).

Further work in 1956 by Dartmouth's summer research project brought significant improvement of artificial intelligence and neural networks (McCarthy et al., 1955; Aish et al., 2015). These positive developments also improved applied intelligence while additional contributions by John Von Neumann in later years suggested imitating simple neuron functions through the use of telegraph relays or vacuum tubes. In the late 1950s, Frank Rosenblatt worked on the perceptron of an electronic device which was constructed in line with biological principles and the perceptron algorithm was invented in 1958 (Seising, 2018; Wang and Raj, 2017; Macukow, 2016). Following neural network developments and contributions by many researchers or organizational structures over the years, the single layer artificial neural network for the application in real world problems was developed by Bernard Widrow and Marcian Hoff and since then ANNs have gained significant interest (Baykal and Yildirim, 2013). This includes advancements and wide application of ANNs in numerous fields of research including various engineering fields (Abiodun et al., 2019). ANNs are characterized by large degrees of freedom and therefore can be able to model non-linear problems that are commonly found in real processes (Sun, 2005).

2.5.1.1 Single layer perceptron (SLP)

A SLP is one of the simplest basic and initial form of feedforward neural network that was developed. Figure 2-1 shows the SLP structure and components with feedforward mechanism. In terms of structure, the SLP has a single layer of weighted connection which is in between the inputs and outputs. Also, the SLP ANN is only limited and capable to learn linear problems through application of perceptron learning rule (PLR) or delta rule (Ebhota et al., 2018; Silva et al., 2018). As shown in Figure 2-1, the perceptron algorithm includes the summation of the weighted input values and bias which is followed by the application of a specific activation function and generation of the output, ***y***.

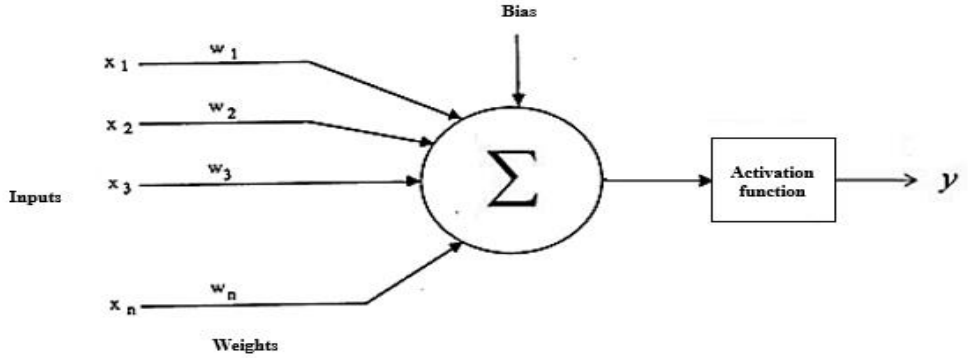

Figure 2-1: The single layer perceptron structure

The perceptron in Figure 2-1 consists of:

- a neuron and
- a transfer function

The training process in a perceptron requires calibration of weights which are assigned random values during the beginning of training processes. In Figure 2-1,the inputs multiply the X_i values with weights W_i and the weighted inputs are:

$$\sum = WX = w_1x_1 + w_2x_2 + w_3x_3 + \ldots + w_nx_n \quad (2.1)$$

The output signal from the summing function, $Z = b + \sum_{i=1}^{n} w_i x_i$ (2.2)

Where

- X represents input to the neuron
- W represents weight
- n represents the number of inputs
- b represents a bias term
- i represents an interger from 1 up to n

The output with activation function following summing function:

$$y = f(b + \sum_{i=1}^{n} w_i x_i) \quad (2.3)$$

The learning process of the perceptron is through the algorithm which calibrates the weights based on the error function. The error (E) is the difference between the desired output-O_d and the actual output, O_a will be generated and the error equation is mathematically given by:

$$E = O_d - O_a \quad (2.4)$$

The ANNs are also useful and capable to model even more complex relationships in data. Unlike ANNs, most of the existing empirical models require theoretical assumptions and guesses in relation to underlying laws or functions governing the system from which raw data was produced (Zhang et al., 1998). Contrary, the ANN often performs a learning process from a series of input-

output data sets based on training data sets presented to the network which often has unknown a-priori mathematical assumptions or trends. Furthermore, it maps subtle functional trends among the training data irrespective of the degree of complexity in data, for instance when dealing with hard to describe data (Zhang et al., 1998).

2.5.1.2 Feedforward artificial neural network (FFANN) structure

Figure 2-2 shows the common ANN design structure and three forms of layers, namely input, hidden and output layers. Based on Figure 2-2, the ANN is composed of multiple layers and these layers are central and useful for the learning process of the network. Each ANN layer consists of interconnected processing elements known as neurons which form a structure of processing information within the ANN. As shown in Figure 2-2, the ANN neurons or nodes are connected by synapses and each neuron receives a number of connections with other neurons and this constantly receives input signals. During this time, the strength of their connection to one another is assigned a certain value in proportion to their strength of connection which could be minimum or maximum (Turkson et al., 2016).

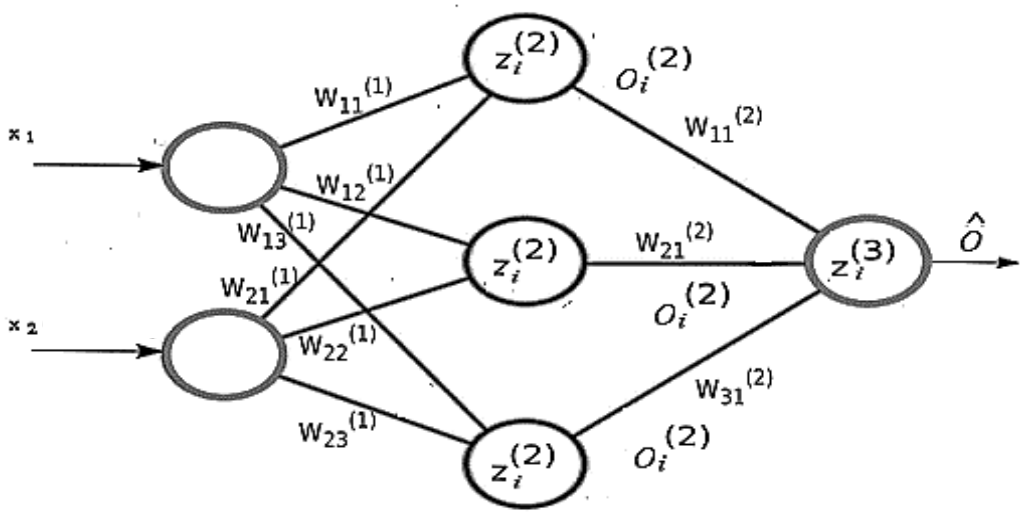

Figure 2-2: FFANN design architecture

Based on Figure 2-3, the ANN can have multiple hidden layers to ensure that the network successfully handles any degree of complexity in the input data (Turkson et al., 2016). In the ANN, the input data is stored in the input layer. The output layer is responsible for the prediction of the output in ANN while the hidden layer(s) ensures that ANN is able to obtain an optimum solution

even for complex structures in the data. The input layer/nodes take in information in meaningful form which can be expressed numerically and the information is expressed and presented as activation values where each node is assigned a number which could be either low or high. If the threshold value is higher, the greater will be the activation and this is passed throughout the network (Turkson et al., 2016).

As for training, each node makes its computation based upon the weighted sum of its inputs and the activation values are presented from node to node based on the transfer functions and weight values which could be high or low. The new calculated ANN values then becomes the new inputs that feed the next ANN layer. The process continues throughout until the final output is obtained. The iteration will proceed and a signal will be constantly received in case the summation of signals exceeds a certain threshold (Alom et al., 2019). In Figure 2-3, the ANN can have different architecture or structure, however, it is generally classified into two types of basic structures, the feedforward and feedback structure (Zhang, 2000). The feedforward structure of the ANN takes the form in Figure 2-3 and it contains the input, hidden and output layers and the signals of the network can only flow/travel in one direction.

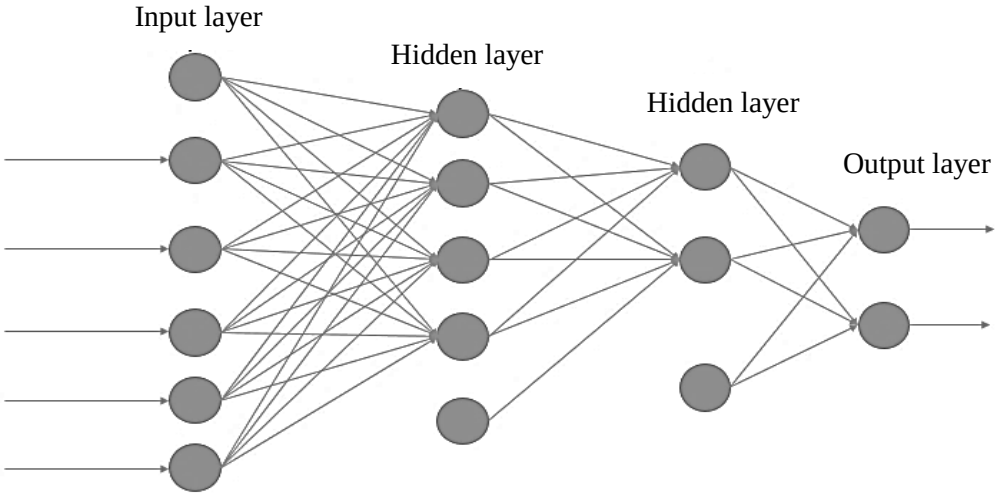

Figure 2-3: FFANN of multiple hidden layers

2.5.1.3 Multilayer perceptron and deep neural network

The three major types of deep learning include multilayer perceptron (MLP) ANN, recurrent ANN and convolutional ANN (Abiodun et al., 2018; Abiodun et al., 2019). The feedforward ANN can be extended to the concept of MLP which consists of input, hidden and output layers. Compared

to the SLP network, MLP ANN is more useful to perform the learning process beyond the abilities of SLP as it is capable to accurately learn both linear and non-linear problems or patterns based on the single or multiple hidden layer (Mas and Flores, 2007; Hornik et al., 1989). The MLP ANN with single hidden layer is normally termed shallow and the MLP ANN made up of input layer, output layer and multiple hidden layers is termed deep neural network (DNN) and can perform complex learning from the given data set (Wang et al., 2020). The MLP ANN is often used for supervised learning problems such as machine translation technology and speech recognition (Bermant et al., 2019). Moreover, the supervised MLP adjusts weights and biases of the network, thus, reducing the error function using mathematical and iterative rules and procedures (Asady et al., 2014). On the other hand, the deep ANNs for instance are often used in image shapes or texture features (Alom et al., 2019).

RNN (Figure 2-4) is a class of ANN in which a feedback network has a feedback path in that the output obtained from a previous step is fed as the input to the current step while capturing the information in relation to the correlation between current data and previous steps (Marhon et al., 2013). Thus, it generates an output and then copies that output and loops or recycles it to the network and in making decisions, therefore, the RNN considers the present and previous learning information that it has received during the decision making process (Salehinejad et al., 2017). Therefore, the RNN applies weights to the current and previous inputs and further modifies the weights through a gradient descent algorithm and back propagation through time. The RNN has the ability to memorize some parts of the inputs and can use them in the process of making good and accurate predictions (Koudjonou and Rout, 2019). The most common neural network (NN) structures in RNN are Elman recurrent neural network, Jordan recurrent neural network and Hopfield recurrent neural network (Szkoła et al., 2011; Ghanbari et al., 2014).

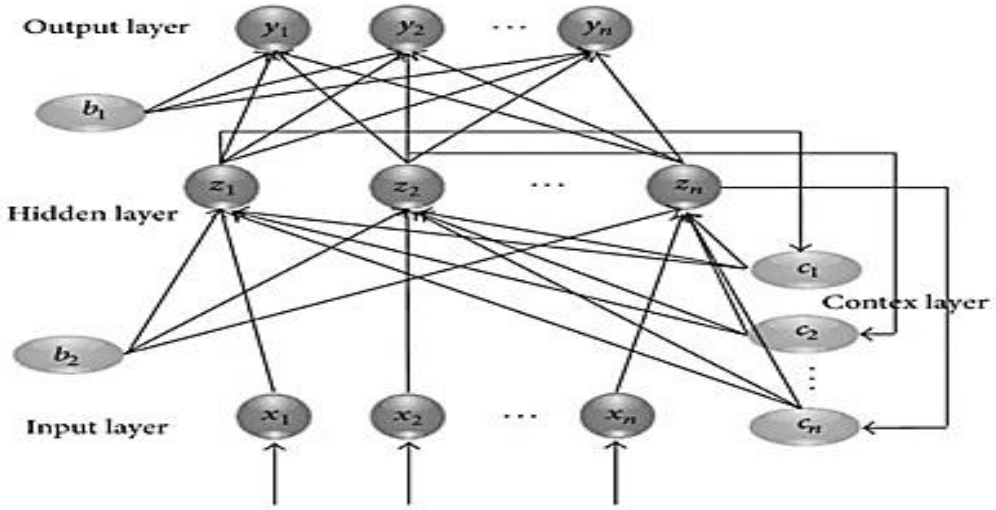

Figure 2-4: Elman RNN structure (Jiang et al., 2015)

CNN (Figure 2-5) is a special form of deep learning artificial neural networks that contains multiple layers of modelling input data or high dimensional input data (Lin et al., 2020). The CNN is also multilayer perceptron neural networks which are made up of a special structure for mapping image data classification and recognition in areas involving face recognition and object detections. This includes high accuracy in recognition because of the good and robust training and performance abilities (Lin et al., 2020).

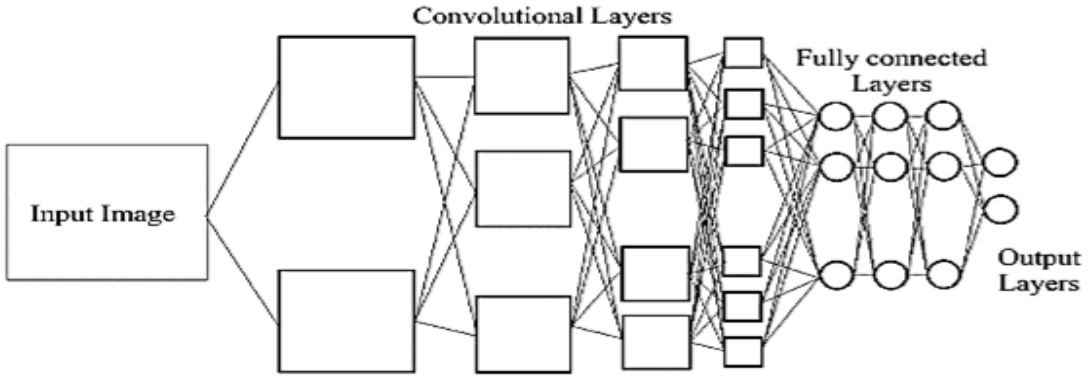

Figure 2-5: Architecture of deep convolutional neural network (Nguyen et al., 2016)

RBFNN is a form of ANN that was developed by Broomhead and Lowe in 1988 that contains three layers, namely, the input, hidden and output layers (Safavi and Ahmadi, 2015). Unlike other ANN types that can have several hidden layers, the RBFNN is simply limited to a single hidden

layer (Erol et al., 2008). Within the hidden layer, a network signal corresponding to an input vector and in proportion to this signal the network, produces a response. The RBFNN uses radial basis functions as activation functions for the application to supervised learning problems such as regression, time series prediction and classification (Wu et al., 2012). Figure 2-6 shows the RBFNN structure which consists of input, hidden and output layers.

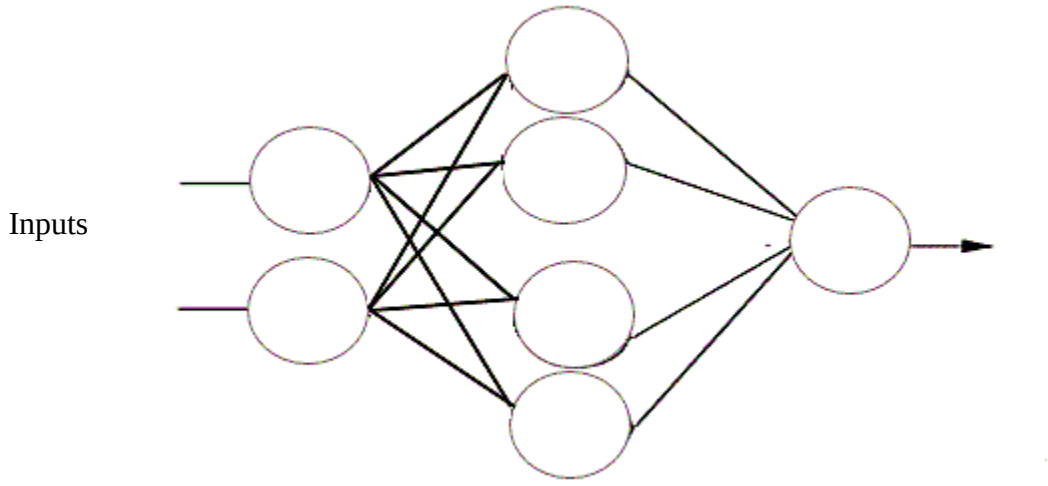

Figure 2-6: RBFNN structure

2.5.1.4 Supervised learning

Supervised learning allows optimization of performance in order to solve various real-world problems using supervised learning techniques (Uddin et al., 2019; Fister et al., 2015). Supervised learning is a learning technique of ANN where, during training, the ANN input vector is presented to the network which then generates the output vector. The output is compared with the desired output and an error signal is generated based on the difference between the output and actual target. The weights get adjusted until the real output of the network matches the desired output (Yang and Rai, 2019). Post training phase, the network should be able to model the new data and assign outputs which were unseen during the training steps. The two types of supervised learning methods are regression and classification. The regression method deals with fitting the data and reproducing the actual output while classification deals with separating the data (Yahia et al., 2020; Ripley, 1994; Bock et al., 2019).

2.5.1.5 Unsupervised learning

Unsupervised learning is a learning technique where there is no supervision on the model but instead the model is allowed to work on its own to discover information (Rojas, 1996). The unsupervised ANNs have no target outputs and the actual duty of the network is to group information which has no particular order according to patterns, differences and similarities without any form of prior training of the data (Lau et al., 2019). Its aim is uncovering hidden structure within the data and therefore clustering and dimensionality reduction techniques are important in unsupervised networks. Therefore, unsupervised learning can be useful to find patterns in data including useful features for categorization of data based on real time learning (van Engelen and Hoos, 2019).

2.5.1.6 Activation functions

Activation functions ensure that ANN learning in each neuron in the hidden layer occurs. In a neuron, these mathematical functions are responsible for ANN learning by taking the input, multiply it by weight vector, add the bias value, apply activation function and then returns the outputs (Gramatikov, 2017). The purpose of the activation functions is to perform complex computations and transfer network results to the output layer while introducing non-linearity in ANN. The non-linearity properties of ANN in the activation function allows to increase the network power to learn and model complex data structures (Nwankpa et al., 2018). The activation function is a decision maker for ANN by calculating the net output of the network. In this regard, there are several and various activation functions that are used in ANN modelling and are commonly classified as binary step activation function, linear and non-linear activation function (Nwankpa et al., 2018).

In binary step activation functions (Figure 2-7), the function generates binary output and is, therefore, useful for binary classification problems. The function generates a value 1 when the input passes the threshold limit value and produces a value 0 if the input fails to pass the threshold (Sharma et al., 2020).

$$f(x) = \begin{cases} 1, x>=0 \\ 0, x<0 \end{cases}$$

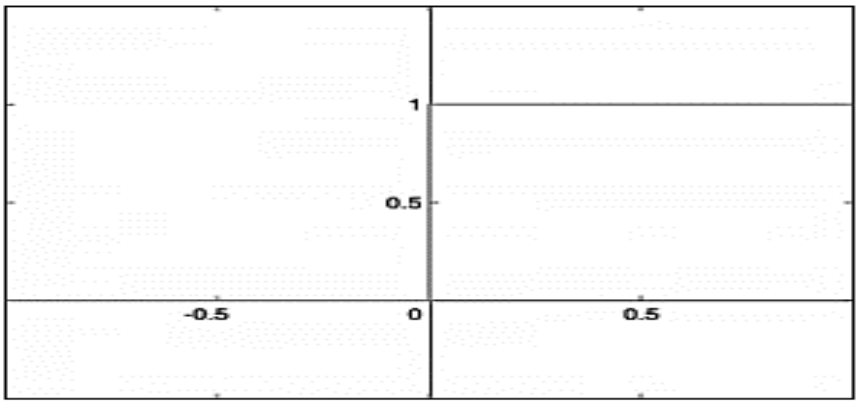

Figure 2-7: Binary step activation function (Sharma et al., 2020)

Based on Figure 2-8, linear activation function is a straight line function whereby activation is proportional to the input and the output of the functions will not be limited between any range since the function takes a linear form ((Feng and Lu, 2019). The linear activation function takes:

$$f(x) = aX \tag{2.5}$$

For this linear activation function, the derivative will be a constant, thus, gradient does not depend on x and therefore, modifications made by back propagation will be constant irrespective of the changes in the input-delta x. This linear activation function can be of minimum use with complex parameters which are often in real data that is given or fed to the ANN (Sharma et al., 2020).

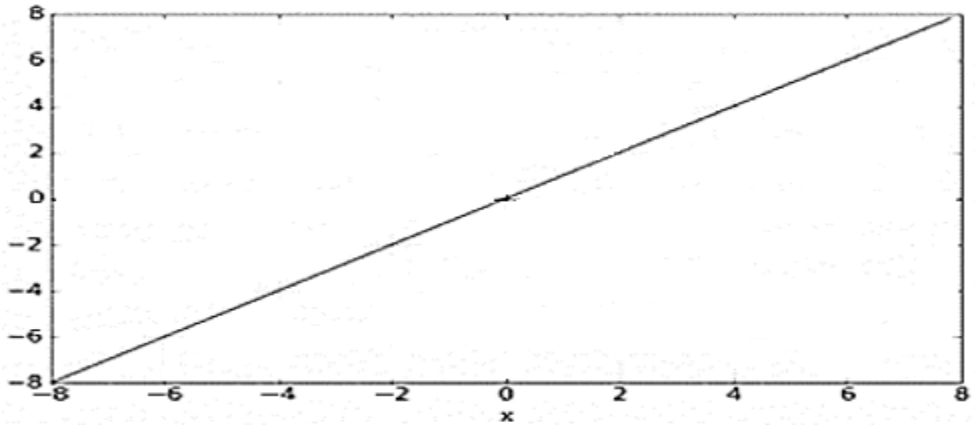

Figure 2-8: The linear activation function (Feng and Lu, 2019; Sharma et al., 2020)

Figure 2-9 presents an exponential linear unit (ELU) activation function which is the common activation function in convolutional neural networks that is often used due to its accuracy. ELU is one of the ANN functions that speeds up the ANN training while alleviating the problem of a

vanishing gradient. ELU can produce negative outputs as it takes negative values and has a non-zero gradient for x < 0 (Sharma et al., 2020).

$$f(x) = \begin{cases} x, & \text{if} > 0 \\ \alpha \exp(x) - 1, & \text{if } x \leq 0 \end{cases} \quad f(a, x) = e^{x} - 1 \tag{2.6}$$

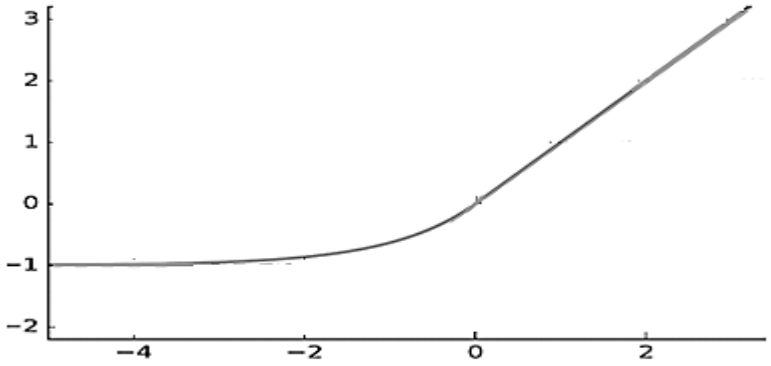

Figure 2-9: ELU activation function (Sharma et al., 2020)

The rectifier linear unit (RELU) in Figure 2-10 is also one of the most used activation function in ANN particularly in convolutional neural network or deep learning which takes a linear form, good performance and speed (Nwankpa et al., 2018). For instance, the RELU activation function uses only the maximum function and it is faster to compute than other activation functions, give sparsity in the model and has non-saturation characteristics for large positive inputs (Nwankpa et al., 2018). RELU has linear behavior, that is, it looks and acts like a liner activation function, however, in case neurons' weights become updated to the degree that the weighted sum of neuron's input is negative, neurons vanish and stop generating anything other than zero values. The derivative of RELU could be either 0 or 1, it outputs 0 when $x \leq 0$ and certain x value when $x > 0$ thus the output is linear if the input is positive (Apicella et al., 2021).

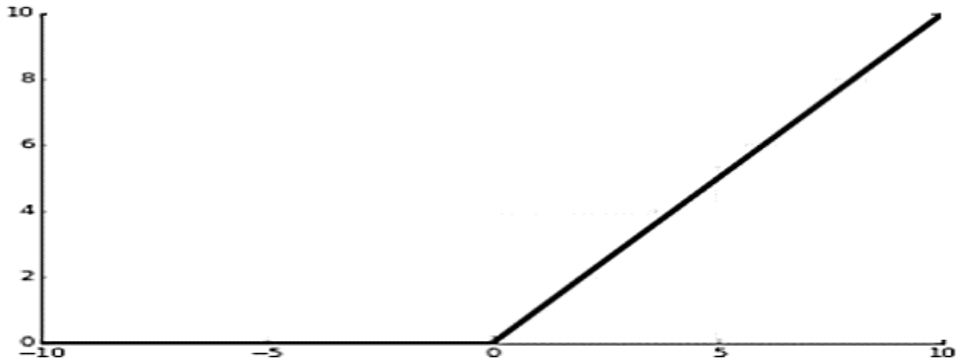

Figure 2-10: RELU activation function (Apicella et al., 2021)

Leaky rectified linear unit (Leaky RELU) in Figure 2-11 is regarded as an improved version of the RELU function as it modifies the issue of dead neurons during the back propagation process. The RELU function was defined as 0 for negative values of x. Unlike RELU, the Leaky RELU activation function allows for small negative x value or non-zero constant gradients during the back propagation step. It is also well known for its efficiency in dealing with complex classification problems (Apicella et al., 2021).

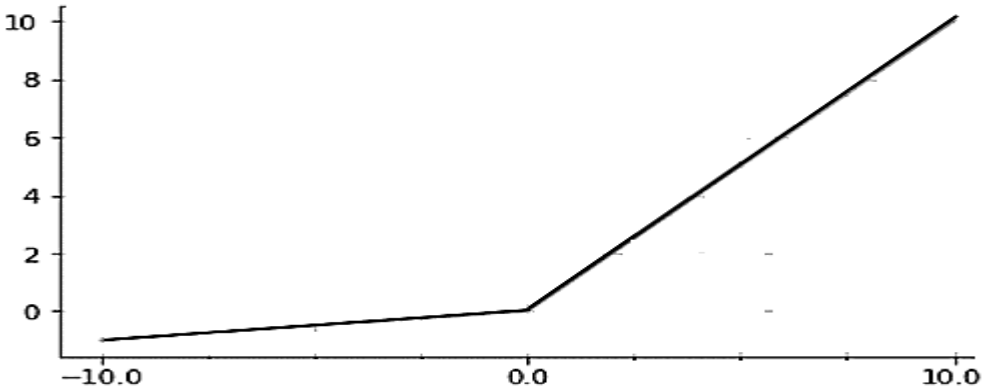

Figure 2-11: Leaky RELU activation function (Apicella et al., 2021)

Parametric rectified linear unit (PRELU) is the activation function similar to RELU with the exception that the slope values of the negative part are learned from the data rather than predefined. PRELU introduces an alpha parameter that modifies this parameter through gradient descent during training and tends to perform better than RELU in many instances (Wang et al., 2020). The gradient becomes an adaptable parameter during learning instead of predefining the gradient of the function.

Sigmoid function is an activation function with the graphical shape in Figure 2-12. It introduces non-linearity in the model by mapping the outputs in the range 0-1 which allows better fit of the data and accurate predictions. By multiplying the neurons having the sigmoid activation function, produces a non-linear output (Feng and Lu, 2019). It has an s-shaped or sigmoid curve otherwise known as a logistic function. It is the ANN function of the form:

$$f(x) = 1/(1 + e^{-x}) \tag{2.7}$$

Where f (x) is the output and *x* is the input

As shown in Figure 2-12, the sigmoid function has good performance characteristics, for instance the time to change from 0 to 1 proves to be less, thus making the sigmoid function a preferred

function for classification and gives a smooth gradient, although it could give rise to a vanishing gradient. The sigmoid is non-zero cantered, therefore, this affects optimization efficiency and it also diminishes the gradient due to saturation effect.

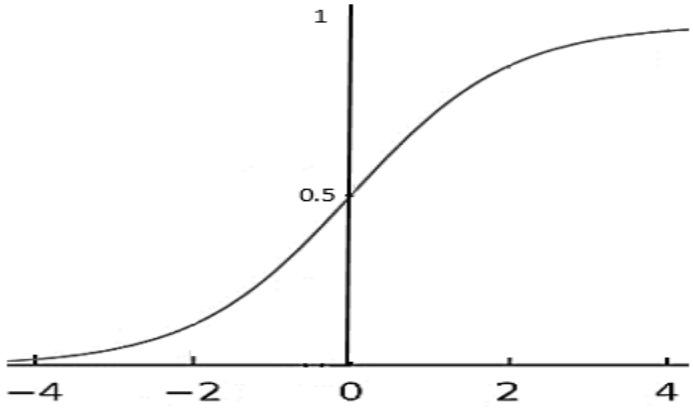

Figure 2-12: Graphical representation of sigmoid function (Feng and Lu, 2019)

Tanh activation is a non-linear activation function for ANN which scales the outputs in the range between -1 and 1 (Figure 2-13). When weighted sum of the inputs are applied to tanh x, the values are scaled in range between -1 and 1 and large negative and positive values will be scaled towards -1 and 1, respectively (Feng and Lu, 2019). Tanh activation is given by:

$$f(x) = \frac{(e^{x} - e^{-y})}{(e^{x} + e^{-y})} \tag{2.8}$$

Tanh function is more favorable for an application in ANN problems because it is continuous and has differentiable characteristics at all the points. The slope does not quickly decrease like that of the sigmoid function, therefore, its gradient does not vanish quickly.

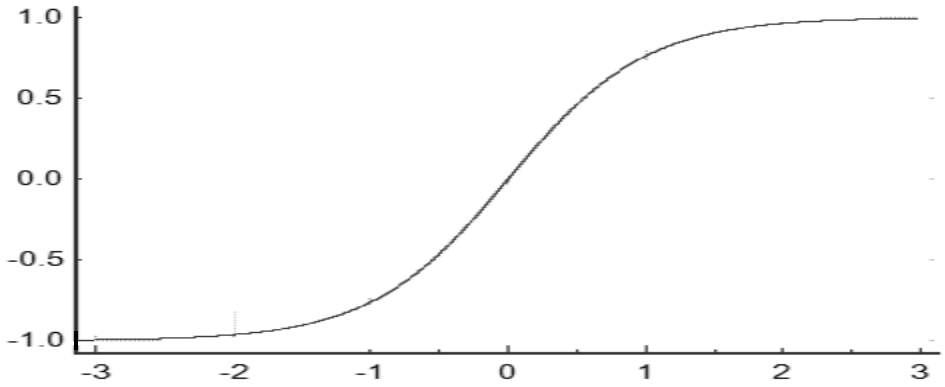

Figure 2-13: Graphical representation of tanh function (Feng and Lu, 2019)

2.5.1.7 Gradient descent (GD) optimization and back propagation algorithm

Gradient Descent is one of most learning algorithm that is often used to perform optimization in neural networks (Azar, 2013). The GD performs learning through minimizing the objective function in the neural network model. This is done through GD back propagation which involves computing the gradient of the objective function. In supervised learning, the objective function will be the error function between the target value and the network output (Emmert-Streib et al., 2020). The network subsequently updates parameters based on the computed gradients and the gradient takes into account the model's parameters and updates them to the opposite direction of the gradient of the cost function. The training cycle is repeated until the minima point of the cost function is attained (Lin and Sun, 2020).

In ANNs, the common method that is used to train an ANN is the back propagation algorithm which is often applied in training feedforward NNs for regression and classification problems. The back propagation can either be backward or forward pass, where in forward pass the output is evaluated based on the given input. In backward pass, the partial derivatives are propagated back to the network (Luo et al., 2017; Ganatra et al., 2011). The function of the back propagation is to optimize the weights which allows or improve the NN learning process in mapping given inputs to the outputs (Xu et al., 2015). During the training phase, the back propagation continuously adjusts the weights based on the existing/incurred training error for the output and the training phase terminates when the error is minimized to the lowest degree.

The three variants of gradient descent include batch, stochastic and mini-batch gradient descent (Ghatak, 2019). Each has its own specific characteristics in terms of performance and optimization procedure. In the instance where stochastic gradient descent was used in Figure 2-14, the training sample or data would be passed through the NN and the weights of each layer would be updated with the calculated gradient. The network, therefore, updates the weights of the network after calculating the error function of every training sample data.

Incase Figure 2-14 was optimized based on batch gradient, the batch gradient descent calculates the loss function for each example and subsequently updates the weights of all training examples at the end of each epoch. The weights are updated once after all training samples have been presented to the NN. If mini-batch gradient was used in Figure 2-14, the training data would be

divided into multiple batches and each batch will consist of a number of training samples. For the ANN structure with six neurons for the input-output layer with one hidden layer, back propagation algorithm and output error in neural network is computed as follows:

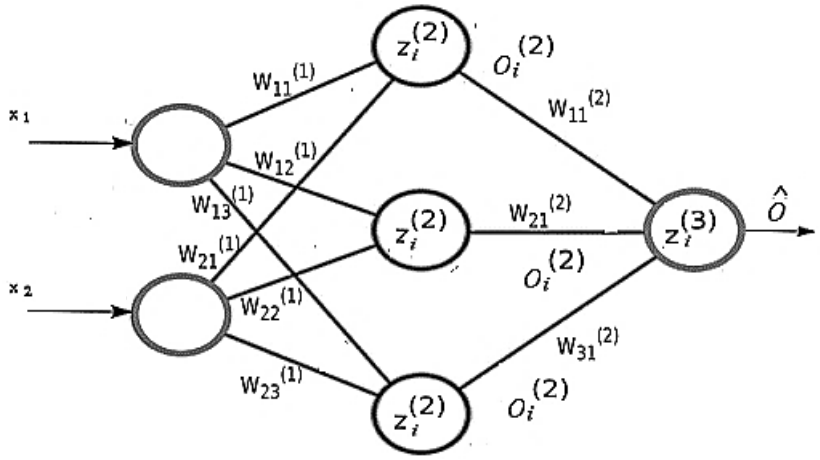

Figure 2-14: Back propagation algorithm and output error in a neural network

For the neural network in Figure 2-14, trained using gradient descent**,** the back propagation error can be computed using a cost function and sigmoid activation function:

$$f(z) = \frac{1}{1 + e^{-z}} \tag{2.9}$$

Error with respect to the network output, $\hat{O}$ is:

$$E = \sum_{i=1}^{N} (o_i - \hat{o}_i)^2 \tag{2.10}$$

O_i in equation (2.10) is the target value in the output layer for i equals to 1 and the output layer gradient is:

$$\frac{\partial E}{\partial W^{(2)}} = \frac{\partial \left(\sum \frac{1}{2} (o_i - \hat{o}_i)^2 \right)}{\partial W^{(2)}} \tag{2.11}$$

and O_i being constant

$$\frac{\partial E}{\partial W^{(2)}} = -\sum (o - \hat{o}) \frac{\partial \hat{o}}{\partial W^{(2)}} \tag{2.12}$$

$$\hat{o} = f\left(z^{(3)}\right) \tag{2.13}$$

$$z^{(2)} = \sum X_i W_i^{(1)} \tag{2.14}$$

$$z^{(3)} = \sum o_i^{(2)} W_i^{(2)} \tag{2.15}$$

$$o_i^{(2)} = f\left(z^{(2)}\right) \tag{2.16}$$

Given the error with *W* and $\hat{o}$ and accounting for other network parameters

$$\frac{\partial E}{\partial W^{(2)}} = -\sum (o - \hat{o}) \frac{\partial \hat{o}}{\partial W^{(2)}} \tag{2.17}$$

$$\hat{o} = f\left(z\right) \tag{2.18}$$

$$\hat{o} = f\left(z^{(3)}\right) \tag{2.19}$$

Based on the equations above and equation 2.17,

$$\frac{\partial E}{\partial W^{(2)}} = -\sum (o - \hat{o}) \frac{\partial \hat{o}}{\partial z^{(3)}} \frac{\partial z^{(3)}}{\partial W^{(2)}} \tag{2.20}$$

and based on equation 2.9 sigmoid activation function the derivativ $\hat{o}$ with Z:

$$\frac{\partial \hat{o}}{\partial z^{(3)}} \cdot = f'(z^{(3)}) \tag{2.21}$$

Substituting equation 2.21 in 2.20

$$= (\hat{o} - o) f'(z^{(3)}) \frac{\partial z^{(3)}}{\partial W^{(2)}} \tag{2.22}$$

2.5.1.8 ANN application in various water systems

The ANN has been widely applied in the various fields of water, hydrology, wastewater/water quality, water resources engineering domestic water and wastewater treatment plants (WWTPs)

(Mi et al., 2004). Its application has produced efficient and useful results and accurate estimates in various water bodies including environmental studies (Mi et al., 2004; Chu et al., 2013). For instance, the feedforward ANN has also been applied along with traditional water modelling techniques for instance modelling various water units for the estimation of efficacy of those water units (O'Reilly et al., 2018). This include prediction of reservoirs, streams and ground water quality (Abdolmaleki et al., 2013).

Rafiee and Jahangiri-Rad (2015) used ANN to predict the Chlorophyll-a (Chl-a) concentration in water of Aras dam reservoir in Iran. In this study, the ANN results showed high accuracy in predicting Chl-a concentration with satisfactory MSE and correlation coefficient values including good agreement between ANN output and actual data. The predicted output proved to be beyond the acceptable standard thus indicating the possibility of eutrophication mainly in the fall season. Also, the correlation coefficient between measured data and predicted values was 0.7 and a root mean square error (RMSE) value below 0.2 for all developed models was obtained.

Another ANN application was conducted by Huo et al. (2013) involving the investigation of a correlation between water quality indicators and eutrophication in Lake of Southwest in China. The study was carried out through the application of ANN back propagation algorithm and using water quality indicators such as total phosphorus (TP), dissolved oxygen (DO), chlorophyll-a (Chl-a) and secchi disk depth (SD) in lake Fuxian and the output/eutrophication indicators used for this study were DO, Chl-a, total nitrogen (TN) and SD. In this study, the ANN yielded robustness, as a useful and informative tool for the effective water quality monitoring and management.

Nwobi-Okoye and Igboanugo (2013) focused on modelling water levels at Kainji dam in Nigeria using ANN. This was through the collection of daily water level data for the development of five ANN models and Autoregressive Integrated Moving Average (ARIMA) model with the aim to fit the 10 year water level data. The ANN prediction accuracy models were found to correlate positively with an increasing number on model inputs. The best model with relative error of 0.039% was reported with ARIMA followed by 0.062% with ANN which was developed based on four modelling inputs whereas the single input ANN model reported least performance than the rest of the models. Based on the findings of this study, the ANN showed better performance than the ARIMA model due to its prediction efficiency and simplicity.

Kheradpisheh et al. (2015) conducted a study to assess ground water quality for 13 wells of Yazd regional water company in Iran using ANN. For evaluation of the influence of key inputs, the chlorine, EC, SO_4, and NO_3 parameters were estimated and compared with measured parameters and input training parameters were physico-chemical parameters, evaporation, water level and temperature. The results of the study using ANN with back propagation proved to be accurate in predicting qualitative variables of groundwater (chlorine, EC, SO_4) while results showed less accuracy with modelling including NO_3. Therefore ANN proved to be a fast and cost-effective technique for water management practices mainly in emergency occasions.

Solaimany-Aminabad et al. (2013) studied water quality of Sanandaj waste treatment plant (WTP) in Iran using ANN with a feedforward back propagation non-linear autoregressive neural network. A successful and useful model was developed and produced for the prediction of the influent water quality. The models proved their effectiveness for the use and for analyzing non-linear behaviour of the influent water quality of Sanadaj WTP. Using ANN, Tümer and Edebali (2015) investigated the performance of feedforward ANN using back propagation based on TSS of Konya waste water treatment plant (WWTP). The ANN structures were developed using MATLAB software and by varying training parameters of ANN such as hidden layers, neurons including training algorithms while measuring the ANN performance using MSE and *R* correlation coefficients. The ANN was useful and capable in predicting the plant performance and proved to be a valuable tool for plant personnel and decision makers.

Türkmeler and Pala (2017) studied an advanced biological WWTP using ANN for the prediction of effluent (BOD) based on BOD, COD, SS, TN, TP and flowrate input parameters. Satisfactory results with ANNs were obtained for the prediction of BOD in WWTP with good values of performance parameters MAPE, high sum of square error (SSE), absolute fraction of variance (R^2), root mean square (RMS) and percentage coefficient of variation. Using brewery wastewater (BWW), Hassen and Asmare (2019) applied ANN to predict the COD, pH and TN by building different structures of ANN ranging from MIMO, single-input single-output (SISO) and multi-input single-output (MISO). The ANN models were developed taking into account various training parameters and MIMO was the best ANN model for pH and TN and SISO was the best ANN model for COD.

Nasr et al. (2012) applied ANN studying a WWTP in Egypt to predict COD, BOD and TSS. Results showed high correlation between measured and predicted output values above 0.9 and acceptable generalization trends and therefore, it was concluded that ANN could be an effective tool to simulate the performance of WWTPs. Furthermore, Rene and Saidutta (2008) focused on the petrochemical industry wastewater from the effluent treatment plant by applying ANN to predict BOD and COD concentrations. The ANN was trained with TSS, TDS, phenol concentration, ammoniacal nitrogen, total organic carbon and Kjeldahl's nitrogen and twelve ANN models were proposed. In this research, prediction results recorded satisfactory statistical significance based on performance parameters and less percentage average relative error for testing was also evident.

ANNs are becoming widely applicable and have gained interest amongst researchers over traditional modelling techniques due to the fact that they offer improved performance, applicability and reliability characteristics (Türkmenler and Pala, 2017). Unlike ANNs, most of the traditional modelling tools have limitations to account for chemistry, meteorology, physics and hydraulic factors while ANNs prove to have good modelling characteristics (Liu et al., 2019). The ANNs handle well with uncertain and non-linear problems and are self-organizing, self-teaching and can deal with multi-complex variables without imposing restrictions on the number of input vectors as they have better and effective computational power than other modelling techniques (Luan and Zhu, 2011). Moreover, the ANNs relative to traditional predictive modelling techniques has the ability to detect trends/extract patterns and meanings from complex and imprecise data.

Nidhisha and Kuruvila (2019) modelled river BOD and COD concentrations using ANN and factor analysis. The training was through a trial and error method by varying non-linear training algorithms, neurons in hidden layers and the number of epochs. Results showed better performance of feedforward ANN with back propagation when combined with factor analysis which is a data reduction tool. Also, Hamada et al. (2018) applied ANN and multiple linear regression (MLR) for the prediction of WWTP BOD, COD and TSS in the Gaza Strip. In this work, five ANN models were developed for predicting water quality efficiency and results were compared with MLR and RBF neural networks and model performances were evaluated using quantitative error metric. Results showed higher performance with ANN than conventional modelling method.

In India, Abba et al. (2017) used multi linear regression, ANN and adaptive neuro-fuzzy inference system (ANFIS) to predict DO concentration for downstream river water in Agra City. The input variables at the upstream, middle and downstream were DO, pH, BOD, and water temperature. The significant results were obtained with ANN and ANFIS for the prediction of DO concentration and ANN model performance outperformed ANFIS and MLR models. In another study, Mas and Ahlfeld (2007) also compared the performance of binary logistic regression, ordinary least squares and ANNs in predicting surface water faecal coliform (FC) concentrations in mixed land-use watershed suing temperature, precipitation data, streamflow and conductivity as input vectors. From the data analysis, the ANNs were able to correctly classify 69% and 85% of FC concentrations in class A and B water quality standards, respectively, compared to the results that were observed for regression models. The good performance of ANN models was also evident when only meteorological input variables were used and ANN models correctly classified 72% and 81% of the cases for class A and B water quality standards, respectively.

The comparison of the performance of ANN and RSM studies were carried out by Khayet et al. (2011) for the prediction and optimization of a reverse osmosis (RO) desalination process. In this study, the central composite design (CCD) was used for RSM upon the performance of RO. The modelling variables were sodium chloride, feed temperature, feed flowrate and operating pressure. For data analysis, the analysis of variance (ANOVA) was used to access the significant performance of ANN and RSM model abilities through plotting the generalization graphs. Both models generally showed good performance and similar trends, however, the best and optimal conditions were obtained by ANN representing global optimal solution for the RO pilot plant that was tested.

Another study on ANN and RSM was conducted by Behin and Farhadian (2016) to predict decolourization efficiency of the reactive red 33 using the O3/UV process in a bubble column reactor. In this study, the ANN and 3-level CCD factors were time, superficial gas velocity, initial concentration of dye and pH. The comparison of the RSM and ANN results showed that ANN was good in fitting the data and showed good capability of better predicting the decolourization efficiency of the reactive red 33 well within the range of training than the RSM model. Similarly, Hamid et al. (2018) used ANN and RSM for the prediction of the capability of oxidized cellulose nanowhisker (CNW) adsorbents for remediation of copper investigated under optimal operating

conditions. The adsorption experiments were carried out using wastewater effluent spiked with Cu (II) where the response variable was Cu (II) removal from wastewater effluent. The findings from this study revealed that CNW adsorbents showed good capability in remaining spiked Cu (II) of wastewater effluent.

Al-Araimi et al. (2019) also used two modelling strategies, namely ANN and RSM for the assessment of optimum dosage of chlorine for the municipal water disinfection in Muscal city of Oman. The ANN was primarily used to forecast the residual chlorine in urban water at any specific given location and therefore, ANN variables were pH, inlet concentration of chlorine and the initial temperature. The RSM and DOE was employed in the study for initial optimization of chlorine disinfection, total organic carbon (TOC) and BOD based on pH, chlorine dosage and time factors. Results showed significant performance of ANN in predicting residual chlorine.

Abdolmaleki et al. (2013) used ANN in drinking water to predict heavy metal copper concentration in Chahnimeh1 reservoir in Iran using electrical conductivity (EC), total dissolved solids (TDS), temperature and pH. The training algorithm was the Levenberg-Marquardt training algorithm and good performance for ANN was obtained with seven neurons with low MSE, high *R* correlation values for training, testing, validation and all data. Another study by Farah et al. (2019) also applied ANN to predict daily water consumption in France for two cases, district metered area and end user case. In this work, the ANN training was carried out using historical data values at daily time and hourly time intervals including variation between hourly time and type of days. The findings showed that the ANN was capable to predict water consumption and peak values for both daily time and hourly time intervals and a MSE of 0.07 was achieved for the district metered area and 0.059 at the end user case.

In Poland, focasting for daily water consumption was investigated by Piasecki et al. (2018) using ANN and Multiple Linear Regression (MLR) based on humidity focasting and three antecedent data of water consumption. Their effects on water consumption was assessed through using correlation coefficients. In this study, only humidity had a significant effect on water consumption while other variables such as temperature, rainfall and wind speed were not considered for focasting models. Also, the ANN outperformed the MLR model while MAPE difference was

largely limited. This study showed that these focasting approaches that were applied in this study can also be applied in various parts of water and wastewater systems.

Liang (2013) conducted a study for the prediction of urban annual water consumption in Tianjin using back propagation ANN. The ANN vectors were industrial water recycling rate, urban population, daily water consumption, city gross domestic product (GDP), industrial output value, industrial water recycling rate and income levels. The neurons in hidden layers that were investigated were 10, 15 and 20. Good results were obtained using ANN with the back propagation algorithm. The best efficiency was obtained with 10 hidden neurons with low average deviation and a high R^2 value of 0.9587. A study by Shah et al. (2018) used RNN and feedforward neural network to predict daily water demand for central Indiana. The models were formulated for two different time intervals, namely, daily and monthly time intervals and the input features were temperature, rainfall, snow depth, median income, number of customers, day of the year and holidays. Based on this study, a good performance was obtained with RNNs which showed high accuracy and low average error in prediction of 1.69% and 2.29%. Therefore, ANNs proved useful for effecting operational decisions for daily and monthly time intervals.

Suh and Ham (2016) conducted a study on water demand for a residential building in Korea using back propagation neural network (BPNN). The training data to estimate water demand was obtained from other sources including climate variables, residential buildings, types and geometric variables. Results showed that the proposed BPNN was able to successfully predict water demand estimated outputs as water demand and water use for residential buildings in Korea is a massive issue. Therefore, the proposed BPNN model in this study was useful in decision making and for water management policy in Korea.

2.5.2 First-principles models

Over the years various water models have been developed and extensively applied in various water bodies to model water quality in surface water, discharge streams, river streams and potable water quality monitoring (Wang et al., 2004; Wang et al., 2013; Wang et al., 2009). With this understanding, the application of water quality models as the monitoring strategies of various pollutant contaminants is useful for better control of negative effects in water quality and an ecological environment (Altenburger et al., 2019). This includes the use as decision support tools

in water systems and analysis of risk factors (Bello et al., 2019). In effect, water quality models have a long history since their inception in 1925 where Streeter and Phelps built the first major water quality model which was used for simulating BOD and dissolved oxygen (DO) in a river system in the United States of America (USA) (Wang et al., 2013; Huang et al., 2017). Currently, more than 100 water quality models for surface water have been developed including numerous models that are based on various theories and computing techniques (Wang et al., 2013; Manivanan, 2017).

The water quality models are generally classified based on a number of characteristic features such as model complexity, the number of water quality parameters, the simulation method used and the type of water quality parameter or indicator (Yuceer, 2016). To this end, some of the water quality models that have been widely applied include AQUATOX model, QUASAR model, QUAL 2E model, water quality analysis simulation program (WASP model), WASP 7 model, CE-QUAL-RIV1 model, CE-QUAL-W2 model, soil water assessment tool (SWAT model) and simulated catchment model (SIMCAT model), MIKE11 model (Wang et al., 2013; Olowe and Kumarasamy, 2018).

2.5.2.1 QUASAR model

The QUASAR model is described as a water quality and flow model for the river networks which were developed based on the Bedford Ouse model by Whitehead (Whitehead et al., 1997). The model uses one dimensional (1D) ordinary equation principles to access the impact of pollutants in the river water systems (Whitehead et al., 1979; Whitehead et al., 1981). The model uses the concepts of mass balance in relation to flow based on stochastic and dynamic simulation principles. The QUASAR model was previously used effectively based on the Monte-Carlo framework to assess the distribution of water quality for high river streams (Whitehead and Young, 1979).

In river systems, the model was initially used within real-time focasting with collating telemetered data including producing focasts at abstraction sites. Due to its effectiveness, other researchers have applied water quality modelling to study mass balance in river systems with major pollutant problems (Warn and Brew, 1980; Warn and Matthews, 1984). Other researchers have applied river water quality modelling to study heavy metal pollution and the movement of nitrates and algae

content within the river systems (Whitehead and Williams, 1984; Whitehead and Hornberger, 1984).

The advantage for the application of QUASAR model is that a number of inputs can be investigated or assessed including tributaries, ground waters, inflows, runoffs, effluents and storm water as well as chemical and biological process assessment along the river system. The QUASAR model also consists of an easier formulation based on ordinary differential equations and therefore it consists of easier calibration and model evaluation. Furthermore, this water model seems to be suitable for modelling large river water systems and therefore requires sufficient data (Cox, 2003).

2.5.2.2 Water quality analysis simulation program (WASP) model

The WASP model is one of the commonly used water models that was developed by United States Environmental Protection Agency (USEPA) (Ambrose et al., 2009; Mbuh et al., 2019). The model is useful to interpret and predict the presence of pollutants in surface water processes. Currently, WASP has been used in various aquatic systems, rivers, estuaries, coastal waters, ponds, lakes and reservoirs (Mateus et al., 2018). In essence, WASP is a dynamic model that can be used for modelling one to three dimensional structures. The model has two independent components, DYNHYD - a hydrodynamic procedure involving an exercise equation and a continuous equation and the WASP standalone computer program which consists of 7 versions, namely, WASP to WASP 7 (Hao et al., 2012).

WASP 7 can be applied as a one dimensional (1D), two dimensional (2D) and three dimensional (3D) models in water quality assessment based on analysis of water systems and pollution types (Mateus et al., 2018; Ziemińska-stolarska and Skrzypski, 2012; Wang et al., 2013). With this model system, DYNHYD and WASP could be used independently or in a combined form. Also, the model is derived based on the principles of mass conservation and requires input data to account for balances in the system that is being modelled (Olowe and Kumarasamy, 2018). WASP is also well capable to address processes occurring in water columns and simulation of organic chemicals, for instance, nutrients-eutrophication, BOD, dissolved oxygen dynamics, coliform bacteria, toxic chemical amounts and synthetic organic compounds (Wool et al., 2020). Larico et al. (2019) used the WASP model to assess eutrophication in El Pane reservoir in Peruvian Andes. Results of the

study were used to analyze national water quality standards (NWQS) using physical, chemical and biological water quality variables.

Other researchers have used WASP to examine eutrophication and phosphorus loading in rivers and water supply reservoirs as eutrophication affects taste, odour and water quality (Lung and Larson, 1995; Jin et al., 1998; Mark and Owens, 2009). Zhang and Rao (2012) used the WASP 7 model in Lake Winnipeg to examine eutrophication while taking into account the average value of phytoplankton biomass as well as phytoplanketon components. Although the WASP model has been widely used and proven useful as a water quality model for the application in water resource management, its limitations include the ability to handle some variables and processes. Other limitations include the inability to readily be operated on batch mode, separation of eutrophication and toxicant fate modules and large external hydrodynamic files (Ghadai et al., 2020).

2.5.2.3 CE-QUAL-RIV1 model

The CE-QUAL-RIV1 model is a dynamic flow and 1D water quality model applicable for rivers or streams. It was developed by US Army Engineers Waterways Experiment Station (WES) dating back in 1991 (Sharma and Kansal, 2012; Ambrose et al., 2009). The model consists of hydrodynamic code-RIV1H and water quality code-RIV1Q and RIV1H which was applied to the case of a water column to calculate river hydraulics based on geometric characteristics and boundary conditions (Olowe and Kumarasamy, 2018). Following the RIV1H, the output was used by the water quality model for simulation. In addition, RIV1H solved St. Venant equations using a four-point implicit method to predict flows, depths, velocities and hydraulic parameters (Ziemińska-stolarska and Skrzypski, 2012). In the main, RIV1Q uses two-point fourth order, accurate finite difference to solve the mass balance concept equation that was developed by Holly and Prassmann (1977) to solve the mass balance concepts based on river geometry, water flow characteristics and concentration including meteorological data.

In Korea, Hwang et al. (2013) used the CE-QUAL-RIV1 model to assess Seonakdong River water quality while varying influent and effluent flowrates for the predictions of long-term water quality. The steady state was found inadequate based on modelling and the variation in water flowrates and water quality during the operation of water gate. From this study findings, recommendations included an optimum plan for evaluating and restoring water quality including period and duration

in relation to gate operation. Also, in a study conducted by Batick (2011), the CE-QUAL-RIV1 model was applied in river modelling using water parameters and peaking hydropower dam which consisted of irregular flowrates varying between 16 to 240 m^3/s. The model was able to predict well water parameters such as temperature including predicting stages and low-flow stage.

2.5.2.4 CE-QUAL-W2 model

The CE-QUAL-W2 model is a 2D hydrodynamic water quality model that was developed by the US Army Corps of Engineers (ASACE) (Zhu et al., 2017). The model is useful in modelling surface water bodies, river basins, estuaries, lakes and eutrophication processes including predicting the fate and transport of pollutants in water bodies and other water quality variables such as DO, nutrients, organic matter, algae, pH, dissolved solids and SS (Martin et al., 1999). Also, the CE-QUAL-W2 model assumption is a lateral homogeneity method, therefore, it is best suited for long and deep narrow water bodies (Cole and Buchak, 1995). In modelling, various researchers have used the CE-QUAL-W2 model in numerous water quality bodies such as rivers, lakes, estuaries and reservoirs including water quality investigations and as a management tool for evaluating water quality in point and non-point pollution sources (Gao and Li, 2014).

The model has also been applied by Zhu et al. (2017) in Xiaxi river in China to simulate mercury transport and cycling in water. The results showed that the model was capable to predict mercury concentrations in Xiaxi river. In Korea, Kim and Kim (2006) applied the CE-QUAL-W2 model in deep reservoir by accounting temporal distribution and spatial distribution of water temperature in a reservoir in Soyang including movements of density currents. The water motion and thermal stratification were both simulated by 2D CE-QUAL-W2 and the model was successful in simulating all characteristics of the stratification regime and the formation of the turbid intermediate layer in the reservoir.

In Canada, Lindenschmidt et al. (2019) effectively used the CE-QUAL-W2 model to study the effect of dam out flow on temperature, nutrients and DO. The model focused on analyzing six scenarios of water extraction by looking 5 m elevation above the reservoir surface at the dam and other elevations which was increased by 10 m incremental values to 55 m elevation. The measurements were water temperature, algae production, biological and physico-chemical parameters. Other researchers have used CE-QUAL-W2 in modelling dam flow control and other

impacts on water quality on rivers and multi-reservoirs while other studies have investigated the effect of water dams and flow regulation in relation to downstream nutrient loads and outflow temperature for the downstream and reservoir scenarios (Chang et al., 2015; Lindenschmidt, et al., 2019).

2.5.2.5 Soil water assessment tool (SWAT) model

The soil water assessment tool (SWAT) model was developed by United States Department of Agriculture (USDA) and Agricultural - based Research Service (ARS) (Neitsch et al., 2002). The model is useful to quantify the effect of land management and practices in watersheds environment (Arnold et al., 1998; Arnold and Fohrer, 2005; Santhi et al., 2006). The model is able to deal or address problems related to surface runoffs, water quality systems, quantification of water and water resources, soil erosion, river systems and ecosystems including studying the effects of climate change and land use (Abbaspour et al., 2019). It is also a strong function of quality parameters and characteristics such as topographic characteristics, vegetation, soil properties, weather, and type of water system (Dai et al., 2017). The model operates on the basis of a daily time step and produces simulations based on dividing watershed into a number of sub basins in series configurations which are also subdivided into hydrologic response units (Arnold et al., 2012). In spite the robustness of the SWAT model in water modelling with readily available data, the non-spatial feature of the hydrological response units makes the model suitable for simplicity application while the model accounts no pollutant routing in a sub-watershed. As a result, the model formulas remain empirical and has limitations to account for erosion and sediment transport and snow melt modelling (Cox, 2003).

A number of studies on the SWAT model has been reported in the literature on water quality assessments, quantitative water analysis, climate change and water resources assessment (Torabi Haghighi et al., 2019; Li and DeLiberty, 2020; Kumar et al., 2017; Kwarteng et al., 2020; Johnston and Kummu, 2011; Rossi et al., 2009). This includes SWAT model application to study sediment and nutrients, concentrations of pollutants and loads (Hallouz et al., 2018; Krysanova and Arnorld, 2008). Liew and Garbrecht (2003) also investigated the ability of the SWAT model to predict streamflow under varying climate conditions from three nested sub water sheds in little Washita river in Southwestern Oklahoma. The model was calibrated based on wet climate conditions and

results showed that the model was capable of predicting streamflow variables for dry climate conditions, likewise, with average and wet climate conditions.

In West-central Iowa, Jha et al. (2007) reported accurate and satisfactory results on SWAT model application on streamflow in Raccoon River. In South Africa, Govender and Everson (2005) applied the SWAT model to model streamflow from two small experimental catchments to examine the capability of the SWAT model to simulate hydrological processes in daily time steps. The streamflow results were significant and the SWAT model performed well under different climate conditions, although the model showed limitation to simulate growth of the Mexican weeping pine (Govender and Everson, 2005). Winchell et al. (2018) reported positive results with the SWAT model for the prediction of annual maximum pesticide concentration exposure in flowing water schemes based on high vulnerability watersheds. The model was applied in 27 watersheds using the approach of uncalibrated parameterization.

2.5.2.6 SIMCAT model

The SIMCAT model was developed by United Kingdom (UK) environment which has been largely used in UK as a water quality modelling tool and as a decision making tool for river water quality management and planning (McIntyre et al., 2003). The SIMCAT model is a 1D steady state water quality model which predicts river water characteristics and is regarded as a cost-effective and a simple water quality model that requires relatively less amount of data for operation (Kannel et al., 2011). The SIMCAT model is a stochastic model that uses the Monte Carlo simulation technique and can be used to assess the effect of pollutants that are discharged in water bodies (Warn, 2007; Olowe and Kumarasamy, 2018).

The SIMCAT model takes into account solutes that are conserved in water, non-conserved substances and dissolved oxygen and the model is best suitable for modelling water bodies that are independent of sediment interactions (Kannel et al., 2011; Cox, 2003). This model offers no allowance for temporal variability and variation in reaeration rate with flow. Other limiting factors include the fact that the SIMCAT model accounts for no photosynthesis, respiration and sediment oxygen demand (Cox, 2003; Ranjith et al., 2019). Hankin et al. (2016) applied the SIMCAT water quality model for catchment scale sensitivity and uncertainty to predict nitrate and soluble reactive phosphorus contents in four monitoring regimes. The four regimes had different spatial and

temporal sampling occurrences. The modelling results showed overall positive improvement of the SIMCAT model. In North England, Crabtree et al. (2006) used the SIMCAT model to predict water quality impacts in the district national park. Results showed that the content on effluent discharge was more than necessary and could allow major targets to meet required standards including control of other sources of pollution.

2.5.2.7 AQUATOX and QUAL 2E models

The AQUATOX model is a simulation model for the aquatic ecosystem that was developed by United States Environmental Protection Agency (USEPA). The model is widely applied in aquatic systems to predict the effects and fate of various environmental pollutants on the ecosystem based on nutrients, organic chemicals, sediments, flow and temperature in the aquatic ecosystem (Park et al., 2008). The model is also useful for the comparison of perturbed and control simulations including photosynthetic limitations. It also allows the use to compute results in graphical and tabular form, sensitivity and uncertainty analysis based on nominal range (Park and Clough, 2004). Researchers have applied the model in river streams, estuaries, lakes and ponds including artificial streams and the model can well explain the causal and effect correlations given the aquatic life water quality and ecological environment (Park et al., 2008). AQUATOX has limitations to solve hydraulic equations including modelling toxic organic pollutants but cannot model organometals (Anagnostou et al., 2017).

The QUAL 2E model was developed by USEPA for predicting pollutants in stretching river streams and well mixed water lakes (Cox, 2003; Brown and Barnwell, 1987; Ning et al., 2001; Pelletier et al., 2006). The model can effectively operate as either a dynamic model or steady state model and can simulate up to a limited number of water quality parameters (Parveen and Singh, 2016), for instance simulation of pollutant loadings, flow and stream temperature including chemical and biological pollutants. This model has limitations to address transient stream flow, storm water flow instances, non-point source pollution including dimensional limitations. The model limits only 20 computational elements per reach and the reaches should not be more than 25 (Olowe and Kumarasamy, 2018; Shanahan et al., 1998).

Paliwal et al. (2006) applied the QUAL 2E model to simulate BOD and dissolved oxygen (DO) content in Yamuna River. The findings were well within acceptable literature studies on river water

modelling. Ning et al. (2001) investigated the impact of water resources and redistribution including water quality management and practices in Kao-Ping River. Findings showed that there was a need to address pollution in the up-stream area both in wet and dry seasons. The findings also showed good capability of QUAL2E in predicting BOD, DO, total phosphate-phosphorus and ammonia-nitrogen content.

2.6 Summary

Based on literature review, extensive research on scientific water issues, treatment technologies and water management techniques is becoming central over the years for adequate water supply and availability. It is also evident from the previous studies that water quality and treatment standards remain the major priority in any useful water treatment technology. As a result, a large number of studies has focused on water quality monitoring including water quality modeling such as first principles modelling for the analysis and control of water quality and water treatment processes. As shown in the previous studies, the significant contribution of water quality studies cannot be underestimated particularly in water treatment processes.

To this date, numerous water quality studies on water quality modelling involving data driven models, wastewater reclamation or reuse and wastewater reuse application and management are also emerging in many countries. These studies are largely aimed to explore and address water challenges facing a large number of communities around the globe. The application of empirical modelling studies have long history in the field of water treatment. However, studies on data driven models for the prediction of water quality are becoming important for the monitoring and control of water treatment processes. These modelling techniques remain necessary due to their robustness and prediction power in modelling high dimensional water data with non-linear trends. In this study, the ANN was selected for the application in HRF for the prediction of multi-parameters of domestic greywater effluent. In this study, the ANN was considered due to its flexibility and predictive power in modelling water quality within the HRF based on mixed domestic greywater.

Chapter 3

Methodology

3.0 Background

This chapter presents the methodological approach used in this study while investigating different aspects of this research which is presented in four main sections. Part of the methods focused on investigating greywater quality details for a better qualitative understanding of domestic greywater which is presented in the section on characterization of greywater. Other parts of the methods deal with detailed concepts of HRF operation and performance for domestic greywater treatment which is presented in the section on controlling factors of a HRF system. The section that followed focused on the methodological approach in identifying significant variables affecting the efficacy of HRF including optimization techniques applicable in HRF equipment. The final details focused on methods on the proposed ANN model structures which were developed for the prediction of various parameters in HRF including different forms of ANNs for single and multi-output parameters for the HRF equipment.

3.1 Methodology on characterization of greywater

Study area

The study was conducted in a low income peri-urban settlement located in Umlazi which is in the southern part of Durban. The place is densely populated and lacks sanitation facilities with high volumes of domestic water runoffs around the area. A total number of seventy five households with 240 inhabitants consisting 48% adult women, 35% adult men and 17% under the age of 18 were randomly identified and selected to conduct the study. The sampling of domestic greywater generated from laundry, bathing and kitchen sources through washing activities in households were carried out and analyzed for all types of pollutants.

Greywater sampling

The analysis of greywater samples was carried out and assessed independently for physical and chemical characteristics. The greywater sample sets were collected from the seventy five households over a period of 4 weeks during weekdays including grab samples which were collected once a day from each of the three sources within two hours from generation and this was

conducted mainly in the afternoon using sterilized sampling bottles. The samples were sealed and placed in an ice cooler box in order to control the thermal effect and the influence of the surrounding on greywater samples. The collection of greywater sources including kitchen greywater was from the kitchen sink while shower greywater was directly from the shower and laundry greywater was collected from the washing stations. The samples were immediately analyzed or stored in a cooler with a temperature below 4 °C where samples could not be immediately analyzed.

Physico-chemical analysis

The collected greywater samples were analyzed for conductivity, COD, BOD, pH and total solids and these analyses were carried out using Standard Methods for the Examination of Water and Wastewater (APHA, 2012). The conductivity and pH parameters were determined in situ through an Orion Star A215 and turbidity through a turbidimeter-TB300 IR Orbeco-Hellige. The calibration was carried out following instructions and procedures outlined for Orion Star A215 benchtop pH-conductivity meters. Three point buffers were used and the pH electrode was prepared according to the meter instructions provided in the electrode use guide. For conductivity, the conductivity standards were used for calibration and the conductivity cell was prepared following the calibration procedure for the conductivity cell. The accuracy for temperature was in order of ± 0.1°C, 0.5% reading ± 1 digit for conductivity and ± 0.002 for pH. The BOD parameter was determined using the 5-day procedure incubation at 20°C with OxiTop manometric equipment while COD was determined using the open reflux method (APHA, 2012). The total solids content was quantified through a gravimetric analysis procedure which was carried out in the laboratory environment.

The analysis of E. coli and total coliforms

The microbes in domestic greywater were analyzed based on enumeration method by Petrifilm method (Cirolini et al., 2013). The microbe analysis was carried out for all collected greywater samples and 1.0 ml volume aliquot of each sample was plated onto a single 3M Petrifilm Rapid E and all samples were duplicated for E. coli and coliform count plate. The plates were incubated at 32-36 °C for a total of 48 hours to allow for the micro bacterial growth in the samples. The analysis was carried out and the plates were enumerated for E. coli and total coliforms. The E. coli content in a water sample was indicated by blue-green coloured colonies with and without the presence of

gas bubbles. The total coliform count content was identified through red coloured colonies with gas.

Data analysis

The statistical analysis and comparisons of the characteristics of greywater were performed using univariate analysis of variance (ANOVA) tests followed by post-hoc Scheffe tests (Brownlee, 1966). Therefore, the univariate ANOVA test was carried out in this study for the statistical comparison of means for all greywater sources. In addition, the post-hoc Scheffe test was used as an additional exploration of the differences among means of greywater sources as it was needed to provide specific information on means that were significantly different from each other. Therefore post-hoc tests are a critical step in the univariate ANOVA test as they allow for the determination of which means are significantly different from the others and therefore, it was used to determine if there exists significant differences in the quality of greywater from the identified sources within households using the Statistical Package for the Social Sciences (SPSS) 22.0 software package.

3.2 Methodology on the operation of the HRF equipment

3.2.1 Methods on the operation of the HRF equipment for the treatment of domestic greywater

Greywater source

This investigation was carried out to evaluate the performance of the HRF equipment for the treatment of greywater from a peri-urban community located in Durban. The greywater sources from the laundry, bathing and kitchen were collected in random order from 30 households within the community to carry out experimental runs using the HRF unit. Over 500 litres of greywater were collected and supplied to the HRF in each occasion for the entire duration of the study.

Experimental set-up and procedures

The experimental work was carried out in a pilot scale HRF equipment (Mtsweni, 2016). The pilot scale HRF was constructed using design principles in Wegelin (1996) and Galvis et al. (1998) and Table 3.1 presents the summary of the HRF design guidelines including specifications, principles and concept adopted for the design of a HRF equipment. In terms of material of construction, a

polyethylene plastic material with metal frames was used in the HRF. The HRF was partitioned into three adjustable compartments as indicated in Table 3.1.

Table 3.1: Summary of the design guidelines for the HRF (Mtsweni, 2016)

Design parameter		**Recommended literature value**	**Actual design parameters**
Gravel media	Compartment 1 (mm)	20-12[(i)]	15-12.2
	Compartment 2 (mm)	12-8[(i)]	12.2-9.5
	Compartment 3 (mm)	8-4[(i)]	8-6.7
Gravel type		(granite. quartz, local) [(i)]	Quartzite
Filter depth (m)		0.2-0.3[(ii)]	0.3
Area of the filter (m^2)			1
Hydraulic velocity m/hr)		0.3-1.5[(i)]	0.3
Uniformity coefficient		<2[(i)]	
Filter length (m)	Compartment 1 (m)		1.5
	Compartment 2 (m)		1
	Compartment 3 (m)		0.5
Filter width (m)		1-2.3[(i)]	1

[(i)]Wegelin (1996); [(ii)]Galvis et al. (1998)

Each filter compartment was partitioned using perforated plates which separate gravel media fractions contained in each compartment while allowing the minimum flow of greywater across the entire filtration system. The filter lengths from the first to the last compartments were 1.5, 1 and 0.5 m respectively. Each filter bed compartment was packed with washed gravel media fractions of different sizes. Firstly, the gravel size in the first compartment was 12.2 to 15 mm while the second compartment was packed with gravel sizes of 9.5 to 12.2 mm and the last compartment with gravel sizes of 6.7 to 8 mm. The media fractions were classified through crushing and grain size distribution. The inflow of greywater across the compartments followed the direction of decreasing pattern of filter media sizes from the first to the last compartment of the filter as the three compartments were in series arrangement. The filter was equipped with a

feed pump, the feed water tank and adjustable influent flow control device with a pre-calibrated valve forming a loop with the HRF equipment.

Figure 3-1 shows the design components of the HRF equipment that was used in this study and the design was based on the aspects of availability, cost and reliability.

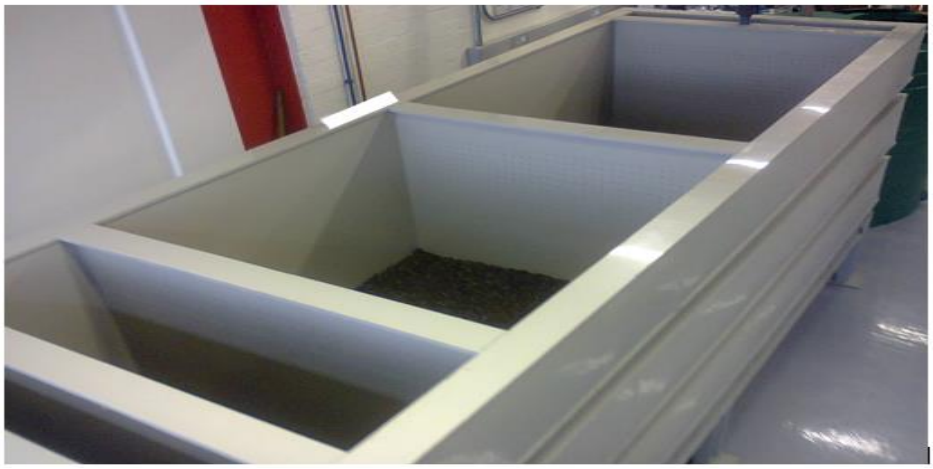

Figure 3-1: The configuration of the three compartment HRF equipment set up (Mtsweni, 2016).

Filter operation

To conduct experiments, the pilot HRF system was operated for 12 weeks and sampling was conducted twice a week and all analyses were carried out immediately after the sampling. The filtration rates in the HRF during the operation were fixed in order to allow for the stabilization in the filter prior to sampling steps. The values and the range of filtration rates for the HRF are presented in Table 3.1 above. The sampling points were located from the inlets and outlets of the HRF system which were carried out in order to analyze the influent and effluent characteristics of the greywater following treatment within the HRF. The HRF was operated at a low filtration rate of 0.3 m/h which is highly recommended for achieving good removal efficiency (Boller, 1993).

Analytical methods

The influent greywater samples were characterized for conductivity, COD, total solids, and turbidity for the evaluation of the removal efficiencies of the HRF equipment. The analysis was carried out using Standard Methods for the Examination of Water and Wastewater according to APHA (2012).

Turbidity

Turbidity is one of the important physical parameters in the analysis of water quality and its presence depends on the quantity of suspended insoluble matter in the greywater. High turbidity amounts in water correlates with poor water quality. Therefore, the removal of turbidity is often necessary for good water quality. In this study, the influent and effluent turbidity of greywater from HRF was measured using a calibrated TB300 IR Orbeco Hellige turbidimeter.

COD parameter

COD is one of the chemical parameters that was measured for the analysis of greywater quality for both the influent and effluent greywater. In water, the COD is described as the quantity of oxygen required to oxidize the organic content in the greywater. The value of COD normally exceeds that of BOD due to the presence of larger amounts of substances that can be oxidized through chemical processes than biological processes. The quantification of COD is therefore important for the assessment of the potential pollution strength of greywater sample. In this study, the COD measurement procedure was through the open reflux procedure based on Standard Methods for the Examination of Water and Wastewater (APHA, 2012).

Conductivity

The conductivity parameter in greywater is an indicator of the dissolved soluble salts often present in the greywater. High conductivity in greywater is often associated with the presence of high proportions of soluble salts. In this study, conductivity of both the influent and effluent greywater samples were measured using a calibrated Orion Star A215 conductivity meter.

Total solids

The total solid parameter indicates all the colloidal, suspended, and dissolved solids present in the greywater. In this study, the total solids was measured for the influent and effluent greywater samples. The total solids were determined through evaporating greywater samples and allowing them to dry in crucible vessels in an oven at 103 to 105 °C followed by weighing the residue in order to determine the total solids present in the greywater sample.

The E. coli and total coliforms

The amounts of E. coli and total coliforms in domestic greywater was estimated using the enumeration method analysis outlined in section 3.1.

3.2.2 Methods on investigation of the controlling and design variables of the HRF equipment

Sampling

The study used was mixed greywater which was collected to run experiments in HRF in order to analyze the combined effect for the selected design factors on filter performance. The greywater was obtained from low income community households from all washing sources and washing stations within the study area. The greywater sources collected were mixed and charged in the feed water tank in order to carry out all experimental runs with this mixed greywater.

Design of experiments

In this study, the operating parameters of the HRF were studied with the aim to investigate their effect on the HRF performance. The investigation was carried out using DOE as it allows the analysis of complex relationships amongst the factors and also allows the effect of a factor to be investigated at several levels of other factors. The one factor-at-a-time experimental method is not useful to study and capture the relationships existing amongst the factors. Therefore, factorial design was conducted in this study to investigate factors affecting the performance of the HRF equipment by varying the design variables of the HRF in Table 3.1. Experiments were conducted in random order to investigate the effect of factors on the response-turbidity.

Design factors

The HRF design variables for carrying out DOE were filtration rate (X_1), filter bed height (X_2), filter length (X_3), gravel media (X_4) and inlet perforated baffle plate (X_5), all which were used as design factors. The design variables and their selection criteria was mainly informed by literature relating and linking the dependence of filter performance with some of these design variables (Wegelin, 1996, 1986, Galvis, 1998). The filtration rate strongly correlates with filter capacity and removal efficiency and all design variables have a strong effect in the removal efficiency. The design matrix was developed based on a 2^5 full factorial design with high and low level values for

each factor. Table 3.2 presents the DOE factors and levels for this experimental work and high and low level values for each design factor were coded by +1 and -1 values as shown in Table 3.2. The factors considered for HRF were derived from experimental design and through knowledge of the process on the operation of the filter.

Table 3.2: Factors and levels for experimental design

Factor	Label	Low level (-)	High level (+)
Mean gravel size (mm)	A	7	14
Filter bed height (m)	B	0.3	0.6
Filter length (m)	C	1	2
Filtration rate (m/hr)	D	0.3	0.6
Perforated inlet baffle screens (mm)	E	3	4

Statistical analysis

The analysis of variance (ANOVA) test was conducted to investigate the significance of factors and their interactions on the response variable. The probability value (p-value) analysis was used to determine significant effects and the interactions existing in this study. Also, the factor significant effect was measured for p-value less than 5% where 95% confidence level was considered. Moreover, the relative importance of the main effects and interactions were further investigated using standardized main effects through Pareto charts and half-normal probability plots.

Accuracy

In this work, the accuracy and goodness of fit criteria was investigated and assessed using R^2 values such as coefficient of determination (R^2) and adjusted R-squared (adj-R^2). The acceptable goodness of fit values should be high and range from 0.9 to 1 for all coefficients, (Moalla et al., 2018) while validation was carried out for generalization ability for the prediction/estimation of the response variable.

DOE software

The factorial design analysis and results of the experimental design were all analyzed using Minitab 14 statistical software. This statistical tool is useful to evaluate and carryout analysis such as graphical and statistical plots after the data analysis such as standardize main effects plots, Pareto charts, normal and half-normal probability plots, descriptive statistics including other useful DOE statistical measures.

3.2.3 Methods on the optimization of the HRF equipment using RSM

For the optimization of the HRF equipment, filter length, filtration rate, the filter bed height and gravel media fractions were used. During experimental design, these design variables were identified to have a significant effect and therefore, were considered for use in the optimization of the HRF.

Sampling and greywater quality

This study was carried out using mixed domestic greywater which was collected from the informal settlement households. In this aspect, mixed greywater from all different sources was collected to carryout experimental runs. Greywater quality strongly depends on the number of social conditions, the pollution load and management including duration left unused which significantly affects its quality. To control variability in greywater quality, the collected amount of greywater with constant quality in terms of pollutants was used throughout experimental runs for overall representation of constant greywater quality.

Accuracy

The statistical testing of the significance of the RSM parameters in this work was assessed through the ANOVA test. Other statistical parameters such as the coefficient of determination (R^2) and adjusted coefficient of determination (adj R^2) were also measured to assess the significance of the parameters and the goodness of fit computation of the ANOVA test. The significance or lack of fit was also assessed through the F-test and probability value (p-value).

Software

The Design Expert 10.02 software package was used to carry out optimization of filter efficiency of the HRF based on the dependent variable and independent variables and their factor settings.

The surface response plots, contour plots and ANOVA for the filtered non- linear mathematical model for the optimization of the response variable were also produced.

3.3 Methodology on ANN modelling and optimization

3.3.1 ANN methods for the prediction of turbidity

The study was conducted at Umlazi, an informal settlement that was identified as the study area. Experimental work was conducted in the study in order to generate ANN training data for a period of 12 months and a total number of 1001 data cases. The ANN model for the prediction of turbidity, based on domestic greywater quality, was generated for this work. In terms of social status, the study area lacks social facilities and this limits efficiency of domestic greywater reuse. Above that, the study area is without proper potable and reuse water facilities while greywater is largely in abundance and produced through different forms of washing activities.

Experimental work

The input and output training data for the development of ANN for the prediction of turbidity was generated through conducting experiments in a three compartment HRF (Figure 3-1). The HRF system was operated for the treatment of greywater while recording physico-chemical parameters for the influent-effluent streams of mixed greywater using a low filtration rate of 0.3 m/h with a total length of 3 m. The mean gravel size was 9 mm for the mean compartment and the size ranging between 14-7 mm for coarse and small fractions with perforated baffle screens of 3 mm. The selection and design criteria of the study was based on the available greywater literature and previous studies on operation of roughing filtration systems related to wastewater treatment (Morel and Diener, 2006).

Data normalization

The data normalization was performed for all input variables for the training of the ANN model. All ANN architectures were developed based on this normalization of training data which is a useful technique for multi input variables. The normalization is a good modelling approach in this study due to inequalities and different units existing in the input data. All inputs were normalized based on equation 3.1 which takes into account individual data points, minimum and maximum values for the training data. The training data was normalized in range between 0-1 to ensure

training efficiency in the neural network. Mathematically, the normalization equation was given by:

$$x_i = \frac{x - x_{min}}{x_{max} - x_{min}} \quad (3.1)$$

Based on equation 3.1, x represents input. The minimum and maximum data points are represented by x_{min} and x_{max}, respectively.

ANN software and ANN training Parameters

Prior to ANN training, the ANN data was preprocessed in Microsoft excel in order to carryout descriptive statistics and training data cleaning. Thereafter, the modelling was carried out using MATLAB software R2015a which is the robust ANN modelling tool. The feedforward NN with back propagation was used to train the neural network for the prediction of turbidity. For the ANN training, the inputs were temperature, electrical conductivity, pH and turbidity and the output was the effluent turbidity. Figure 3-2 shows the ANN structure and proposed training parameters for the prediction of turbidity.

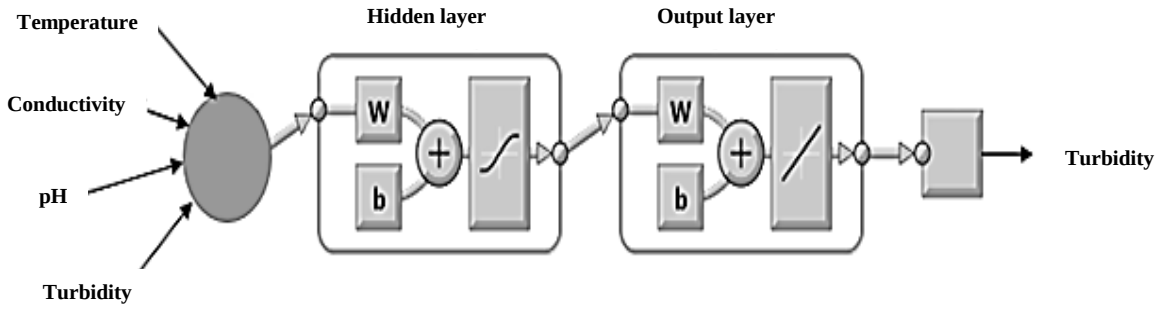

Figure 3-2: ANN structure and proposed training parameters for the prediction of turbidity

Table 3.3 shows the ANN average variables that were used for the development of the ANN model for the predicted turbidity. The ANN was trained with electrical conductivity (EC), temperature, pH and turbidity with the following range of values: EC ranged from 300 to 1200 µS/cm, the pH was from 8-12, turbidity ranged from 210-350 NTU and greywater temperature ranged from 25-29 °C. For turbidity, the effluent value of turbidity was observed ranging between 24.1-30.9 NTU. Also, the measuring instrument for turbidity was a calibrated TB 300 IR Turbidity meter and a

multiline Orion Star A215 conductivity meter. Lastly, the measuring instrument for temperature and pH was Fisher Model 805 meter.

Table 3.3: The mean values of ANN inputs for the prediction of turbidity

	Inputs				Output
	Temperature (°C)	pH	Turbidity (NTU)	EC (µS/cm)	Turbidity (NTU)
Mean	26.5	10	279	510	27.5
Min	25	8	210	300	24.1
Max	29	12	350	1200	30.9
SD	2.9	1.5	89	160	1.6

Development of ANN and model accuracy

Several ANN models were developed for the prediction of turbidity in greywater from the HRF. The ANN models were developed based on the back propagation algorithm and the proposed ANN model was a three layered ANN back propagation structure. The study used empirical rules as well as trial and error techniques to optimize the connection weights of ANN. During training, the number of ANN models with different neurons in the hidden layer, transfer functions and training algorithms on MATLAB were developed. The neurons in the hidden layer ranging between 5-9 neurons were investigated including different transfer functions and algorithms available in MATLAB.

In building the model, the ANN data was randomly divided into training, testing and validation sets with 70% training, 15% testing and 15% validation. During training the maximum iterations were set at 1000 and the target error was 0.1%. The early stopping procedure was used in this study to ensure avoidance of overfitting of the designed ANN during the training process. Table 3.4 shows different types of training algorithms for MATLAB and learning functions that were used in this study.

Table 3.4: Different types of training algorithm and learning functions for MATLAB for ANN training for the prediction of turbidity

Training Functions	Definition: Training function	Learning functions
trainbfg	BFGS quasi-Newton back propagation	Tansig-Purelin
		Logsig-purelin
trainbr	Bayesian regularization	Tansig-Purelin
		Logsig-purelin
traincgb	Powell -Beale conjugate gradient back propagation	Tansig-Purelin
		Logsig-purelin
traincgf	Fletcher-Powell conjugate gradient back propagation	Tansig-Purelin
		Logsi-purelin
traincgp	Polak-Ribiere conjugate gradient back propagation	Tansig-Purelin
		Logsig-purelin
traingd	Gradient descent back propagation	Tansig-Purelin
		Logsig-purelin
traingda	Gradient descent with adaptive lr back propagation	Tansig-Purelin
		Logsig-purelin
traingdx	Gradient descent with momentum and adaptive lr back propagation	Tansig-Purelin
		Logsig-purelin
trainlm	Levenberg-Marquardt back propagation	Tansig-Purelin
		Logsig-purelin
trainoss	One step secant back propagation	Tansig-Purelin
		Logsig-purelin
trainr	Random order incremental training with learning functions	Tansig-Purelin
		Logsig-purelin
trainrp	Resilient back propagation	Tansig-Purelin
		Logsig-purelin
trainscg	Scaled conjugate gradient back propagation	Tansig-Purelin
		Logsig-purelin

ANN performance and accuracy

The statistical parameters were used to check the accuracy of the developed ANN model. The performance measures that were used to compare accuracy of the best ANN were MSE, and *R* correlation coefficient for the training, testing, validation and all data sets. The best or optimally trained ANN model amongst the numerous developed models that displayed low errors and goodness of fit between predicted and observed data was selected as the best ANN model. The training was finally terminated when the performance criteria was met using coefficient of determination and MSE values based on the comparison of the performance parameters during ANN training steps.

3.3.2 Methods on ANN for the prediction of COD of domestic greywater from the outlet stream of a HRF unit

Study area

The area selected to conduct the study was a low income informal settlement found in a certain area of Umlazi Township with high dense population. The area generates domestic greywater in high volumes through various forms of daily washing activities from household activities. The area remains without basic and formal greywater handling schemes and due to social and economic status in households, the variation in greywater quality exists. Therefore, greywater sampling was performed in this area and experimental analysis was done in the laboratory environment.

HRF equipment

The HRF was operated for the treatment of greywater under a constant filtration rate of 0.5 m/h for a period of 1 year. A three compartment filter 3 m length, 1 m height and 1 m width was used in this study with coarse gravel size (12.2-15 mm), medium size (12.2-9.5 mm) and small gravel fractions (8-6.7 mm) which were all charged into the filter. The ANN training data was obtained through the sampling in the HRF equipment.

ANN parameters

The ANN input parameters that were used for the development of ANN for the prediction of COD were solids, pH and turbidity and the output layer consisted of COD as the output variable. The ANN set up and parameters were chosen to configure the ANN based on the literature and HRF theory. Figure 3-3 presents ANN parameters that were used to train the network including the proposed ANN structure for the prediction of COD.

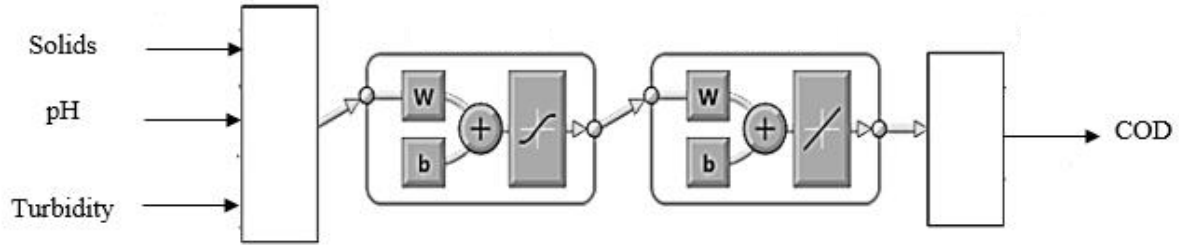

Figure 3-3: ANN architecture and proposed training inputs for COD prediction

Data normalization

The data normalization was also carried out for the input-output to ensure that all variables are scaled in the required range for ANN training. The ANN training data was standardized in order to increase the learning efficiency of ANN. The standardization also removes biasness in neural networks due to a variable scale existing within the experimental data. In this work, the training data was standardized as some of the parameters had larger effects compared to other parameters. The standardization procedure in training data was carried out based on equation 3.1 for the prediction of COD.

MATLAB script for network training

In this study, the network was trained using MATLAB script which was generated and customized for the training of the network. The input and target data sets were imported into MATLAB Workspace for the processing of the ANN training steps using MATLAB command window. The MATLAB script takes into account the adjustment of all training parameters such as transfer functions, training algorithms and the number of neurons in the hidden layer through trail-and-error. The activation functions such as purelin, logsig and tansig were used in training the neural network (Hagan et al., 1996). The MSE was chosen as the network performance criteria and the network was trained and the MSE was adjusted until a low error between the network and target outputs was satisfactory.

The feedforward neural network with back propagation algorithm was used during training of ANN. A number of multi-layer ANNs with different transfer functions and training algorithms in the hidden layer were investigated for the prediction of COD and turbidity using the iterative method. The linear transfer function in the output layer was used for all ANN models that were developed through training. In this study, all ANN MATLAB training algorithms were investigated in order to obtain the best training algorithm based on Table 3.4. The ANN data was divided into three subsets, training, testing and validation. In training the ANN, 700 data cases were used for training, 150 cases for testing and also 150 cases for validation.

ANN accuracy

At the end of the ANN training process, the MSE and R^2 values were recorded after each ANN training step. The training of the network was performed through the trail-error method for different training parameters and the best ANN architecture was selected based on the minimum MSE and maximum coefficient of determination (R^2) values in the training, validation, testing and all data sets. Therefore, the best model was selected based on outlined satisfactory performance criteria.

3.3.3 ANN methods on prediction of filter duration in a HRF equipment

ANN parameters

The training variables and experimental data summary for the development of feedforward ANN is presented in Table 3.5.The ANN training parameters were turbidity, electrical conductivity, filtration rate and pH for the prediction of filter duration and turbidity. The training parameters were obtained by means of experimental runs in a HRF equipment and were quantified through different types of measuring instruments in the laboratory. Table 3.5 also summarizes the mean, upper and lower values of the collected data in unstandardized form.

Table 3.5: Summary of input-output variables for the development of ANN

	ANN Inputs				ANN Outputs	
	Flowrate m/h	pH -	Turbidity NTU	EC µS/cm	Filter duration days	Turbidity NTU
Mean	0.6	8.5	220	696	20	39
Min	0.3	7.5	120	300	15	18
Max	0.9	11.4	320	1095	25	60

Sampling and ANN training data

The ANN training data was generated through experiments conducted in the laboratory using the HRF and the data generated was used for training the neural network for the prediction of filter duration. To carryout experimental work, domestic greywater from the kitchen source was collected from the low income community and was placed in the feed water tank connected to the filter. In the input layer, the total dissolved solids, conductivity, turbidity, pH and output values of turbidity were analyzed in the filter compartments to the last compartment. The output layer

consisted of conductivity, turbidity and pH as dependent variables for the proposed ANN. All ANN variables were analyzed using measuring devices and experimental analyses in the laboratory space according to the standard method and guidelines on APHA (2012). Figure 3-4 shows the ANN structure and proposed training parameters for the prediction of filter duration and turbidity.

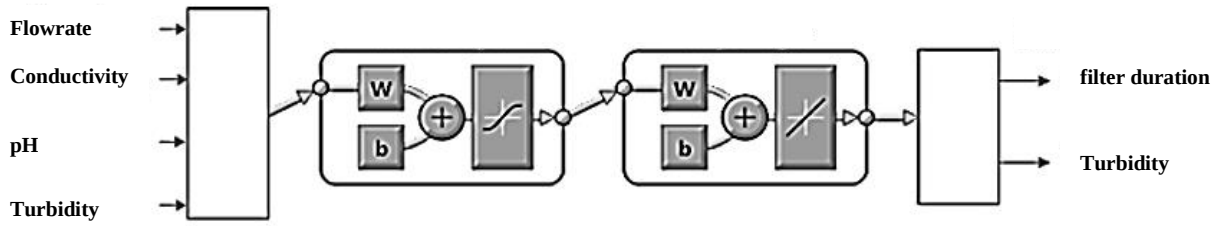

Figure 3-4: ANN structure and proposed training parameters for the prediction of filter duration and turbidity

Conductivity

In this work, electrical conductivity in greywater samples were measured through a use of a calibrated Orion Star A215 conductivity meter. The conductivity was also used as input during ANN training.

Turbidity

The analytical instrument used for measuring turbidity in greywater was a calibrated TB300 IR Orbeco Hellige turbidity meter. The turbidity of greywater was also selected for training the ANN.

pH

The other network parameter was pH of greywater which was also used as the input parameter for training the ANN. The pH of greywater was estimated through a calibrated Fisher Model 805 meter.

Flowrate

The inflow of greywater across the filter bed should be maintained constant and the filter was equipped with feed pump which is useful to direct greywater into the HRF bed. The adjustable influent flow control device with a pre-calibrated valve was used for flow regulation. In this study, the flowrate was used amongst the inputs for ANN training.

ANN model set up

The raw data was pre-processed and analyzed on Microsoft excel and MATLAB R2015a software package for ANN tools to assess the data variability, outliers, missing data points and data distribution. The training data was also assessed through descriptive statistics prior to ANN training. For good convergence in neural network training, the variability in input data was eliminated through standardizing the training data in the input and output layer in range of 0-1 using equation 3.1. In this study, the feedforward neural network with back propagation algorithm was chosen as the network structure for modelling HRF. The ANN training involved the iteration of neural network architecture, the number of hidden neurons, training functions, learning function, performance function and output transfer function. Therefore, an iterative procedure was adopted for this study for each proposed neural network modelling for the prediction of filter duration.

Measuring network accuracy and validation

The network performance at the end of the training phase was measured based on the minimum value of MSE and *R* correlation coefficient values for all data sets. The optimal ANN model is desired to have a low MSE value and maximum correlation coefficient values in training, testing, validation and all data regression. There were 637 data cases in this study and 70% was assigned for training, 15% for testing and the reminder for validation. In this work, the trained ANN was validated using the validation data set which was set at 15% of the total experimental data.

3.3.4 Methods on ANN for the prediction of multi-output parameters of domestic greywater from the outlet stream of the HRF equipment

ANN training data and parameters

In this work, the aim to predict selected physico-chemical variables of greywater in the outlet stream of the HRF. The sampling of greywater from mixed sources was carried out in the study area and experimental runs and analyses were conducted in the laboratory. The ANN training data consisted physico-chemical parameters which were obtained through experimental runs conducted in HRF. In the input layer, there were seven input variables and these were solids, temperature, turbidity, flowrate, conductivity, pH and COD. The multi-output variables that were

simultaneously predicted using feedforward ANN were pH, COD, solids and turbidity. Table 3.6 summarizes the input-output parameters that were used for training the ANN in this study.

Table 3.6: ANN parameters for the prediction of multioutput variables of greywater effluent stream from the HRF unit

	ANN Inputs							ANN Outputs			
Parameter	Flowrate m/h	pH	Solids (mg/l)	Turbidity NTU	EC µS/cm	Temperature (°C)	COD (mg/l)	pH	Turbidity NTU	COD mg/l	Solids mg/l
Mean	0.6	9	1400	280	600	27	1700	10	40	600	350
Min	0.3	8	900	200	400	23	900	7	30	350	200
Max	1	12.5	1900	450	2000	29	2300	12	120	700	500

Figure 3-5 below presents the feedforward NN structure and the input parameters proposed for ANN training parameters for the prediction of pH, COD, solids and turbidity for the effluent greywater stream from the HRF equipment.

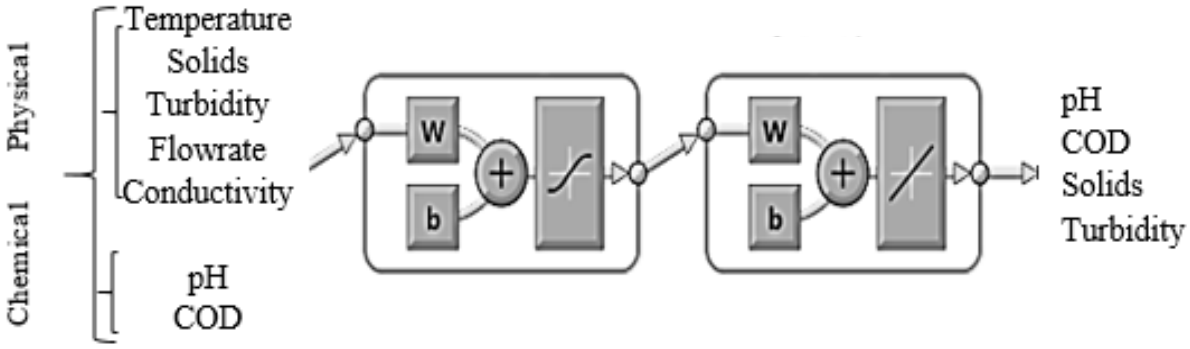

Figure 3-5: ANN architecture and proposed training parameters for the prediction of multi-output variables

ANN software and data normalization

The ANN models were developed using MATLAB R2015a software which is suitable programme consisting of a tool box for modelling applications including implementing ANNs. A MATLAB script was developed using automatic neural network function. The ANN data for MATLAB workspace was normalized using equation 3.2 for efficient training of the ANN modelling. The normalization of the training data was carried out using the following general equation:

$$Z_i = \frac{x - \mu}{\sigma} \tag{3.2}$$

From equation 3.2, Z_i represents the normalized x using μ, the mean value of the data and σ, the standard deviation of the data.

ANN training: MATLAB script

The MATLAB script developed for ANN was used for training which took in to account the properties of ANN. The script was used as the basis of training the network and was continuously adjusted until the MSE value was minimized to the satisfactory level. Through an iterative approach, the adjustments on the number of hidden neurons in the hidden layer, the number of neurons and 13 training algorithms on MATLAB neural network toolbox were tested. Other training parameters that were adjusted included learning rate and epochs while other ANN training parameters contained in MATLAB were kept constant.

ANN training procedure: training steps and training parameters

Step 1: Training with COD and pH as input parameters

In MATLAB script, a trial-and-error technique was used to develop a three layered feedforward NN for the prediction of four main multi-output parameters of domestic greywater from the outlet stream of a HRF using the feedforward ANN. Initially, the training was carried out using COD and pH as input vectors for the prediction of multioutput parameters as shown in Figure 3-6.

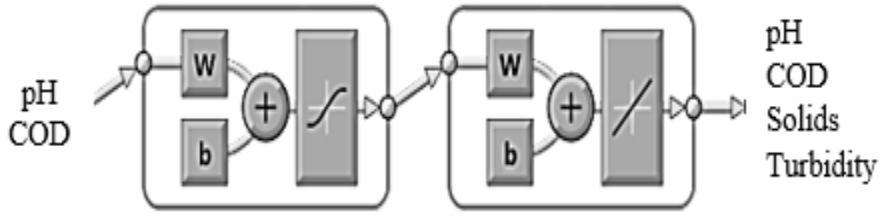

Figure 3-6: Training of ANN with COD and pH input parameters

Step 2: Training with temperature, solids, turbidity, flowrate and conductivity

The next ANN models were trained using a new set of input vectors including flowrate, conductivity, temperature, turbidity and solids. The four multi-output parameters in the output layer remained pH, COD, solids and turbidity (Figure 3-7).

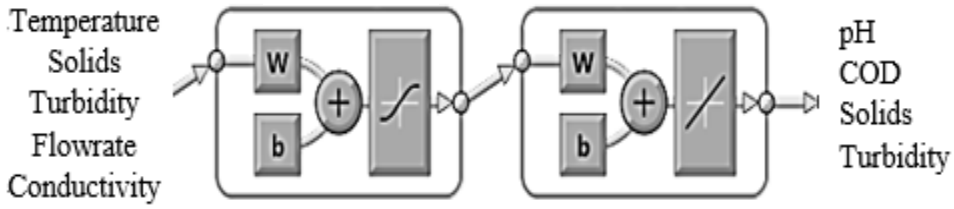

Figure 3-7: Training of ANN with physical parameters for the prediction of multioutput vectors

Step 3: Training with step 1 and 2 training parameters

Figure 3-8 shows the next training attempt to develop the optimal ANN using the combination of physical and chemical parameters as input vectors for the prediction of multi output parameters.

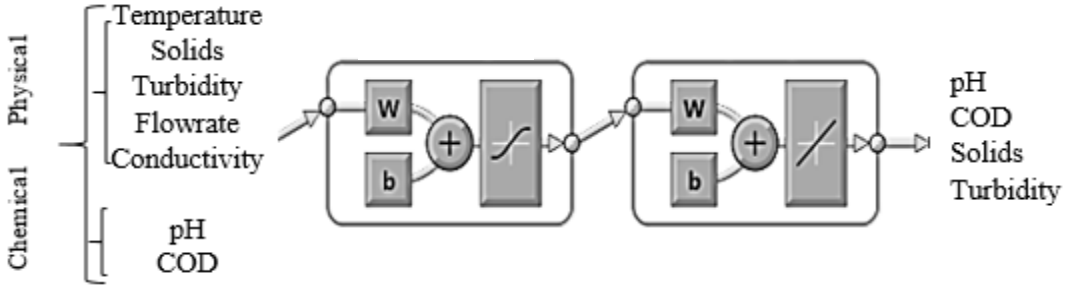

Figure 3-8: Training of ANN with physico-chemical parameters for the prediction of multioutput variables

ANN Accuracy

The best fitting neural network was evaluated for the performance and correlation between predicted data and measured data. Therefore, the accuracy of each developed ANN model was examined using statistical parameters such as *R* correlation coefficient for the training, testing, validation and all data sets and MSE values.

Chapter 4

Results on domestic greywater characterization

4.0 Introduction

This section presents published findings on domestic greywater characteristics for a qualitative assessment of household greywater from kitchen, laundry and bath sources. The greywater sources were investigated and analyzed in order to understand quality composition. The greywater was analyzed for biological and physico-chemical parameters using greywater quality analysis methods that was discussed in the previous section. Figure 4-1 shows experimental results of greywater quality analysis in terms of turbidity for the three investigated greywater sources. Amongst the three greywater sources, the kitchen source ultimately recorded the highest level of turbidity of 252 NTU and low turbidity values were recorded for the laundry and bathing greywater sources. This can be largely related to a high number of pollutants and different types of pollutants in greywater which are often found in kitchen greywater sources used to carry out washing activities (Couto et al., 2013; Edwin et al., 2014).

Moreover, the laundry greywater source was evidently less turbid and simply recorded 170 NTU compared to the kitchen greywater source. Of all these greywater sources, the quality differences could be attributed to low pollution load and probably the absence of food particles, fats and other forms of wastes. Furthermore, the lowest turbidity is desirable and is associated with good water quality (Edwin et al., 2014). It was also observed from the plot in Figure 4-1 that the lowest turbidity of 120 NTU was obtained in bathing greywater source and can be highly useful for reuse with application of the right treatment system (Hernandez, 2010). For these greywater sources, the ANOVA test was carried out and showed significant difference amongst greywater sources at 5% significant level.

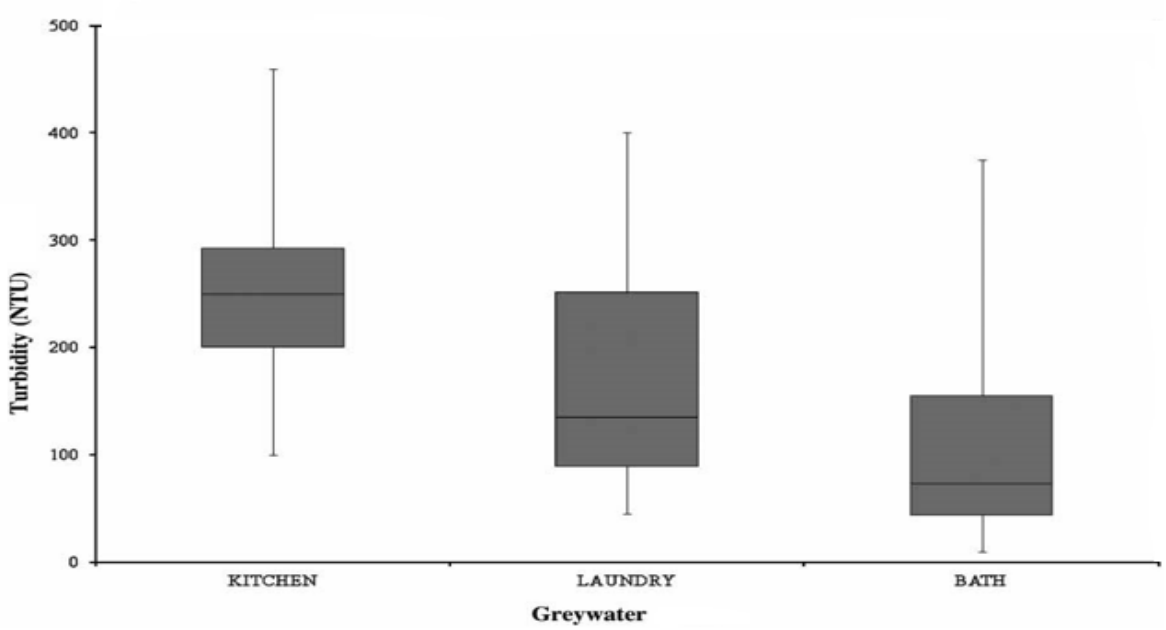

Figure 4-1: Experimental results on the comparison of turbidity values in bathing, kitchen and laundry greywater sources

Electrical conductivity is one of the parameters of greywater which measures the salinity of all dissolved matter contained in greywater. The electrical conductivity in greywater could generally range between 14 and 3000 µS/cm (Oteng-Peprah et al., 2018). In this regard, the findings of Figure 4-2 summarizes conductivity values of the three greywater sources. For these greywater sources the laundry source recorded the highest conductivity value of 680 µS/cm compared to kitchen and bathing greywater sources which reported relatively low values of conductivity of 320 and 156 µS/cm, respectively. In this study, significant quality differences observed in conductivity could be effectively due to the characteristics of detergents in terms of quality or any solute contents dissolving in greywater. These findings are in agreement with Kotut et al. (2011) study on greywater pollutants, conductivity and high and low conductivity trends of laundry and both bathing and kitchen greywater sources, respectively. The ANOVA test which was undertaken to analyze existing differences within greywater sources and a significant difference amongst the three greywater sources at 0.05 statistical significance level was evident.

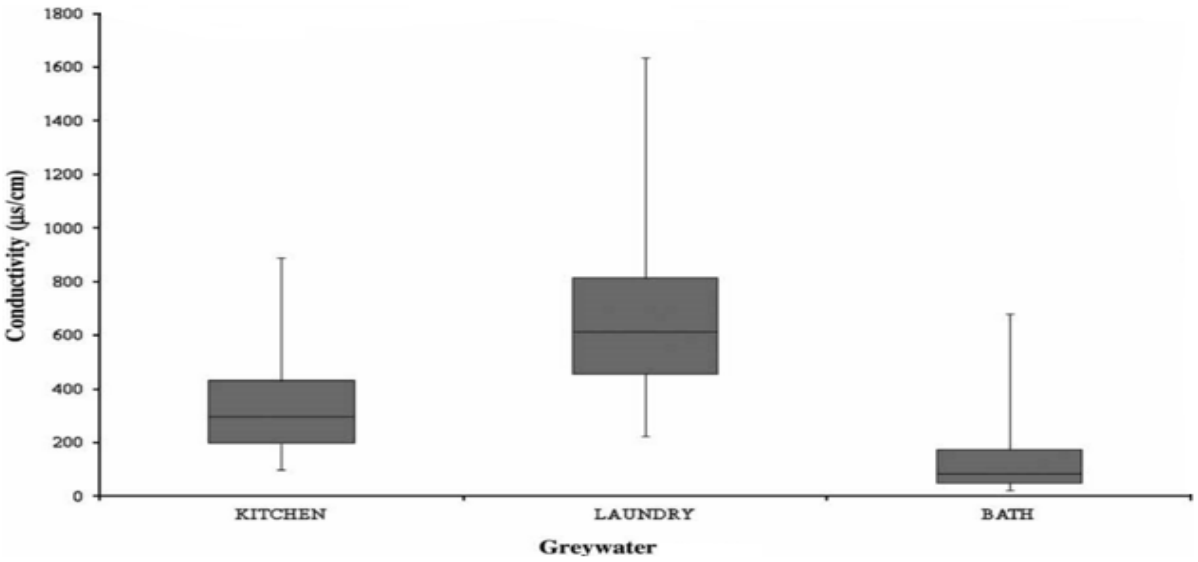

Figure 4-2: Experimental results on the comparison of conductivity values in bathing, kitchen and laundry greywater sources

Figure 4-3 presents experimental results on the comparison of pH level in bathing, kitchen and laundry greywater sources. The pH could be within the range of 5-12. As observed in the plot, the average pH within the three greywater sources showed basic characteristics and recorded a mean value of 8.35. Furthermore, the highest pH amongst the greywater sources was recorded in laundry greywater with an average value of 9.58. This can be attributed to the quality impact and the presence of detergents that could be alkaline in nature. The deposition of high concentration of alkaline detergents in greywater likely affected the pH level in greywater as can be observed in the study by Morel and Diener (2006). For the analysis of pH, a low value of pH of 6.25 was exhibited by kitchen greywater which could be attributed to the interaction on greywater source, chemical quality and low alkaline materials.

To this end, a low/high pH value could significantly have an effect on the acidity level of greywater. As observed in the plot, the bathing greywater source recorded a slightly lower pH of 9.24 than laundry greywater. In agreement with previous findings, the laundry greywater source will generally display high pH due to the presence of alkaline detergents (Oteng-Peprah et al., 2018). For the statistical analysis of pH amongst the three sources, an ANOVA test was conducted for the comparison of means; a significant level at 5% for the three greywater sources was consequently confirmed on the findings of conductivity.

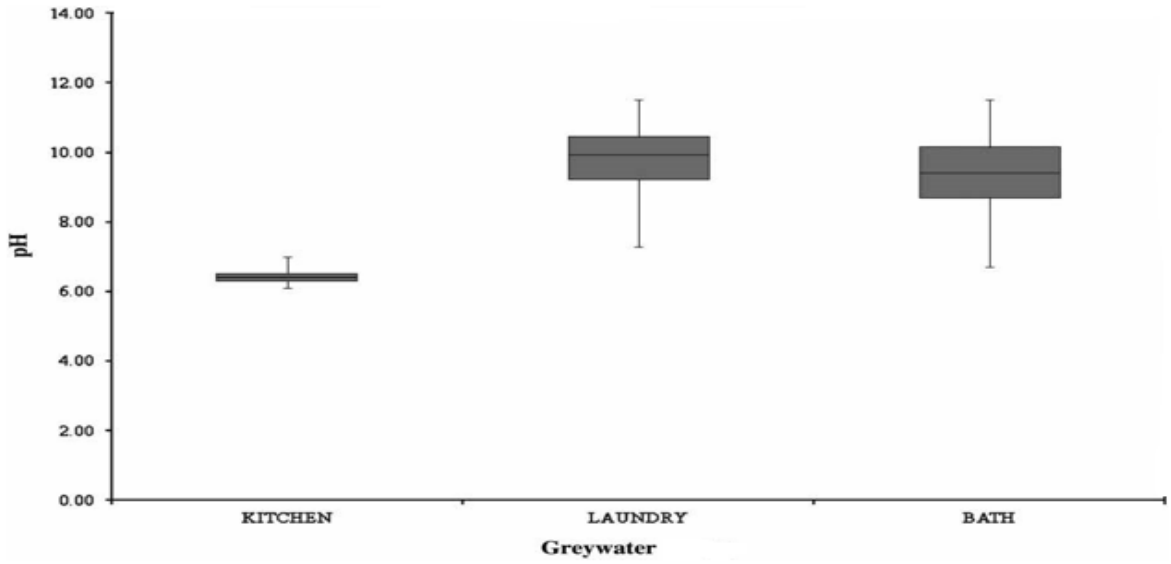

Figure 4-3: Experimental results on the comparison of pH values in bathing, kitchen and laundry greywater sources

Figure 4-4 depicts results on the comparison on greywater quality in terms of total solids for the analysis of the three greywater sources. Amongst the three greywater sources, the kitchen greywater source recorded the highest value of total solids of 3589 mg/l compared to laundry and bath greywater sources. Based on the plot, the lowest concentration of total solids were obtained in bathing greywater with a value of 504 mg/l followed by laundry greywater source with a value of 736 mg/l. It is important to note that high concentrations of total solids in greywater is directly associated with the nature of washing activities in kitchen sinks, hand basin and dishwashers including detergents, fats and food matter/particles. As a result and compared to other greywater sources, the kitchen greywater will tend to have high total solids due to high levels of contamination/solids contained in it (Oteng-Peprah et al., 2018). For the total solids, the statistical analysis of ANOVA test was carried out within the three greywater sources using 5% significant level and the ANOVA test confirmed significant difference on total solids within the three greywater sources.

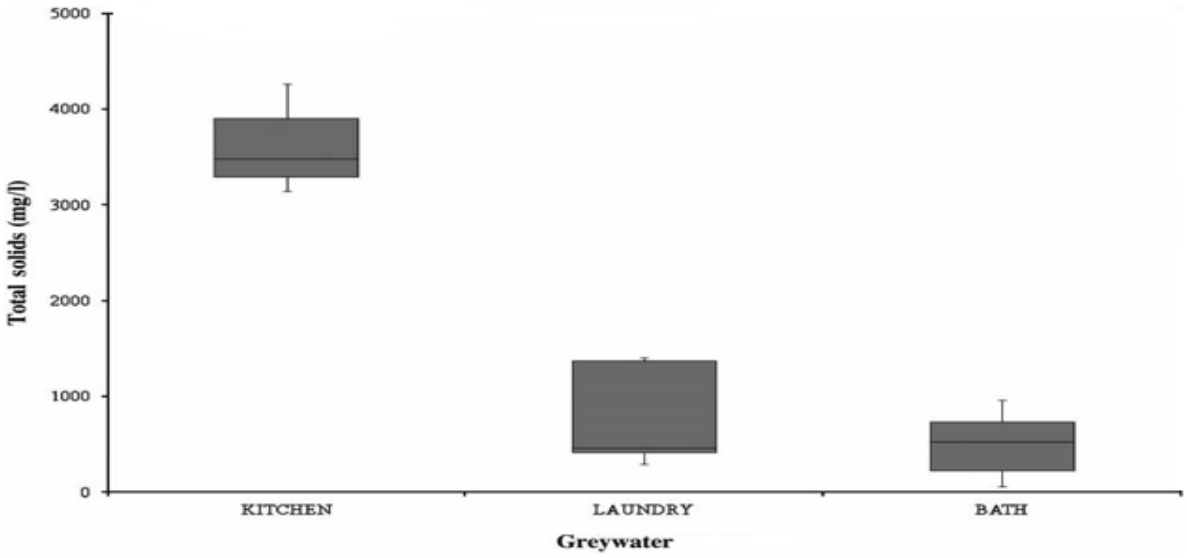

Figure 4-4: Experimental results on the comparison of total solids in bathing, kitchen and laundry greywater sources

The graphical plot in Figure 4-5 compares mean variation of BOD findings in kitchen, bathing and laundry greywater sources. In greywater, the analysis of BOD is useful and provides the insight on the amount of oxygen used by microorganisms to degrade organic matter present under aerobic settings (Morel and Diener, 2006). Based on the plot, a BOD value of 604.5 mg/l was obtained in greywater sources originating from kitchen which was far above laundry and bathing greywater sources. The observed trend in BOD could be attributed to a higher level of organic matter present in kitchen greywater than the other two greywater sources (Morel and Diener, 2006). The BOD content in laundry greywater was 413.75 mg/l and the smallest value of BOD obtained in greywater originating from the bath was 185.25 mg/l. The low biodegradability ratio for the three greywater sources was obtained ranging from 0.13 to 0.29, therefore indicating non-biodegradability of most of the organic matter in greywater sources. The statistical analysis of an independent ANOVA test of means was conducted in order to investigate the significant difference observed in greywater sources. The statistical test showed the existence of significant difference in greywater sources at a p-value below 0.05.

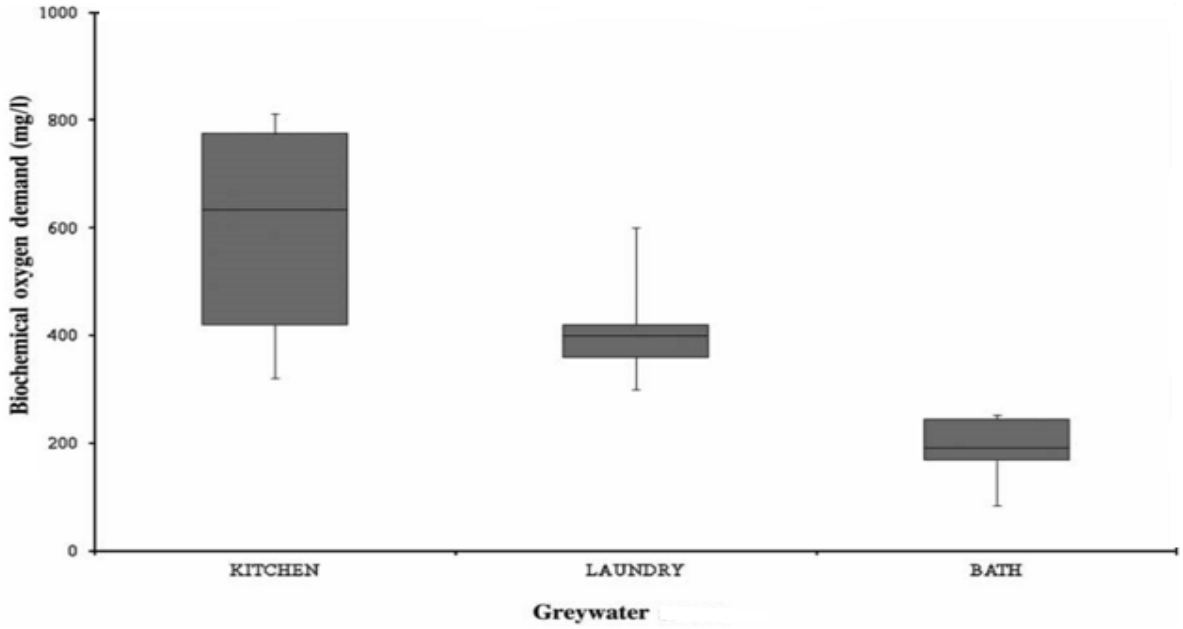

Figure 4-5: Experimental results on the comparison of BOD values in bathing, kitchen and laundry greywater sources

Figure 4-6 presents COD results after characterization of various parameters in kitchen, laundry and bathing greywater sources. The quantitative analysis of COD in greywater is a useful indicator of the amount of oxygen content required to oxidize pollutants present in greywater due to the presence of organic and inorganic substances. Based on COD results, the dominance of COD content in kitchen and laundry greywater was evident with an average COD value of 2074.5 and 1628 mg/l, respectively. In this study, the factor of high COD value obtained in greywater originating from kitchen could be a function of the organics and physical pollutants present in kitchen greywater. As shown in Figure 4-6, the less polluted sample with the lowest value of COD was observed in greywater source originating from the bath with an average COD of 1426.37 mg/l. Also, the trend in average COD observed in bathing greywater could be attributed to a low level of contamination. The significant difference in greywater sources was confirmed by an ANOVA test which was obtained at a 0.05 significant level.

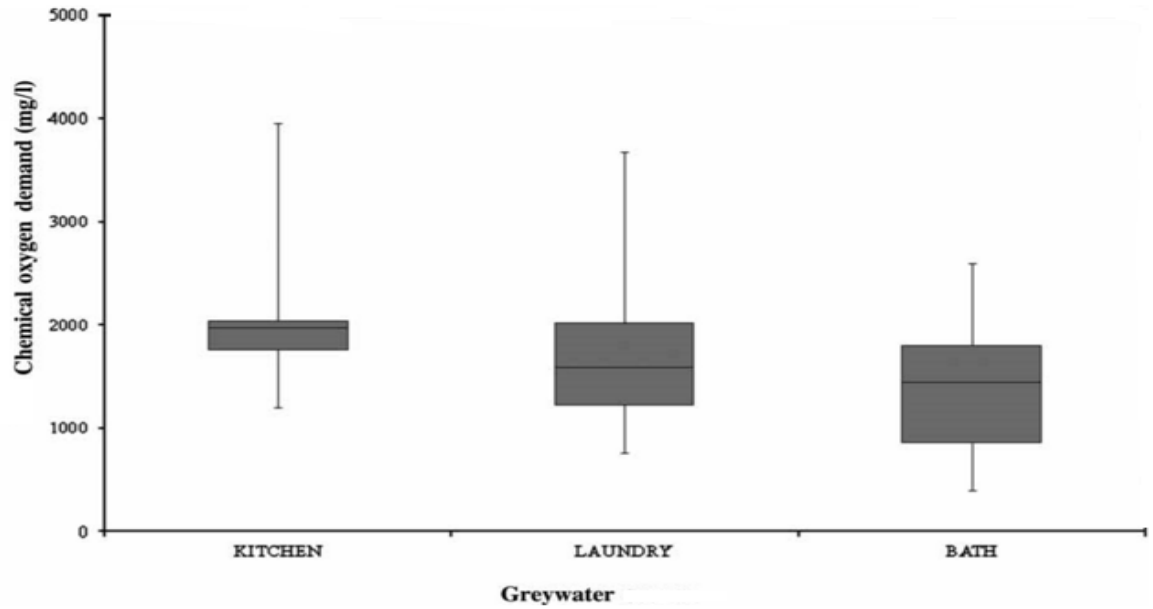

Figure 4-6: Experimental results on the comparison of COD values in bathing, kitchen and laundry greywater sources

The pollutants such as total coliforms and E. coli can cause significant effects in human health particularly in human beings in contact with contaminated domestic greywater (Shi et al., 2018). Figure 4-7 presents the characteristics of greywater influent in terms of microorganisms, the E. coli and total coliforms as biological indicator parameters of greywater quality. The existence of biological pollutants were detected in greywater samples following the analysis of 30 samples of greywater. In this analysis, the E. coli ranged between 0-39 CFU/ml with an average value of 6.6 CFU/ml while the total coliforms ranged between 0-19 CFU/ml with a mean value of 4.5 CFU/ml. Also, the E. coli in greywater was detected greywater samples including total coliforms, thus indicating the level of contamination in greywater samples, particularly, the presence of pathogenic bacteria/microbes.

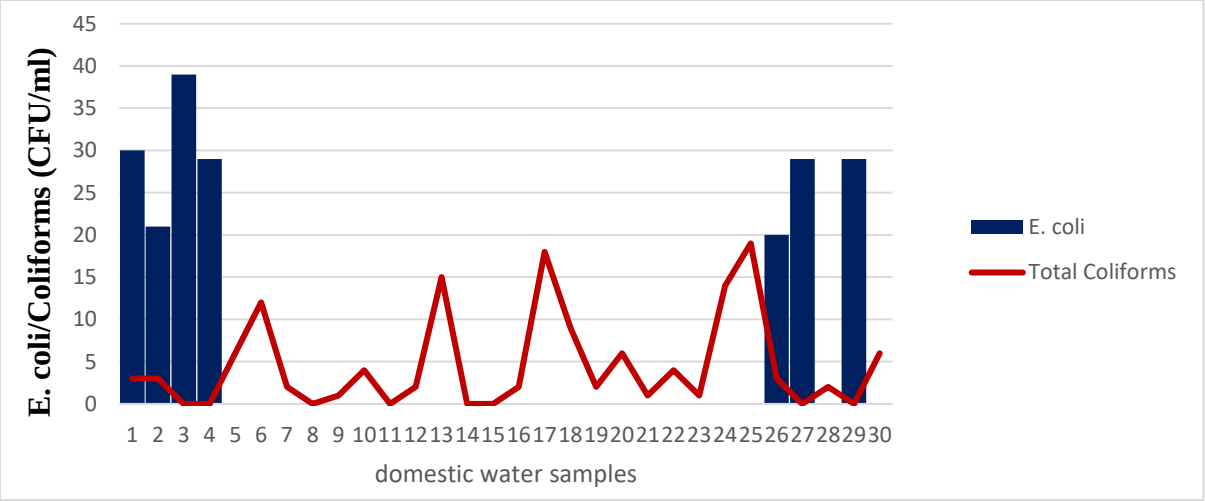

Figure 4-7: Experimental results on the analysis of pathogenic matter in terms of E. coli and total coliforms in domestic greywater

Chapter 5

Results on the operation of a HRF equipment

5.1 The performance of a HRF equipment for the treatment of domestic greywater

This section discusses published findings on domestic greywater characteristics and its qualitative assessment which was investigated through the application of HRF technology as it is used as a treatment unit for domestic greywater. The performance of the HRF system was investigated using physico-chemical parameters and microbiological parameters following domestic greywater treatment. The removal efficiency based on different influent and effluent measured parameters was evaluated and the parameters were turbidity, conductivity, COD, solids, E. coli and total coliforms. Figure 5-1 presents the findings on the influent-effluent turbidity profiles obtained after domestic greywater treatment. The HRF was able to remove large amount of turbidity by removing large suspended particles and other contaminants present in the water. As shown in the plot, the HRF was significantly effective in removing turbidity in the effluent stream from high turbidity concentrations in the influent stream.

Moreover, the average reduction of turbidity in HRF was relatively high with a mean value of 90% from the influent turbidity ranging from a value of 156 to 420 NTU. The effluent quality in terms of turbidity was highly improved up to the range of 14 to 53 NTU. In this work, the statistical matched pair *t*-test was conducted to investigate and analyze the significant difference on average mean on turbidity and the difference was significant at 5% significant level. The good removal of turbidity obtained in a HRF could be largely attributed to the effective filtration process and increased filter retention with low filtration within the HRF unit (Wegelin, 1996).

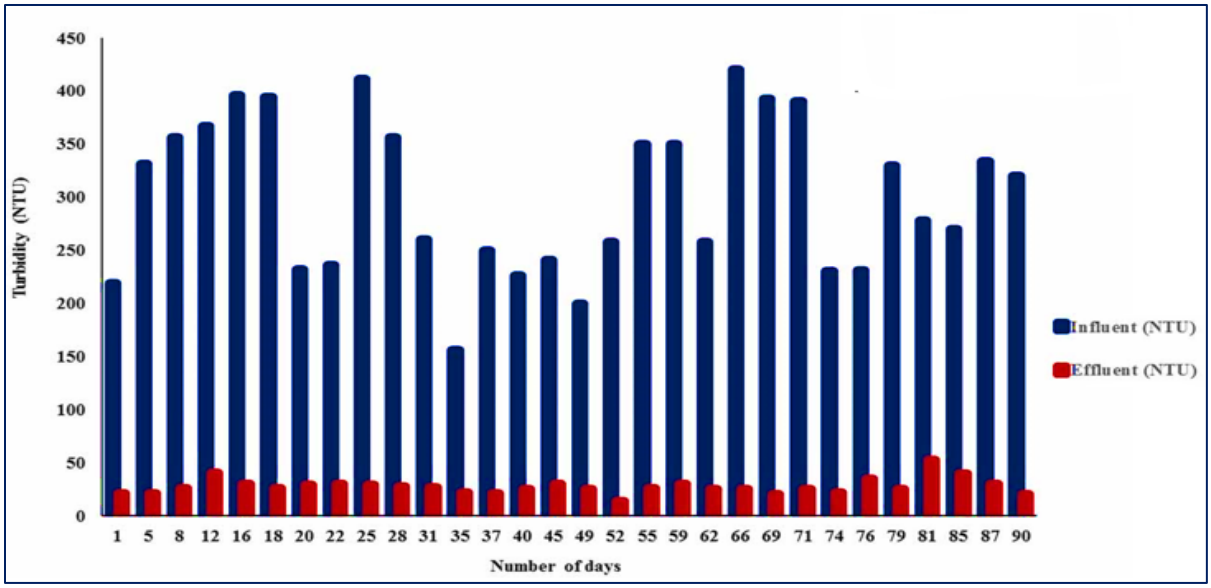

Figure 5-1: Greywater influent and effluent treatment results in terms of turbidity profile over time within a HRF equipment operated at a fixed filtration rate of 0.3 m/hr

The removal of chemical pollutants in HRF is an important step for improving quality of greywater in any water treatment process. Figure 5-2 shows the comparison of COD removal for the influent and effluent streams of greywater after performing the treatment in a HRF which was investigated at a filtration rate of 0.3 m/hr. As shown in the plot, the reduction of COD in the effluent stream of domestic greywater from the HRF was evidently recorded. The trend also shows high COD contents in the influent domestic greywater samples ranging from 1020-2640 mg/l. This relates to chemical quality of greywater with the presence of chemical matter in domestic greywater. The lowest COD values were obtained in the effluent stream greywater after the occurrence of filtration process in a HRF system. Also, the COD obtained in the outlet stream was lower than the influent stream with COD content in range between 304 and 806 mg/l and the average COD reduction of 50-70% was subsequently attained and this was confirmed by *t*-test and the significant difference on COD was obtained at a p-value below 0.05.

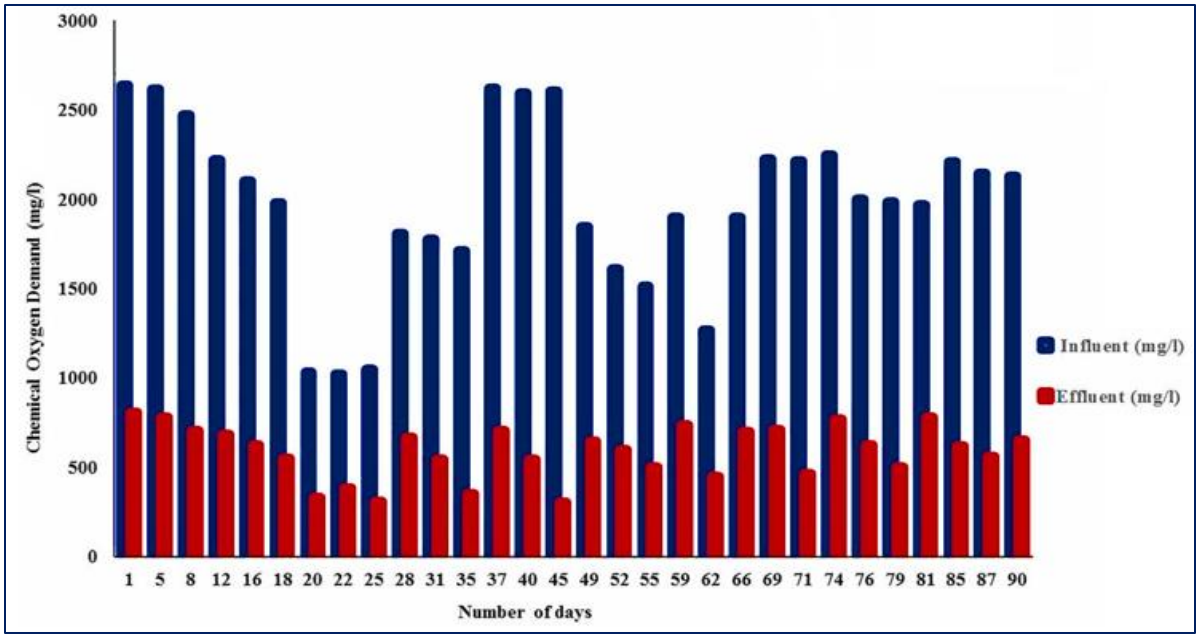

Figure 5-2: Greywater influent and effluent treatment results in terms of COD profile over time within the HRF equipment operated at a fixed filtration rate of 0.3 m/hr

A significant removal efficiency on conductivity of 86% was obtained in a HRF. Figure 5-3 shows the conductivity trends of the influent and effluent streams after domestic greywater treatment in HRF. As an indicator of total dissolved matter, the conductivity patterns in Figure 5-3 showed that the reduction on conductivity was obtained in the effluent stream following domestic greywater treatment. The conductivity in the range between 95-420 µS/cm was obtained with the reduction of conductivity in the effluent stream while the conductivity in the inlet stream showed a much higher range between 1055 and 2591µS/cm. The statistical *t*-test on conductivity was analyzed and the significant difference was confirmed at 0.05 significant level. For this water quality parameter, the significant reduction on conductivity within the HRF could correlate with effectiveness of the filtration mechanism and dissolved matter in greywater.

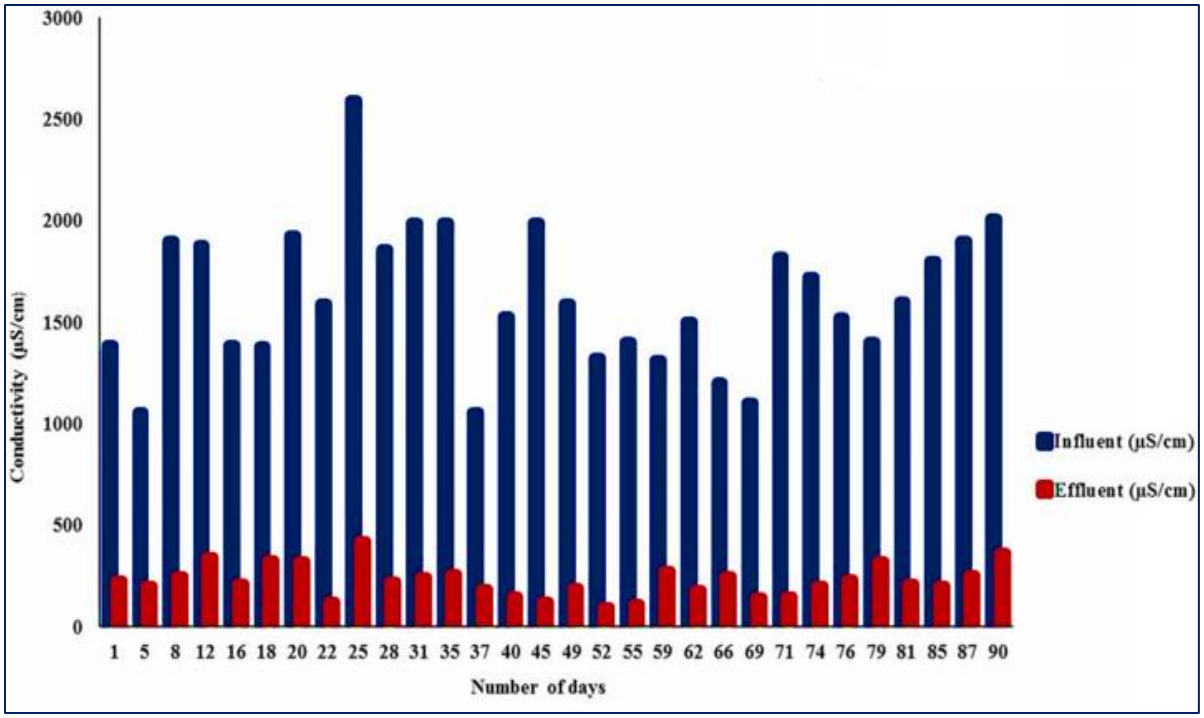

Figure 5-3: Greywater influent and effluent treatment results in terms of conductivity profile over time within a HRF equipment operated at a fixed filtration rate of 0.3 m/hr

Figure 5-4 shows graphical comparison on reduction of total solids of domestic greywater from the HRF. The plot shows high total solids in the influent stream prior to the actual treatment in HRF and the significant reduction of total solids in the effluent stream was evident after the treatment in HRF was effected. The reduction for total solids after treatment was between 95-350 mg/l compared to the influent which ranged between 1055 to 1847 mg/l. Also, the effectiveness of the HRF was evident with high percentage reduction of total solids in the effluent stream of up to 84%. The statistical test for the analysis of total solids based on matched pair *t*-test was applied in order to analyze the observed mean difference in total solids within the roughing filtration equipment. As a result, a significant reduction of total solids within the HRF was obtained at a probability level of 5%. In agreement with the removal/operation mechanism of matter in HRFs, the reduction of total solids following water treatment is essential for meeting effluent quality standards and this can be attributed to good filtering capacity and settling activity (Wegelin, 1996).

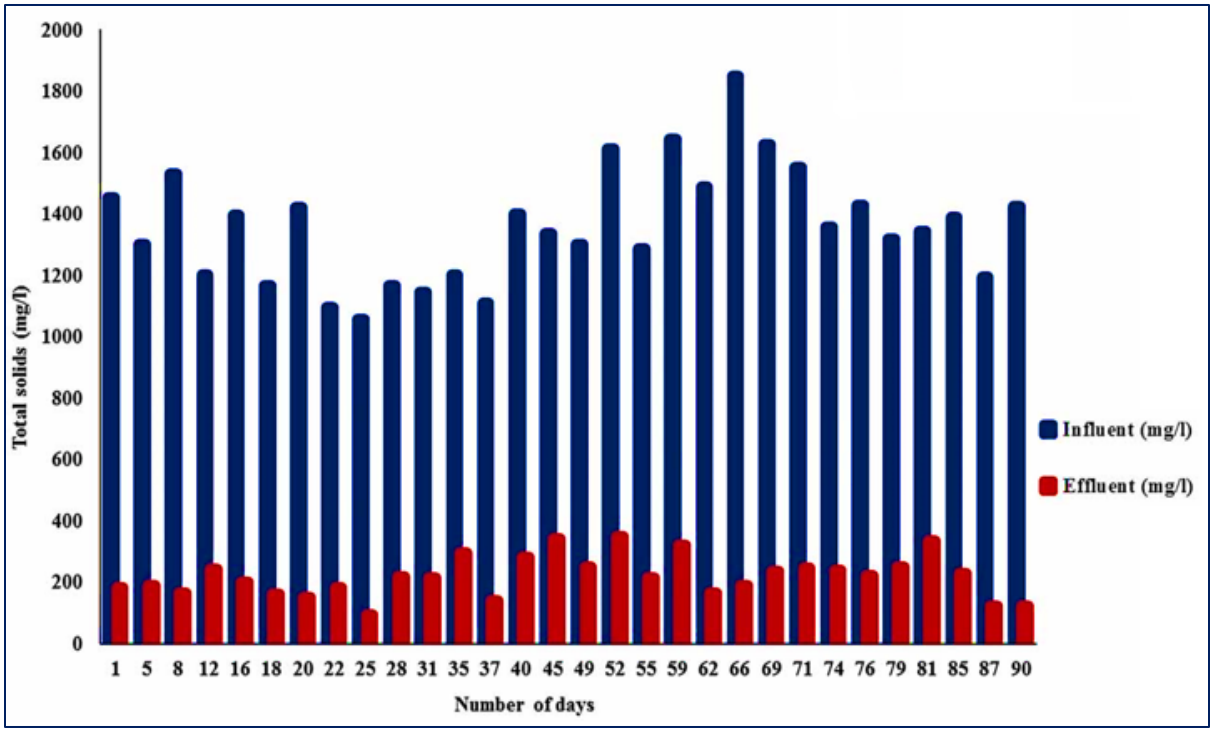

Figure 5-4: Greywater influent and effluent treatment results in terms of total solids over time within a HRF equipment operated at a fixed filtration rate of 0.3 m/hr

Figure 5-5 shows the E. coli profile for the influent and effluent mixed greywater samples. The removal of E. coli ranged between 10 and 87% within the HRF for the 30 samples of greywater that were analyzed for the presence of E. coli. Although the HRF showed significant capability of reducing E. coli in greywater samples, the greywater quality can be highly improved in terms of removal efficiency with further water treatment steps and suitable water treatment processes of greywater in order to ensure that water meets greywater reuse standards. In water, the complete removal of microorganisms including E. coli is extremely important in terms of health and good water quality standards (Oteng-Peprah et al., 2018). Meanwhile, the presence of E. coli is undesirable in water as it is associated with faecal pollution content in water.

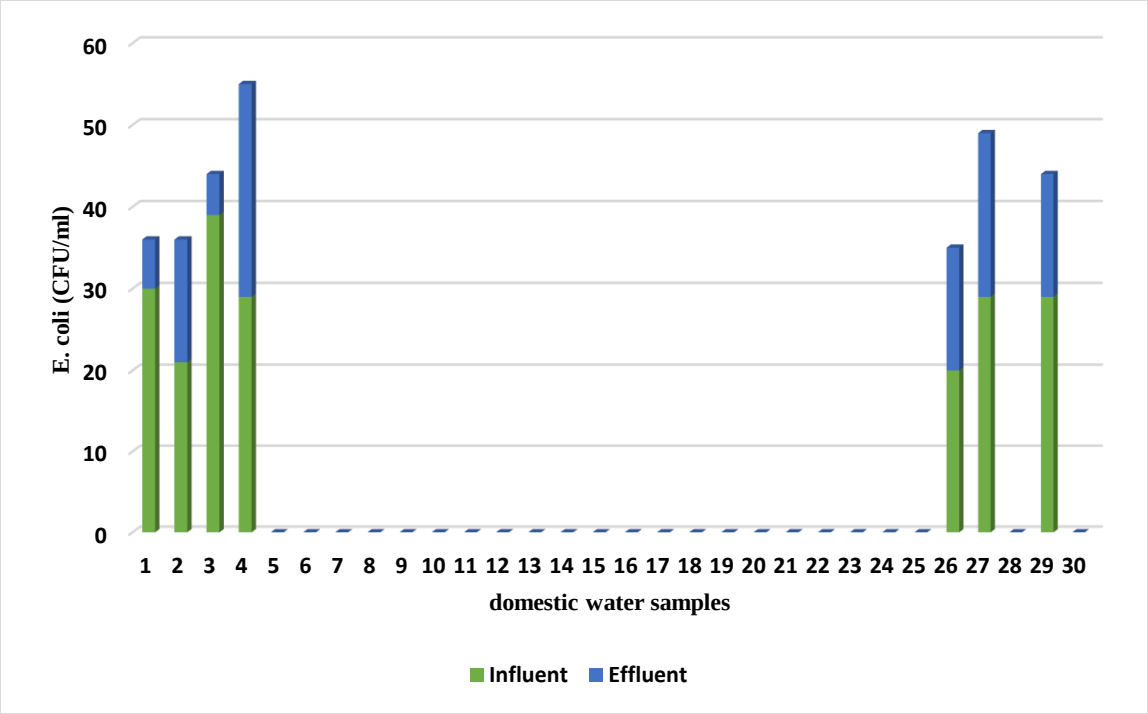

Figure 5-5: The HRF performance in terms of E. coli removal in domestic greywater samples

Figure 5-6 presents the total coliforms in the HRF equipment and the effectiveness of the HRF equipment was highly evident. The removal of total coliforms obtained in HRF was significantly high as shown in Figure 5-6 and in terms of performance, the observed absence of total coliforms in the effluent stream typically confirms the effectiveness and the capability of roughing filtration to deal with microorganism pollutants (Dastanaie et al., 2007; Gross et al., 2007). The amount of total coliforms in greywater is an indirect indicator of the presence of faecal content in greywater and it remains highly useful in terms of assessment of health and hygiene risk related to greywater reuse. Based on the findings of the study, the HRF performance in terms of removal of some of the parameters including turbidity, conductivity, pH and microbes was in accordance with greywater reuse standards for irrigation and toilet flushing as outlined by Rodda et al. (2010b).

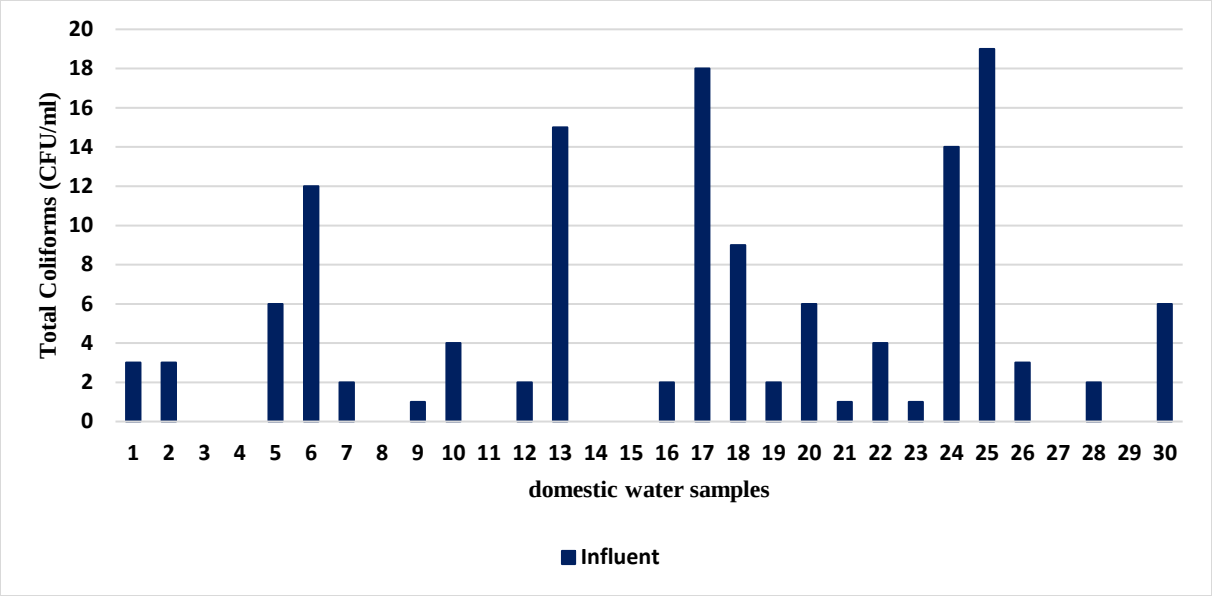

Figure 5-6: The HRF performance in terms of the removal of the total coliforms in domestic greywater samples

5.2 Investigation of the controlling and design variables of the HRF equipment

This section focuses on the findings of the design of experiments, principles and algorithms related to filter performance in the HRF. The controlling factors with design matrix for all design factors of the study are shown below with the total number of runs and the response variable which is the average turbidity from the HRF following filtration runs. The influential effect of these factors on response turbidity was studied with a total of 32 experimental runs that were conducted.

Table 5.1: Factorial design matrix for turbidity removal (%)

Standard order	Factorial design variables				
	A	B	C	D	E
1	-1	-1	1	1	1
2	1	1	1	1	-1
3	-1	-1	1	1	-1
4	1	-1	-1	-1	-1
5	1	-1	-1	1	1
6	1	-1	1	-1	-1
7	-1	1	1	1	1
8	1	1	-1	-1	1
9	1	1	-1	-1	-1
10	1	1	1	1	1
11	1	1	-1	1	-1

12	1	-1	1	1	-1
13	1	1	1	-1	-1
14	-1	-1	-1	-1	1
15	-1	-1	-1	1	1
16	1	-1	1	1	1
17	-1	-1	-1	-1	-1
18	1	1	-1	1	1
19	-1	1	-1	1	-1
20	-1	-1	1	-1	-1
21	1	1	1	-1	1
22	-1	1	1	1	-1
23	1	-1	-1	-1	1
24	1	-1	-1	1	-1
25	-1	1	-1	-1	1
26	-1	1	-1	1	1
27	-1	1	1	-1	1
28	-1	-1	1	-1	1
29	-1	-1	-1	1	-1
30	-1	1	-1	-1	-1
31	-1	1	1	-1	-1
32	1	-1	1	-1	1

Table 5.2 presents results on significant controlling factors of the HRF that were investigated using two level factorial DOE. In this study five factors with 31 degrees of freedom were studied. Results show the relationship between independent factors and response variables and examines significant factors, the linear, 2-way and quadratic interactions within this study through analysis of ANOVA. The analysis of ANOVA was also used for the evaluation at 95% confidence limits. Other useful statistical parameters for computation of ANOVA such as the adjusted sum of squares, adjusted mean square including F-test statistics are presented along with p-values.

The significant factors considered for the removal of turbidity at low and high levels were gravel media, filtering bed, filter length and filtration rate. Factor E was not significant at a 0.05 probability level. Also, the regression assumptions were met based on an adequacy check criteria which was assessed by R^2 and adjusted R^2 with large values observed (Phanphet et al., 2018).

Table 5.2: Experimental results of the ANOVA test for the removal of turbidity (%)

Source	DF	Adj SS	Adj MS	F-Value	P-Value
Model	15	11407,7	760,51	1106,20	0,000
Linear	5	7296,7	1459,33	2122,66	0,000
A	1	1092,8	1092,78	1589,50	0,000
B	1	504,0	504,03	733,14	0,000
C	1	1582,0	1582,03	2301,14	0,000
D	1	4117,8	4117,78	5989,50	0,000
E	1	0,0	0,03	0,05	0,834
2-Way Interactions	10	4111,1	411,11	597,97	0,000
A*B	1	195,0	195,03	283,68	0,000
A*C	1	472,8	472,78	687,68	0,000
A*D	1	1845,3	1845,28	2684,05	0,000
A*E	1	1,5	1,53	2,23	0,155
B*C	1	1237,5	1237,53	1800,05	0,000
B*D	1	87,8	87,78	127,68	0,000
B*E	1	148,8	148,78	216,41	0,000
C*D	1	0,8	0,78	1,14	0,302
C*E	1	69,0	69,03	100,41	0,000
D*E	1	52,5	52,53	76,41	0,000
Error	16	11,0	0,69		
Total	31	11418,7			

R-sq(R^2) = 99.90; R-sq (Adj) = 99.81; R-sq(Pred) = 99.61

Figure 5-7 presents a Pareto chart of effects which shows five main effects A, B, C, D and E including 2-factor interactions. The t-value obtained was 2.12 on the Pareto chart of standardized effects as shown in Figure 5-7. The plot shows that the main effect A, B, C and D had significant effects on the removal of turbidity at 5% significance level while effect E was insignificant. The significant 2-factor interactions at 5% significance level were AD, BC, AC, AB, BE, BD, CE and DE while AE and CD were not significant at p-value of 5%.

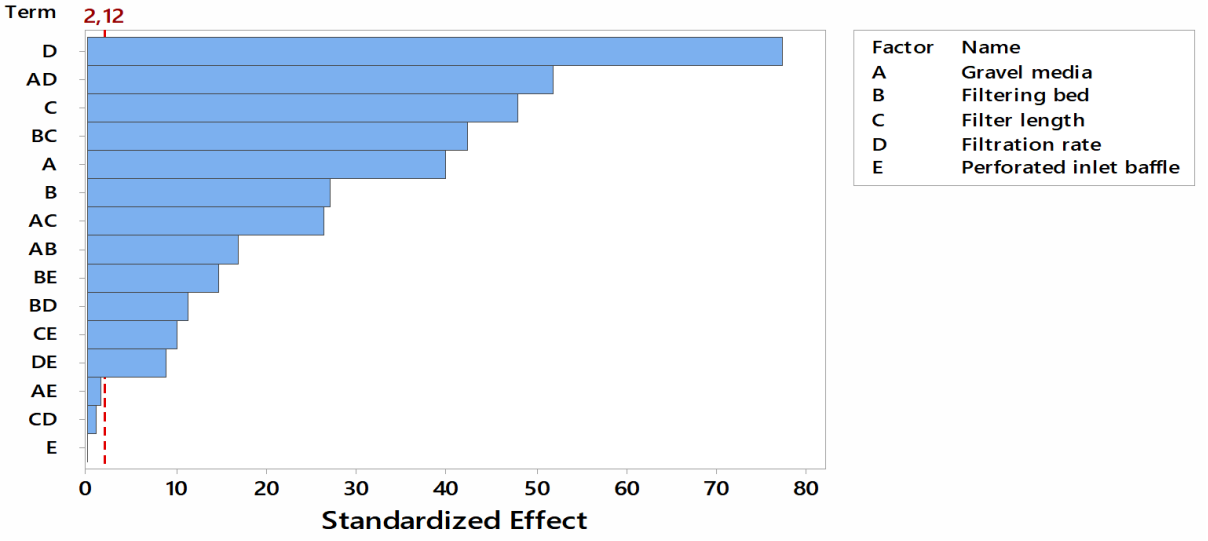

Figure 5-7: The Pareto chart of the standardized effects, response is % removal at a significant level of 5%

Figure 5-8 depicts the half normal probability plot of standardized effect for the removal of turbidity which is useful to evaluate the magnitude and the significance of the effects. The results of the studied effects and interactions could be significant or insignificant as shown in Figure 5-8. The four statistical significant factors at 0.05 level were A, B, C and D and compared to other factors, the largest effect was due to filtration rate as shown in the plot. The significant 2-way interactions at 0.05 statistical significance level were AD, BC, AC, AB, BE, BD, CE and DE. Amongst the significant interactions, the largest 2-way interaction was due to AD.

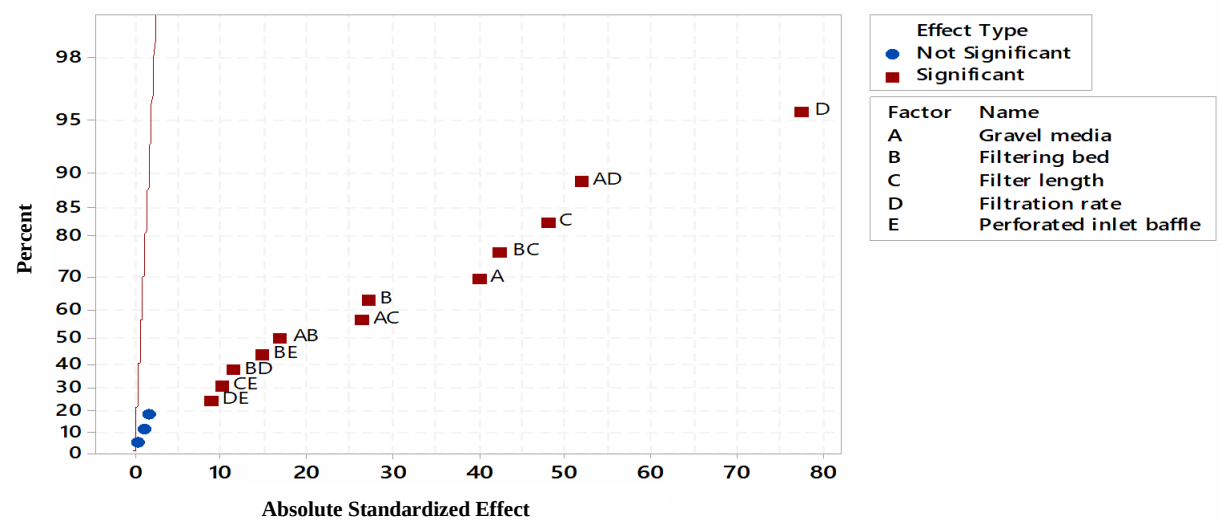

Figure 5-8: Half normal plot of standardized effects, response is % removal at p-value of 0.05

Figure 5-9 represents the histogram of residuals that show the distribution of residuals of all observations. This plot is useful to evaluate the characteristics of residuals and the concept of normality of residuals in the experimental data. Figure 5-9 essentially shows a bell shaped curve which suggests that the errors did not show any deviations from the symmetric bell-shape but characteristics of normal distribution and mean zero were evident. This suggest that the experimental data clearly met the normality assumptions.

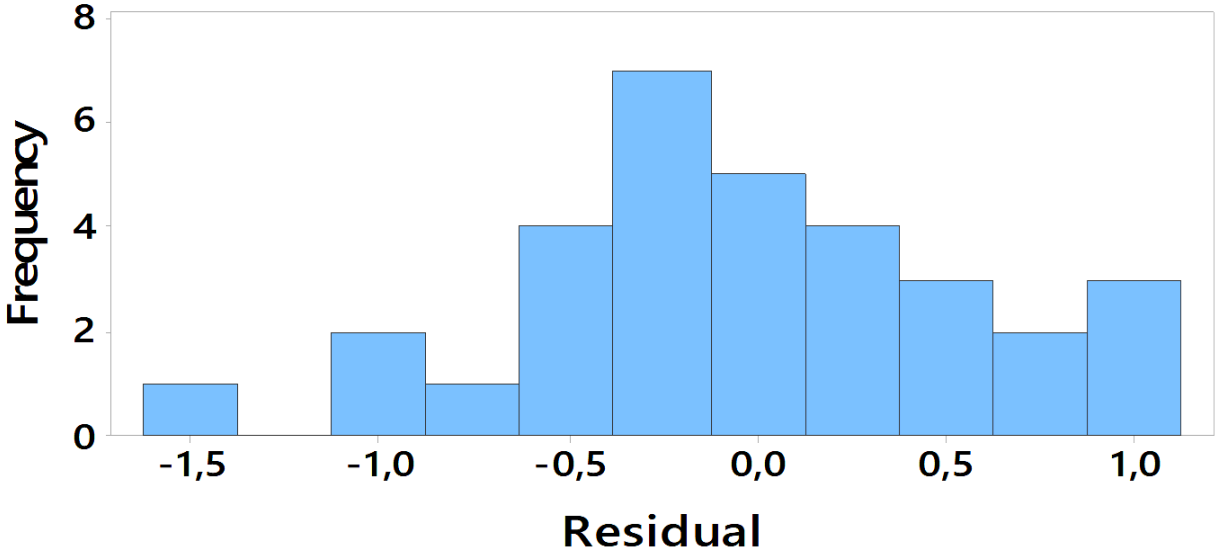

Figure 5-9: The histogram plot of residuals indicating the distribution of residuals of observations

A graphical plot showing residuals against fitted values was produced in order to evaluate randomness and constant variance assumptions (Figure 5-10). The graph is a scatter plot of the standardized residuals against the fitted value. The plot is a good indicator of the randomness of the residuals and the spread of residual values with fitted values. Based on Figure 5-10, it can be observed that a random pattern of residuals on both sides of the zero line existed and were valid. The plot further shows no recognizable pattern in the residuals therefore suggesting validity of constant variance assumptions.

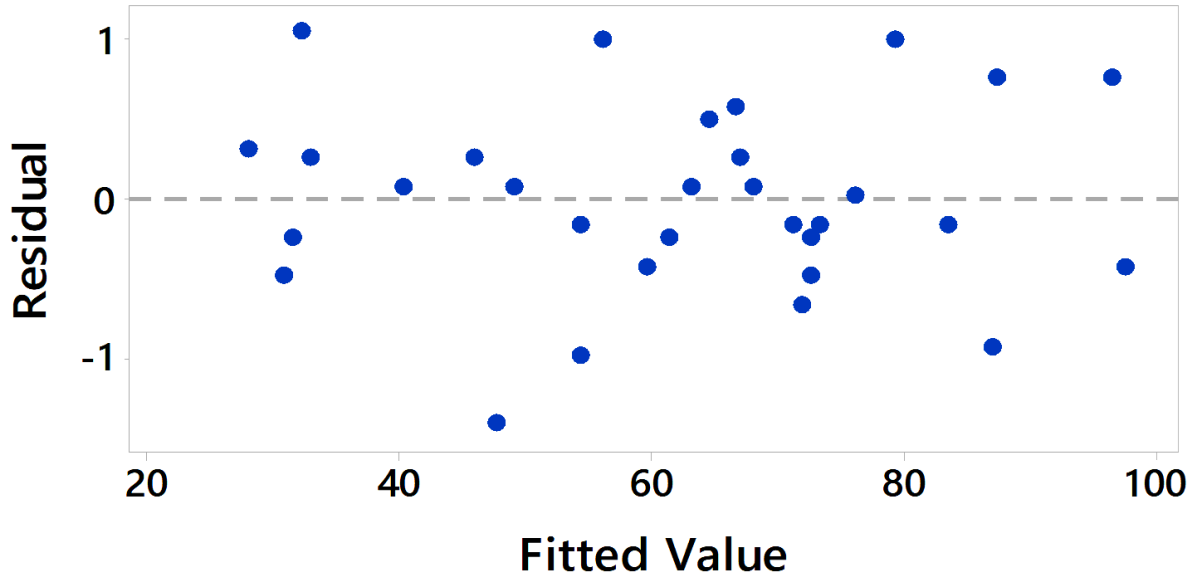

Figure 5-10: A scatter plot of the standardized residuals with fitted values

Figure 5-11 shows the normal probability plot of residuals that were constructed for validation of the assumption of normality in data. The normal plot is a useful graphical technique to evaluate the normality of the data through plotting normal probability of residuals. The difference between predicted and observed values will be the residuals. As shown in Figure 5-11, the normality plot showed that the residuals were reasonably aligned with the straight line which suggest that the experimental data came from the normal population.

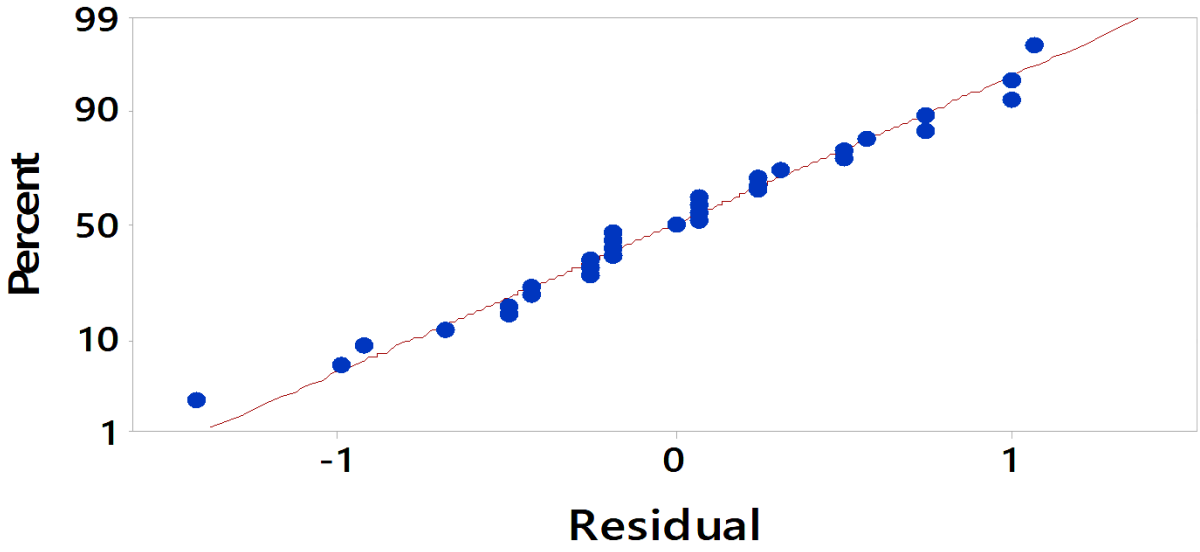

Figure 5-11: The normal probability plot between predicted and observed values (residuals)

Figure 5-12 presents another useful graphical plot of positive and negative residuals plotted against observation order with the aim to examine the assumption that residuals are fully independent from one another. From the graphical plot, it can be observed that the residuals had no obvious trends displayed on the residuals but maintained a random order on either side of the zero line. This verifies the assumption that the residuals versus order were independent from one another.

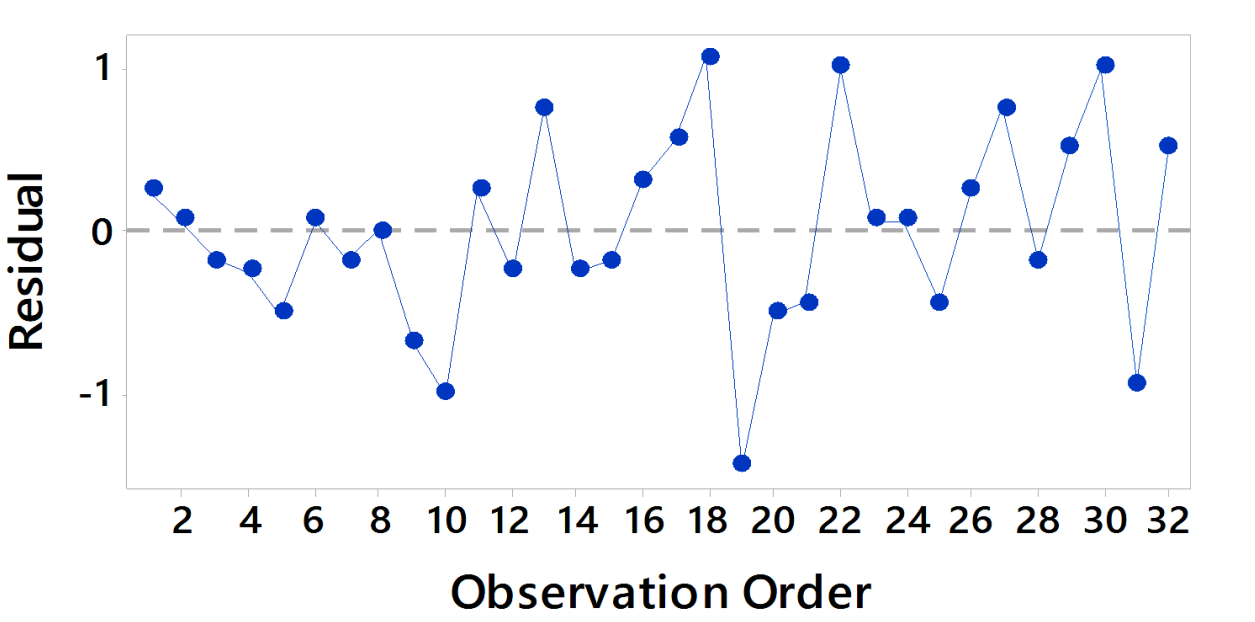

Figure 5-12: The plot of positive and negative residuals with the number of observation order

5.3 The optimization of a HRF equipment using DOE/RSM

This section deals with the mathematical approach used to gain an understanding of the operational aspect of the roughing filter and the approach used for the operation of the horizontal roughing filter. The central composite design set up is presented in Table 5.3 with the number of runs, experimental factors for the predicted and experimental results of the response variable. In this study, each factor was coded into three levels in design matrix as -1, 0 and +1 and the dependent variable was effluent turbidity from the HRF equipment. Based on the RSM, the repeated runs at the central point, the factor settings and response values were carried out through experimental work as outlined in Table 5.3

Table 5.3: The design matrix and experimental factors of RSM with error predictions

Std Order	Run	A	B	C	D	Predicted efficiency	Experimental efficiency	Error (%)
28	1	0	0	0	0	76.2	75.4	1.06
11	2	-1	1	-1	1	72.4	72.6	0.27
3	3	-1	1	-1	-1	73.3	73.3	0.00
4	4	1	1	-1	-1	73.9	74.0	0.14
18	5	2	0	0	0	71.9	72.0	0.14
31	6	0	0	0	0	76.2	76.6	0.52
6	7	1	-1	1	-1	75.0	75.0	0.00
26	8	0	0	0	0	76.2	76.6	0.52
5	9	-1	-1	1	-1	75.9	76.0	0.13
16	10	1	1	1	1	72.7	73.0	0.41
10	11	1	-1	-1	1	70.5	70.4	0.14
21	12	0	0	-2	0	72.0	72.0	0.00
23	13	0	0	0	-2	75.9	76.0	0.13
27	14	0	0	0	0	76.2	75.8	0.53
25	15	0	0	0	0	76.2	76.8	0.78
30	16	0	0	0	0	76.2	76.9	0.91
9	17	-1	-1	-1	1	74.1	74.3	0.27
29	18	0	0	0	0	76.2	75.5	0.93
12	19	1	1	-1	1	70.1	70.0	0.14
8	20	1	1	1	-1	75.2	75.0	0.27
24	21	0	0	0	2	72.1	72.0	0.14
17	22	-2	0	0	0	75.2	75.0	0.27
20	23	0	2	0	0	73.5	73.5	0.00
7	24	-1	1	1	-1	74.7	75.0	0.40
22	25	0	0	2	0	75.1	75.0	0.13
15	26	-1	1	1	1	75.1	75.0	0.13
14	27	1	-1	1	1	72.1	72.0	0.14
13	28	-1	-1	1	1	75.9	76.0	0.13
19	29	0	-2	0	0	75.0	75.0	0.00
1	30	-1	-1	-1	-1	75.5	75.4	0.13
2	31	1	-1	-1	-1	74.7	74.7	0.00

The RSM allowed investigation and determination of the relationship between variables and assessment of response variable as a function of independent variables. All experiments were analyzed as per the CCD experimental design matrix with recorded experimental and observed turbidity removal. Experiments were conducted in triplicates using all design points. The model performance related to the accuracy, reliability, the correlation between the observed and predicted data and error variances were extracted using diagnostic plots.

After considering and assessing significant variable terms, the predicted response (y) for the HRF efficiency could be mathematically expressed with the following second order polynomial coded equation 5.1:

$$\text{Efficiency} = 76.23 - 0.8125\times A - 0.3708\times B + 0.7625\times C - 0.9625\times D + 0.3563\times AB - 0.0312\times AC - 0.7187\times AD + 0.2438\times BC + 0.1063\times BD + 0.3188\times CD - 0.6749\times A^2 - 0.4874\times B^2 - 0.6749\times C^2 - 0.5499\times D^2 \quad (5.1)$$

Table 5.4 presents ANOVA results for the fitted quadratic polynomial for the removal of turbidity. The fitted polynomial was found to be significant at 95% confidence level by the F-test static and with all p-values of regression ≤ 0.05. In addition, the accuracy in terms of the lack of fit at a significant level of 5% was found insignificant as shown in Table 5.4. A measure of the model's overall performance using R^2 coefficient of determination was obtained to be 0.9727 which is much higher and close to a value of 1. Furthermore, it was observed that R^2 adjusted coefficient of determination was 0.9488 and the R^2 predicted coefficient of determination recorded was 0.9477 which is in agreement with the adjusted coefficient of determination as shown in Table 5.4. All terms of the model can be observed to be statistical significant and the significance of each term/coefficient was obtained through F-value and p-value. The turbidity removal showed a strong dependency as a function of the independent variables with significant level below 5% and quadratic terms were significant at $p < 0.05$.

Table 5.4: The ANOVA test results of fitted quadratic response surface model for the HRF

Source	Sum of Squares	df	Mean Square	F-value	p-value
Model	100.12	14	7.15	40.74	0.0001
A-Gravel	15.84	1	15.84	90.26	0.0001
B-Bed height	3.30	1	3.30	18.80	0.0005
C-Length	13.95	1	13.95	79.50	0.0001
D-Flowrate	22.23	1	22.23	126.67	0.0001
AB	2.03	1	2.03	11.57	0.0037
AC	0.0156	1	0.0156	0.0890	0.7693
AD	8.27	1	8.27	47.09	0.0001
BC	0.9506	1	0.9506	5.42	0.0334
BD	0.1806	1	0.1806	1.03	0.3255
CD	1.63	1	1.63	9.26	0.0077
A^2	13.02	1	13.02	74.19	0.0001
B^2	6.79	1	6.79	38.69	0.0001
C^2	13.02	1	13.02	74.19	0.0001

D^2	8.65	1	8.65	49.25	0.0001
Residual	2.81	16	0.1755		
Lack of Fit	0.3542	10	0.0354	0.0866	0.9995
Pure Error	2.45	6	0.4090		
Cor. Total	102.93	30			

R-Squared: 0.9727; R-Squared Adj.: 0.9488; R-Squared Pred.: 0.9477; Adeq. Std.Dev.: 0.4190; Mean: 74.38; C.V.%: 0.5633; Precision: 20.8718

Figure 5-13 presents the profile for the quadratic response surface in a form of a graphical plot representing the effect of gravel media size and flowrate in the optimization of turbidity removal. The response surface plot presented a surface with a maximum removal efficiency. The removal increased within the HRF as the flowrate and gravel approached decreasing trends. The high removal of turbidity was 77% with low gravel media sizes and low filtration rate. Wegelin (1996) reported higher filter performance in roughing filters with low filtration rates and gravel media fractions. A decreasing trend or low efficiency of turbidity removal with the effect of gravel and flowrate was observed in this study with the application of coarse gravel media size and increased filtration rate. Therefore, low filtration rate and gravel media size favored high effective removal of turbidity within the HRF.

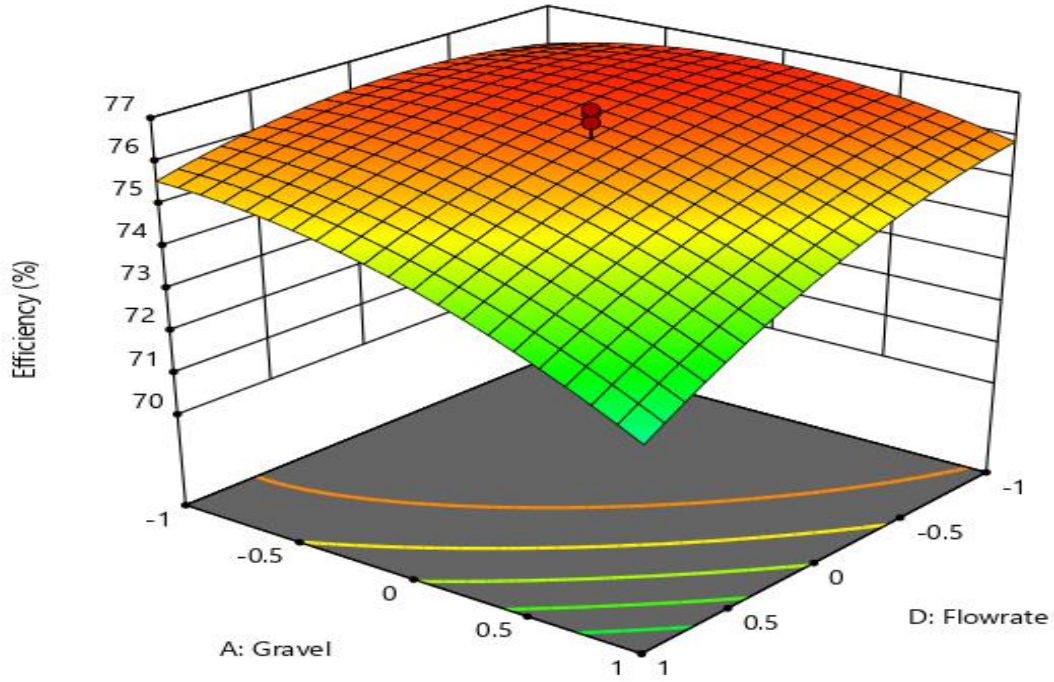

Figure 5-13: Response surface and contour plot for the interaction effect of gravel media and filtration rate for the turbidity removal (%)

Figure 5-14 presents surface response plot following the assessment of flowrate and filter length on turbidity removal within the HRF equipment. The removal of turbidity was strongly affected by both filtration rate and filter length. The increased turbidity removal was observed with the increasing filter length and reduced filtration rate from maximum to minimum value. Based on Figure 5-14, it was clearly observed that effectiveness or removal efficiency decreased significantly within the HRF with the reduction of filter length and increased filtration rate. These conditions can be attributed to the fact that extended filter length and the minimum flowrate favors increased filtration time removal within the HRF and these findings are in agreement with previous studies on roughing filtration (Wegelin, 1996).

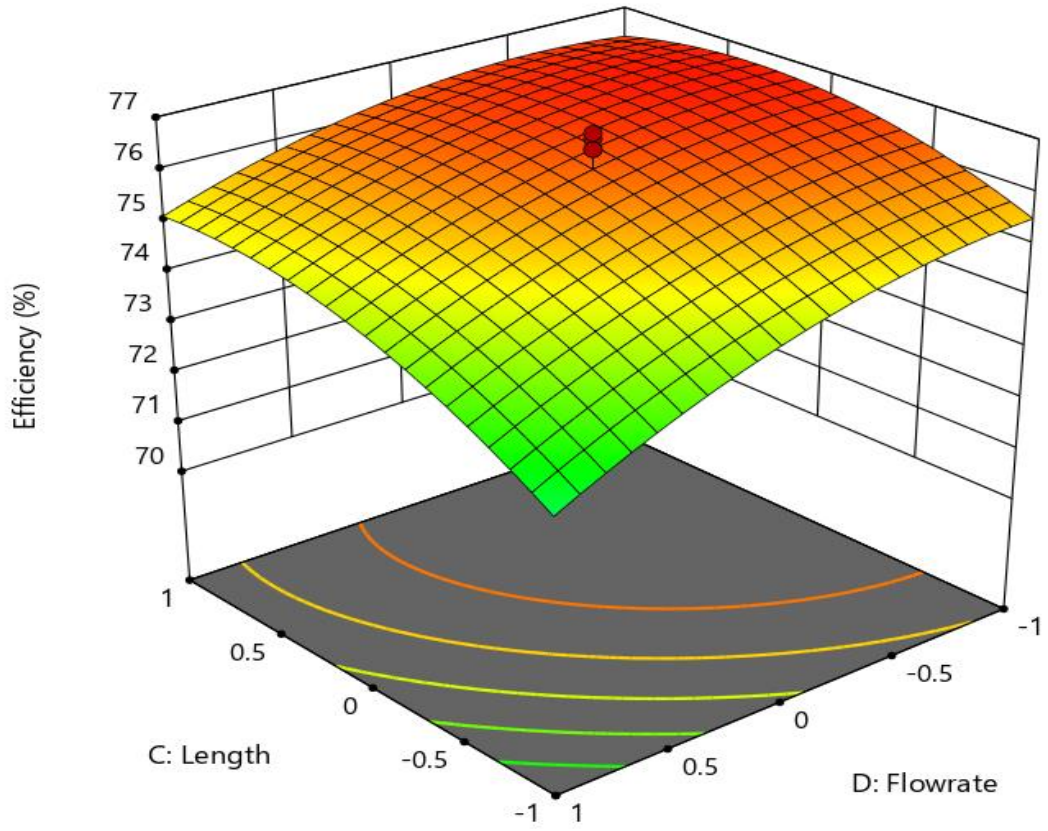

Figure 5-14: Response surface and contour plot for the interaction effect of filter length and filtration rate for the turbidity removal (%)

The response surface graphical plot investigating the effect of two variables, filtration rate and bed height on the removal of turbidity is presented in Figure 5-15. This graphical plot demonstrate the effect of filtration rate and bed height on HRF for the removal turbidity. Based on Figure 5-15, it

was observed that turbidity removal showed growth with low filtration rate over a certain value of filter bed height after which, decreasing trend was observed. Both factors had negative effects on the response variable and a low value of removal of turbidity was evident when filtration rate and bed height were increased. Therefore, the bed height and flowrate had a significant impact on turbidity removal in HRF (Lin et al., 2006).

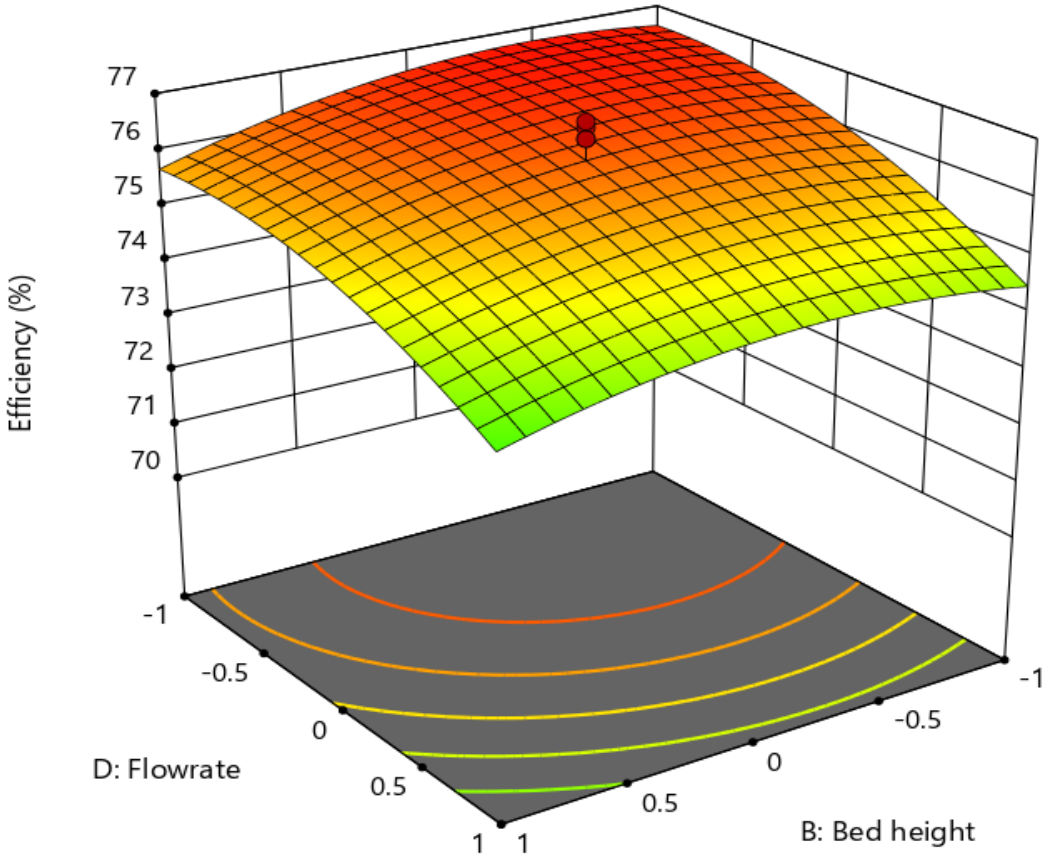

Figure 5-15: Response surface and contour plot for the interaction effect of filtration rate and filter bed height for the turbidity removal (%)

Figure 5-16 describes the effect of filtration length and bed height on the removal of turbidity in the HRF; the filtration length showed a positive effect on the removal turbidity as shown in the plot. The bed height showed a negative effect on the removal of turbidity and for increased length of the filter, an increased removal of turbidity was observed with a reduced filter bed height based on Figure 5-16. A removal of turbidity could be achieved with reduced filter length and bed height above mid-range height. A decline in the removal of 70% was observed when filter bed height was

maximized while using a shorter filtration length. Therefore, it is evident that the improvement in turbidity removal can be achieved under the right factor settings within the HRF. As can be observed, the filter length and filter bed height significantly affects the filter removal (Lin et al., 2006; Cleary, 2005).

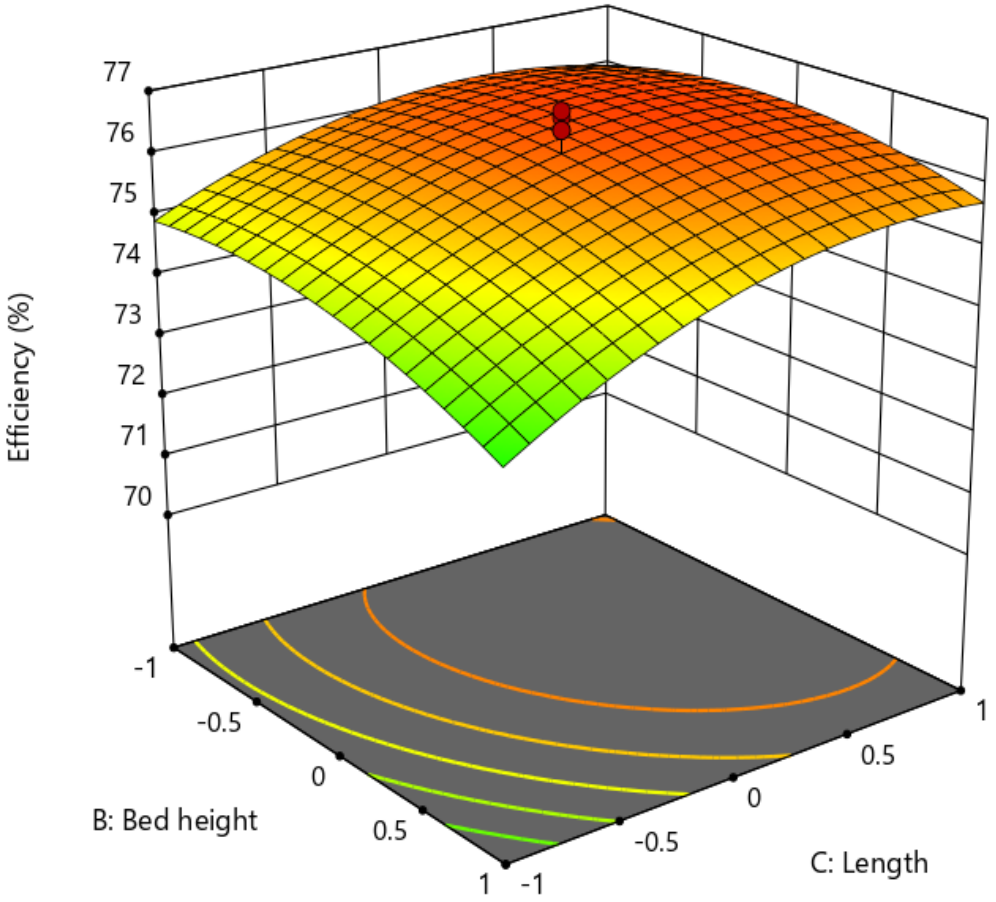

Figure 5-16: Response surface and contour plot for the interaction effect of filter bed height and filter length for the turbidity removal (%)

Figure 5-17 presents the response surface plot of gravel media size and filter bed height for the removal of turbidity. Based on Figure 5-17, the negative interaction effect of bed height and gravel media size was evident for the removal of turbidity. The ascending trend in the removal of turbidity was observed with the decrease in gravel media size and bed height. The gravel and bed height parameters are important parameters and have an effect on filter performance. These parameters are correlated with filtering capacity and the effectiveness of the sedimentation process within the

HRF. Also, the increased efficiency in HRF with reduced filtering media was further evident in some previous studies (Lin et al., 2006; Wegelin, 1996). In this graphical plot, the lower removals occurred with increased filter bed height and gravel media size within the filter equipment.

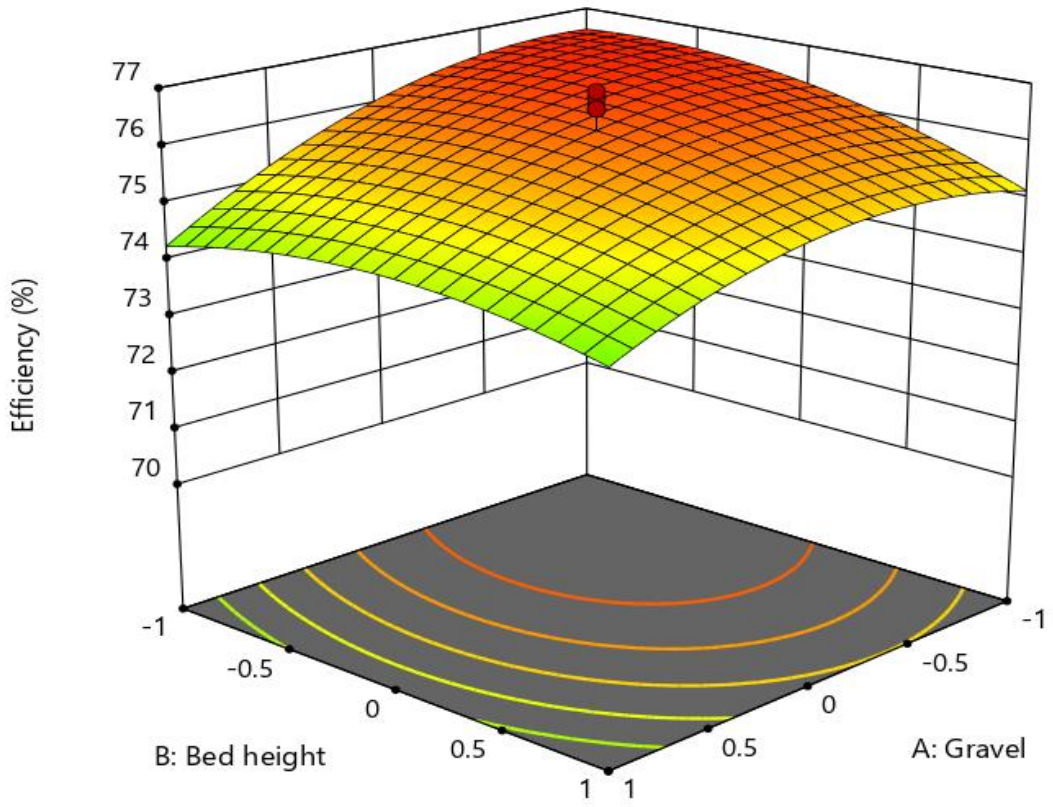

Figure 5-17: Response surface and contour plot for the interaction effect of filter bed height and gravel media for the turbidity removal (%)

Figure 5-18 presents results of the response surface plot representing the effect of gravel media and filter length on turbidity removal. As shown, the turbidity removal showed an increasing trend with increasing filter length and with the reduction of gravel media size. The removal of 76% was obtained with a combination of low gravel media size and increased/maximum filter length settings. The removal was reduced to 73% with coarse gravel media size and reduced filter length settings. Therefore, it can be observed that the interaction between gravel media size and filter length had an interaction effect and significant impact in influencing the removal of turbidity. The higher performance was evident in HRF with reduced gravel media and increased filter length (Cleary, 2005).

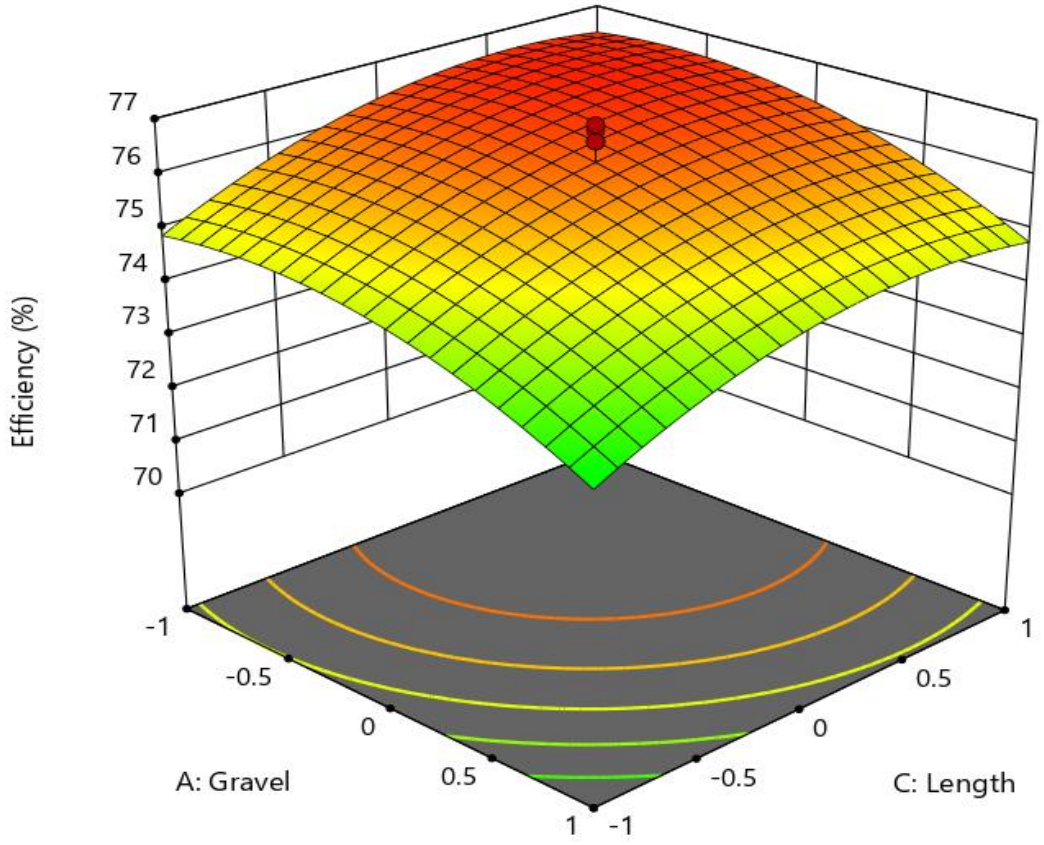

Figure 5-18: Response surface and contour plot for the interaction effect of gravel media and filter length for the turbidity removal (%)

Figure 5-19 show the normal plot of residuals with externally standardized residuals between the actual and predicted response values. This graphical plot is useful to observe the standard deviations patterns in data between the actual and predicted response values. As shown in the plots, the normal distribution trend was observed as data points were reasonably in a straight line plot which confirms the assumption of normally distribution of errors. The same trend was observed with actual and experimental values as the data points were found distributed on a straight line, therefore showing satisfactory correlation and good match between experimental and actual response values.

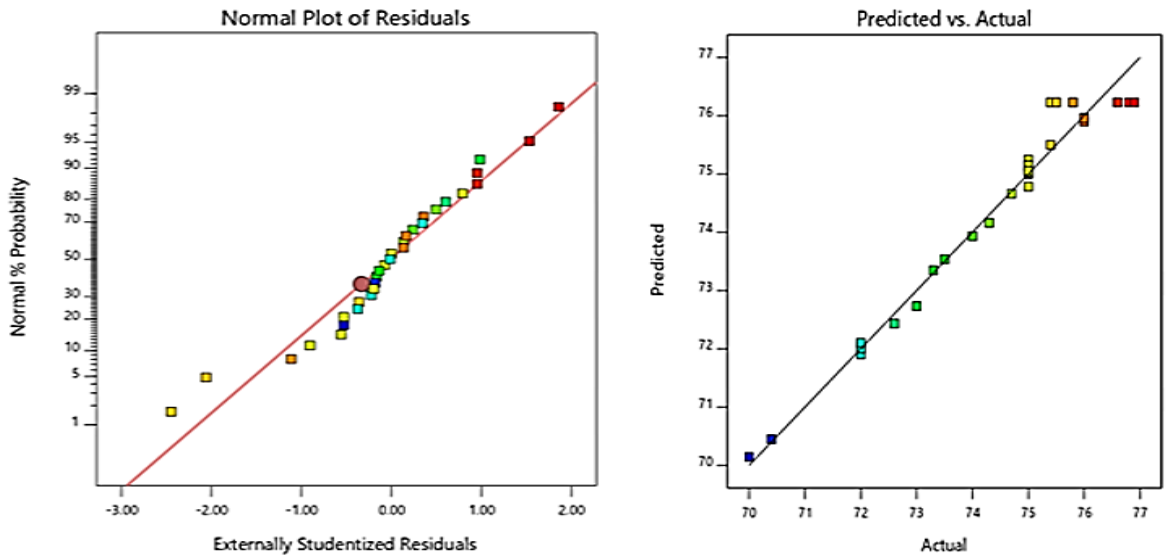

Figure 5-19: The normal plot of residuals and the plot of predicted versus actual values for turbidity removal (%)

Figure 5-20 present the standardized residuals against predicted and run number for the optimization of HRF equipment. As observed, it was evident that all data points were randomly distributed and no particular trend was observed in the data suggesting non constant variance assumptions in this RSM modelling. From the plots, the distribution of externally standardized residuals was evidently observed to fall in the range between -3 and 3.

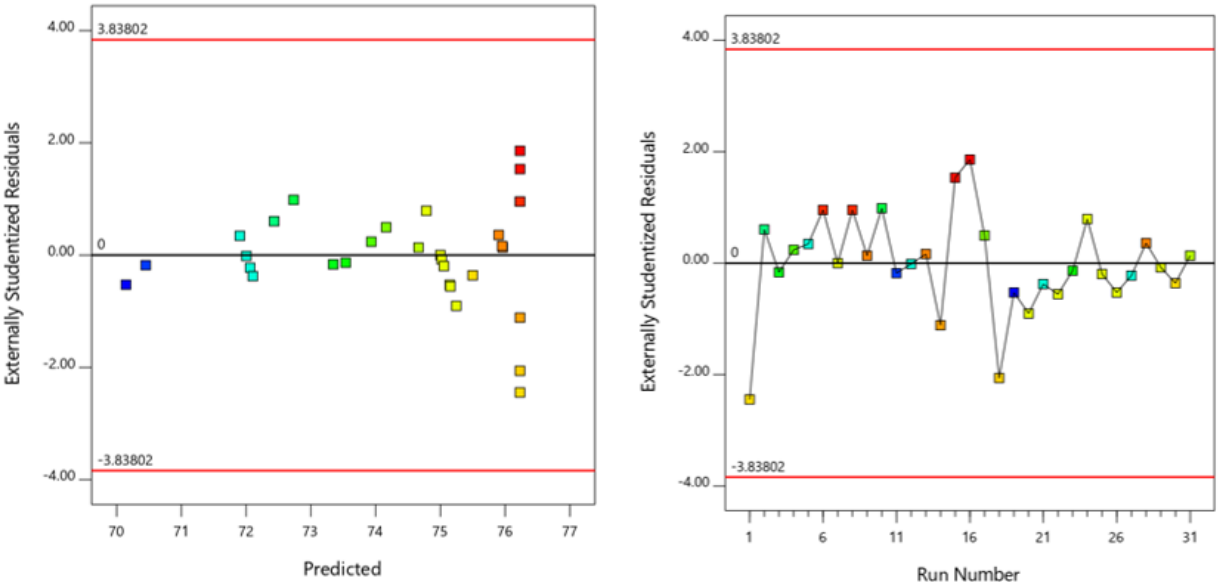

Figure 5-20: The graphical representation of externally standardized residuals versus predicted and run number

The optimization steps were carried out for turbidity removal with all input variables considered for optimization. The optimal conditions that support maximizing removal efficiency in the filter as a desirable outcome were investigated with all input variables considered for optimization. The numerical optimization was carried out as the aim was to maximize removal efficiency. The lower and upper limits for gravel media, filter bed height, filter length and filtration rate as constraints were optimized for gravel media fractions (8 mm), a minimum flowrate (0.365 m/h) and filter bed with depth of 0.39 m for a removal efficiency exceeding 76%. A low experimental error in experimental data with a coefficient of determination higher than 0.9 was evident for the optimized removal efficiency within the filter equipment.

Chapter 6

Results on ANN modelling and optimization

6.1 The prediction of turbidity from the HRF system

This section covers aspects related to neural network algorithms and its potential application in modelling the roughing filter for the prediction of turbidity of domestic greywater from the HRF unit. In this study, an ANN supervised learning was used for the prediction of turbidity after pre-treatment of greywater in the HRF. Table 6.1 shows ANN training results with performance parameters such as mean square error, the number of neurons in the hidden layer, training function and *R*-correlation coefficient values, all of which were used to construct the neural network. Results on ANN training with back propagation algorithm for the prediction of turbidity from the HRF are summarized in Table 6.1. The ANN model structures show different types of hidden layer properties and learning functions and network performance values/parameters obtained after the training phase.

Amongst various training algorithms investigated using MATLAB R2015a, the most significant training results were obtained with trainlm, trainbr and trainscg training functions with hidden neurons in hidden layers ranging from 5 to 9. Based on the significant training function, the accuracy of prediction was evaluated using MSE and the correlation coefficient using training data. As shown in Table 6.1, the correlation coefficient values were significantly higher than 0.9 although some of the ANN models showed low performance in terms of MSE values and correlation coefficient values.

A low value of MSE and high correlation coefficient values for train, test, validation and all data was obtained for a well-trained and best ANN model which indicates good fitting characteristics between ANN outputs and target data. The best ANN model with trainlm obtained was 4-7-1 with Logsig-Purelin transfer functions in the hidden-output layer, respectively and the MSE value of 0.0010 was obtained. The ANN trainlm model outperformed trainbr with 4-6-1 structure and MSE of 0.0046 including trainscg with 4-5-1 structure and the MSE of 0.0051. Other training functions also showed insignificant performance compared to trainlm algorithm.

Table 6.1: ANN results on different architectures of ANN training for the prediction of turbidity

Training Functions	Learning functions	No of hidden neurons					Performance
		5	**6**	**7**	**8**	**9**	
		Performance (MSE)					(R)
Trainbfg	Tansig-Purelin	0.00930	0.0248	0.0173	0.0141	0.0111	>0.999
	Logsig-purelin	0.0110	0.0107	0.0115	0.0098	0.0097	>0.999
trainbr	Tansig-Purelin	0.00572	0.0046	0.0052	0.0060	0.0057	>0.999
	Logsig-purelin	0.00605	0.0055	0.0052	0.0061	0.0055	>0.999
traincgb	Tansig-Purelin	0.0375	0.0141	0.0146	0.0143	0.0141	>0.999
	Logsig-purelin	0.0250	0.0140	0.0104	0.0110	0.0100	>0.999
traincgf	Tansig-Purelin	0.0357	0.0282	0.0257	0.0228	0.0188	>0.999
	Logsi-purelin	0.0183	0.0182	0.0144	0.0107	0.0098	>0.999
traincgp	Tansig-Purelin	0.0171	0.0342	0.0152	0.0148	0.0145	>0.999
	Logsig-purelin	0.0287	0.0169	0.0147	0.0128	0.0118	>0.999
traingd	Tansig-Purelin	0.0848	0.0790	0.0788	0.0680	0.0681	>0.999
	Logsig-purelin	0.0897	0.0895	0.0785	0.0744	0.0740	>0.988
traingda	Tansig-Purelin	0.1320	0.3390	0.1630	0.1500	0.1210	<0.988
	Logsig-purelin	0.2240	0.1390	0.1230	0.1130	0.1200	<0.988
traingdx	Tansig-Purelin	0.0909	0.1230	0.0788	0.0718	0.0604	<0.988
	Logsig-purelin	0.0842	0.0747	0.0547	0.0500	0.0688	<0.988
trainlm	Tansig-Purelin	0.0091	0.0056	0.0088	0.0068	0.0080	>0.999
	Logsig-purelin	0.0094	0.0077	0.0010	0.0072	0.0049	>0.999
trainoss	Tansig-Purelin	0.0316	0.0146	0.0267	0.0187	0.0186	<0.988
	Logsig-purelin	0.0174	0.0167	0.0162	0.0132	0.0126	<0.988
trainr	Tansig-Purelin	0.0116	0.0173	0.0168	0.0185	0.0180	<0.988
	Logsig-purelin	0.0560	0.0282	0.0164	0.0153	0.0152	<0.988
trainrp	Tansig-Purelin	0.0205	0.0120	0.0304	0.0205	0.0171	>0.988
	Logsig-purelin	0.0237	0.0141	0.0135	0.0124	0.0101	>0.988
trainscg	Tansig-Purelin	0.0051	0.0199	0.0110	0.0124	0.0121	>0.999
	Logsig-purelin	0.0151	0.0133	0.0165	0.0111	0.0112	>0.999

Table 6.2 summarizes the performance of the three ANN training functions based on MSE and gradient descent with momentum weight and bias learning functions (learngdm). The trainlm recorded highest training accuracy, lower MSE and lower training iterations than trainbr and trainscg and the decreasing pattern in training iterations in the direction of high performing training functions was also observed. For the trainscg: 4-5-1 model, 241 training iterations were recorded followed by trainbr: 4-6-1 model which recorded 126 iterations. The best ANN for trainlm with 4-7-1 structure recorded 86 iterations which was the least amongst the training algorithms in Table 6.2. Thus, the best ANN model showed good performance including accelerated training speed than the other training algorithms in Table 6.2.

Table 6.2: ANN results with three network training functions for the prediction of turbidity

	trainlm		trainbr		trainscg	
Neurons	Train function	Adapt. Learning Learngdm	Train function	Adapt. Learning Learngdm	Train function	Adapt. Learning Learngdm
5	Logsig	0.0094	Logsig	0.0060	Logsig	0.0151
	Tansig	0.0091	Tansig	0.0057	Tansig	0.0051
6	Logsig	0.0077	Logsig	0.0055	Logsig	0.0133
	Tansig	0.0056	Tansig	0.0046	Tansig	0.0199
7	Logsig	0.0010	Logsig	0.0052	Logsig	0.0165
	Tansig	0.0088	Tansig	0.0052	Tansig	0.0110
8	Logsig	0.0072	Logsig	0.0061	Logsig	0.0111
	Tansig	0.0068	Tansig	0.0060	Tansig	0.0124
9	Logsig	0.0049	Logsig	0.0055	Logsig	0.0112
	Tansig	0.0080	Tansig	0.0057	Tansig	0.0121

To investigate the training accuracy of the ANN models, results on regression plots and training state of the designed ANN models were examined. The graphical representation of the regression plots and training state plots for trainlm, trainbr and trainscg are presented in Figures 6-1 to 6-8. Figure 6-1 shows the performance of trainlm in terms of regression plots at the end of neural network training for the prediction of turbidity. Based on the plot, the regressions are for the training, testing, validation and all data sets which are all represented in linear regression format. The plots show the extent the estimated outputs match the actual ANN targets with the ideal plot. The targets and corresponding predicted outputs can be observed scattered around solid lines coded in green, red, blue and grey which all represent best fit linear regression lines between output and

targets. In general, the final regression plots at the end of ANN training obtained showed good accuracy as data cases are distributed around the 45° diagonal line as shown in the regression plot, although few data points deviated from the targets. The high correlation coefficients for training, test, validation and all data were obtained which ideally confirmed the relationship between the model outputs compared to the actual target values therefore confirming the good fit for ANN performance based on trainlm algorithm.

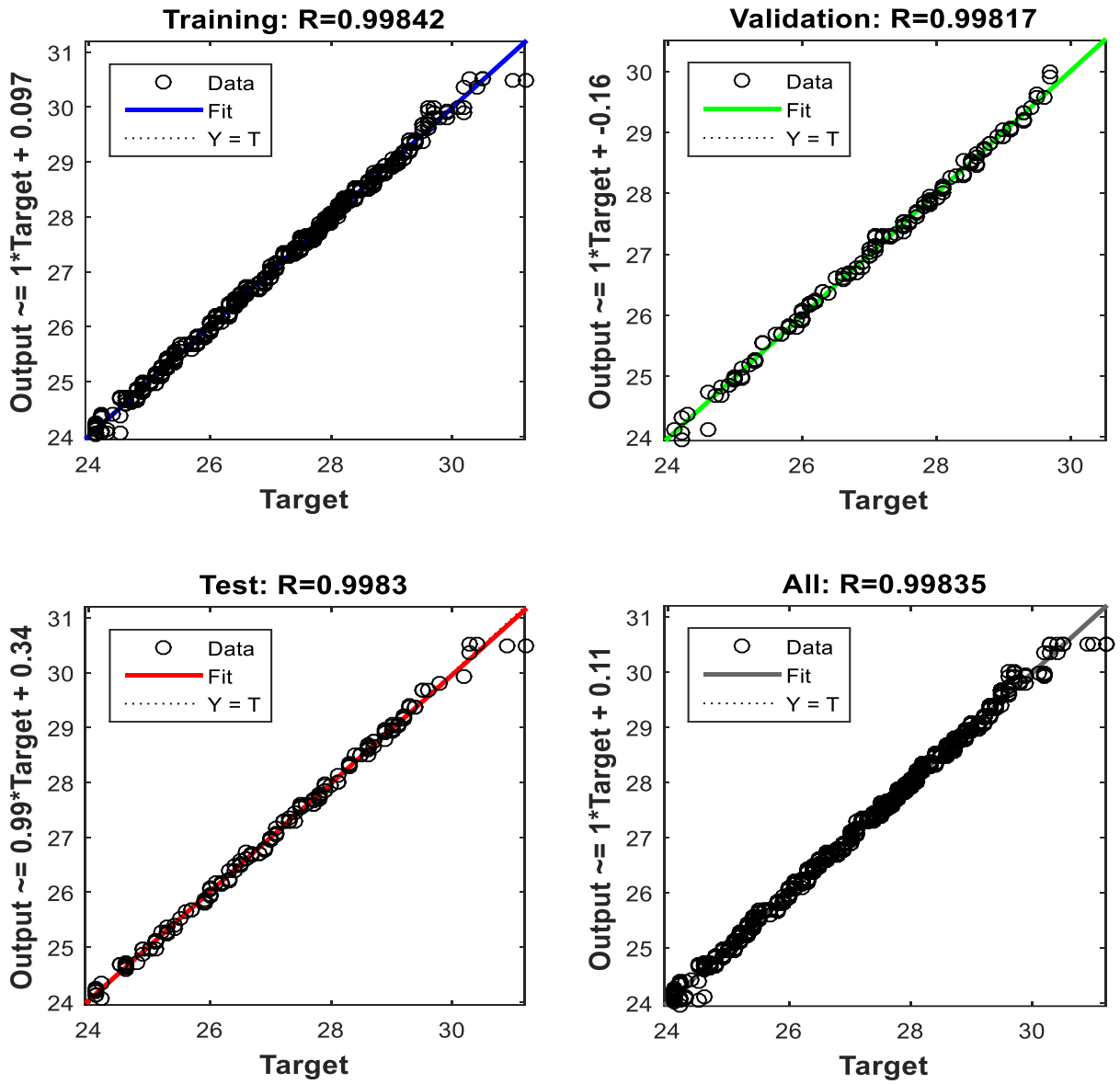

Figure 6-1: ANN performance on regression outputs for best fit model with trainlm for the prediction of turbidity

The effect of training state parameters were also examined for trainlm, trainbr and trainscg by taking into account the momentum parameter, gradient and validation check with respect to the number of epochs as shown in Figure 6-2. The summary of the ANN training state results are directly presented and discussed for trainlm, trainbr and trainscg at the end of the neural network training phase. The end or termination of the training phase is mainly a function of the magnitude of gradient, the number of validation checks and momentum factor which controls the training speed of ANN. Based on Figure 6-2, the final gradient, momentum factor and validation check simply converged to 1e-05, 0.015291 and 6, respectively at epoch value of 8. From Figure 6-2, the ANN training was finally terminated as the momentum factor and gradient were gradually reduced while validation performance reached its maximum limit value.

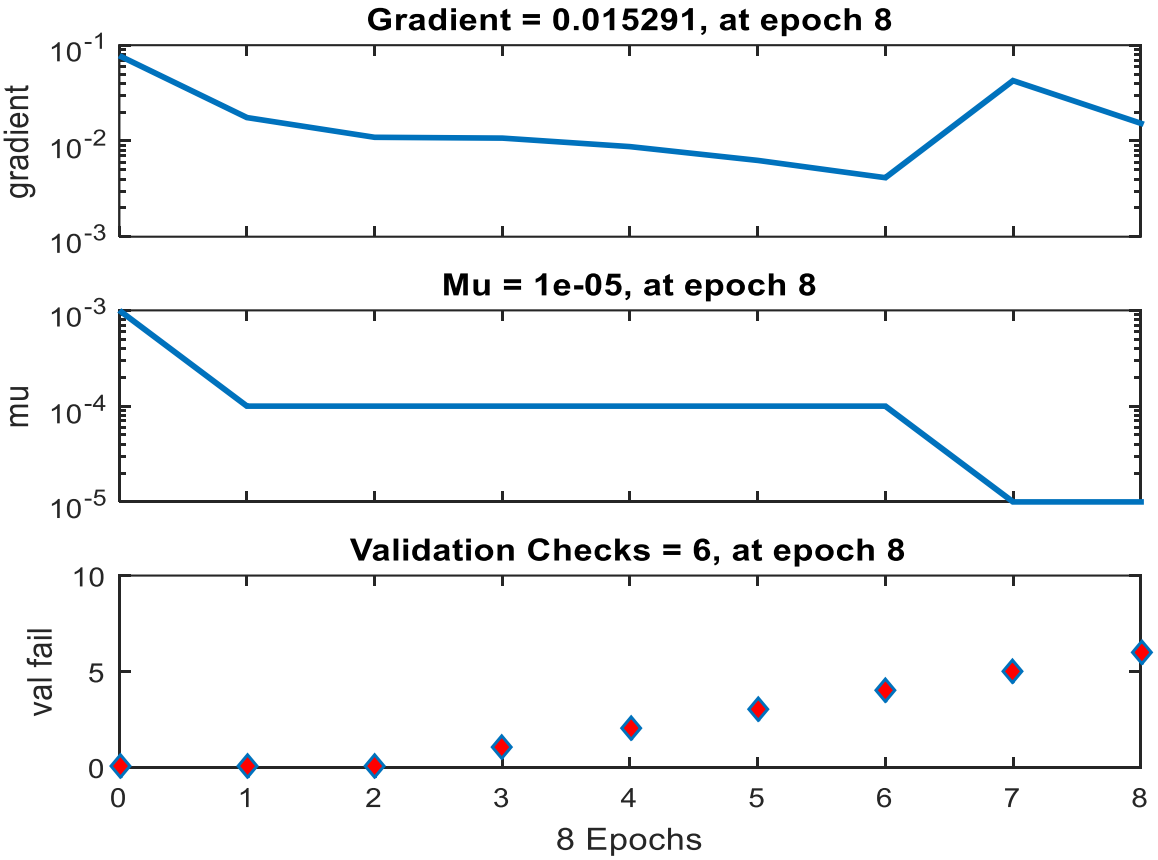

Figure 6-2: ANN performance in terms of gradient parameter, momentum factor and validation checks with trainlm algorithm

The regression plot for trainbr following the neural network training phase is presented in Figure 6-3 in the form of regressions. The three regression graphs represent the ANN data for training, testing and all data for the prediction of turbidity. The plots show the relationship between the network outputs and the corresponding targets at the end of the ANN training steps. As shown in Figure 6-3, the regression plots essentially show the good overall accuracy of trainbr in fitting the ANN target and output data. The best fit linear regression lines between outputs and targets were also evident and the data points matched very well with the target-output line for training, testing and all data with correlation coefficients values all greater than 0.998. Based on Figure 6-3, the network showed satisfactory performance in predicting turbidity for the given ANN inputs.

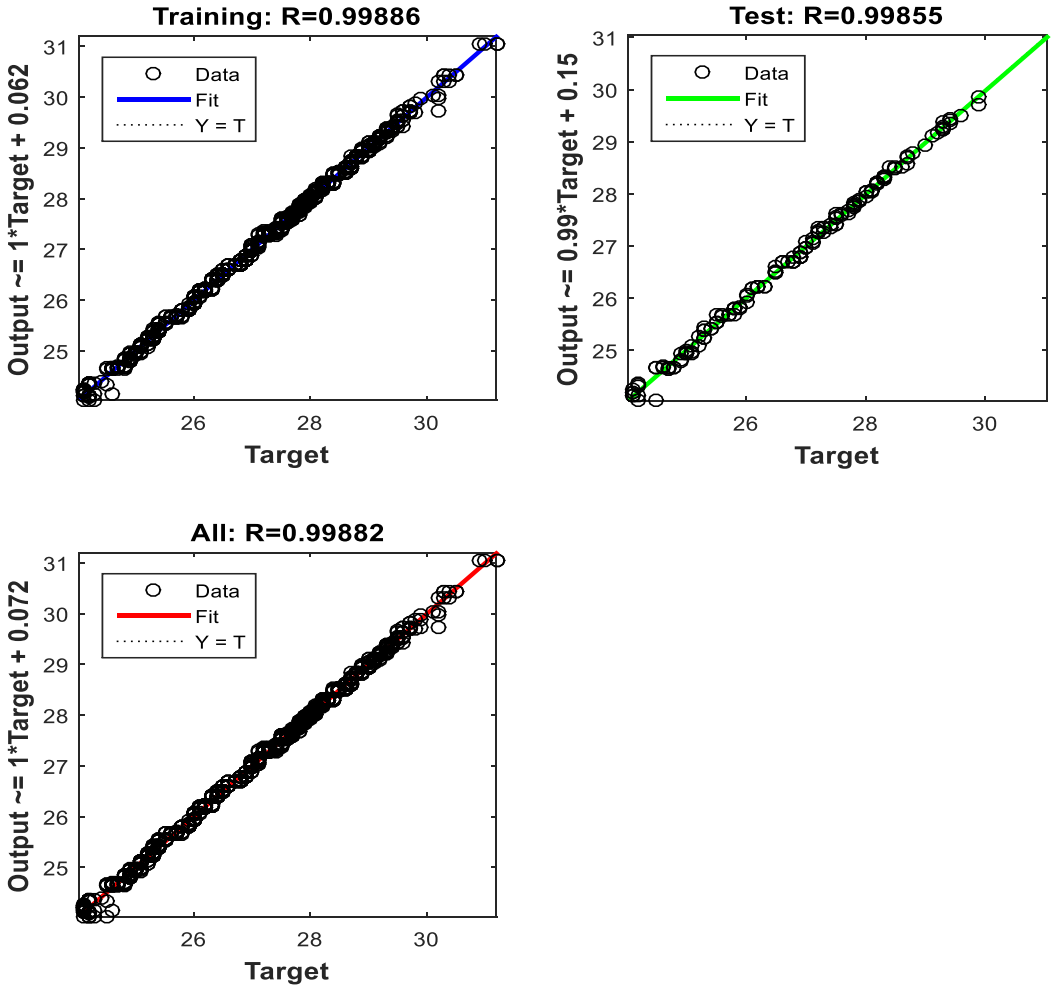

Figure 6-3: ANN performance on regression outputs for best fit model with trainbr

The ANN training results showing the training state of ANN with trainbr algorithm is presented in Figure 6-4. The graphical plot shows the training state with ANN training parameters which are

useful for the network validation. These include gradient, momentum parameter and validation checks plotted against the number of epochs. During the training phase, the gradient and momentum parameters were adjusted by the network as they were approaching minimum values as shown in Figure 6-4. The final gradient parameter obtained was 0.0081711 and momentum factor subsequently reached a value of 0.5 and both were recorded at an epoch value of 14 by the network. As it can be observed in Figure 6-4, the validation checks gradually increased and reached a value of 6 and the ANN training finally ceased.

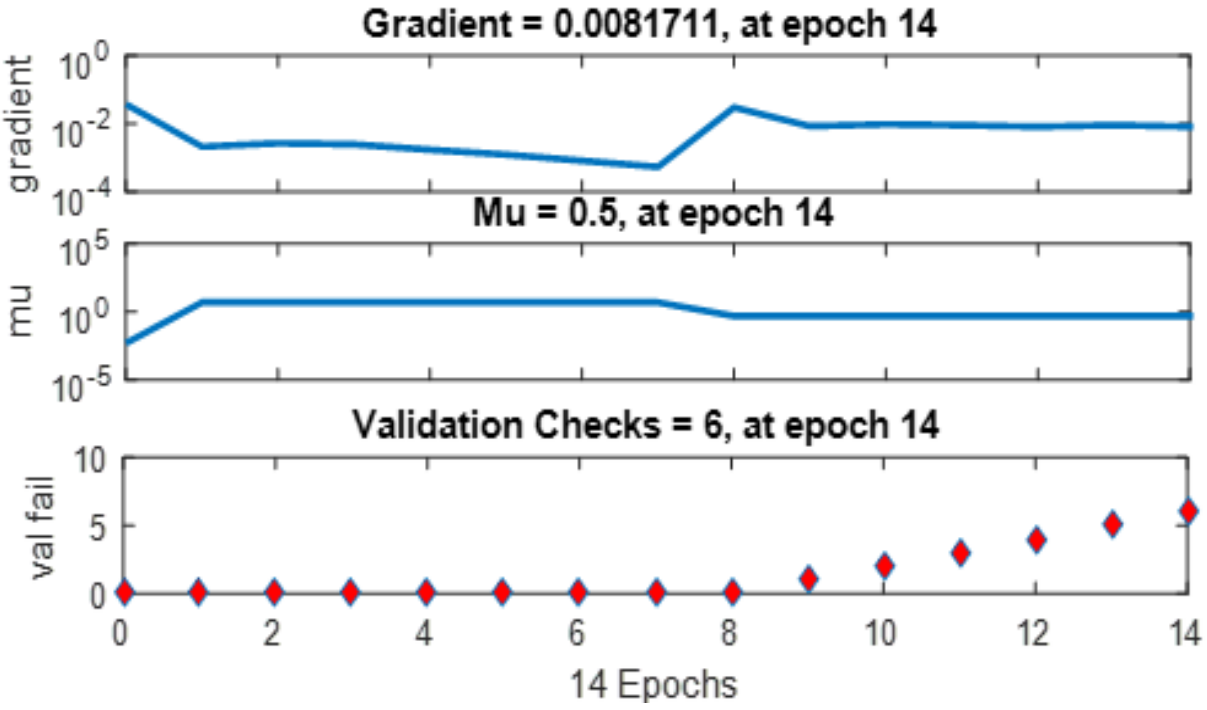

Figure 6-4: ANN performance in terms of gradient parameter, momentum factor and validation checks for the trainbr algorithm

Figure 6-5 summarizes the regression plots for trainscg at the end of the ANN training phase. The ANN linear regression plots for the network outputs versus targets for all training subsets are evident. The four linear regression plots for training, validation, testing an all data in terms of correlation coefficient values and the degree of linearity between the outputs and targets were well within a satisfactory range after ANN training. Each graphical plot showed good performance in terms of distribution around the best linear regression plot and only a few deviations were observed in data cases with respect to the 45° diagonal line relative to the targets. It is evident that the ANN

training showed good fit and good linear relationship between outputs and corresponding targets with large correlation coefficients in training, test, validation and all data sets. Based on Figure 6-5, the correlation coefficient values exceeding 0.996 were obtained with the trainscg algorithm which this confirms the predictive ability of the developed ANN model for the prediction of turbidity.

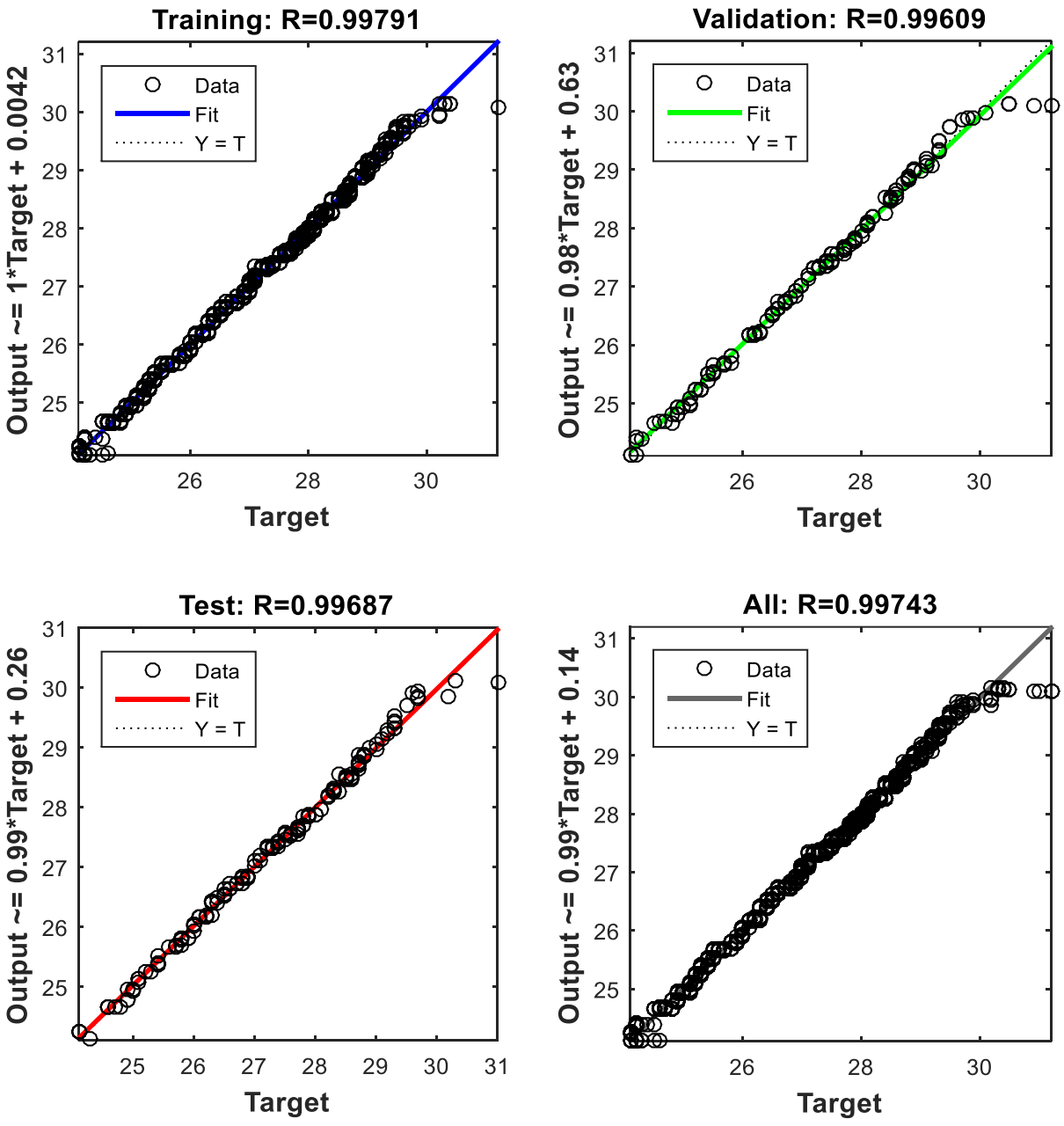

Figure 6-5: ANN performance on regression output for best fit model with trainscg algorithm

The ANN performance with trainscg algorithm is presented in Figure 6-6. The graphical plot shows the training state results which are useful indicators in monitoring the training progress of ANN. The ANN training vectors were gradient and validation checks which are plotted and presented along with the number of epochs. The training progress values of gradient and validation check at epoch 60 were 0.070115 and 6 respectively when the trainscg was examined. The ANN eventually reached a maximum training phase as the validation performance increased to a maximum value while the gradient value gradually decreased reaching the minimum limit of 0.070115.

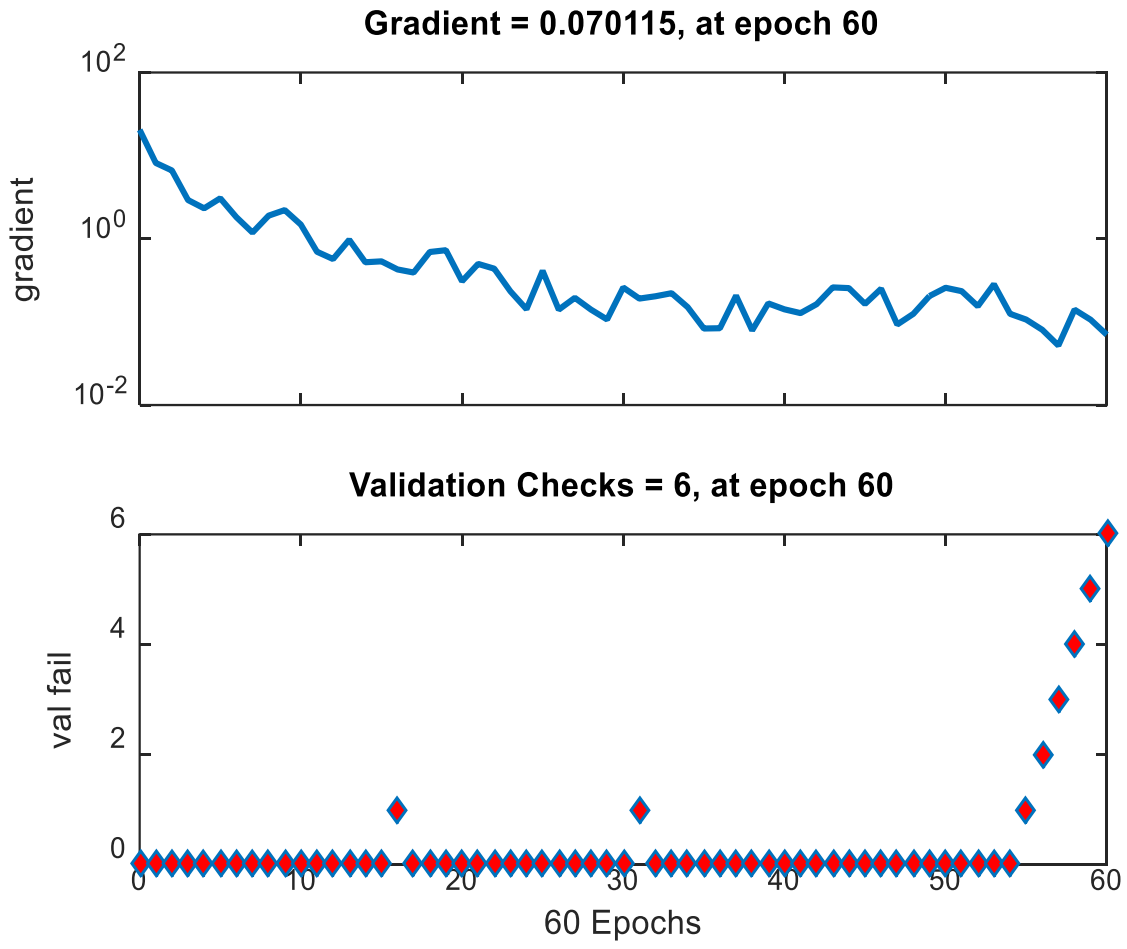

Figure 6-6: The ANN training state in terms of validation checks and gradient parameter with trainscg

The optimal ANN model with trainlm was subsequently used to carry out the prediction of turbidity from the HRF based on the new sample of data with only 61 data cases consisting of experimental input vectors. The experimental data cases and predicted ANN outputs can be observed in Figure 6-7. The graphical plot result typically shows the comparison pattern between sampling data cases and network outputs. A good agreement and satisfactory performance from the plot using trainlm was achieved. Figure 6-7 confirms a good match between the outputs and target data and this was observed with most of the errors obtained near zero between predicted and target data and the low average error below 1% was finally obtained.

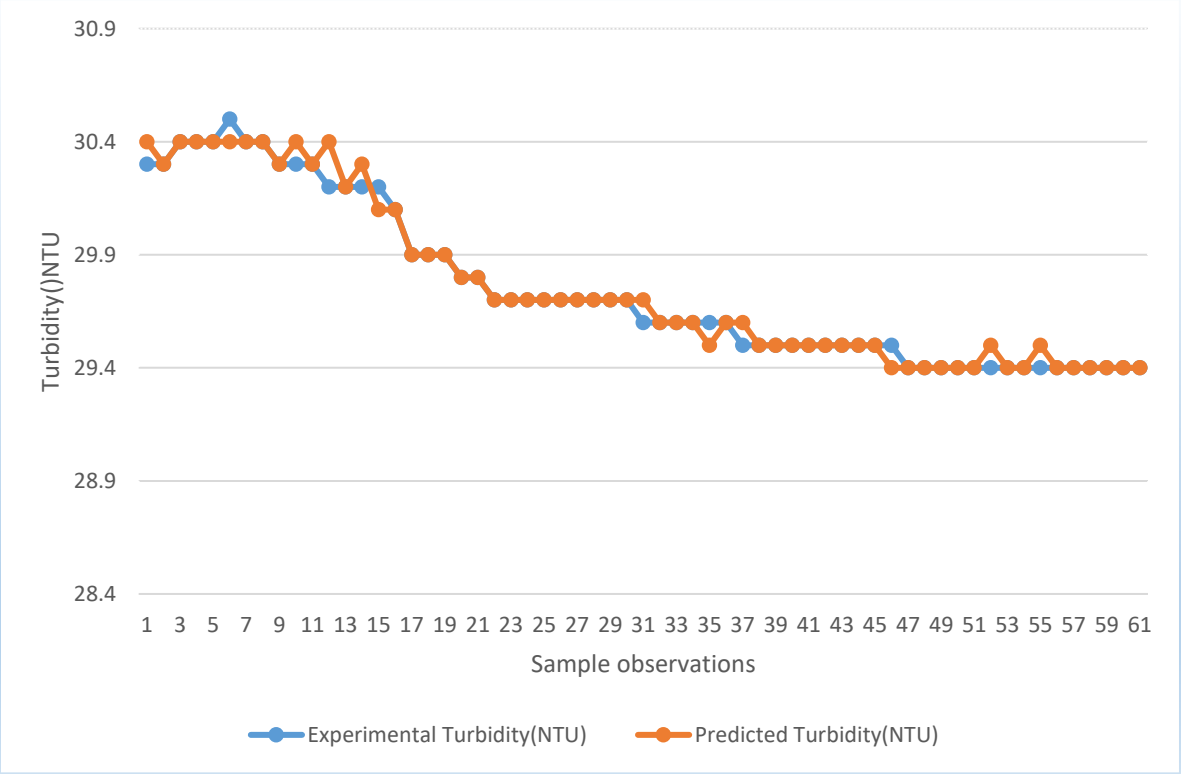

Figure 6-7: The graphical plot showing the comparison pattern between sampling data cases and network outputs

The sensitivity analysis on the performance of the neural network in prediction of turbidity was investigated. The effect of variables in the model was investigated and estimated by studying the percentage of contribution of the variable effect on the value of *R*-correlation coefficient values and through the value of estimated MSE. Figure 6-8 depicts results on sensitivity analysis with trainlm for the prediction of turbidity. The ANN input variables were temperature, turbidity, pH and conductivity and the most significant variables with trainlm were turbidity and conductivity. The highest percentage contribution was evident for turbidity and correlation coefficient value of approximately 0.97.

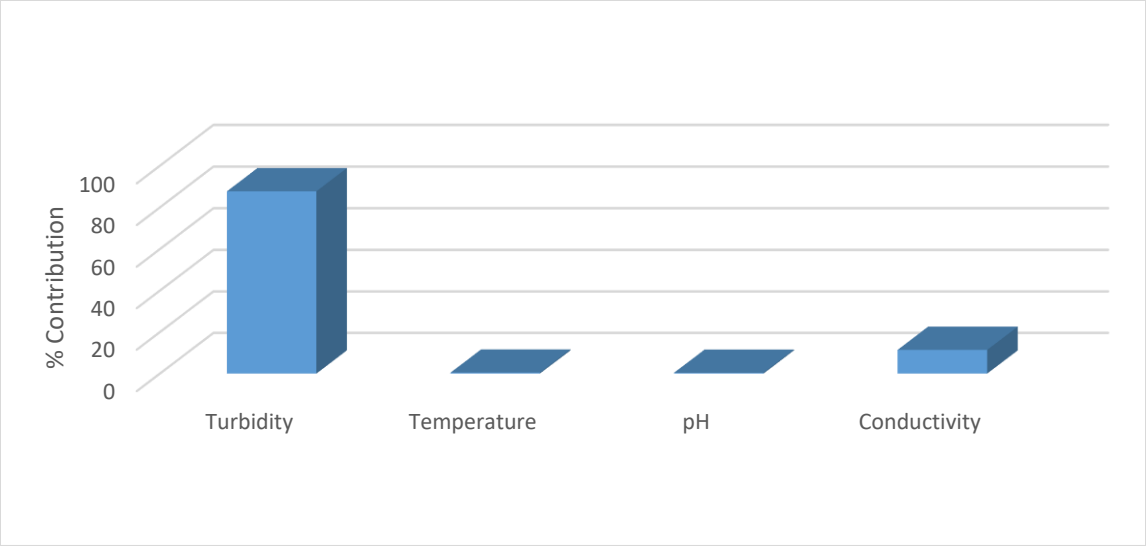

Figure 6-8: Results on sensitivity analysis with trainlm for the prediction of turbidity

6.2 The prediction of COD from the effluent stream of a HRF equipment

This section presents findings of ANN application in modelling HRF equipment for the prediction of COD of domestic greywater effluent from the HRF unit. The network is feedforward with back propagation connection for the supervised learning. This architecture was trained with three inputs which were turbidity, solids and pH. The proposed network architecture has one input layer, hidden layer and the output layer. The ANN training results reflect testing which was developed with different training functions and algorithms, the number of neurons and values of performance index through iteration process steps based on experimental data.

Different types of ANN models for COD prediction were developed while varying MATLAB R2015a training functions and parameters with the summary of the best ANN models presented in

Table 6.3. The ANN results obtained from the models were compared in terms of MSE, MAE, MAPE and correlation coefficient values. The optimal ANN model was obtained with the trainlm algorithm based on its satisfactory performance as the minimum MSE and lower MAE and MAPE containing 10 neurons in the hidden layer. As shown in Table 6.3, all other ANN models with trainbr were outperformed by the trainlm training algorithm. The trained ANN model with trainlm algorithm achieved higher prediction accuracy with lower values of MSE, MAE and MAPE performance parameters.

Table 6.3: ANN results on different structures of NN training for the prediction of COD

Neuron	ANN model trainlm						ANN model trainbr				
	Train function	Train R	Test R	MSE	MAE	MAPE	Train R	Test R	MSE	MAE	MAPE
2	Logsig	0.9941	0.9939	0.00208	0.0382	5.0589	0.9961	0.9949	0.00307	0.0383	4.7044
	Tansig	0.9978	0.9967	0.0072	0.0697	9.7851	0.9982	0.9979	0.00204	0.0381	4.5281
3	Logsig	0.9981	0.9966	0.00367	0.0481	7.6185	0.9959	0.9956	0.00205	0.0373	4.7044
	Tansig	0.9984	0.9961	0.00206	0.0377	3.1207	0.9968	0.9965	0.00211	0.0254	0.4965
4	Logsig	0.9980	0.9981	0.00211	0.0339	3.3974	0.9979	0.9972	0.00105	0.0247	0.4240
	Tansig	0.9969	0.9985	0.00209	0.0386	4.6069	0.9983	0.9982	0.00291	0.0260	0.8384
5	Logsig	0.9978	0.9982	0.00150	0.0326	2.2296	0.9984	0.9983	0.00211	0.0249	0.4288
	Tansig	0.9982	0.9988	0.00211	0.0383	4.6702	0.9984	0.9984	0.00155	0.0251	0.5014
6	Logsig	0.9980	0.9984	0.00170	0.0350	3.2102	0.9986	0.9983	0.00191	0.0245	0.6032
	Tansig	0.9979	0.9984	0.00122	0.0289	3.6314	0.9986	0.9985	0.00121	0.0252	0.5597
7	Logsig	0.9984	0.9983	0.00110	0.0257	0.5869	0.9989	0.9988	0.00192	0.2581	0.5280
	Tansig	0.9984	0.9982	0.00130	0.0285	1.1093	0.9984	0.9981	0.00190	0.2480	0.5280
8	Logsig	0.9995	0.9989	0.00172	0.0357	3.5423	0.9981	0.9980	0.00193	0.0255	0.5939
	Tansig	0.9988	0.9987	0.00110	0.0226	0.4987	0.9988	0.9987	0.00151	0.0257	0.5548
9	Logsig	0.9995	0.9994	0.00142	0.0241	0.4992	0.9990	0.9991	0.00111	0.0251	0.3593

	Tansig	0.9996	0.9992	0.00150	0.0282	0.7147	0.9992	0.9991	0.00112	0.0250	0.5514
10	Logsig	0.9998	0.9989	0.00111	0.0264	0.7262	0.9995	0.9993	0.00101	0.0247	0.2883
	Tansig	0.9998	0.9995	0.00099	0.0240	0.1686	0.9995	0.9992	0.00141	0.0249	0.4481

In order to examine the detailed overall performance of the ANN models and the underlying trends in ANN with the trainlm training algorithm, the MSE, MAE and MAPE were directly analyzed. Figure 6-9 shows MSE, neurons and training functions following ANN training with the trainlm training algorithm. A low MSE value which is the average squared difference between the network outputs and targets was observed to vary with the number of neurons ranging from 0.0072 to 0.001. The low value of MSE was 0.001 and the optimum number of neurons in hidden layers was 10 based on the Tansig activation function. During ANN training, the performance parameters including average MAE and MAPE were used in order to evaluate the model accuracy. Compared to the trainbr training algorithm, the trainlm recorded a lower value of MAE and MAPE of 0.0240 and 0.1686, respectively.

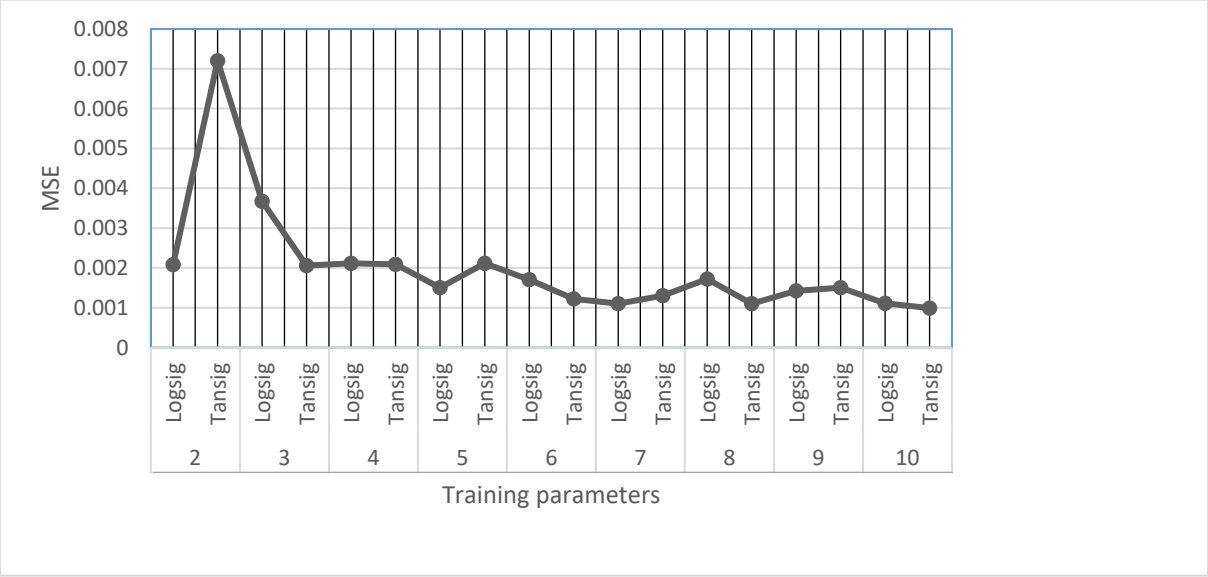

Figure 6-9: ANN performance in terms of MSE with the size of hidden layer neurons and the type of activation function based on the trainlm training algorithm

Figure 6-10 shows the distribution of network errors in terms of an error histogram plot of 20 bins for the ANN with the trainlm algorithm containing 10 neurons in the hidden layer with training, testing and validation data sets. The error histogram is a good indicator in evaluating the quality of error distributions based on ANN predictions after the training stage. The blue bars represent training data set, red coded bars represent testing data and the green bars represent the validation data set. Based on the plot, it is evident that most of the errors are normally distributed with large errors distributed around the zero error line. The small errors were also distributed in both ends of the zero error line showing a downward trend away from the zero error line. Therefore, Figure 6-10 confirms the good performance and good error distributions of the developed ANN model with the trainlm training algorithm.

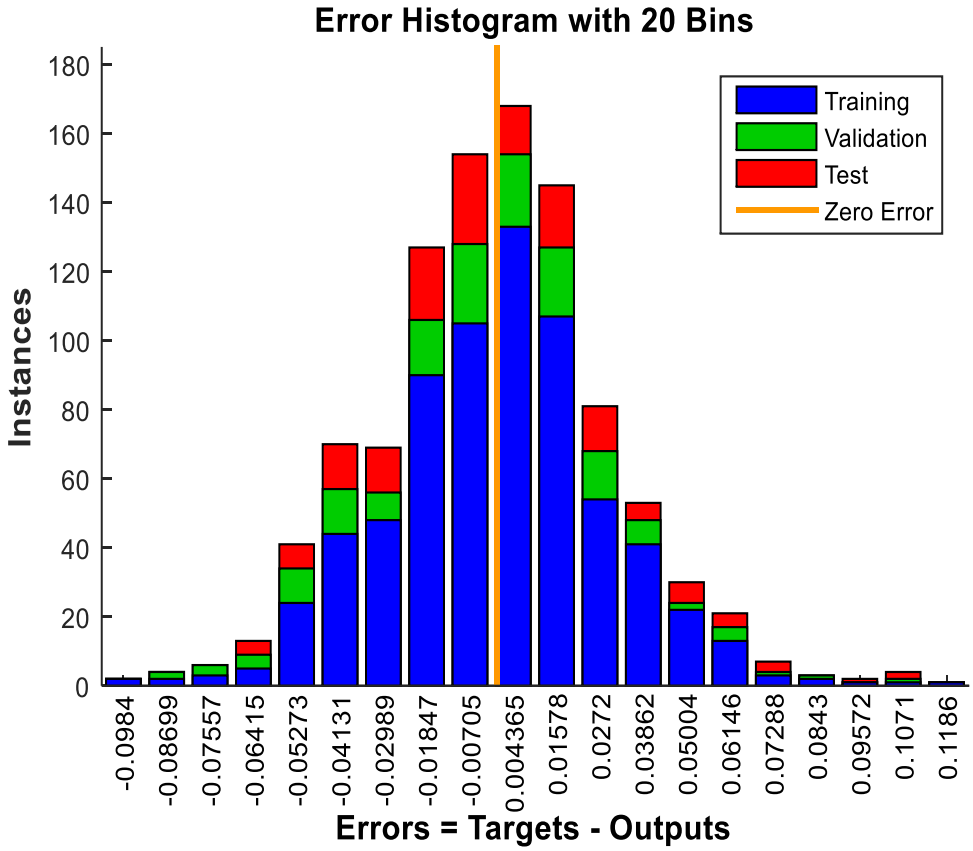

Figure 6-10: Graphical plot of error histogram for 20 bins with the trainlm training function

Figure 6-11 shows simulation results of COD in terms of the relationship between independent experimental COD from the HRF equipment and COD predicted by the neural network for a total

of 30 independent samples. In this case, the network response results were satisfactory as it was observed that the outputs tracked the targets very well for the sampling cases. A high correlation coefficient between measured and predicted output COD values was observed for almost all data cases. The error values between the measured predicted outputs of COD were also observed with the data cases with an overall small error for the prediction of COD values. Based on the analysis of simulation results for COD, the ANN model developed with the trainlm algorithm showed good accuracy and generalization capability in predicting COD of domestic greywater from the HRF equipment with a high R^2 value of 0.9998.

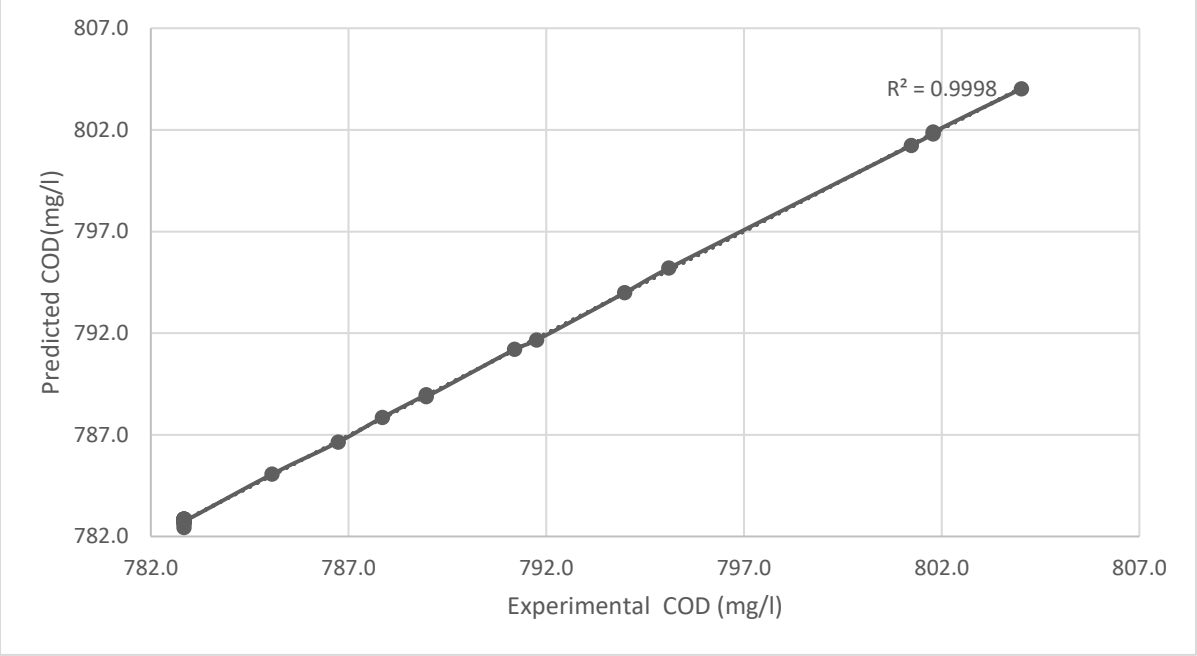

Figure 6-11: The graphical plot showing ANN performance with a new sample observation for the prediction of COD

Figure 6-12 presents ANN performance in terms of MSE, neurons and training functions for the trainbr training algorithm following the ANN training phase. The MSE during the training stage was in range from 0.00307 to 0.001. The decreasing pattern in MSE with improved training neurons in hidden layers was evident which showed the improvement in learning abilities of ANN with the trainbr training function. The lowest MSE value obtained with the trainbr training function was 0.00101 containing 10 neurons in the hidden layer. The accuracy of the model was also evaluated with an average MAE and MAPE performance parameters during training steps. The

values of MAE and MAPE recorded were 0.0247 and 0.2883, respectively. These accuracy measures were well above that obtained with the trainlm training function.

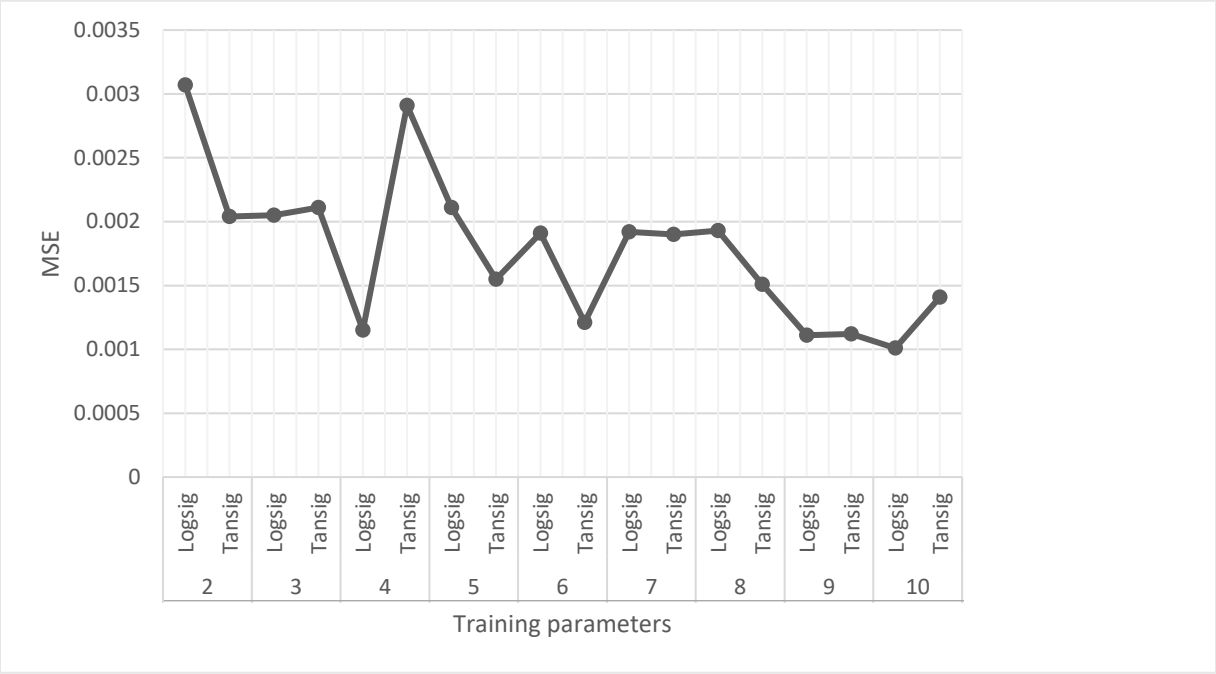

Figure 6-12: ANN performance in terms of MSE with the size of hidden layer neurons and the type of activation function based on the trainbr algorithm

Figure 6-13 illustrates the distribution of network errors in terms of an error histogram plot of 20 bins for the ANN with the trainbr algorithm. The blue bars represent training data and red bars represent test data. The plot shows the performance of ANN in terms of error distributions with a normal shaped error histogram. Based on the histogram plot, it was observed that the errors showed characteristics of normal distribution with a large number of errors occurring near the centre or zero error line. The small errors were also observed to be evenly distributed around the zero error line and shows a decreasing pattern at both ends of the zero error line.

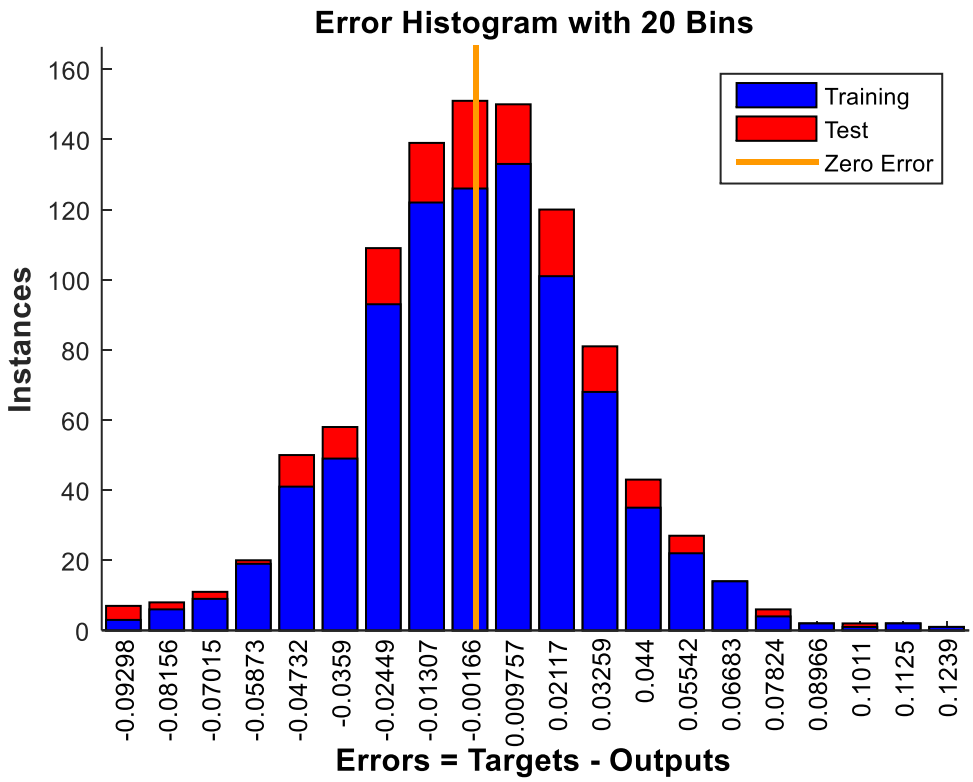

Figure 6-13: Graphical plot of error histogram for 20 bins with the trainbr training function

6.3 The prediction of filter duration in a HRF system

This section presents findings related to feedforward ANN application in modelling HRF for the prediction of filter duration based on the use of domestic greywater from the kitchen source in a HRF system. As discussed in the method section, the development of the ANN model for the prediction of filter duration involved steps such as data collection, the selection of ANN architecture, training and validation based on experimental data from HRF. The ANN training process is non-linear and therefore the use and selection of ANN architecture, model training and validation techniques for the prediction of filter duration was investigated. In this study, the ANN with a single hidden layer was trained using available training functions in MATLAB and training input parameters that were previously presented in Table 3.7.

The performance of all different types of ANNs that were developed were compared in order to select the best ANN model using MSE and correlation coefficients for the training, testing, validation and all data sets. The ANN architecture that met the criteria of highest correlation coefficient and low MSE was selected as the optimal ANN model. The correlation coefficients for

training, testing, validation and all data should be close to an ideal value of 1 with a low value of MSE which should be close to zero. Therefore, good performance parameters and low error difference in a successfully trained and the optimal ANN model were the ultimate target.

The summary of the two training algorithms based on their performances were mainly trainlm and trainscg which are presented and discussed in this section. Table 6.4 presents training results and varying performance of ANN models for the prediction of filer duration and turbidity using the trainlm algorithm. The ANN architecture was obtained with 8 neurons in one hidden layer with Tansig-Purelin activation functions and learngdm as the best learning function. Also, the gradient descent weight and bias learning function (learngd) was outperformed by learngdm. From Table 6.4, the lowest MSE was recorded for the optimal model and high correlation coefficients for training, testing, validation and all data set.

Furthermore, the ANN showed success in learning experimental data from the HRF system and the ANN with 4-8-2 structure was selected as the optimal and the best network for the prediction of filter duration and turbidity in a HRF equipment. In this study, the ANN filter duration obtained was drastically reduced with more kitchen greywater source used in HRF. This is due to low quality of kitchen greywater and high solid particulates which limit efficacy in HRF.

Table 6.4: The ANN results for the prediction of filter duration and turbidity with trainlm algorithm

Train function	**Activation function**	**Adapt. learning**	**Train (R)**	**Test (R)**	**Val (R)**	**All (R)**	**MSE**	**Model**
trainlm	logsig/purelin	learn gdm	0.99990	0.99998	0.99970	0.99980	3.21e-10	4-4-2
trainlm	tansig/purelin	learn gdm	0.99979	0.99969	0.99977	0.99978	1.14e-10	4-4-2
trainlm	logsig/purelin	learn gd	0.99990	0.99980	0.99970	0.99990	1.35e-10	4-4-2
trainlm	tansig/purelin	learn gd	0.99990	0.99970	0.99960	0.99970	1.85e-10	4-4-2
trainlm	logsig/purelin	learn gdm	0.99990	0.99927	0.99928	0.99979	7.35e-11	4-5-2
trainlm	tansig/purelin	learn gdm	0.99990	0.99970	0.99980	0.99990	3.80e-10	4-5-2
trainlm	logsig/purelin	learn gd	0.99978	0.99926	0.99932	0.99964	1.77e-05	4-5-2

trainlm	tansig/purelin	learn gd	0.99990	0.99970	0.99960	0.99980	4.76e-11	4-5-2
trainlm	logsig/purelin	learn gdm	0.99990	0.99980	0.99970	0.99990	2.88e-09	4-6-2
trainlm	tansig/purelin	learn gdm	0.99990	0.99970	0.99970	0.99990	1.10e-09	4-6-2
trainlm	logsig/purelin	learn gd	0.99990	0.99980	0.99980	0.99990	7.10e-11	4-6-2
trainlm	tansig/purelin	learn gd	0.99990	0.99940	0.99950	0.99980	6.59e-10	4-6-2
trainlm	logsig/purelin	learn gdm	0.99990	0.99990	0.99989	0.99998	8.58e-08	4-7-2
trainlm	tansig/purelin	learn gdm	0.99990	0.99980	0.99970	0.99998	2.07e-10	4-7-2
trainlm	logsig/purelin	learn gd	0.99990	0.99990	0.99990	0.99990	5.63e-11	4-7-2
trainlm	tansig/purelin	learn gd	0.99958	0.99816	0.99810	0.99914	9.26e-08	4-7-2
trainlm	logsig/purelin	learn gdm	0.99990	0.99980	0.99980	0.99990	2.96e-10	4-8-2
trainlm	tansig/purelin	learn gdm	0.99998	0.99995	0.99993	0.99997	1.90e-12	4-8-2
trainlm	logsig/purelin	learn gd	0.99990	0.99990	0.99990	0.99990	5.52e-10	4-8-2
trainlm	tansig/purelin	learn gd	0.99855	0.99309	0.99372	0.99707	7.37e-11	4-8-2
trainlm	logsig/purelin	learn gdm	0.99990	0.99980	0.99980	0.99980	3.73e-10	4-9-2
trainlm	tansig/purelin	learn gdm	0.99990	0.99990	0.99990	0.99990	1.45e-10	4-9-2
trainlm	logsig/purelin	learn gd	0.99990	0.99990	0.99980	0.99980	4.07e-10	4-9-2
trainlm	tansig/purelin	learn gd	0.99990	0.99990	0.99990	0.99990	9.01e-11	4-9-2
trainlm	logsig/purelin	learn gdm	0.99890	0.99790	0.99770	0.99880	1.00e-09	4-10-2
trainlm	tansig/purelin	learn gdm	0.99990	0.99990	0.99990	0.99990	1.47e-10	4-10-2
trainlm	logsig/purelin	learn gd	0.99990	0.99990	0.99990	0.99990	8.96e-10	4-10-2
trainlm	tansig/purelin	learn gd	0.99990	0.99980	0.99970	0.99990	1.57e-08	4-10-2

The downward trend on MSE of the ANN model with trainlm is graphically presented in Figure 6-14. The plot illustrates the values and the trends on MSE for the training, testing and validation data sets with increasing number of iterations/epochs. Based on the graphical plot, MSE clearly showed the continuous downward pattern with the increase of the iteration number and the train, test and validation sets all showed a similar downward pattern. The downward trend of MSE was observed until the network reached epoch 1000 and the training was terminated. As observed in Figure 6-14, the best validation performance of the network was reached when a low MSE value was 1.5577e-10 at epoch 1000.

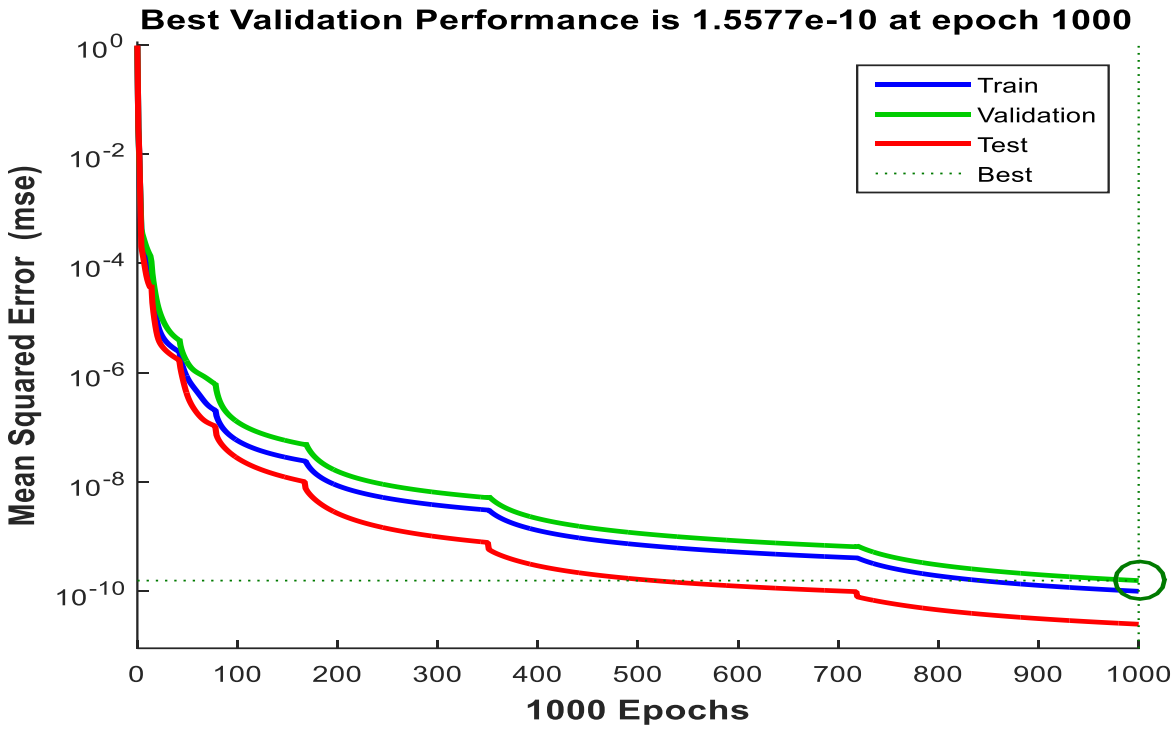

Figure 6-14: ANN performance of the trainlm algorithm for the prediction of filter duration and turbidity

The ANN performance in terms of regression plots for trainlm and trainscg algorithms were also examined and this is essential in evaluating the performance of ANN models after being designed. Figure 6-15 shows the regression plots for the trainlm algorithm in terms of correlation coefficients for training, testing, validation and all data at the end of the training phase. All values were found greater than 0.99 and this confirms good performance of the network in fitting data subsets after training. The actual correlation coefficient values for training, testing, validation and all data were

0.99998, 0.99995, 0.99993 and 0.99997, respectively. From the plot, the good distribution of the majority of data cases within the 45° line showed the good match between the network outputs with target data. Therefore, predictive power of the model with the trainlm algorithm which was illustrated by low error difference between the targets and outputs in Figure 6-15.

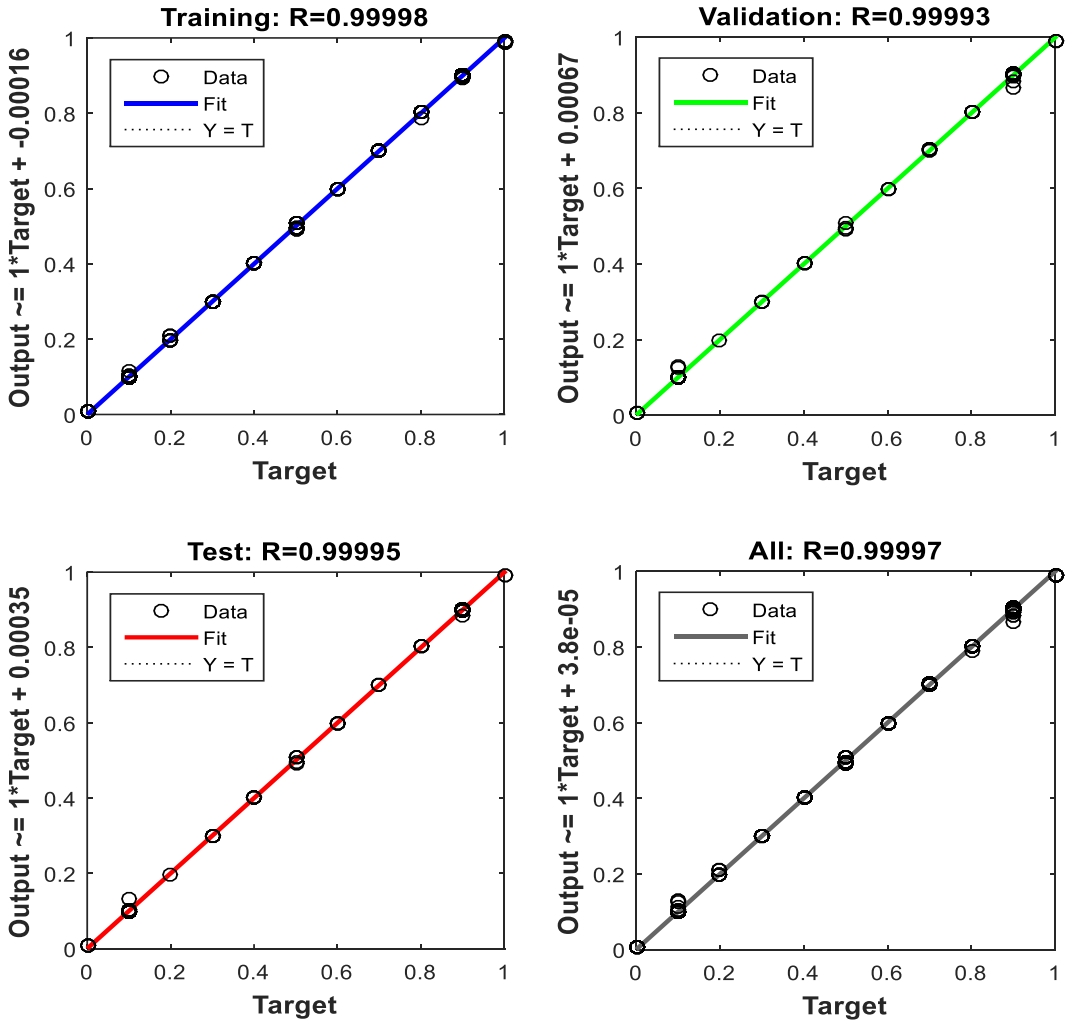

Figure 6-15: Regression plot showing correlation coefficient values for the trainlm algorithm for the prediction of filter duration and turbidity

Figure 6-16 shows the error histogram plot of the network with 20 bins which was obtained with the trainlm algorithm. The errors between observed data and predicted data of the network were generated to evaluate the performance of the network for the training, validation and testing data after ANN training. In this plot, the blue coding represents training data, the red coding represents test data and green bars represent validation data. The errors are distributed around the zero error

where mainly large errors and no abnormalities were observed with the error trends as shown in this plot. Therefore, the graphical plot is actually useful for confirmation of good fit of the network in terms of performance for the prediction of filter duration and turbidity.

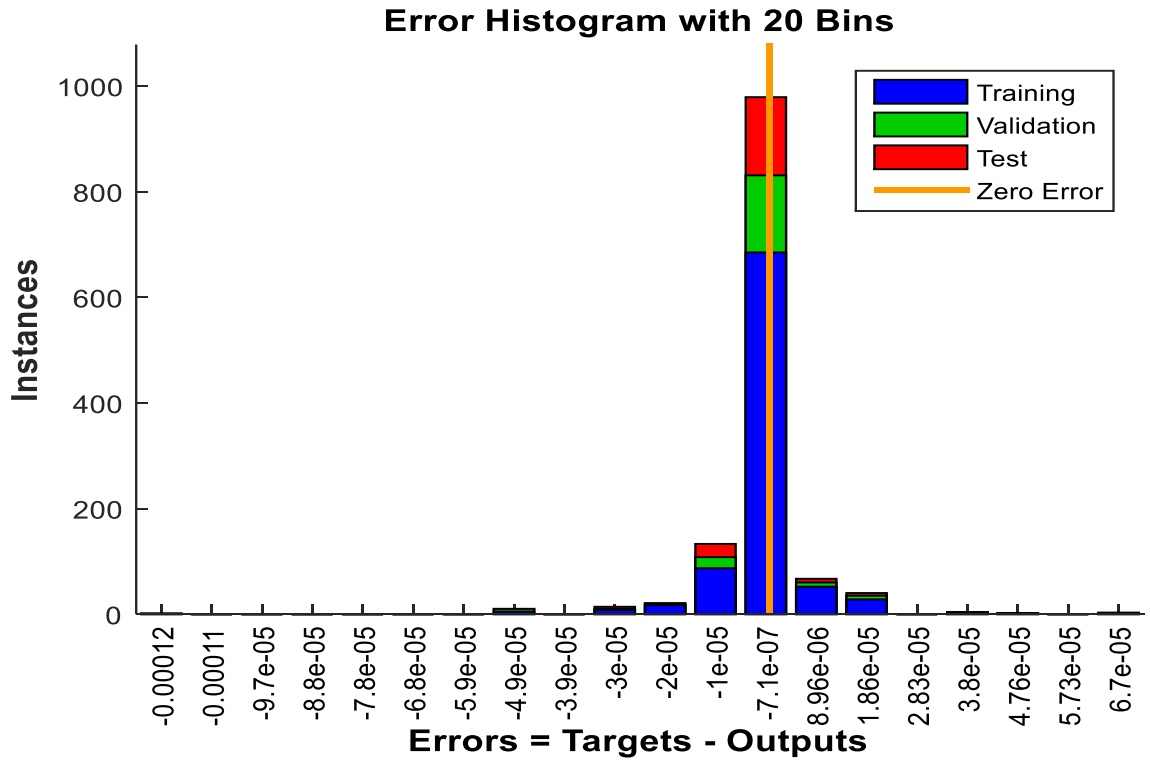

Figure 6-16: Graphical plot of error histogram for 20 bins with the trainlm algorithm

Table 6.5 summarizes the trainscg training results of ANN for the prediction of filter duration and turbidity in HRF equipment which was trained using training parameters in Table 3.7, which was discussed in Chapter 3. The six ANN neurons were subsequently obtained for the optimized architecture with Logsig activation function and Purelin function in the output layer. The performance of different types of ANN models were based on MSE and correlation coefficients for the training, testing, validation and all data sets as shown in Table 6.5. In addition, the trainscg with ANN architecture 4-6-2 recorded the lowest MSE value and higher correlation coefficient values in all data subsets than the rest of the ANN models. Based on the findings of this study it was clearly evident that the trainscg algorithm had underperformed compared to the trainlm algorithm for the prediction of filter duration and turbidity in the HRF unit.

Table 6.5: The ANN results with trainscg algorithm for the prediction of filter duration

Train function	Train function	Adapt. learning	Train (R)	Test (R)	Val (R)	All (R)	MSE	model
trainscg	logsig/purelin	learn gdm	0.99630	0.99385	0.99411	0.99560	0.00094	4-4-2
trainscg	tansig /purelin	learn gdm	0.98178	0.97716	0.97177	0.97955	0.00480	4-4-2
trainscg	logsig/purelin	learn gd	0.99750	0.99603	0.99666	0.99972	0.00060	4-4-2
trainscg	tansig/purelin	learn gd	0.99896	0.99895	0.99862	0.99880	0.00027	4-4-2
trainscg	logsig/purelin	learn gdm	0.99977	0.99930	0.99904	0.99889	0.00029	4-5-2
trainscg	tansig /purelin	learn gdm	0.99995	0.99991	0.99988	0.99994	1.17e-05	4-5-2
trainscg	logsig/purelin	learn gd	0.99054	0.98824	0.99042	0.99017	0.00251	4-5-2
trainscg	tansig/purelin	learn gd	0.99980	0.99975	0.99981	0.99980	4.73e-05	4-5-2
trainscg	logsig/purelin	learn gdm	0.99991	0.99989	0.99988	0.99990	8.42e-07	4-6-2
trainscg	tansig /purelin	learn gdm	0.99993	0.99983	0.99988	0.99991	7.85e-07	4-6-2
trainscg	logsig/purelin	learn gd	0.99997	0.99991	0.99986	0.99995	9.76e-08	4-6-2
trainscg	tansig/purelin	learn gd	0.99975	0.99922	0.99921	0.99959	8.63e-07	4-6-2
trainscg	logsig/purelin	learn gdm	0.99913	0.99878	0.99888	0.99878	0.00023	4-7-2
trainscg	tansig /purelin	learn gdm	0.99939	0.99867	0.99869	0.99918	0.00013	4-7-2
trainscg	logsig/purelin	learn gd	0.99990	0.99990	0.99990	0.99990	6.25e-05	4-7-2
trainscg	tansig/purelin	learn gd	0.99972	0.99924	0.99938	0.99959	6.71e-05	4-7-2
trainscg	logsig/purelin	learn gdm	0.97232	0.96683	0.95857	0.96966	0.00620	4-8-2
trainscg	tansig /purelin	learn gdm	0.99376	0.98643	0.99008	0.99214	0.00198	4-8-2
trainscg	logsig/purelin	learn gd	0.99862	0.99843	0.99774	0.99846	0.00027	4-8-2
trainscg	tansig/purelin	learn gd	0.99999	0.99990	0.99988	0.99998	2.35e-05	4-8-2

trainscg	logsig/purelin	learn gdm	0.99990	0.99970	0.99973	0.99980	5.64e-05	4-9-2
trainscg	tansig /purelin	learn gdm	0.99975	0.99960	0.99961	0.99970	0.00012	4-9-2
trainscg	logsig/purelin	learn gd	0.99376	0.98632	0.99007	0.99214	0.00149	4-9-2
trainscg	tansig/purelin	learn gd	0.99962	0.99924	0.99928	0.99959	0.00520	4-9-2
trainscg	logsig/purelin	learn gdm	0.99929	0.99857	0.99859	0.99918	0.00012	4-10-2
trainscg	tansig /purelin	learn gdm	0.99994	0.99993	0.99992	0.99993	1.51e-05	4-10-2
trainscg	logsig/purelin	learn gd	0.99993	0.99992	0.99992	0.99993	1.83e-05	4-10-2
trainscg	tansig/purelin	learn gd	0.99946	0.99939	0.99914	0.99943	0.00013	4-10-2

The graphical plot in Figure 6-17 presents the network performance for trainscg in terms of MSE for 1000 epochs. The plot essentially shows performance trends for training, validation and testing data sets with the number of iteration settings increasing from 0 to 1000 when the network training was carried out. The ANN training with the trainscg algorithm significantly showed the decreasing pattern up to a low MSE of 7.4656e-07 for a total of 1000 iterations and the network training finally stopped. As shown in Figure 6-17, the good performance of ANN was evident and no over fitting problems were observed. Although with trainscg, the training algorithm achieved low MSE following training, the lowest MSE was, however, achieved with trainlm algorithm and was adopted as the best training algorithm.

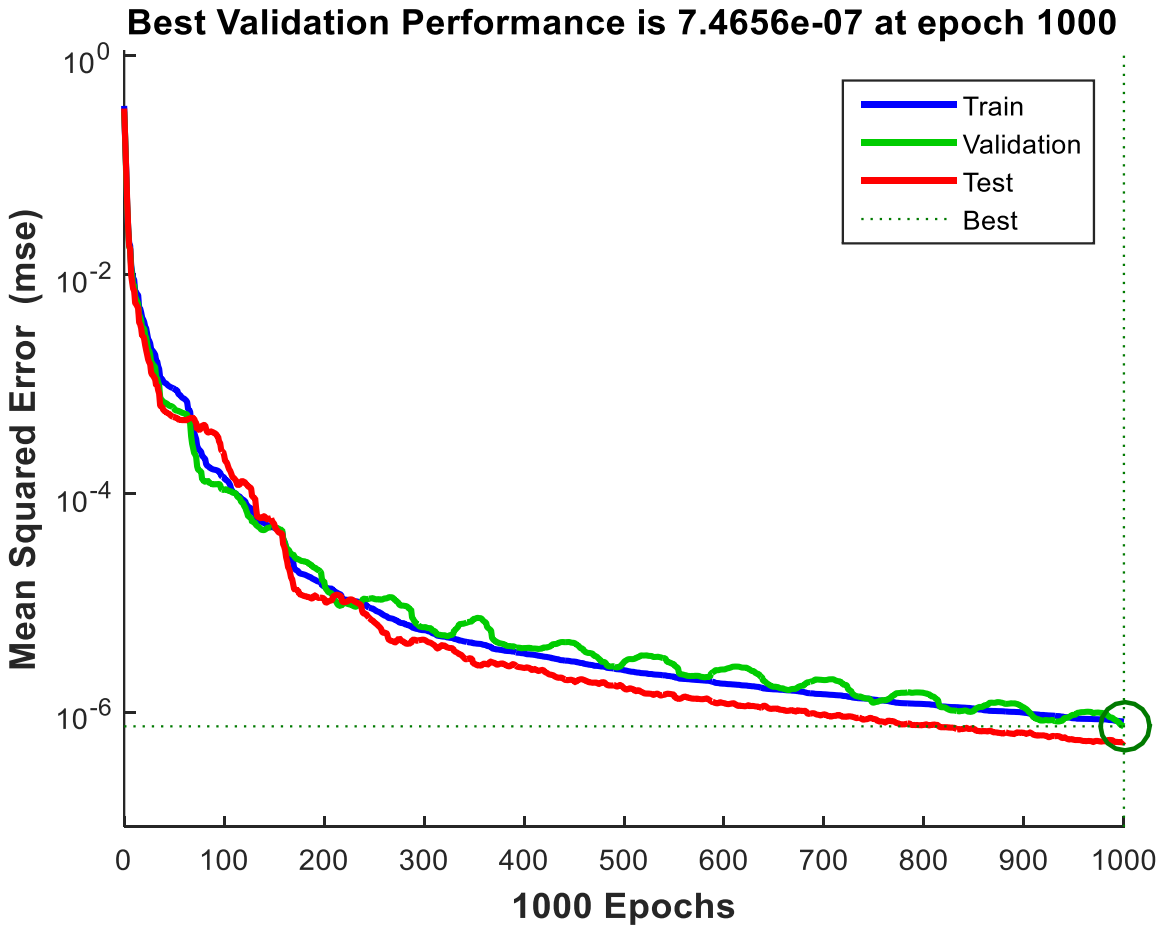

Figure 6-17: ANN performance of the trainscg training function for the prediction of filter duration and turbidity

Figure 6-18 depicts the network regression plots for training, test, validation and all data which were obtained with trainscg. Although it was clearly observed that trainlm recorded the better performance than trainscg, the coefficient of determination values of trainscg recorded were satisfactory and closer to a value of 1 which explains a desirable and perfect correlation between targets and network outputs. The actual correlation coefficients obtained for testing, training, validation and all data were high as observed in the graphical plot in Figure 6-18. The data points were largely centered on the 45° line which confirmed a reasonable fit and good generalization between the targets and network predictions.

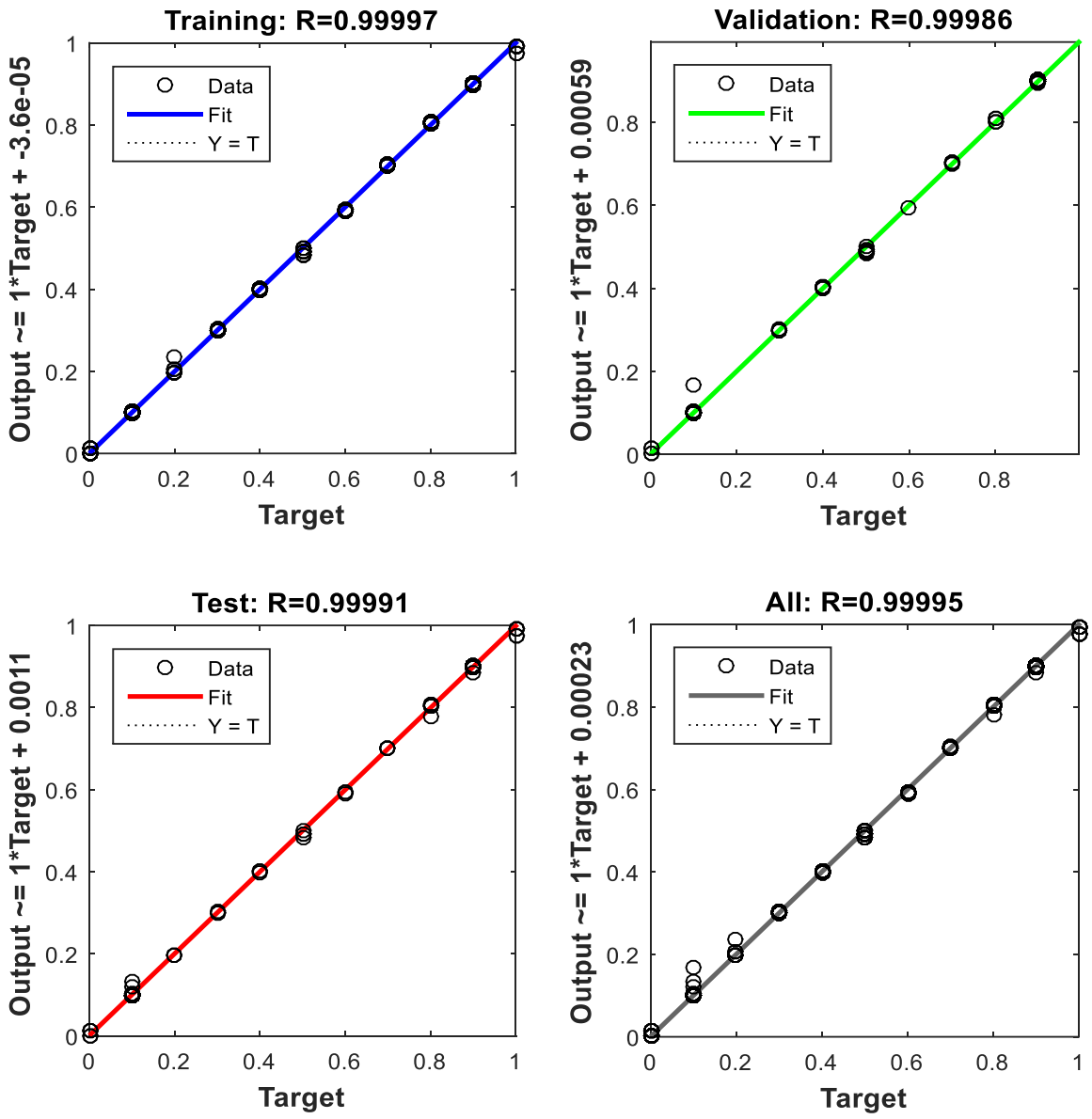

Figure 6-18: Regression plot showing correlation coefficient values for trainscg for the prediction of filter duration and turbidity

The graphical plot showing the error histogram for 20 bins with trainscg at the end of ANN training is presented in Figure 6-19. The error histogram shows error distributions which were produced by the network with three sets of data which was training, testing and validation. As shown in the histogram plot in Figure 6-19, the blue, green and red coded bars represent train, validation and test data sets, respectively. The large errors were mainly distributed near the zero error line and a

small percentage of errors were located away from the zero error line. Most of the observed error values were within the range between -0.030 and 0.037.

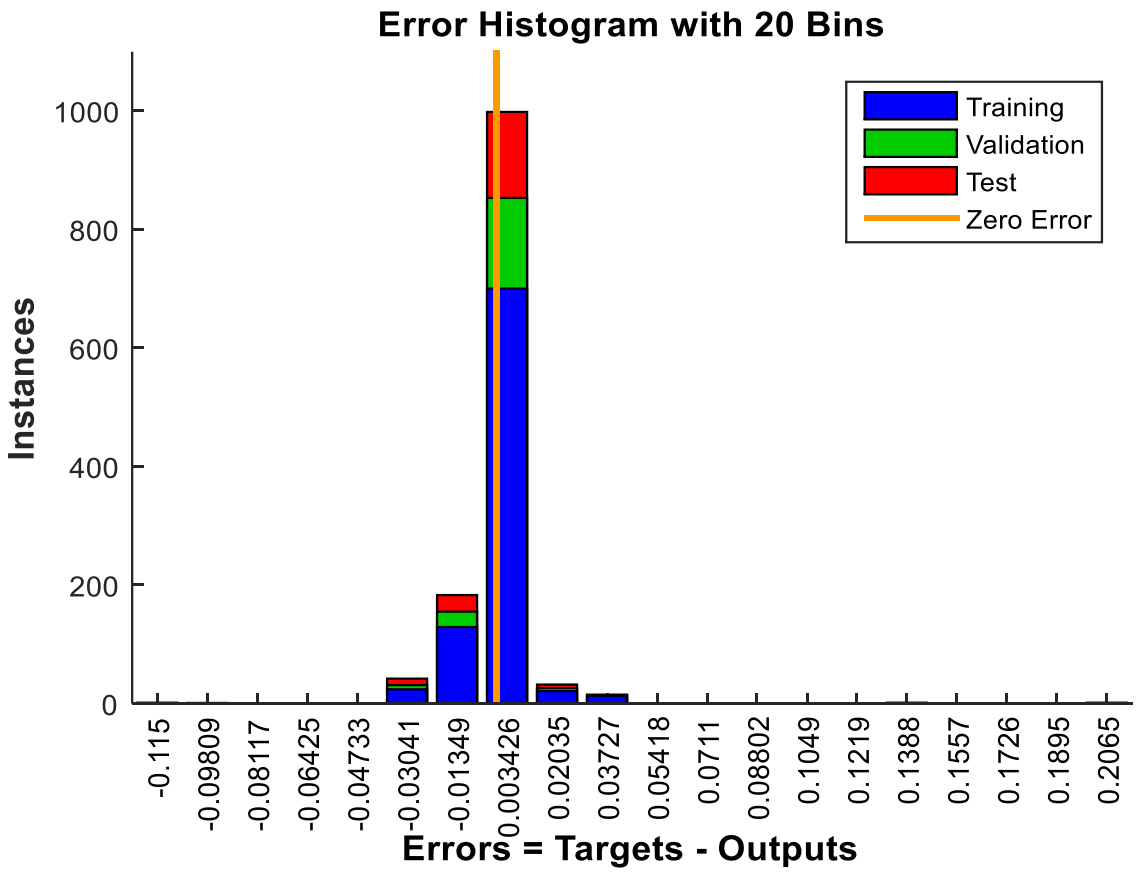

Figure 6-19: Graphical plot of error histogram for 20 bins with trainscg

6.4 The prediction of physico-chemical variables of domestic greywater of the outlet stream of the HRF equipment

This section presents the findings on feedforward ANN modelling of the HRF system for the prediction of multi-output parameters; these were pH, COD, solids and turbidity of domestic greywater following pre-treatment using HRF equipment. The ANN feed forward with back propagation algorithm has been examined in this section for the modelling of the HRF in order to describe the filter performance behavior and ANN capability to map the inputs and output parameters of greywater following the treatment of greywater in a HRF. In this task, the aim was to develop a three layered feedforward ANN for the prediction of four main multi-output parameters of domestic greywater from the outlet stream of the HRF using the feedforward ANN. The predicted multi-output parameters using feedforward ANN were pH, COD, solids and turbidity. In an attempt to develop optimal ANN, the training was initially carried out using only COD and pH as inputs for the prediction of the four multi-outputs that include pH, COD, solids and turbidity. The performance of the ANN obtained in terms of values of the MSE and R correlation coefficient obtained is presented in Figures 6-20 and Figure 6-21. It was noted that ANN showed some learning ability based on reduction of MSE. The summary of the number of neurons in the hidden layer and 14 investigated MATLAB training algorithms is presented in the ANN plots (Figure 6-20 and Figure 6-21).

It was also observed that the ANN in terms of MSE values showed minimal performance on decreasing pattern for the most of the ANN training algorithms with varying number of neurons in the hidden layer as illustrated in Figure 6-20. As observed in the plot, the ANN learning did not show significant improvement during training despite the adjustment of the hidden layer neurons. Therefore, based on this plot, the MSE in almost all ANN models did not show significant improvement with the application of proposed chemical parameters as ANN input vectors for the prediction of pH, COD, solids and turbidity. Figure 6-21 shows the performance of ANN models in terms of *R* correlation coefficient based on the training data set. All ANN models recorded low *R* correlation coefficient values below 0.7. Ideally, the *R* correlation coefficient values should approach a target value of 1 for an optimal ANN model. For all ANN models, the number of neurons that were investigated ranged from 3 to 20 using one hidden layer and different training functions on MATLAB tool.

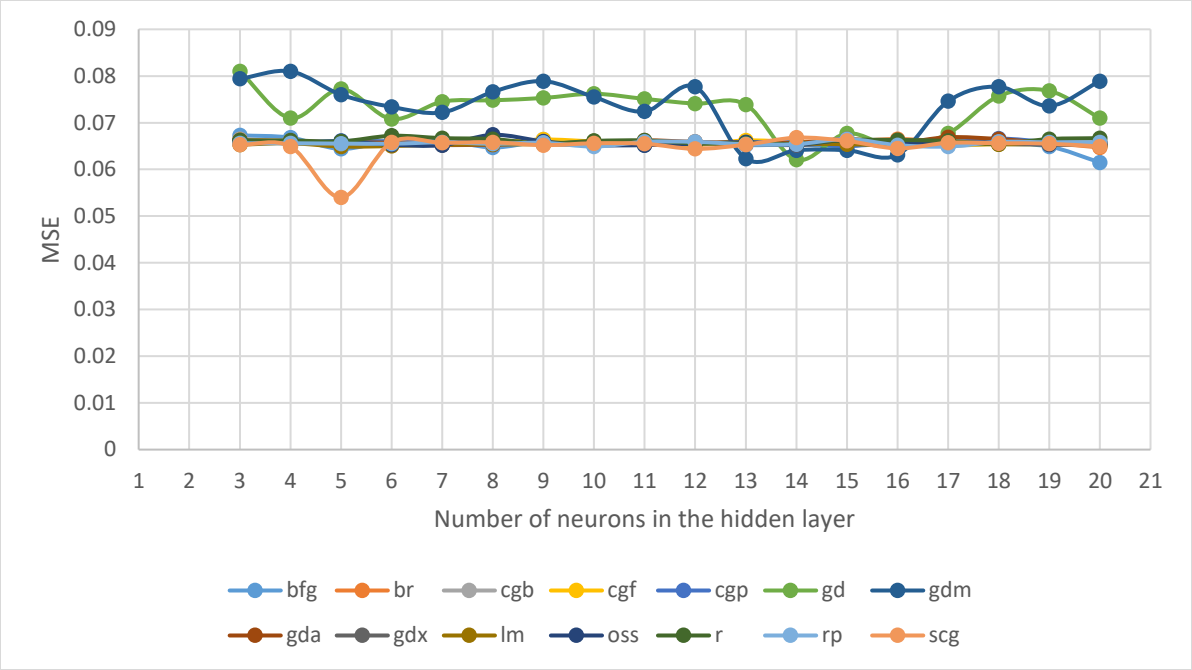

Figure 6-20: The comparison of various training functions in terms of MSE values for ANN trained with COD and pH as inputs for the prediction of multi-output parameters

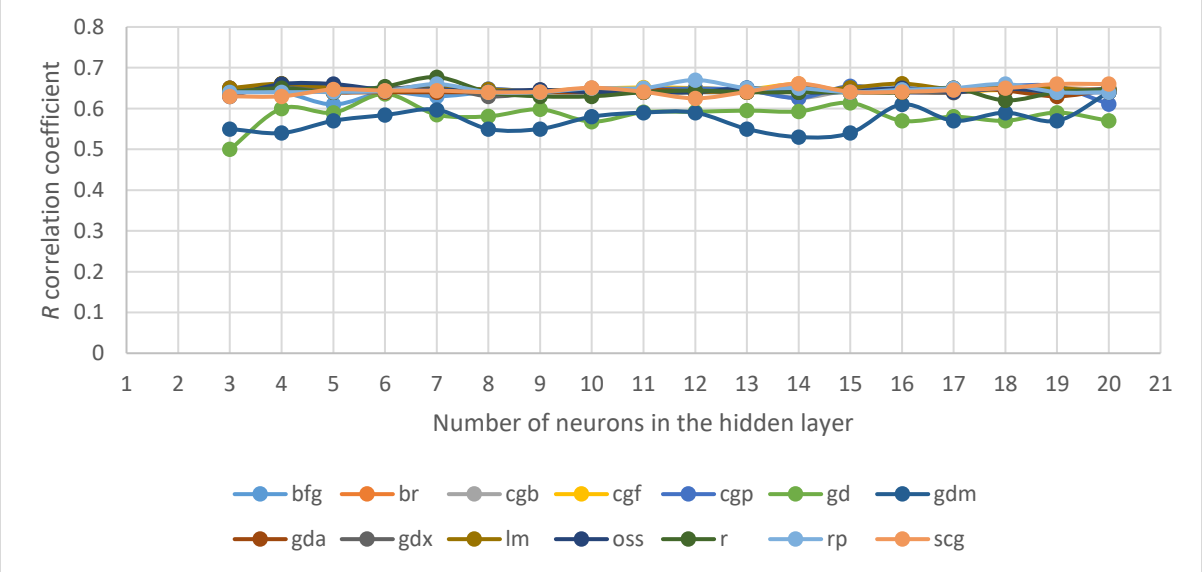

Figure 6-21: The comparison of various training functions in terms of correlation coefficient values for ANN trained with COD and pH as inputs for the prediction of multi-output parameters

Following unsatisfactory performance of the designed ANN models with COD-pH input vectors for the prediction of pH, COD, solids and turbidity. The next ANN models were designed using a new set of input vectors which essentially included flowrate, conductivity, temperature, turbidity and solids as described in Chapter 3. The four multi-output parameters in the output layer remained unchanged and these were pH, COD, solids and turbidity. Figure 6-22 to Figure 6-23 show training results of various ANN models at the end of the training state. The ANN models were trained with the number of neurons varying between 3 and 20 in order to avoid under fitting and overfitting challenges and 14 MATLAB training algorithms.

As shown in Figure 6-22, the ANN models showed better predictions of pH, COD, solids and turbidity than ANN modes with COD and pH as input variables with additional training parameters and low MSE and high correlation coefficient values. In all ANN models, the training algorithms exhibited almost identical performance trends and improved values of MSE and correlation coefficient values. Some fluctuations were observed for the training functions with MSEs greater than 0.03 and generally decrease with increasing number of neurons. This be attributed to the power and learning characteristics of training functions of ANN during the training period.

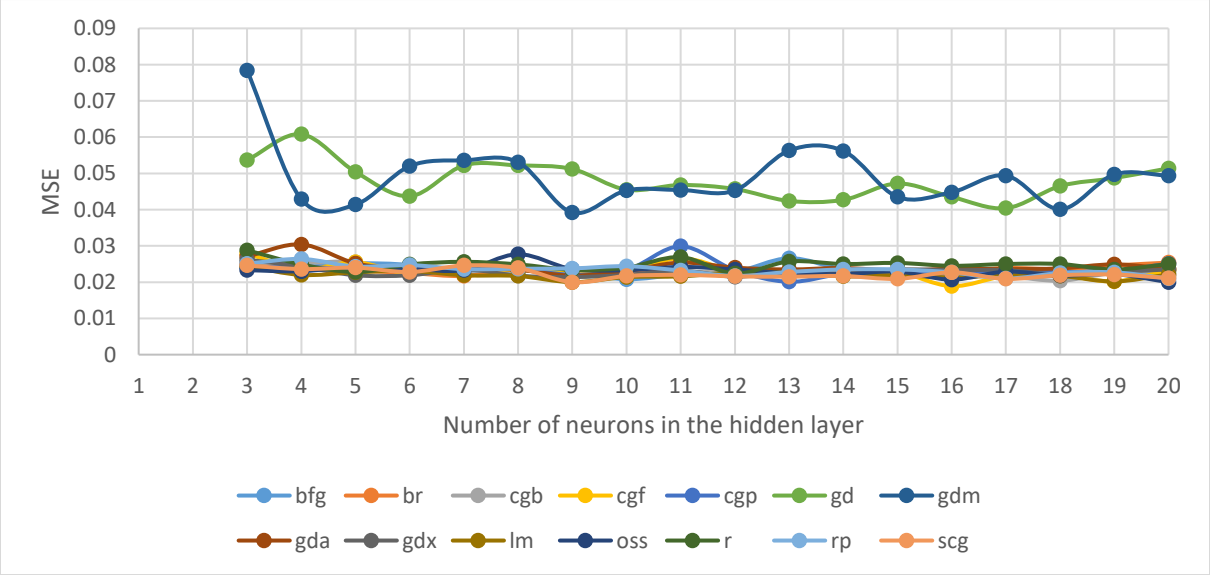

Figure 6-22: The comparison of various training functions in terms of MSE values for ANN trained with physical parameters as inputs for the prediction of multi-output parameters

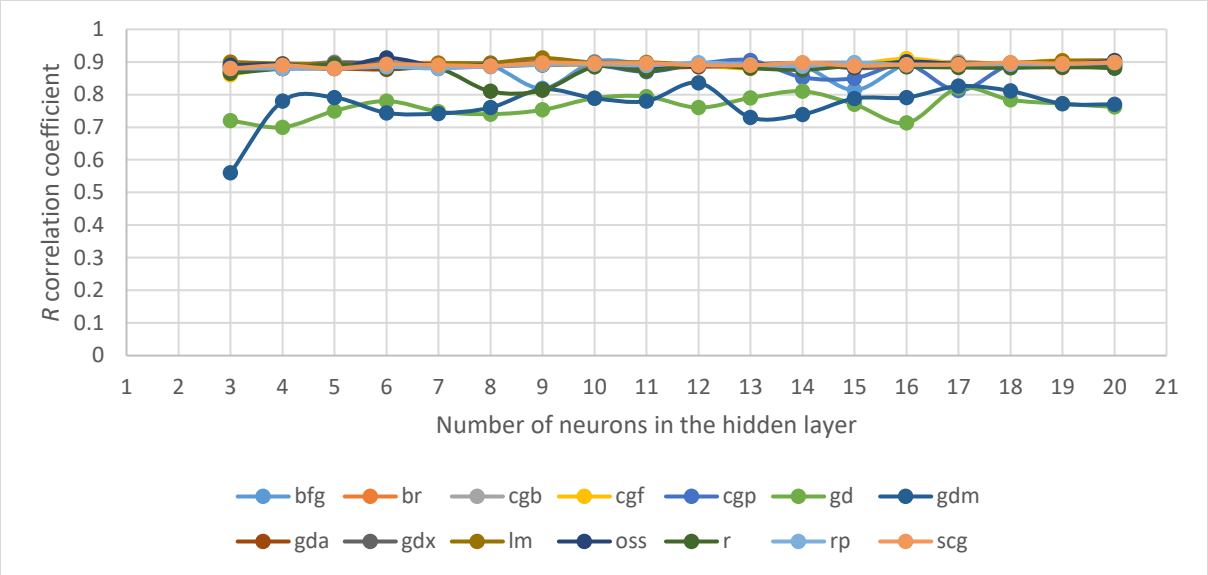

Figure 6-23: The comparison of various training functions in terms of correlation coefficients for ANN trained with physical parameters as inputs for the prediction of multi-output parameters

In the final attempt to develop the optimal ANN model, a combination of physical and chemical parameters were selected and used as input vectors for the prediction of pH, COD, solids and turbidity following method in Chapter 3. The ANN models were trained through trial and error steps. This was carried out through varying training parameters such as training algorithms, the number of neurons in the hidden layer and the training functions. During training, the number of neurons varying between 3 and 20 were investigated. In general, all ANN models showed high degree of learning ability based on the improvement of MSE values and *R* correlation coefficient values as a function of the hidden layer size including training input vectors.

The MSE values showed a decreasing pattern for all training algorithms and the lowest MSE amongst the training algorithms was obtained with trainbr (Figure 6-24). It was also found that most of the ANN models recorded high correlation coefficient values (Figure 6-25), therefore showing good fit and low error values between the targets and the network outputs. The best ANN was obtained with 15 neurons in the hidden layer, thus the 7-15-4 ANN architecture was selected as the optimal ANN model. The corresponding training algorithm for the optimal model was trainbr, whereas, the activation function was the Tansig and Purelin function in the hidden layer and output layer, respectively.

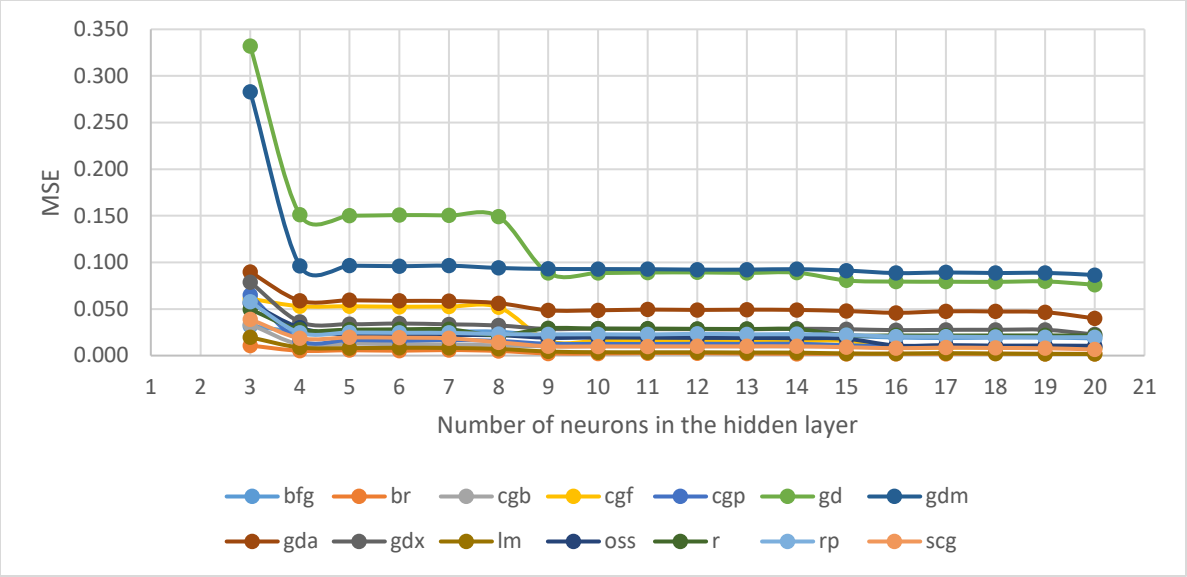

Figure 6-24: The MSE values for ANN trained with physico-chemical parameters for the prediction of multi-output parameters

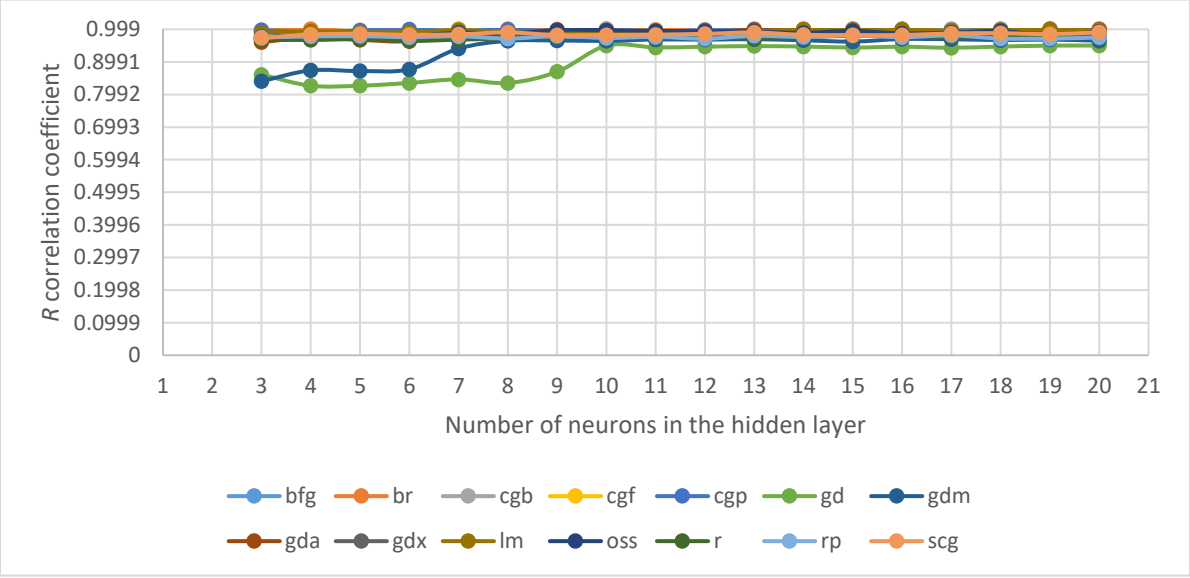

Figure 6-25: The *R* correlation coefficients for various training functions of ANN for the prediction of multi-output parameters

After successful learning activity of the feedforward ANN, the fully trained optimal ANN model was presented with a new sample of data containing input vectors. Figure 6-26 presents the graphical plot showing solids profile with 30 observations. The graphical plot presents the network

predictions along target data with a varying number of observations. The plot showed a good fit on predicted and target data as the predicted values almost matched target values. The low error values are desirable in well-trained ANN models and based on this plot, it was also evident that there were low error values between predicted and target values for almost all the observations. This ANN model showed good predictive power and high accuracy in predicting solids content.

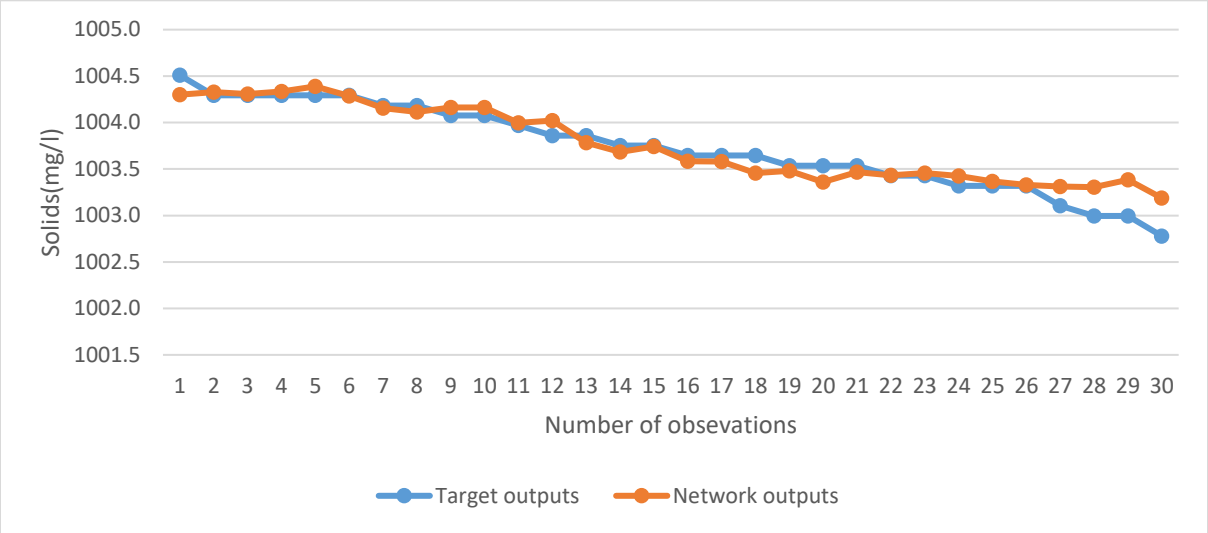

Figure 6-26: The multi-output ANN performance in the case of total solids profile in terms of network predictions and target outputs with the number of sample observations

The optimal ANN model also showed good performance in predicting turbidity as shown in Figure 6-27, where turbidity profile with the number of sample observations is presented. The plot shows predicted ANN outputs of turbidity compared against known target values. Based on this plot, the a good fit between predicted and target turbidity values with all sample data points/observations was evident. For approximately all observations, low error distributions were also evident between targets and the predicted output turbidity, and only a few observations suffered a minor loss of precision or accuracy as illustrated in Figure 6-27. The experimental and predicted values of turbidity were between 30.5 and 32.2 NTU as shown in this graphical plot.

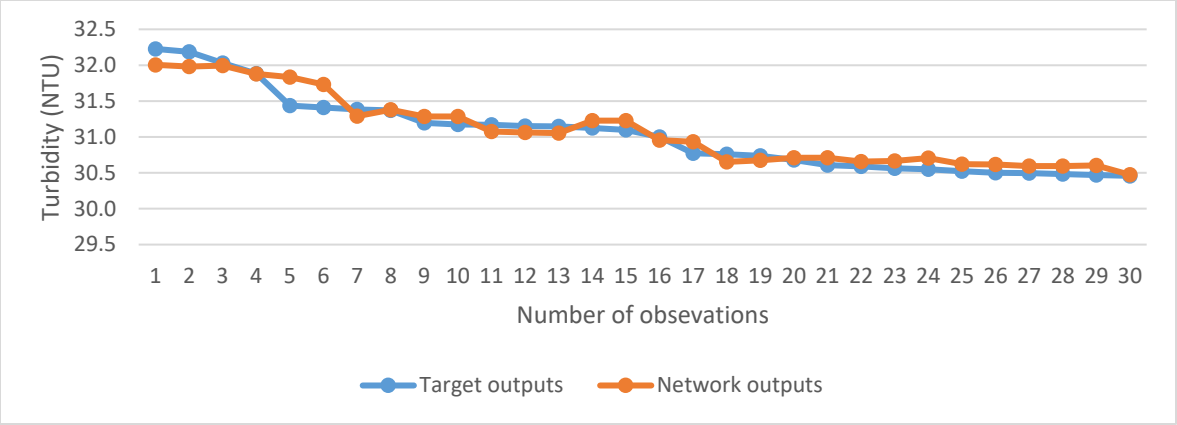

Figure 6-27: The multi-output ANN performance in the case of turbidity profile in terms of network predictions and target outputs with the number of sample observations

Figure 6-28 shows the performance of the optimal ANN model in predicting COD for the given ANN sample with 30 observations. The plot shows target COD plotted with respect to the predicted COD along the sample observations. A good fitting pattern between the predicted and target COD values was evident and low error difference in most data cases. Although the ANN was capable of capturing of showing reasonable prediction accuracy as the matching pattern between targets and predicted COD was reasonably evident. However, the ANN model showed a certain degree of limitation in accurately predicting COD within the HRF system. This could be due to greywater quality variations obtained in different sources and the low prediction accuracy was evident for COD.

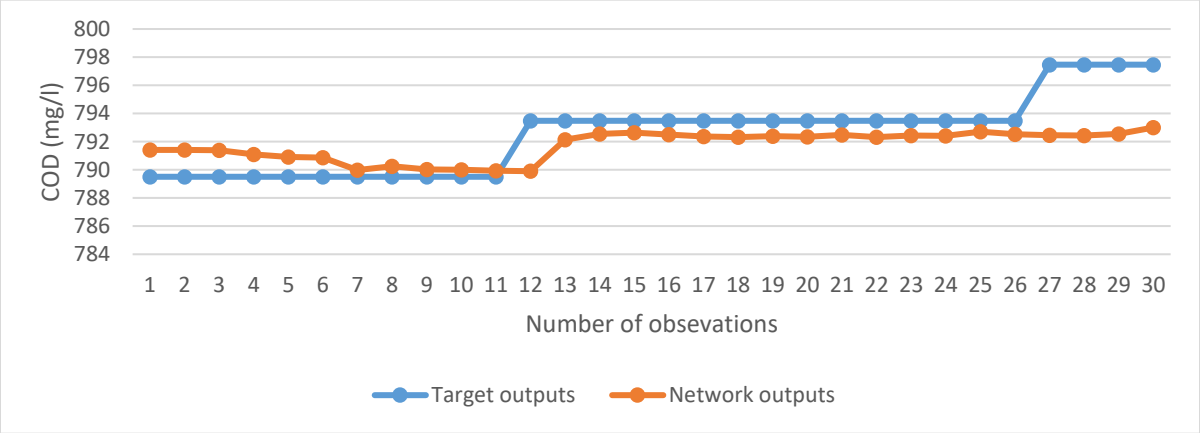

Figure 6-28: The multi-output ANN performance in the case of COD profile in terms of network predictions and target outputs with the number of sample observations

The optimal ANN model was also used for the prediction of pH as shown in the graphical plot profiling pH patterns in Figure 6-29 with the number of observations. As shown in the Figure 6-29, the plot shows good data fitting with *R* correlation coefficient above 0.9 between predicted and the actual outputs for the variable pH. The accuracy of the ANN with predicted and the target outputs for all 30 observations was observed in the plot. The plot also displays minimal error profile with respect to the target outputs including low deviations between predicted and target outputs. Therefore, the good agreement between predicted results in relation to the known target values confirmed the usefulness of the optimal ANN model.

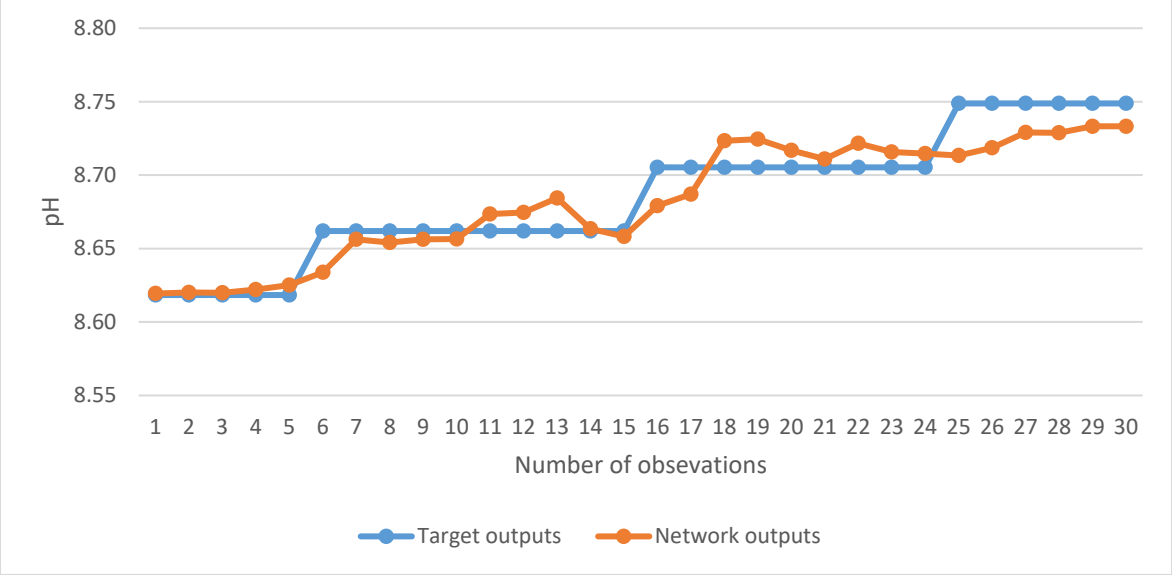

Figure 6-29: The multi-output ANN performance in the case of pH profile in terms of network predictions and target outputs with the number of sample observations

Chapter 7

7.1 Conclusions and recommendations

The first aspect of this research work was the investigation of quality of domestic greywater from a peri-urban community in terms of the content of biological and physico-chemical pollutants. The aim was to understand and quantify the concentration of pollutants in domestic greywater sources originating from kitchen, bath and laundry sources. This aspect was investigated in order to gain in depth understanding related to domestic greywater quality and for the selection of the effective and right water treatment methods. Based on the results, it was observed that the greywater from kitchen, laundry and bath showed significant difference in terms of biological, physical and chemical content. In this study, the kitchen source recorded higher pollution strength and lower treatability characteristics than other greywater sources at $p<0.05$ significant level. Also, the biodegradability of kitchen greywater was low and the BOD/COD ratio of 0.5 was obtained.

The difference in quality was also observed in greywater sources due to daily households' social conditions and practices. The E. coli and total coliforms in domestic greywater samples were also recorded in this study. This confirmed the requirement of the treatment aspect on domestic greywater in order to minimize the significance of health related risks related to domestic greywater reuse. Based on the microbes obtained in domestic greywater, the treatment of domestic greywater prior to reuse should also be considered in order to ensure conformity of greywater with greywater reuse standards.

In the HRF, the filter performance through the treatment of mixed domestic greywater was also investigated. The aim was to study the level of effectiveness of the HRF and its ability in treating mixed domestic greywater which was operated at a low filtration rate of 0.3 m/h and based on the selected gravel media sizes within the filter compartments. The filter performance was evaluated based on the biological, chemical and physical parameters of the greywater streams within the HRF equipment. Based on the results related to this investigation, the removal of pollutants was generally satisfactory within the HRF and significant removal was evident in the greywater stream from the HRF in terms of biological and physico-chemical pollutants at a significant level of 5%.

The physical pollutants were highly removed by the HRF. Based on the findings, an average turbidity removal of 90% was obtained in the HRF. The removal of conductivity was also satisfactory and a value of 86% was recorded. In addition, a value of 84% for the removal of solids and 50-70% removal of COD were also recorded within the HRF equipment. Other experiments were performed in a HRF for the analysis of the biological pollutants. A good removal of E. coli and total coliforms was also obtained for the treated greywater. Also, the HRF performance in terms of removal of some of the parameters including turbidity, conductivity, pH and microbes was in accordance with greywater reuse standards for irrigation and toilet flushing. However, further treatment of chemical pollutants remain necessary to make greywater fit for reuse purposes.

The aspect of design variables of the HRF was also investigated in this study based on the DOE/RSM method in order to study and understand the multi-effect influence of design variables on the HRF performance. The design parameters were perforated inlet baffle, filtration rate, filter length, bed height and gravel media size. In this study, the significant variables were filtration rate, filter length bed height and gravel media size at 5% significant level while perforated inlet baffle was found insignificant based on the findings of the factorial design. Amongst the significant design variables, it was observed based on Pareto chart analysis and half-probability plot that the most significant design variable within the HRF was filtration rate compared to filtration length, filter bed height and gravel media size.

Therefore, it was evident that right factor settings on design variables in HRF is important and is highly necessary for the optimal performance in HRF. Based on four design variables, that is, filtration rate, filter length, bed height and gravel media sizes, a single compartment of the filter was optimized using RSM. Furthermore, the filtration rate, gravel media, bed height and filter length had an effect on the overall removal of turbidity. Therefore based on this study, the selection and use of the right design factor settings is the key step in HRF performance. The other aspect of this work was investigated using ANN through the development of different ANN structures. This was done in order to study the applicability and prediction accuracy of ANN following domestic greywater treatment within the HRF equipment. For this aspect, the modelling of HRF using ANN was carried out based on the selected ANN training parameters and different ANN structures were developed varying from MISO to MIMO models. The ANN models that were developed include:

- ANN model to predict turbidity in HRF equipment.

- ANN model to predict COD of domestic greywater in the outlet stream of the HRF equipment.
- The feedforward ANN model to estimate and predict filter duration of the HRF equipment.
- MIMO ANN model, based on the physico-chemical parameters, to predict multi-output variables of domestic greywater effluent from the HRF equipment.

For the prediction of turbidity, the ANN with 4-7-1 structure was obtained using the trainlm algorithm. The MSE obtained was below 10% with *R* correlation coefficients all greater than 0.9 for the training, testing, validation and all data sets. The next objective on ANN was the prediction of COD for mixed domestic greywater from the HRF. The optimal ANN architecture obtained was 3-10-1 which was obtained with the trainlm training algorithm. Results of this ANN also showed satisfactory low MAPE and MAE values and good *R* correlation coefficient values close to 1 for the training and testing data sets. These findings showed good ability and accuracy of ANN in predicting COD from the HRF stream.

The study also investigated the aspect of filter duration of the HRF system using ANN based on turbidity, pH, conductivity and solids as input variables. An ANN with 4-8-2 architecture was obtained based on the trainlm algorithm for the prediction of filter duration and turbidity. In addition, the *R* correlation coefficients obtained for training, testing, validation and all data were also satisfactory and the values were 0.99998, 0.99995, 0.99993 and 0.99997, respectively and a value below 10% on MSE was also recorded for this optimal model. However, the filter duration using ANN obtained was highly affected by low domestic greywater quality based on kitchen greywater containing high pollutants. The final objective was investigated using ANN for the prediction of multi-output variables following HRF performance. The predicted variables using ANN were pH, COD, solids and turbidity. Form this investigation, the feedforward MIMO ANN model recorded good accuracy in predicting these multi-output variables of domestic greywater from the HRF. In this aspect, different models of ANN were developed by varying training functions, neurons and combination of physico-chemical parameters and learning functions. The optimal ANN model after training was 7-15-4. Also, the MSE value of 0.001 based on training data was obtained and the *R* correlation coefficient values above 0.9 for training, test, validation and all data sets was obtained. As for the validation of the model, the optimal ANN showed good prediction and satisfactory accuracy when a sample with 30 data cases was presented.

7.2 Recommendations

The research study presented in this thesis investigated and explored the option of domestic greywater reuse through modelling of the HRF equipment for the optimization of HRF performance. The thesis recommends:

- Characterization of the remainder of pollutants in domestic greywater for the overall representation of domestic greywater quality while this study mainly investigated the major physico-chemical pollutants and microbial activities which were reported in this work.
- The critical analysis of all microbes in domestic greywater for the community due to their direct effect in human wellbeing as they can even cause infectious diseases with greywater reuse below reuse standards.
- Further investigation on design and different types of filtering media in HRFs for the treatment of low biodegradable domestic greywater in order to meet domestic greywater reuse standards and overcome water shortages in peri-urban communities.
- The combination of empirical and ANN studies to study filter duration for highly polluted domestic greywater for the optimization of HRF performance for the exploration and analysis on cost effective operation within the HRFs.
- The development of universal ANN water quality modelling for monitoring efficiency in HRFs within water treatment remain necessary for the flexible and instant water quality modelling.

References

ABBA, S.I., HADI, S.J. AND ABDULLAHI, J. (2017). River water modelling prediction using multi-linear regression, artificial neural network, and adaptive neuro-fuzzy inference system techniques. *Procedia Computer Science*, 120, 75-82.

ABBASPOUR, K.C., VAGHEFI, S.A., YANG, H. AND SRINIVASAN, R. (2019). Global soil, landuse, evapotranspiration, historical and future weather databases for SWAT Applications. *Scientific Data*, 6(1), 1-11.

ABDOLMALEKI, A.S., GHOLAMALIZADEH AHANGAR, A. AND SOLTANI, J. (2013). Artificial Neural Network (ANN) Approach for Predicting Cu Concentration in Drinking Water of Chahnimeh1 Reservoir in Sistan-Balochistan, Iran. *Health Scope*, 2(1), 31-38.

ABIODUN, O.I., JANTAN, A., OMOLARA, A.E., DADA, K.V., MOHAMED, N.A. AND ARSHAD, H. (2018). State-of-the-art in artificial neural network applications: A survey. *Heliyon*, 4(11), 00938-00979.

ABIODUN, O.I., KIRU, M.U., JANTAN, A., OMOLARA, A.E., DADA, K.V., UMAR, A.M., LINUS, O.U., ARSHAD, H., KAZAURE, A.A. AND GANA, U. (2019). Comprehensive Review of Artificial Neural Network Applications to Pattern Recognition. *IEEE Access*, 7, 158820–158846.

AFFAM, A. AND ADLAN M. (2013). Operational performance of vertical up-flow roughing filter for pre-treatment of leachate using limestone filter media. *Journal of Urban and Environmental Engineering*, 7(1), 117-125.

AHSAN, T. (1995). Process analysis and optimization of direct horizontal-flow roughing filtration. *PhD thesis report in Water Engineering*. Delft University of Technology, Holland.

AISH, A.M., ZAQOOT, H.A. AND ABDELJAWAD, S.M. (2015). Artificial neural network approach for predicting reverse osmosis desalination plants performance in the Gaza Strip. *Desalination*, 367, 240-247.

AL-ARAIMI, M.M., JOY, V.M., RAO, L.S.N. AND FEROZ, S. (2019). Optimization and Assessment of Residual Chlorine using Response Surface Methodology (RSM) and Artificial Neural Network (ANN) Modeling, *International Journal of Recent Technology and Engineering* (IJRTE), 8(3), 258-263.

AL-JAYYOUSIE, O.R. (2003). Greywater reuse: towards sustainable water management. *Desalination*, 156(1), 181-192.

ALLEN, L., CHRISTIAN-SMITH, J. AND PALANIAPPAN, M. (2010). *Overview of Greywater Reuse*: *The Potential of Greywater Systems to Aid Sustainable Water Management*, Pacific Institute Report, Oakland, CA.

ALMEIDA, M., BUTLER, D. AND FRIEDLER, E. (1999). At-source domestic wastewater quality. *Urban Water Journal*, 1(1), 49-55.

ALOM, M.Z., TAHA, T.M., YAKOPCIC, C., WESTBERG, S., SIDIKE, P., NASRIN, M.S., HASAN, M., VAN ESSEN, B.C., AWWAL, A.A.S. AND ASARI, V.K. (2019). A State-of-the-Art Survey on Deep Learning Theory and Architectures. *Electronics*, 8(3), 1-66.

ALTENBURGER, R., BRACK, W., BURGESS, R.M., BUSCH, W., ESCHER, B.I., FOCKS, A., MARK HEWITT, L., JACOBSEN, B.N., DE ALDA, M.L., AIT-AISSA, S., BACKHAUS, T., GINEBREDA, A., HILSCHEROVÁ, K., HOLLENDER, J., HOLLERT, H., NEALE, P.A., SCHULZE, T., SCHYMANSKI, E.L., TEODOROVIC, I., TINDALL, A.J., DE ARAGÃO UMBUZEIRO, G., VRANA, B., ZONJA, B. AND KRAUSS, M. (2019). Future water quality monitoring: improving the balance between exposure and toxicity assessments of real-world pollutant mixtures. *Environmental Sciences Europe*, 31(1), 1-17.

AMBROSE, R.B., WOOL, T.A. AND BARNWELL, T.O. (2009). Development of Water Quality Modeling in the United States. *Environmental Engineering Research*, 14(4), 200-210.

AMERICAN PUBLIC HEALTH ASSOCIATION (APHA) (2012). *Standard Methods for the Examination of Water and Wastewater*, 20th edn. American Water Works Association and Water Environmental Federation, Washington, DC.

ANAGNOSTOU, E., GIANNI, A. AND ZACHARIAS, I. (2017). Ecological modeling and eutrophication-A review, *Natural Resource Modeling*, 30(3), e12130.

APICELLA, A., DONNARUMMA, F., ISGRÒ, F. AND PREVETE, R. (2021). A survey on modern trainable activation functions. *Neural networks*: *the official journal of the International Neural Network Society*, 138(1), 14-32.

ARNOLD, J.G. AND FOHRER, N. (2005). SWAT2000: current capabilities and research opportunities in applied watershed modelling. *Hydrological Processes*, 19(3), 563-572.

ARNOLD, J.G., SRINIVASAN, R., MUTTIAH, R.S. AND WILLIAMS, J.R. (1998). Large area hydrologic modeling and assessment. Part I: Model development. *Journal of the American Water Resources Association*, 34(1), 73-89.

ARNOLD, J.G., MORIASI, D.N., GASSMAN, P.W., ABBASPOUR, K.C., WHITE, M.J., SRINIVASAN, R., SANTHI, C., HARMEL, R.D., VAN GRIENSVEN, A., VAN LIEW, M.W., KANNAN, N. AND JHA, M.K. (2012). SWAT: Model Use, Calibration and Validation. *American Society of Agricultural and Biological Engineers*, 55(4), 1491-1508.

ASADY, B., HAKIMZADEGAN, F. AND NAZARLUE, R. (2014). Utilizing artificial neural network approach for solving two-dimensional integral equations. *Mathematical Sciences*, 8(1), 117.

ASANOA, T. (2006). Special Feature on Groundwater Management and Policy: Water Reuse via Groundwater Recharge, *International Review for Environmental Strategies*, 6(2), 205 – 216.

AULENBACH, D.B. (1993). Manual of Design for Slow Sand Filtration by David Hendricks, AWWA Research Foundation and the American Water Works Association, Denver, CO.

AYENI, A.O., BALOGUN, I.I. AND SONEYE, A.S.O. (2011). Seasonal Assessment of Physico-chemical Concentration of Polluted Urban River: A Case of Ala River in South- western Nigeria. *Research Journal of Environmental Sciences*, 5(1), 21-35.

AZAR, A.T. (2013). Fast neural network learning algorithms for medical applications. *Neural Computing and Applications*, 23(3-4), 1019-1034.

BAILEY, J.R., AHMAD, S. AND BATISTA, J.R. (2020). The Impact of Advanced Treatment Technologies on the Energy Use in Satellite Water Reuse Plants. *Water*, 12(2), 1-17.

BAKARE, B.F., MTSWENI, S. AND RATHILAL, S. (2017). Characteristics of greywater from different sources within households in a community in Durban, South Africa. *Journal of Water Reuse and Desalination*, 7(4), 520-528.

BAKARE, B.F., MTSWENI, S. AND RATHILAL, S. (2019). Pilot study of a horizontal roughing filtration system treating greywater generated from peri-urban community in Durban, South Africa, *Journal of Water Reuse and Desalination*, 9(3), 330-337.

BAKER, M.N. (1948). The quest for pure water. *The American Water Works Association Inc*., New York, 7-76.

BATICK, B.M. (2011). *Modeling temperatue and dissolved oxygen in the Cheatham reservoir with CE-QUAL-W2*. Dissertation, Nashville Tennessee Graduate School of Vanderbilt University.

BAYKAL, H. AND YILDIRIM, H.K. (2013). Application of Artificial Neural Networks (ANNs) in Wine Technology. *Critical Reviews in Food Science and Nutrition*, 53(5), 415–421.

BEHIN, J. AND FARHADIAN, N. (2016). Response surface methodology and artificial neural network modeling of reactive red 33 decolorization by O3/UV in a bubble column reactor. *Advances in Environmental Technology*, 2(1), 33-44.

BELLO, O., ABU-MAHFOUZ, A., HAMAM, Y., PAGE, P., ADEDEJI, K. AND PILLER, O. (2019). Solving Management Problems in Water Distribution Networks: A Survey of Approaches and Mathematical Models. *Water*, 11(3), 562.

BERMANT, P.C., BRONSTEIN, M.M., WOOD, R.J., GERO, S. AND GRUBER, D.F. (2019). Deep Machine Learning Techniques for the Detection and Classification of Sperm Whale Bioacoustics. *Scientific Reports*, 9(1), 12588.

BOANO, F., CARUSO, A., COSTAMAGNA, E., RIDOLFI, L., FIORE, S., DEMICHELIS, F., GALVÃO, A., PISOEIRO, J., RIZZO, A. AND MASI, F. (2020). A review of nature-based solutions for greywater treatment: Applications, hydraulic design, and environmental benefits. *Science of the Total Environment*, 711, 134731.

BOCK, F.E., AYDIN, R.C., CYRON, C.J., HUBER, N., KALIDINDI, S.R. AND KLUSEMANN, B. (2019). A Review of the Application of Machine Learning and Data Mining Approaches in Continuum Materials Mechanics. *Frontiers in Materials*, 6, 110.

BOLLER, M. (1993). Filter mechanisms in roughing filters. *Journal of Water Supply Research and Technology – Aqua*, 42(3), 174 -185.

BOWDEN, G.D., PICHLER, B.J. AND MAURER, A. (2019). A Design of Experiments (DoE) Approach Accelerates the Optimization of Copper-Mediated 18F-Fluorination Reactions of Arylstannanes. *Scientific Reports*, 9(1), 11370.

BOYACIOGLU, H., BOYACIOGLU, H. AND GUNDUZ, O. (2005). Application of factor analysis in assessment of surface water quality in Buyuk Menderes River Basin, *European Water Journal*, 9(10), 43-49.

BROWN, L.C. AND BARNWELL, T.O. (1987). *The enhanced stream water quality models QUAL2E and QUAL2E-UNCAS. Documentation and user manual*, report EPA/600/3-87/007, U.S. EPA, Athens, GA. USA.

BROWNLEE, K. A. (1966). *Statistical Theory and Methodology in Science and Engineering*. Wiley, New York.

CARDEN, K., ARMITAGE, N., SICHONE, O., WINTER, K. AND RIVETT, U. (2006). Management options for the safe use and disposal of greywater in the non-sewered areas of South Africa. *Paper presented at the 3rd International Conference on Ecological Sanitation, 23-26 May 2005, Durban, South Africa*.

CHANG, C.-H., CAI, L.-Y., LIN, T.-F., CHUNG, C.-L., VAN DER LINDEN, L. AND BURCH, M. (2015). Assessment of the Impacts of Climate Change on the Water Quality of a Small Deep Reservoir in a Humid-Subtropical Climatic Region. *Water*, 7(12), 1687-1711.

CHEN, Z., NGO, H.H. AND GUO, W. (2013). A Critical Review on the End Uses of Recycled Water. *Critical Reviews in Environmental Science and Technology*, 43(14), 1446-1516.
CHEN, Z., NGO, H.H. AND GUO, W.S., (2012). A critical review on sustainability assessment of recycled water schemes. *Science of the Total Environment*, 426, 13-31.

CHU, H.B., LU, X.W AND ZHANG, L. (2013). Application of Artificial Neural Network in Environmental Water Quality Assessment, *Journal of Agricultural Science and Technology*, 15(2), 343-356.

CIROLINI, A., BASEGGIO, A.M., MIOTTO, M., RAMOS,R.J., CATTANI, C.S.O. AND VIEIRA, C.R.W. (2013). Evaluation of the PetrifilmTM and TEMPO® systems and the conventional method for counting microorganisms in pasteurized milk, *Food Science and Technology*, 33(4), 784-789.

CLARKE, B.A., LLOYD, B.J., CROMPTON, J.L. AND MAJOR, I.P. (1996). Cleaning of up-flow gravel pre-filters in multi-stage filtration water treatment plants. In: Graham, N. and Collins, R. (eds.). *Advances in slow sand and alternative biological filtration*, Wiley and Sons, Chichester.

CLEARY, S.A. (2005). *Sustainable drinking water treatment for small communities using multistage slow sand filtration*. Master's thesis in Applied Science. Waterloo, Ontario, Canada.

COLE, T. AND BUCHAK, E.M. (1995). CE-QUAL-W2: *A two dimensional, laterally averaged, hydrodynamic and water quality model*, Version 2.0, User Manual. U.S. Army Corps of Engineers, Waterways Experiment Station, Vicksburg, MS 39180-6199.

COUTO, E.A., CALIJURI, M.L., ASSEMANY, P.P., SANTIAGO, A.F. AND CARVALHO I.C. (2013). Greywater production in airports: Qualitative and quantitative assessment. *Resources, Conservation and Recycling*, 77, 44-51.

COX, B.A. (2003). A review of currently available in-stream water-quality models and their applicability for simulating dissolved oxygen in lowland rivers. *The Science of the Total Environment*, 314-316(1), 335-377.

CRABTREE, B., SEWARD, A.J. AND THOMPSON, L. (2006). A case study of regional catchment water quality modelling to identify pollution control requirements. *Water Science and Technology*, 53(10), 47-54.

DAI, J., CHEN, J., LÜ, G., BROWN, L.C., GAN, L. AND XU, Q. (2017). Application of SWAT99.2 to sensitivity analysis of water balance components in unique plots in a hilly region. *Water Science and Engineering*, 10(3), 209-216.

DASTANAIE, J., NABI, G. R., NASRABADI, T., HABIBI, R. AND HOVEIDI, H. (2007). Use of horizontal flow roughing filtration in drinking water treatment. *International Journal of Environmental Science and Technology*, 4(3), 379-382.

DE ROOS, A.J., GURIAN, P.L., ROBINSON, L.F., RAI, A., ZAKERI, I. AND KONDO, M.C. (2017). Review of Epidemiological Studies of Drinking-Water Turbidity in Relation to Acute Gastrointestinal Illness. *Environmental Health Perspectives*, 125(8), 086003.

DEJAEGHER, B. AND HEYDEN, Y.V. (2011). Experimental designs and their recent advances in set-up, data interpretation, and analytical applications. *Journal of Pharmaceutical and Biomedical Analysis*, 56(2), 141-158.

DURSTEWITZ, D., KOPPE, G. AND MEYER-LINDENBERG, A. (2019). Deep neural networks in psychiatry. *Molecular Psychiatry*, 24(11), 1583-1598.

EBHOTA, V.C., ISABONA, J. AND SRIVASTAVA, V.M. (2018). Investigating Signal Power Loss Prediction in A Metropolitan Island Using ADALINE and Multi-Layer Perceptron Back Propagation Networks, *International Journal of Applied Engineering Research*, 13(18), 13409-13420.

EDOKPAYI, J.N., ODIYO, J.O. AND DUROWOJU, O.S. (2017). Impact of Wastewater on Surface Water Quality in Developing Countries: A Case Study of South Africa. In *Water Quality*, Intech: Vienna, Austria, 401-416.

EDWIN, G. A., GOPALSAMY, P. AND MUTHU, N. (2014.) Characterization of domestic gray water from point source to determine the potential for urban residential reuse: a short review. *Applied Water Science*, 4, 39-49.

EMMERT-STREIB, F., YANG, Z., FENG, H., TRIPATHI, S. AND DEHMER, M. (2020). An Introductory Review of Deep Learning for Prediction Models with Big Data. *Frontiers in Artificial Intelligence*, 3.

ENQVIST, J.P. AND ZIERVOGEL, G. (2019). Water governance and justice in Cape Town: An overview. *Wiley Interdisciplinary Reviews*: *Water*, 6(4), 1-15.

ERIKSSON, E., BAUN, A., SCHOLES, L., LEDIN, A., AHLMAN, S., REVITT, M., NOUTSOPOULOS, C. AND MIKKELSEN, P.S. (2007). Selected storm water priority pollutants - a European perspective. *Science of the Total Environment*, 383(1-3), 41-51.

EROL, R., OĞULATA, S.N., ŞAHIN, C. AND ALPARSLAN, Z.N. (2008). A Radial Basis Function Neural Network (RBFNN) Approach for Structural Classification of Thyroid Diseases. *Journal of Medical Systems*, 32(3), 215-220.

FARAH, E, ABDALLAH, A. AND SHAHROUR, I. (2019). Prediction of water consumption using Artificial Neural Networks modelling (ANN), *MATEC Web of Conferences* 295(3), 01004.

FENG, J. AND LU, S. (2019) Performance Analysis of Various Activation Functions in Artificial Neural Networks, *Journal of Physics*: *Conference Series*, 1237(2):111-122.

FINLEY, S., BARRINGTON, S. AND LYEW, D. (2009). Reuse of domestic greywater for the irrigation of food crops. *Water, Air, Soil and Pollution*, 199(1-4), 235-245.

FISTER, I., SUGANTHAN, P.N., FISTER, I., KAMAL, S.M., AL-MARZOUKI, F.M., PERC, M. AND STRNAD, D. (2015). Artificial neural network regression as a local search heuristic for ensemble strategies in differential evolution. *Nonlinear Dynamics*, 84(2), 895-914.

FRIEDLER, E. (2004). Quality of individual domestic greywater streams and its implication for on-site treatment and reuse possibilities. *Environmental Technol*ogy, 25(9), 997-1008.

GAJBHIYE, S., SHARMA, S.K. AND AWASTHI, M.K. (2015). Application of Principal Components Analysis for Interpretation and Grouping of Water Quality Parameters. *International Journal of Hybrid Information Technology,* 8(4), 89-96.

GHADAI, M., SATAPATHY, D.P. AND NARASIMHAM, M.L. (2020) A brief overview on water quality models, *International Journal of Advanced Research in Engineering and Technology,* 11(10), 535-544.

GALVIS, G., VISSCHER, J.T. AND LATORRE, J. (1998). *Multi-stage filtration and innovation water treatment technology*. International Reference Centre for Community Water Supply and Sanitation. The Hague, Netherlands and Universidad del Valle Instituto CINARA, Cali, Colombia.

GANATRA, A., KOSTA, Y.P., PANCHAL, G. AND GAJJAR, C. (2011). Initial Classification Through Back Propagation In a Neural Network Following Optimization Through GA to Evaluate the Fitness of an Algorithm. *International Journal of Computer Science and Information Technology,* 3(1), 98-116.

GAO, L. AND LI, D. (2014). A review of hydrological/water-quality models. Frontiers of Agricultural Science and Engineering, 1(4), 267-276.

GHANBARI, A., VAGHEI, Y. AND SAYYED NOORANI, S. (2014). Reinforcement Learning in Neural Networks: A Survey, *International journal of Advanced Biological and Biomedical Research*, 2(5), 1398-1416.

GHANIM, A.N. (2014). Optimization of pollutants removal from textile wastewater by electrocoagulation through RSM. *Journal of Babylon University/Engineering Sciences*, 22(2), 375-378.

GHATAK, A. (2019). Optimization. In: *Deep Learning with R. Springer, Singapore*.

GHAWI, A. (2019). Development of the Greywater Domestic Treatment Unit for Irrigation of the Garden in Rural Areas. *Journal of Ecological Engineering*, 20(3), 46-56.

GHRAIR, A.M., AL-MASHAQBEH, O.A. AND MEGDAL, S.B. (2014). Performance of a Grey Water Pilot Plant Using a Multi-Layer Filter for Agricultural Purposes in the Jordan Valley. *CLEAN - Soil, Air, Water*, 43(3), 351-359.

GOVENDER, M. AND EVERSON, C.S. (2005). Modelling streamflow from two small South African experimental catchments using the SWAT model. *Hydrological Processes*, 19(3), 683-692.

GRAMATIKOV, B.I. (2017). Detecting central fixation by means of artificial neural networks in a pediatric vision screener using retinal birefringence canning. *Biomedical Engineering Online*, 16(1), 52.

GROSS, A., KAPLAN, D. AND BAKER, K. (2007). Removal of chemical and microbiological contaminants from domestic greywater using a recycled vertical flow bioreactor (RVFB). *Ecological Engineering*, 31(2), 107-114.

HAGAN, M.T., DEMUTH, H.B. AND BEALE, M.H. (1996). Neural network design, *Pws Publishing Company*, Boston.

HALLOUZ, F., MEDDI, M., MAHÉ, G., ALIRAHMANI, S. AND KEDDAR, A. (2018). Modeling of discharge and sediment transport through the SWAT model in the basin of Harraza (Northwest of Algeria). *Water Science*, 32(1), 79-88.

HAMADA, M., ZAQOOT, H.A. AND JREIBAN, A.A. (2018). Application of artificial neural networks for the prediction of Gaza wastewater treatment plant performance-Gaza strip. *Journal of Applied Research in Water and Wastewater*, 5(1), 399-406.

HAMID, H.A. HARUN, H., SUNAR, N.M., AHMAD, F.H., JASMANI, L. AND SULEIMAN, N. (2018). Predicting the Capability of Oxidized CNW Adsorbents for the Remediation of Copper Under Optimal Operating Conditions Using RSM and ANN Models. *International Journal of Engineering and Technology*, 7(4.30), 264-268.

HAMZAH, F.M., JAAFAR, O., JANI, W.N.F. A. AND ABDULLAH, S.M.S. (2016). Multivariate Analysis of Physical and Chemical Parameters of Marine Water Quality in the Straits of Johor, Malaysia. *Journal of Environmental Science and Technology*, 9(6), 427-436.

HANJRA, M.A. AND QURESHI, M.E. (2010). Global water crisis and future food security in an era of climate change. *Food Policy*, 35(5), 365-377.

HANKIN, B., BIELBY, S., POPE, L. AND DOUGLASS, J. (2016). Catchment-scale sensitivity and uncertainty in water quality modelling. *Hydrological Processes*, 30(22), 4004-4018.

HAO, L., CHENG, L. AND BI, X. (2012). Apply with WASP Water Quality Model, *The 2nd International Conference on Computer Application and System Modelling*, 0714-0717.

HASSEN, E.B. AND ASMARE, A.M. (2019). Predictive performance modeling of Habesha brewery wastewater treatment plant using artificial neural networks. *Chemistry International*, 5(1), 87-96.

HERNANDEZ, L.L. (2010). *Removal of Micropollutants from Grey Water: Combining Biological and Physical/Chemical Processes,* PhD thesis, Wageningen University, Wageningen, The Netherlands

.

HERNÁNDEZ-LEAL, L., ZEEMAN, G., TEMMINK, H. AND BUISMAN, C. (2007). Characterisation and biological treatment of greywater. *Water Science and Technology*, 56(5), 193-200.

HINTON, G.E. (1992). How Neural Networks Learn from Experience. *Scientific American*, 267(3), 144-151.

HOLLY, F.M.JR AND PREISSMANN, A. (1977). Accurate calculation of transport in two dimensions. *Journal of the Hydraulics division*, 103(11), 1259-1277.

HORNIK, K., STINCHCOMBE, M. AND WHITE, H. (1989). Multilayer feedforward networks are universal approximators. *Neural Networks*, 2(5), 359-366.

HUANG, J., YIN, H., CHAPRA, S.C. AND ZHOU, Q. (2017). Modelling dissolved oxygen depression in an urban river in China. *Water*, 9(7), 520.

HUO, S., HE, Z., SU, J., XI, B. AND ZHU, C. (2013). Using Artificial Neural Network Models for Eutrophication Prediction. *Procedia Environmental Sciences*, 18, 310-316.

HUSBANDS, P. AND HOLLAND, O. (2012). Warren McCulloch and the British Cyberneticians. *Interdisciplinary Science Reviews*, 37(3), 237-253.

HWANG, J.Y., KIM, Y.D., KWON, J.H., PARK, J.H., NOH, J.W. AND YI, Y.K. (2013). Hydrodynamic and water quality modeling for gate operation: A case study for the Seonakdong River basin in Korea. *KSCE Journal of Civil Engineering*, 18(1), 73-80.

IBRAHIM, S., WAHAB, N.A., ANUAR, A.N. AND BOB, M. (2017). Parameter Optimization of Aerobic Granular Sludge at High Temperature Using Response Surface Methodology, *International Journal of Electrical and Computer Engineering (IJECE)*, 7(3), 1522-1529.

IEONG, I.I., LOU, I., UNG, W.K. AND MOK, K.M. (2015). Using Principle Component Regression, Artificial Neural Network, and Hybrid Models for Predicting Phytoplankton Abundance in Macau Storage Reservoir. *Environmental Modeling and Assessment*, 20(4), 355-365.

IVES, K.J. AND SHOLJI, I. (1965). Research on Variables Affecting Filtration. *Journal of Sanitary Engineering Division, ASCE*, 91(SA4), 1-18.

IYER, C.S., SINDHU, M., KULKARNI, S.G., TAMBE, S.S AND KULKARNI, B.D. (2003). Statistical analysis of the physico-chemical data on the coastal water of Cochin, *Journal of Environmental Monitoring*, 2(5), 324-327.

JAYALATH, J.M.J.C. AND PADMASIRI, J.P. (1996). Gravity roughing filter for pretreatment. *Proc. 22nd WEDC Conference on Reaching the Unreached*: *Challenges for the 21st Century*. New Delhi, India 271-272.

JAYALATH, J. (1994). Algae removal by roughing filter. 20th WEDC conference: Manual on water supply and treatment. Ministry of urban development, Government of India, New Delhi.

JEFFERSON, B., PALMER, A., JEFFREY, P., STUETZ, R. AND JUDD, S. (2004). Greywater characterization and its impact on the selection and operation of technologies for urban reuse, *Water Science and Technology*, 50(2), 157-164.

JHA, M.K., GASSMAN, P.W. AND ARNOLD, J.G. (2007). Water Quality Modeling for the Raccoon River Watershed Using SWAT. *Transactions of the ASABE,* 50(2), 479-493.

JHANSI, S. AND MISHRA, S. (2013). Wastewater treatment and reuse: Sustainability options. *Journal of Sustainable Development*, 10(1), 1-15.

JIANG, P., QIN, S., WU, J. AND SUN, B. (2015). Time Series Analysis and Forecasting for Wind Speeds Using Support Vector Regression Coupled with Artificial Intelligent Algorithms. *Mathematical Problems in Engineering*, 2015, 1-14.

JIN, K.R., JAMES, R.T., LUNG, W.S., LOUCKS, D.P., PARK, R.A. AND TISDALE, T.S. (1998). Assessing Lake Okeechobee Eutrophication with Water-Quality Models. *Journal of Water Resources Planning and Management*, 124(1), 22-30.

JOHNSTON, R. AND KUMMU, M. (2011). Water Resource Models in the Mekong Basin: A Review. *Water Resources Management*, 26(2), 429-455.

KANNEL, P.R., KANEL, S.R., LEE, S., LEE, Y.-S. AND GAN, T.Y. (2011). A Review of Public Domain Water Quality Models for Simulating Dissolved Oxygen in Rivers and Streams. *Environmental Modeling and Assessment*, 16(2), 183-204.

KARBOUBI, A., ZOUHRI, A. AND ANOUAR, A. (2014). Characterization of Domestic Waste water and Performance Indicators of the Waste water Treatment Plant of the City of SETTAT, *International Journal of Engineering Research and Technology (IJERT)*, 3(2), 2311-2316.

KARPISCAK, M. M., FOSTER, K. E. AND SCHMIDT, N. (1990). Residential water conservation. *Water Research*, 26(6), 939-948.

KHAYET, M., COJOCARU, C. AND ESSALHI, M. (2011). Artificial neural network modeling and response surface methodology of desalination by reverse osmosis. *Journal of Membrane Science*, 368(1-2), 202-214.

KHERADPISHEH, Z., TALEBI, A., RAFATI, L., GHANEIAN, M.T. AND EHRAMPOUSH, M.H. (2015). Groundwater quality assessment using artificial neural network: a case study of Bahabad plain, Yazd, Iran. *Desert*, 20(1), 65-71.

KIM, Y. AND KIM, B. (2006). Application of a 2-Dimensional Water Quality Model (CE-QUAL-W2) to the Turbidity Interflow in a Deep Reservoir (Lake Soyang, Korea). *Lake and Reservoir Management*, 22(3), 213-222.

KOTUT, K., NGANGA, V.G. AND KARIUKI, F. (2011). Physico-chemical and microbial quality of greywater from various households in Homa Bay Town, *The Open Environmental Engineering Journal*, 4(1), 162-169.

KOUDJONOU, K.M. AND ROUT, M. (2019). A stateless deep learning framework to predict net asset value. *Neural Computing and Applications*, 32, 1-19.

KRYSANOVA, V. AND ARNOLD, J.G. (2008). Advances in Ecohydrological Modelling with SWAT-a review. *Hydrological Sciences Journal*, 53(5), 939-947.

KUMAR, N., SINGH, S.K., SRIVASTAVA, P.K. AND NARSIMLU, B. (2017). SWAT Model calibration and uncertainty analysis for streamflow prediction of the Tons River Basin, India, using Sequential Uncertainty Fitting (SUFI-2) Algorithm. *Modeling Earth Systems and Environment*, 3(1), 30.

KWARTENG, E.A., GYAMFI, C., ANYEMEDU, F.O.K., ADJEI, K.A. AND ANORNU, G.K. (2020). Coupling SWAT and bathymetric data in modelling reservoir catchment hydrology. *Spatial Information Research*, 29, 55-69.

LAAFFAT, J., AZIZ, F., OUAZZANI, N. AND MANDI, L. (2019). Biotechnological approach of greywater treatment and reuse for landscape irrigation in small communities. *Saudi Journal of Biological Sciences*, 26(1), 83-90.

LANGILLE, J. J. AND BROWN, R. E. (2018). The Synaptic Theory of Memory: A Historical Survey and Reconciliation of Recent Opposition. *Frontiers in systems neuroscience*, 12, 52.

LARICO, M., JOHAN, A., MEDINA, Z. AND ADOLFO, S. (2019). Application of WASP model for assessment of water quality for eutrophication control for a reservoir in the Peruvian Andes. *Lakes and Reservoirs*, 24(1), 37-47.

LAU, E.T., SUN, L. AND YANG, Q. (2019). Modelling, prediction and classification of student academic performance using artificial neural networks. *SN Applied Sciences*, 1(9), 982-992.

LEBCIR, R. (1992). *Factors controlling the performance of horizontal flow roughing filter*s. PhD thesis, the University of Newcastle upon Tyne, UK, 1992.

LI, F., WICHMANN, K. AND OTTERPOHL, R. (2009). Review of technological approaches for grey water treatment and reuses. *Science of the Total Environment*, 407(11), 3439-3449.

LI, Y. AND DELIBERTY, T. (2020). Assessment of Urban Streamflow in Historical Wet and Dry Years Using SWAT across Northwestern Delaware. *Environmental Processes*, 7(2), 597-614.

LIANG, B. (2013). Urban Annual Water Consumption Prediction Using Artificial Neural Network. *Applied Mechanics and Materials*, 409-410, 1008-1011.

LIEW, M.W. AND GARBRECHT, J. (2003). Hydrologic simulation of the little Washita river experimental watershed using SWAT. *Journal of the American Water Resources Association*, 39(2), 413-426.

LIN, E., PAGE, D., PAVELIC, P., DILLON, P., MCCLURE, S. AND HUTSON, J. (2006). Evaluation of roughing filtration for pre-treatment of stormwater prior to aquifer storage and recovery (ASR). *CSIRO Land and Water Science Report*, 03/06.

LIN, H. AND SUN, Q. (2020). Crude Oil Prices Forecasting: An Approach of Using CEEMDAN-Based Multi-Layer Gated Recurrent Unit Networks. *Energies*, 13(7), 1543.

LIN, K., ZHAO, H., LV, J., LI, C., LIU, X., CHEN, R. AND ZHAO, R. (2020). Face Detection and Segmentation Based on Improved Mask R-CNN. *Discrete Dynamics in Nature and Society*, 1-11.

LINDENSCHMIDT, K.-E., CARR, M.K., SADEGHIAN, A. AND MORALES-MARIN, L. (2019). CE-QUAL-W2 model of dam outflow elevation impact on temperature, dissolved oxygen and nutrients in a reservoir. *Scientific Data*, 6(1), 312.

LIU, P., WANG, J., SANGAIAH, A., XIE, Y. AND YIN, X. (2019). Analysis and Prediction of Water Quality Using LSTM Deep Neural Networks in IoT Environment. *Sustainability*, 11(7), 2058.

LUAN, Q. AND ZHU, C. (2011). Surface Water Quality Evaluation Using BP and RBF Neural Network. *Journal of Software*, 6(12), 2528-2534.

LUDWIG, A. (2006). *The new create an oasis with greywater*: *oasis design*, Santa Barbara, California.

LUNG, W.-S. AND LARSON, C.E. (1995). Water Quality Modeling of Upper Mississippi River and Lake Pepin. *Journal of Environmental Engineering*, 121(10), 691-699.

LUO, H., FU, J. AND GLASS, J.R. (2017). Adaptive Bidirectional Back propagation: Towards Biologically Plausible Error Signal Transmission in Neural Networks. *ArXiv, abs/1702.07097*.

LUO, Y., ZHANG, W., LI, J., ZHANG, L., ZOU, J., HU, J., YANG, L., XI, Y. AND LIAO, T. (2019). Optimization of uranium removal from uranium plant wastewater by response surface methodology (RSM). *Green Processing and Synthesis*, 8(1), 808-813.

MACUKOW, B. (2016). Neural Networks - State of Art, Brief History, Basic Models and Architecture. *Computer Information Systems and Industrial Management*, 3-14.

MANGIO, H.R., MIRJAT, M.S., RAJPAR, I, TALPUR, M.A., JUNEJO, S.A. AND CUONG , D.M. (2017). Effect of Reed Grasses Treated Grey Water and Normal Water on Growth and Yield of Maize Crop. *Sindh University Research Journal (Science Series)*, 49(2), 271-278.

MANHOKWE, S., SHOKO, S. AND ZVIDZAI, C. (2019). Optimization of biological wastewater treatment for yeast processing effluent using cultured bacteria: Application of response surface methodology. *African Journal of Microbiology Research*, 13(26), 430-437.

MANIVANAN R. (2017). Water Quality Modelling For Ocean Engineering Projects - A Review. *Fisheries and Oceanography Open Access Journal*, 3(4), 555617.

MAREN, A.J., HARSTON, C.T. AND PAP, R.M. (1990). *Handbook of Neural Computing Applications*, Academic Press, Inc. San Diego, USA.

MARHON, S.A., CAMERON, C.J.F. AND KREMER, S.C. (2013). Recurrent Neural Networks. In: BIANCHINI, M., MAGGINI, M. AND JAIN, L. (eds) Handbook on Neural Information Processing. *Intelligent Systems Reference Library, 49. Springer, Berlin, Heidelberg*.

MARK, R.E. AND OWENS, J. (2009). Development and application of a WASP model on a large Texas reservoir to assess eutrophication control, Lake and Reservoir Management, 25(2), 136-148.

MARKRAM, H., GERSTNER, W. AND SJÖSTRÖM, P.J. (2011). A history of spike-timing-dependent plasticity, *Frontiers in Synaptic Neuroscience*, 3(4), 1-24.

MARTIN, J., HESTERLEE, C. AND COLE, T. (1999). TWO-DIMENSIONAL WATER QUALITY MODELING USING CE-QUAL-W2 ON SELECTED RESERVOIRS, *Proceedings of the 1999 Georgia Water Resources Conference*, The University of Georgia.

MARTINS, N.R.B., ANGELICA, A., CHAKRAVARTHY, K., SVIDINENKO, Y., BOEHM, F.J., OPRIS, I., LEBEDEV, M.A., SWAN, M., GARAN, S.A., ROSENFELD, J.V., HOGG, T. AND FREITAS, R.A. (2019). Human Brain/Cloud Interface. *Frontiers in Neuroscience*, 13,112.

MAS, DM.L AND AHLFELD, D.P. (2007). Comparing artificial neural networks and regression models for predicting faecal coliform concentrations, *Hydrological Sciences Journal,* 52(4), 713-731.

MAS, J.F. AND FLORES, J.J. (2007). The application of artificial neural networks to the analysis of remotely sensed data. *International Journal of Remote Sensing*, 29(3), 617-663.

MASHABELA, K. (2015). *Onsite greywater reuse as a water conservation method: A case study of Lepelle-Nkumpi local municipality, Limpopo province of South Africa*. Dissertation, Master of Science in Geography and Environmental Science, Faculty of Science and Agriculture.

MASIH, I., MASKEY, S., MUSSÁ, F.E.F. AND TRAMBAUER, P. (2014). A review of droughts on the African continent: a geospatial and long-term perspective. *Hydrology and Earth System Sciences*, 18(9), 3635-3649.

MATEUS, M., VIEIRA, R., ALMEIDA, C., SILVA, M. AND REIS, F. (2018). ScoRE - A Simple Approach to Select a Water Quality Model. *Water*, 10(12), 1811.

MAUNG, T. (2006). *A study on the performance of limestone roughing filter for the removal of turbidity, suspended solids, biochemical oxygen demand and coliform organisms using wastewater from the inlet of domestic wastewater oxidation pond*. PhD thesis, Universiti Sains Malaysia.

MAZLUM, N., OZER, A. AND MAZLUM, S. (1999). Interpretation of Water Quality Data by Principal Component Analysis. *Turkish Journal of Engineering and Environmental Science*, 23(1), 19-26.

MBUH, M.J., MBIH, R. AND WENDI, C. (2019). Water quality modeling and sensitivity analysis using Water Quality Analysis Simulation Program (WASP) in the Shenandoah River watershed. *Physical Geography*, 40(2), 127-148.

MCCARTHY, J., MINSKY, M. L., ROCHESTER, N. AND SHANNON, C. E. (1955). A Proposal for the Dartmouth Summer Research Project on Artificial Intelligence. *AI Magazine*, 27(4), 12-14.

MCINTYRE, N.R., WAGENER, T., WHEATER, H.S. AND YU, Z.S. (2003). Uncertainty and risk in water quality modelling and management. *Journal of Hydroinformatics*, 5(4), 259-274.

MHASKE, A.R., TALEY, S.M. AND BINIWALE, R.B. (2014). Removal of turbidity from sewage water by phytorid sewage treatment plant : A study using the response surface methodology. *International Journal of Agricultural Engineering*, 7(2), 365-372.

MI, X., SIVAKUMAR, M. AND HAGARE, D. (2004). *A general review of applications of artificial neural network to water industry*. In: MOWLAEI, M., ROSE, A. AND LAMBORN, J. (Eds.), Environmental Sustainability through Multidisciplinary Integration, 234-243. Australia: Environmental Engineering Research Event.

MISRA, A.K. (2014). Climate change and challenges of water and food security. *International Journal of Sustainable Built Environment*, 3(1), 153-165.

MOALLA, R., GARGOURI, M., KHMIRI, F., KAMOUN, L. AND ZAIRI, M. (2018). Phosphogypsum purification for plaster production: A process optimization using full factorial design, *Environmental Engineering Research*, 23(1), 36-45.

MOHAMED, R.M.S.R., AL-GHEETHI A.A.S., AHMAD, M.S.L., BAKAR, S.A., MUSA, S. AND KASSIM, A.H.M. (2019). Ceramic Tile Waste for Treating Laundry Greywater. *Pertanika Journal of Science and Technology*, 27(3), 1051-1059.

MOREL, A. AND DIENER, S. (2006). *Greywater Management in low and middle-income countries: review of different treatment systems for households or neighbourhoods.* Sandec Report

no 16/06, Swiss Federal Institute of Aquatic Science and Technology (Eawag). Dübendorf, Switzerland.

MTSWENI, S. (2016). *Performance of A Horizontal Rouging Filtration System for the pre-Treatment of Greywater*. Master of Engineering Dissertation, Durban University of Technology, Durban, South Africa.

MTSWENI, S., BAKARE, B.F. AND RATHILAL, S. (2019). Performance of a horizontal roughing filter using principal component regression and multiple linear regression treating informal settlement greywater, *Proceedings of the world congress on engineering and computer science* (WCECS), October 22-24, San Francisco, USA.

MUANDA, C. (2009). *Investigation of anaerobic up-flow batch reactor for treatment of greywater in un-sewered settlements.* Master of technology thesis. Cape Peninsula University of Technology.

MUKHOPADHAY, B., MUJUMDER, M., BARMAN, R.N., ROY, P.K. AND MAZUMDAR, A. (2009). Verification of filter efficiency of horizontal roughing filter by Wegelin's design criteria and artificial neural network. *Drinking Water Engineering and Science Discussions*, 2(4), 21-27.

MURDANI, JAKFAR, EKAWATI, D., NADIRA, R. AND DARMADI (2018). Application of Response Surface Methodology (RSM) for wastewater of hospital by using electrocoagulation. *IOP Conference Series: Materials Science and Engineering*, 345(1), 012011.

MURRAY, P.M., BELLANY, F., BENHAMOU, L., BUČAR, D.-K., TABOR, A.B. AND SHEPPARD, T.D. (2016). The application of design of experiments (DoE) reaction optimisation and solvent selection in the development of new synthetic chemistry. *Organic and Biomolecular Chemistry*, 14(8), 2373-2384.

NASR, M.S., MOUSTAFA, M.A.E., SEIF, H.A.E. AND EL KOBROSY, G. (2012). Application of Artificial Neural Network (ANN) for the prediction of EL-AGAMY wastewater treatment plant performance-EGYPT. *Alexandria Engineering Journal*, 51(1), 37-43.

NATHAN, N.S., SARAVANANE, R. AND SUNDARARAJAN, T. (2017). Spatial Variability of Ground Water Quality Using HCA, PCA and MANOVA at Lawspet, Puducherry in India. *Computational Water, Energy, and Environmental Engineering*, 06(03), 243-268.

NEITSCH, S. L., ARNOLD, J.G., KINIRY, J.R., WILLIAMS,J.R. AND KING, K.W. (2002). *Soil and Water Assessment Tool Theoretical Documentation. Version 2000. Temple, Tex.: USDA-ARS*, Grassland Soil and Water Research Laboratory and Texas A&M University, Blackland Research and Extension Center.

NGUYEN, N.G., TRAN, V.A., NGO, D.L., PHAN, D., LUMBANRAJA, F.R., FAISAL, M.R., ABAPIHI, B., KUBO, M. AND SATOU, K. (2016). DNA Sequence Classification by Convolutional Neural Network. *Journal of Biomedical Science and Engineering*, 09(05), 280-286.

NIDHISHA, C. AND KURUVILA, E.C. (2019). Modelling BOD and COD Using Artificial Neural Network with Factor Analysis. *International Research Journal of Engineering and Technology* (IRJET), 06(4).

NING, S.K., CHANG, N.B., YANG, L., CHEN, H.W. AND HSU, H.Y. (2001). Assessing pollution prevention program by QUAL2E simulation analysis for the Kao-Ping River Basin, Taiwan. *Journal of Environmental Management*, 61(1), 61-76.

NKWONTA, O.I. (2010). *Roughing filters: an alternative passive pre-treatment of coal mine water in South Africa*. Masters technology in faculty of engineering and built environment, Tshwane University of Technology.

NKWONTA, O.I., OLUFAYO, O.A., OCHIENG, G.M., ADEYEMO, J.A. AND OTIENO, F.A.O. (2010). Turbidity removal: Gravel and charcoal as roughing filtration media. *South African Journal of Science*, 106(11/12), 1-5.

NSW (2008). *NSW Greywater reuse in sewered, single household residential premises*. Water for life, NSW Government, Sydney, Australia.

NWANKPA, C., IJOMAH, W., GACHAGAN, A. AND MARSHALL, S. (2018). Activation functions: Comparison of trends in practice and research for deep learning, *arXiv:1811.03378*.

NWOBI-OKOYE, C.C. AND IGBOANUGO, A.C. (2013). Predicting water levels at Kainji dam using artificial neural networks. *Nigerian Journal of Technology (NIJOTECH)*, 32(1), 129-136.

O'REILLY,G., BEZUIDENHOUT, C.C AND BEZUIDENHOUT, J.J. (2018). Artificial neural networks: applications in the drinking water sector. *Water Science and Technology*: *Water Supply*, 18(6), 1869-1887.

OH, K.S., LEONG, J.Y.C., POH, P.E., CHONG, M.N. AND LAU, E.V. (2018). A review of greywater recycling related issues: Challenges and future prospects in Malaysia. *Journal of Cleaner Production*, 171, 17-29.

OJHA, V.K., ABRAHAM, A. AND SNÁŠEL, V. (2017). Metaheuristic design of feedforward neural networks: A review of two decades of research. *Engineering Applications of Artificial Intelligence*, 60, 97-116.

OLOWE, K.O. AND KUMARASAMY, V.M. (2018). Assessment of Some Existing Water Quality Models, Nature Environment and Pollution Technology. *An International Quarterly Scientific Journal*, 17(3), 939-948.

ORIMOLOYE, I.R., OLOLADE, O.O., MAZINYO, S.P., KALUMBA, A.M., EKUNDAYO, O.Y., BUSAYO, E.T., AKINSANOLA, A.A. AND NEL, W. (2019). Spatial assessment of drought severity in Cape Town area, South Africa. *Heliyon*, 5(7), 02148.

OTENG-PEPRAH, M., ACHEAMPONG, M.A. AND DEVRIES, N.K. (2018). Greywater Characteristics, Treatment Systems, Reuse Strategies and User Perception-a Review. *Water, air, and soil pollution*, 229(8), 2-16.

PALIWAL, R. SHARMA, P. AND KANSAL, A. (2006). Water quality modelling of the river Yamuna (India) using QUAL2E-UNCAS. *Journal of Environmental Management*, 83(2), 131-44.

PARK, R.A. AND CLOUGH, J. (2004). AQUATOX (Release 2): *Modeling Environmental Fate and Ecological Effects in Aquatic Ecosystems*. Volume 1: User's Manual, U.S. Environmental Protection Agency, Office of Water.

PARK, R.A., CLOUGH, J.S. AND WELLMAN, M.C. (2008). AQUATOX: Modeling environmental fate and ecological effects in aquatic ecosystems. *Ecological Modelling*, 213(1), 1-15.

PARVEEN, N. AND SINGH, S.K. (2016). Application of Qual2e model for river water quality modelling, *International Journal of Advance Research and Innovation*, 4(2), 429-432.

PASINI, A. (2015). Artificial neural networks for small dataset analysis. *Journal of thoracic disease*, 7(5), 953-960.

PATIL, V.B., KULKARNI, G.S. AND KORE, V.S. (2012). Performance of horizontal roughing filters for wastewater: A Review. *International Research Journal of Environmental Sciences*, 1(2), 53-55.

PELLETIER, G. J., CHAPRA, S. C. AND TAO, H. (2006). QUAL2Kw - A framework for modeling water quality in streams and rivers using a genetic algorithm for calibration. *Environmental Modeling and Software*, 21(3), 419-425.

PHANPHET, S., SUKPRASERT, N., WANGMAI, A., BANGPHAN, S. AND BANGPHAN, P. (2018). Application of factorial design to study the effect of moisture and rice of varieties on the production of paddy husker machine, *Proceedings of the World Congress on Engineering, II, WCE*, July 4-6, London, U.K.

PIASECKI, A., JURASZ, J. AND KAŹMIERCZAK, B. (2018). Forecasting daily water consumption: a case study in Torun, Poland. *Periodica Polytechnica Civil Engineering*, 62(3), 818-824.

PIDOU, M., MEMON, F.A., STEPHENSON, T., JEFFERSON, B. AND JEFFREY, P. (2007). Greywater recycling: treatment options and applications, Institution of Civil Engineers. Proceedings. *Engineering Sustainability*, 160, 119-131.

PRAUS, P. (2005). Water quality assessment using SVD-based principal component analysis of hydrological data. *Water SA*, 31(4), 417- 422.

PUSKARCZYK, E. (2019). Artificial neural networks as a tool for pattern recognition and electrofacies analysis in Polish palaeozoic shale gas formations. *Acta Geophysica*, 67(6), 1991-2003.

QIAO, J.-F., MENG, X., LI, W.-J. AND WILAMOWSKI, B.M. (2018). A novel modular RBF neural network based on a brain-like partition method. *Neural Computing and Applications*, 32(3), 899-911.

RAFIEE, M. AND JAHANGIRI-RAD, M. (2015). Artificial Neural Network Approaches to the Prediction of Eutrophication and Algal Blooms in Aras Dam, Iran. *Iranian journal of health science*, 3(1), 25-32.

RAKESH, S.S., RAMESH, P.T., MURUGARAGAVAN, R.., AVUDAINAYAGAM, S. AND KARTHIKEYAN, S. (2020). Characterization and treatment of greywater: A review. *International Journal of Chemical Studies*, 8(1), 34-40.

RAMON, G., GREEN, M., SEMIAT, R. AND DOSORETZ, C. (2004). Low strength greywater characterization and treatment by direct membrane filtration. *Desalination*, 170 (3), 241-50.

RANJITH, S., SHIVAPUR, A.V., KUMAR, P.S.K., HIREMATH, C.G. AND DHUNGANA, S. (2019) Water Quality Model for Streams: A Review. *Journal of Environmental Protection*, 10 (12), 1612-1648.

RATH, J.S., HUTTON, P.H., CHEN, L. AND ROY, S.B. (2017). A hybrid empirical-Bayesian artificial neural network model of salinityin the San Francisco Bay-Delta estuary. *Environmental Modelling and Software*, 93, 193-208.

RENE, E. AND SAIDUTTA, M. (2008). Prediction of BOD and COD of a refinery wastewater using multilayer artificial neural networks. *Journal of Urban and Environmental Engineering*, *2*(1), 1-7.

RIPLEY, B.D. (1994). Neural Networks and Related Methods for Classification. *Journal of the Royal Statistical Society*. Series B (Methodological), 56(3), 409-456.

RODDA, N CARDEN, K AND ARMITAGE, N. (2010b). *Sustainable use of greywater in small-scale agriculture and gardens in South Africa – Guidance Report.* WRC Report no. TT 469/1/10. Water Research Commission, Pretoria, South Africa. ISBN 978-1-4312-0091-7.

ROJAS, R. (1996). Unsupervised Learning and Clustering Algorithms. In: *Neural Networks, Springer, Berlin, Heidelberg*, 99-121.

ROSSI, C.G., SRINIVASAN, R., JIRAYOOT, K., LE DUC, T., SOUVANNABOUTH, P., BINH, N. AND GASSMAN, P.W. (2009). Hydrologic evaluation of the lower Mekong River Basin with the Soil and Water Assessment Tool model. *International Agricultural Engineering Journal*, 18(1-2), 1-13.

RYAD, A., LAKHDAR, K., MAJDA, K. S., SAMIA, A., MARK, A., CORINNE, A. D. AND ERIC, G. (2010). Optimization of the culture medium composition to improve the production of hyoscyamine in elicited Datura stramonium L. Hairy Roots using the Response Surface Methodology (RSM). *International Journal of Molecular Sciences*, 11(11), 4726-4740.

SAFAVI, H.R. AND AHMADI, K.M. (2015). Prediction and assessment of drought effects on surface water quality using artificial neural networks: case study of Zayandehrud River, Iran. *Journal of Environmental Health Science and Engineering*, 13(1), 68.

SALEHINEJAD,H., BAARBE, J., SANKAR, S., BARFETT, J., COLAK, E. AND VALAEE, S. (2017). Recent advances in recurrent neural networks. *arXiv preprint arXiv:1801.01078.*

SANTHI, C., SRINIVASAN, R., ARNOLD, J.G. AND WILLIAMS, J.R. (2006). A modeling approach to evaluate the impacts of water quality management plans implemented in a watershed in Texas, *Environmental Modelling and Software,* 21(8), 1141- 1157.

SARKHOSH, M., ATAFAR, Z., AHMADI, E, REZAEI, S, VOSOGHI, M, NAZARI, S., FAKHRI, Y., MOHSENI, S.M. AND SAGHI, M.H. (2016). Treatment of fresh leachate from

municipal solid waste landfill using horizontal roughing filter. *International Journal of Pharmacy and Technology*, 8(82), 12629-12637.

SEISING, R. (2018). The Emergence of Fuzzy Sets in the Decade of the Perceptron-Lotfi A. Zadeh's and Frank Rosenblatt's Research Work on Pattern Classification. *Mathematics*, 6(7), 110.

SHAH, S., HOSSEINI, M., MILED, Z.B., SHAFER, R. AND BERUBE, S. (2018). A Water Demand Prediction Model for Central Indiana. In *Proceedings of the Thirtieth AAAI Conference on Innovative Applications of Artificial Intelligence(IAAI-18)*, New Orleans, LA, USA.

SHALLUE C.J., LEE, J., ANTOGNINI, J., SOHL-DICKSTEIN, J., FROSTIG, R. AND DAHL, G.E. (2019). Measuring the Effects of Data Parallelism on Neural Network Training. *Journal of Machine Learning Research*, 20 (112), 1-49.

SHANAHAN, P., HENZE M., KONCSOS L., RAUCH, W., REICHERT, P., SOMLYÓDY, L. AND VANROLLEGHEM, P. (1998). River Water Quality Modelling: II. Problems of the art. *Water Science and Technology*, 38(11), 245-252.

SHARMA, D. AND KANSAL, A. (2012). Assessment of river quality models: a review. *Reviews in Environmental Science and Biotechnology*, 12(3), 285-311.

SHARMA, S., SHARMA, S. AND ATHAIYA, A. (2020). Activation functions in neural networks. *International Journal of Engineering Applied Sciences and Technology*, 4(12), 310-316.

SHI, K. W., WANG, C. W.AND JIANG, S. C. (2018). Quantitative microbial risk assessment of Greywater on-site reuse. *The Science of the Total Environment*, 635, 1507–1519.

SHIHAB, S. (1993). Application of Multivariate Method in the Interpretation of Water Quality Monitoring Data of Saddam Dam Reservoir, Confidential 13.

SILDIR, H., AYDIN, E. AND KAVZOGLU, T. (2020). Design of Feedforward Neural Networks in the Classification of Hyperspectral Imagery Using Super structural Optimization. *Remote Sensing*, 12(6), 956.

SILVA, F., SANZ, M., SEIXAS, J., SOLANO, E. AND OMAR, Y. (2020). Perceptrons from memristors. *Neural Networks*, 122, 273-278.

SINGH, V.P. (2017). Challenges in meeting water security and resilience. *Water International*, 42(4), 349-359.

SOLAIMANY-AMINABAD, M., MALEKI, A. AND HADI, M. (2013). Application of artificial neural network (ANN) for the prediction of water treatment plant influent characteristics. *Journal of Advances in Environmental Health*, 1(2), 89-100.

SUH, D. AND HAM, S. (2016). A water demand forecasting model using BPNN for residential building. *Contemporary Engineering Sciences*, 9(1), 1-10.

SUN, Y. (2005). *Exchange rate forecasting with an artificial neural network model: can we beat a random walk model*? Master of Commerce and Management (MCM) thesis, Lincoln University, New Zealand.

SZKOŁA, J., PANCERZ, K. AND WARCHOŁ, J. (2011). Recurrent Neural Networks in Computer-Based Clinical Decision Support for Laryngopathies: An Experimental Study. *Computational Intelligence and Neuroscience*, 289-398.

TAHERIYOUN, M., MEMARIPOUR, A. AND NAZARI-SHARABIAN, M. (2020). Using recycled chemical sludge as a coagulant aid in chemical wastewater treatment in Mobarakeh Steel Complex. *Journal of Material Cycles and Waste Management*, 22(3), 745-756.

TALAEE, P.H. (2014). Multilayer perceptron with different training algorithms for streamflow forecasting. *Neural Computing and Applications*, 24(3-4), 695-703.

TANSEL, B. (2008). New Technologies for Water and Wastewater Treatment: A Survey of Recent Patents. *Recent Patents on Chemical Engineering*, 1(1), 17-26.

TAVAKOL, M., ARJMANDI, R., SHAYEGHI, M., MONAVARI, S.M. AND KARBASSI, A. (2017). Application of Multivariate Statistical Methods to Optimize Water Quality Monitoring

Network with Emphasis on the Pollution Caused by Fish Farms. *Iranian Journal of Public Health*, 46(1), 83-92.

TEPONG-TSINDÉ, R., CRANE, R., NOUBACTEP, C., NASSI, A. AND RUPPERT, H. (2015). Testing Metallic Iron Filtration Systems for Decentralized Water Treatment at Pilot Scale. *Water*, 7(12), 868-897.

TORABI HAGHIGHI, A., DARABI, H., SHAHEDI, K., SOLAIMANI, K. AND KLØVE, B. (2019). A Scenario-Based Approach for Assessing the Hydrological Impacts of Land Use and Climate Change in the Marboreh Watershed, Iran. *Environmental Modeling and Assessment*, 25(1), 41-57.

TORTAJADA, C. AND NAMBIAR, S. (2019). Communications on Technological Innovations: Potable Water Reuse. *Water*, 11(2), 251.

TÜMER, A.E. AND EDEBALI, S. (2015). Prediction of wastewater treatment plant performance using multilinear regression and artificial neural networks, *International Symposium on Innovations in Intelligent Systems and Applications (INISTA)*, Madrid, 1-5.

TÜRKMENLER, H. AND PALA, M. (2017). Performance Assessment of Advanced Biological Wastewater Treatment Plants Using Artificial Neural Networks. *International Journal of Engineering Technologies* (*IJET*), 3(3), 151-156.

TURKSON, R.F., YAN, F., ALI, M.K.A. AND HU, J. (2016). Artificial neural network applications in the calibration of spark-ignition engines: An overview. *Engineering Science and Technology, an International Journal*, 19(3), 1346-1359.

TYE, H. (2004). Application of statistical 'design of experiments' methods in drug discovery. *Drug Discovery Today*, 9(11), 485-491.

UDDIN, S., KHAN, A., HOSSAIN, M.E. AND MONI, M.A. (2019). Comparing different supervised machine learning algorithms for disease prediction. *BMC Medical Informatics and Decision Making*, 19(1), 1-16.

UNAR, M.A. (1999). Ship Steering Control Using Feedforward neural networks. *PhD Thesis, University of Glasgow, Glasgow. Scotland, UK*.

VAN ENGELEN, J.E. AND HOOS, H.H. (2019). A survey on semi-supervised learning. *Machine Learning*, 109, 373-440.

VOULVOULIS, N (2018). Water reuse from a circular economy perspective and potential risks from an unregulated approach. *Current Opinion in Environmental Science and Health*, 2, 32-45.

WAGARACHCHI, M. AND KARUNANANDA, A. (2017). Optimization of Artificial Neural Network Architecture Using Neuroplasticity. *International Journal of Artificial Intelligence*, 15(1), 112-125.

WANG, H. AND RAJ, B. (2017). On the Origin of Deep Learning. *arXiv:1702.07800v4*.

WANG, J.Q., ZHONG, Z. AND WU, J. (2004). Steam water quality models and its development trend, *Journal of Anhui Normal University (Natural Science)*, 27(3), 243-247.

WANG, Q., LI, S., JIA, P., QI, C. AND DING, F. (2013). A Review of Surface Water Quality Models, Wetland Degradation and Ecological Restoration. *The Scientific World Journal*, 1-7.

WANG, Q.G., DAI, W. N., ZHAO, X.H., DING, F., LI, S.B. AND ZHAO,Y. (2009). Numerical model of thermal discharge from Laibin power plant based on Mike 21, *Research of Environmental Sciences*, 22(3), 332-336.

WANG, S.-H., MUHAMMAD, K., HONG, J., SANGAIAH, A.K. AND ZHANG, Y.-D. (2020). Alcoholism identification via convolutional neural network based on parametric ReLU, dropout, and batch normalization. *Neural Computing and Applications*, 32(3), 665–680.

WANG, X., ZHAO, Y. AND POURPANAH, F. (2020). Recent advances in deep learning. *International Journal of Machine Learning and Cybernetics*, 11(4), 747-750.

WANG, Y., LI, Y., SONG, Y. AND RONG, X. (2020). The Influence of the Activation Function in a Convolution Neural Network Model of Facial Expression Recognition. *Applied Sciences*, 10, 1897.

WARN, A. AND BREW, J. (1980). Mass balance. *Water Research*, 14(10), 1427-1434.

WARN, A.E. AND MATTHEWS, P.J. (1984). Calculation of the Compliance of Discharges with Emission Standards. *Water Science and Technology*, 16(5-7), 183-196.

WARN, T. (2007). SIMCAT 10.1-A guide and reference for users. *Environment Agency*, 210.

WEGELIN, M. (1996). *Surface water treatment by roughing filters - A design, construction and operation manual*, SANDEC Report No. 2/96, Dubendorf, Switzerland.

WEGELIN, M. (1986). *Horizontal flow roughing filtration (HRF), design, construction and operation manual*, IRCWD Report No. 06/86, Zurich, Switzerland.

WHITEHEAD, P., YOUNG, P. AND HORNBERGER, G. (1979). A systems model of stream flow and water quality in the Bedford-Ouse river-1. Stream flow modelling. *Water Research*, 13(12), 1155-1169.

WHITEHEAD, P.G. AND HORNBERGER, G.M. (1984). Modelling algal behaviour in the river thames. *Water Research*, 18(8), 945-953.

WHITEHEAD, P.G. AND WILLIAMS, R. (1984). Modelling nitrate and algal behaviour in the River Thames. *Water Science and Technology*, 16, 6521-6633.

WHITEHEAD, P.G. AND YOUNG, P. (1979). Water quality in river systems: Monte Carlo analysis. *Water Resources Research*, 15(2), 451-459.

WHITEHEAD, P.G., BECK, M.B. AND O'CONNELL, P.E. (1981). A systems model of streamflow and water quality in the Bedford Ouse river system-II. Water quality modelling. *Water Research*, 15(10), 1157-1171.

WHITEHEAD, P.G., WILLIAMS, R.J. AND LEWIS, D.R. (1997). Quality simulation along river systems (QUASAR): model theory and development. *Science of the Total Environment*, 194-195, 447-456.

WINCHELL, M.F., PERANGINANGIN, N., SRINIVASAN, R. AND CHEN, W. (2018). Soil and Water Assessment Tool model predictions of annual maximum pesticide concentrations in high vulnerability watersheds. *Integrated Environmental Assessment and Management*, 14(3), 358–368.

WOOL, T., AMBROSE, R.B., MARTIN, J.L. AND COMER, A. (2020). WASP 8: The Next Generation in the 50-year Evolution of USEPA's Water Quality Model. *Water*, 12(5), 1398.

WORLD WIDE FUND FOR NATURE SOUTH AFRICA (WWF-SA) (2016). *Water: Facts and Futures-report*, Published in May 2016 by WWF-SA, Cape Town, South Africa.

WU, Y., WANG, H., ZHANG, B. AND DU, K.-L. (2012). Using Radial Basis Function Networks for Function Approximation and Classification. *ISRN Applied Mathematics*, 1-34.

WUROCHEKKE, A.A., MOHAMED, R.M.S., AL-GHEETHI, A.A. ATIKU, H., AMIR, H.M. AND MATIAS-PERALTA, H.M. (2016). Household greywater treatment methods using natural materials and their hybrid system. *Journal of Water and Health*, 14 (6), 914-928.

WUTTICHAIKITCHAROEN, P. AND BABEL, M.S. (2014). Principal Component and Multiple Regression Analyses for the Estimation of Suspended Sediment Yield in Ungauged Basins of Northern Thailand. *Water*, 6(8), 2412-2435.

XU, B., ZHANG, H., WANG, Z., WANG, H. AND ZHANG, Y. (2015). Model and Algorithm of BP Neural Network Based on Expanded Multichain Quantum Optimization. *Mathematical Problems in Engineering*, 1-11.

YAHIA, S., SAID, S. AND ZAIED, M. (2020). A novel classification approach based on Extreme Learning Machine and Wavelet Neural Networks. *Multimedia Tools and Applications*, 79(19–20), 13869-13890.

YANG, R.-Y. AND RAI, R. (2019). Machine auscultation: enabling machine diagnostics using convolutional neural networks and large-scale machine audio data. *Advances in Manufacturing*, 7(2), 174-187.

YEREL, S. (2010). Water Quality Assessment of Porsuk River, Turkey*, E-Journal of Chemistry*, 7(2), 593-599.

YIN, Y. (2018). Deep Learning with the Random Neural Network and its Applications, *arXive-prints: arXiv:1810.08653* (*misc*).

YUCEER, M. (2016). Modeling Water Quality in Rivers: A Case Study of Beylerderesi River in Turkey. *Applied Ecology and Environmental Research*, 14(1), 383-395.

ZENG, J., CHEN, S., WAN, K., LI, J., HU, D., ZHANG, S. AND YU, X. (2020). Study of biological up-flow roughing filters designed for drinking water pretreatment in rural areas: using ceramic media as filter material. *Environmental Technology*, 41(10), 1256-1265.

ZHANG, G., EDDY PATUWO, B. AND HU, Y.M. (1998). Forecasting with artificial neural networks: The state of the art. *International Journal of Forecasting*, 14(1), 35-62.

ZHANG, W. AND RAO, Y.R. (2012). Application of a eutrophication model for assessing water quality in Lake Winnipeg. *Journal of Great Lakes Research*, 38(3), 158-173.

ZHANG, X.S. (2000). Feedback Neural Networks. In: *Neural Networks in Optimization*. Nonconvex Optimization and Its Applications, 46. Springer, Boston, MA.

ZHANG,Y., ZHAO,X., ZHANG, X. AND PENG, S. (2015). A review of different drinking water treatments for natural organic matter removal, Water Science and Technology: *Water Supply*, 15 (3), 442-455.

ZHU, S., ZHANG, Z. AND LIU, X. (2017). Enhanced Two Dimensional Hydrodynamic and Water Quality Model (CE-QUAL-W2) for Simulating Mercury Transport and Cycling in Water Bodies. *Water*, 9(9), 643.

ZIEMIŃSKA-STOLARSKA, A. AND SKRZYPSKI, J. (2012). Review of Mathematical Models of Water Quality. *Ecological Chemistry and Engineering S*, 19(2), 197-211.

ZIN, M.S.M., JUAHIR, H., TORIMAN, M.E., KAMARUDIN, M.K.A., WAHAB, N.A. AND AZID, A. (2017). Assessment of water quality status using univariate analysis at Klang and Juru river, Malaysia. *Journal of Fundamental and Applied Sciences*, 9(2S), 93-108.

Appendix

Analytical procedures (Adopted from Mtsweni, 2016)

- pH

This is measured using a calibrated pH meter

- Conductivity

This was measured using a calibrated conductivity meter

- Turbidity

Turbidity in water is caused by suspended and colloidal matter such as clay, silt, finely divided organic and inorganic matter, and plankton and other microscopic organisms. Turbidity is an expression of the optical property that causes light to be scattered and absorbed rather than transmitted with no change in direction or flux level through sample.

Determine turbidity as soon as possible after the sample has been taken. Gently agitate all samples before examination to ensure a representative measurement. Sample preservation is not practical; begin analysis promptly. Refrigerate or cool 4 °C, to minimize microbiological decomposition of solids, if storage is required. This is measured using a calibrated conductivity meter.

- Total solids

Total solids is the term applied to the material residue left in the vessel after evaporation of a sample and its subsequent drying in an oven at a defined temperature. The residue consists of organic and inorganic component of the waste.

Apparatus required

- Porcelain crucibles
- Drying oven
- Analytical balance
- Desiccator

Procedure

Heat clean dish to 103-105 °C for 1 hour. Store and cool dish in desiccator until cooled (needed). Weigh immediately before use.

Pipette 50 ml of well mixed sample to pre-weighed crucible

Weigh crucible contained with sample and place in an oven at 103 -105°C for 24 hours. Remove the crucible from the oven and placed in a dessicator to cool. Weigh the crucible
The total solids are therefore calculated as follows:
Total solids (mg/l) = ((A-B) x 1000)/(sample volume, ml)
A = weight of dried residue + dish, (mg)
B = weight of dish, (mg)

- Total dissolved solids

Total dissolved solids, is the portion that passes through the filter. The type of filter holder, the pore size, porosity, area, and the thickness of the filter and the physical nature, particle size, and the amount of material deposited on the filter are the principal factors affecting separation of suspended from dissolved solids. Dissolved solids is the portion of solids that passes through a filter of 2.0 micron metre (or smaller) nominal pore size under specified conditions. Suspended solids is the portion retained on the filter.

Apparatus required

- Porcelain crucibles
- Drying oven
- Analytical balance
- Dessicator
- Vacuum filtration apparatus (glass filter attached)

Procedure
Heat clean dish to 180 °C for 1 hour. Store and cool dish in dessicator until needed. Weigh immediately before use.
Assemble filtering apparatus and filter and begin suction. Filter about 150 ml of well mixed sample using vacuum filtration apparatus. If volume filtered fails to meet minimum yield, increase sample volume up to 1 L. If complete filtration takes more than 10 min, increase filter diameter or decrease sample volume. Continue suction for about 3 min after filtration is complete.

Evaporate the portion that passes through the filter for 24 hours at 180 °C in an oven, cool in a dessicator to balance temperature, and weigh.

The total dissolved solids are therefore calculated as follows:
Total dissolved solids (mg/l) = ((A-B) x 1000)/(sample volume, ml)
A = weight of dried residue + dish, (mg)
B = weight of dish (mg)

- Volatile solids

The volatile solids are required to the fraction of the total solids lost on ignition at 550 °C and serves as a measure of the organic (oxidizable) solids present in each sample analyzed.

Apparatus required

- Porcelain crucibles
- Drying oven
- Analytical balance
- Dessicator
- Muffle furnace

Procedure
Residue from the determination of total solid is ignited in a muffle furnace at 550 °C for 20 mins. The volatile solid is therefore calculated as follows:
Total dissolved solids (mg/l) = ((A-C) x 1000)/(sample volume, (ml))
A = weight of dried residue + dish before ignition, (mg)
C = weight of residue + dish after ignition, (mg)

- Chemical oxygen demand (COD)

COD measures the oxygen equivalent of that portion of the organic matter in a sample that is easily oxidized by a strong chemical oxidant. It is an important and rapidly measured parameter to measure the amount of organic compounds in stream and industrial waste studies, and in

operational control of waste water treatment plants. The sample is digested for 2 hours in a strongly acidic dichromate solution, using silver sulphate as a catalyst and mercuric sulphate as a masking agent to prevent chloride interference. The dichromate is partially reduced by the oxidisable material present in the sample. The excess dichromate is titrated with ammonium iron (II) sulphate and the COD value calculated from the amount of dichromate.

Apparatus required

- Digester unit
- Erlenmeyer flasks
- Pipettes
- 10 ml and 5 ml automatic bottle top dispensers
- Digital titrator

Reagents

Standard potassium dichromate $K_2Cr_6O_7$ digestion solution: 0.0167 M

Add to about 500 ml distilled water and 4.913g $K_2Cr_6O_7$, previously dried at 105 °C for 2 hours.

Add 167 ml conc. sulphuric acid H_2SO_4 and 13.3 g Mercuric sulphate $HgSO_4$.

Dissolve and cool to room temperature before diluting to 1L.

Sulphuric acid H_2SO_4/Silver Sulphate reagent Ag_2SO_4 (COD reagent)

Add 26 g of silver sulphate crystals or powder to 2.5 l of concentrated sulphuric acid using a magnetic stirrer. Shake well and leave for 2 days for dilution.

Ferroin indicator 2 drops

Dissolve 1.485 g 1:10 phenontroline monohydrate and 0.695 g ferrous sulphate ($FeSO_4.7H_2O$) in distilled water and dilute to 100 ml.

Dissolve 39.2g Fe $(NH_4)2(SO_4)2$.$6H_2O$ in distilled water. Add 20 ml conc. sulphuric acid H_2SO_4 and dilute to 1 L. Standardize daily against standard potassium dichromate $K_2Cr_6O_7$ digestion solution.

Standard preparation

Add 3 ml of standard $K_2Cr_6O_7$ digestion solution to 5 ml of distilled water. Add 7 ml COD reagent and cool it down. Prepare a standard $K_2Cr_6O_7$ solution daily to correct any variation in the concentration of the Ferrous Ammonium Sulphate. Titrate with FAS Titrant using 2 drops of ferroin indicator.

Procedure

- Add 5 ml sample to each digester tube
- Add 5 ml distilled water to another vessel (blank)
- Add 3 ml potassium dichromate digestion solution into each vessel
- Add 7 ml sulphuric acid reagent (with silver sulphate) in each vessel

The acid must be poured down the wall of the flask while flask is tilted. If sample is too concentrated it will turn green and a higher dilution of a sample must be used

Prepare a blank with each set of samples consisting of 5 ml distilled water in place of sample together with all reagents and digest together with samples

Digest for 2 hrs at 150 °C

- Transfer contents from tube into 100 ml flasks for titration
- Titrate the excess dichromate in the digest mixture with standard ferrous ammonium sulphate using 2 drops of ferroin indicator
- Titrate from a sharp green /orange to red brown end point
- Take reading.

Calculation

COD (mg/l) = ((Blank-Titration)x(molarity of FASx8000))/(sample (ml))

- Biological oxygen demand (BOD)

BOD is the amount of dissolved oxygen required by aerobic biological organisms in a body of water to break down organic material present in a given water sample at certain temperature over a specific time period. The BOD value is most commonly expressed in milligrams of oxygen consumed per liter of sample during 5 days of incubation at 20 °C and is often used as

a robust surrogate of the degree of organic pollution of water. BOD is the principle test to give an idea of the biodegradability of any sample and strength of the waste.

Apparatus and reagents required

- BOD system
- 300 mL incubation bottles
- A nitrifying inhibitor (ATH) (N-allylthiourea)

Procedure

- Add a sample volume into the incubation bottles, this depends on the range of BOD estimated in the collected sample.
- Add drops of ATH based on the sample size then place in the BOD system for 5 Days. Below (Table A) is the table showing relationship between sample volume and the drops of ATH required.

Table A: Mtsweni (2016)

Sample volume	Measuring range (mg/l)	ATH (drops)
428	0 - 40	10
360	0 - 80	10
244	0 - 200	5
157	0 - 400	5
94	0 - 800	3
56	0 - 2000	3
21.7	0 - 4000	1

General ANN Training Script

The input and the target data is imported to Matlab Workspace and e the Command Window is used to create the ANN.

```
% Import the data
x = input';
t = target';
% Choose the Training Function,  Levenberg-Marquardt back propagation
trainFcn = 'trainlm';
% Create a Fitting Network, different number of neurons for the hidden layer.
hiddenLayerSize = 15;
net = fitnet(hiddenLayerSize,trainFcn);
% Division of Data into 70% for Training, 15% for Validation and 15% for Testing
net.divideParam.trainRatio = 70/100;
net.divideParam.valRatio = 15/100;
net.divideParam.testRatio = 15/100;
% Training the Network
[net,tr] = train (net,x,t);
% Testing the Network (output, error, performance)
y = net(x);
e = gsubtract(t,y);
p = perform(net,t,y)
% View the Network
view(net)
% View the Error Histogram and the Regression Plot
ploterrhist(e);
plotregression(t,y);
```